AN ANALYSIS OF PARAMETERS RELATED TO THE DIRECTIONAL INSTABILITY OF REAR CASTER WHEELCHAIRS

A Thesis

Presented to the

Faculty of the School of Engineering and Applied Science

University of Virginia

In Partial Fulfillment

of the Requirements for the Degree

Master of Science (Mechanical and Aerospace Engineering)

by

Timothy J. Collins

August 1987

This thesis is submitted in partial fulfillment of the

requirements for the degree of

Master of Science (Mechanical and Aerospace Engineering)

Timothy J. Collins

AUTHOR

This thesis has been read and approved by the examining committee:

James J. Kauzlarich

THESIS ADVISOR

John G Thacker

[illegible]

[illegible]

Accepted for the School of Engineering and Applied Science:

Edgar A Starke Jr.

Dean, School of Engineering
and Applied Science

August 1987

ABSTRACT

A five degree of freedom dynamic model which uses a quasi-static approximation for lateral load transfer effects has been developed as a means of investigating the inherent directional instability associated with rear caster wheelchairs. Using a treadmill and test cart, the dependence of lateral wheelchair tire cornering force on variables such as forward speed, inflation pressure, camber angle, slip angle, and vertical load have been experimentally determined. A model has been developed which predicts wheelchair tire-road forces for different operating conditions. A simulation program which utilizes the tire force data to solve the equations of motion written for a body fixed reference frame attached to the wheelchair has been tested. Predictions from the program for trajectory and yaw velocity response are in good agreement with theory and observation for both rear caster and conventional type wheelchairs.

A parametric study of several design variables has delineated the conditions under which a rear caster wheelchair exponentially diverges to a state of uncontrolled and potentially unsafe motion upon being subjected to a slight disturbance. Center of gravity position and other geometric parameters, along with forward speed, have been shown to have a dominant influence on directional control, while tire selection has been shown to play a less important role. The effects of camber, toe, inertial properties, and caster friction have also been investigated.

ACKNOWLEDGEMENTS

The author would like to thank the members of the examining committee. I would like to especially thank Dr. James J. Kauzlarich and Dr. John G. Thacker for all of the help and advice they have given me during my stay at the University of Virginia.

In addition, I would like to say how much I enjoyed the opportunity to work for the Rehabilitation Engineering Center at the University of Virginia. A sincere word of thanks goes to everyone at the center who has helped me in various ways over the past two years. I would like to also thank Beth Todd and Mike Towler for their many helpful comments and suggestions throughout the preparation of this thesis.

Finally, I must express my love and gratitude to Annette. Without her caring and support, I would never have been able to finish this project.

TABLE OF CONTENTS

LIST OF FIGURES

LIST OF TABLES

LIST OF SYMBOLS

* note that terms such as front, rear, left, or right refer to a rear caster wheelchair

A	ground contact point for left caster
a,b,c	empirical tire force coefficients
A_1, A_2	amplitudes of exponential solutions (m/sec^2)
$\hat{a}_1$	longitudinal unit vector for left caster assembly
$\hat{a}_2$	lateral unit vector for left caster assembly
$\vec{a}_c$	acceleration of wheelchair center of mass (m/s^2)
$\vec{a}_{Pa}$	acceleration of left caster pin (m/s^2)
$\vec{a}_{Pb}$	acceleration of right caster pin (m/s^2)
a_x	longitudinal distance from c.g. to point A (m)
a_y	lateral distance from c.g. to point A (m)
B	ground contact point for right caster
$\hat{b}_1$	longitudinal unit vector for right caster assembly
$\hat{b}_2$	lateral unit vector for right caster assembly
b_x	longitudinal distance from c.g. to point B (m)
b_y	lateral distance from c.g. to point B (m)
C	point which locates wheelchair c.g.
$\hat{c}_1$	longitudinal body fixed unit vector
$\hat{c}_2$	lateral body fixed unit vector
$\hat{c}_3$	vertical body fixed unit vector
C_a	point locating c.g. of left caster assembly
C_b	point locating c.g. of right caster assembly
c.g.	center of gravity
C_α	cornering stiffness (N/deg or N/rad)
$C_{\alpha f}$	cornering stiffness of front tires (N/deg or N/rad)

$C_{\alpha r}$	cornering stiffness of rear tires (N/deg or N/rad)
d	width, distance between front wheels (m)
d	test cart half width (m)
D	ground contact point for left front tire
d_1	lateral distance from c.g. to left front wheel (m)
d_2	lateral distance from c.g. to right front wheel (m)
E	ground contact point for right front tire
F_{AX}	longitudinal force on left caster wheel (N)
F_{AY}	lateral force on left caster wheel (N)
F_{AZ}	normal force on left caster wheel (N)
F_{BX}	longitudinal force on right caster wheel (N)
F_{BY}	lateral force on right caster wheel (N)
F_{BZ}	normal force on right caster wheel (N)
f_c	camber coefficient [=1/m] (dimensionless)
$\vec{F}_c$	resultant force acting at wheelchair c.g. (N)
F_{DX}	longitudinal force on left front wheel (N)
F_{DY}	lateral force on left front wheel (N)
F_{DZ}	normal force on left front wheel (N)
F_{EX}	longitudinal force on right front wheel (N)
F_{EY}	lateral force on right front wheel (N)
F_{EZ}	normal force on right front wheel (N)
f_r	coefficient of rolling resistance
F_r	rolling resistance force (N)
F_s	side force (N)
F_{sx}	longitudinal component of side force (N)
F_{sy}	lateral component of side force (N)
F_x	longitudinal force on tire (N)

F_y	lateral cornering force on tire (N)
F_{yf}	cornering force on front wheels, zero width model (N)
F_{yr}	cornering force on rear wheels, zero width model (N)
F_z	normal force on tire (N)
g	acceleration due to gravity (9.8 m/s^2)
h	c.g. height (m), also height of test cart support (m)
I	inertia of wheelchair only about z axis ($kg\text{-}m^2$)
I_z	wheelchair/user moment of inertia about z axis ($kg\text{-}m^2$)
I_{zP}	moment of inertia of casters about caster pins ($kg\text{-}m^2$)
k	roll coefficient (kf/kr)
k_f	front roll coefficient (N-m)/rad
k_r	rear roll coefficient (N-m)/rad
k_t	torsional rigidity of torsional pendulum (N-m)/rad
k_{us}	understeer coefficient
l	caster trail distance (m), also test cart length (m)
l_1	distance from caster pin to caster c.g. (m)
m	slope of cornering force vs camber force curve
m	total mass of wheelchair and occupant (kg)
M	stabilizing or destabilizing moment (N-m)
M_{af}	frictional moment at left caster pin (N-m)
M_{bf}	frictional moment at right caster pin (N-m)
$\vec{M}_c$	resultant moment about wheelchair c.g. (N-m)
m_c	mass of caster assembly
$\vec{M}_{Pa}$	moment on left caster about caster pin (N-m)
$\vec{M}_{Pb}$	moment on right caster about caster pin (N-m)
M_x	overturning moment on tire (N-m)
M_y	rolling resistance moment (N-m)
M_z	self aligning torque on rolling tire (N-m)

M_z	moment about z axis (N-m)
$\hat{n}_1$	unit vector along global X axis
$\hat{n}_2$	unit vector along global Y axis
$\hat{n}_3$	unit vector along global Z axis
P	horizontal force at wheel center (N)
P_a	point locating left caster pin
P_b	point locating right caster pin
r	height of tire axle above ground (m)
R	distance test cart support pin is moved (m)
$\vec{r}_{cPa}$	displacement vector, point C to left caster pin (m)
$\vec{r}_{cPb}$	displacement vector, point C to right caster pin (m)
$\vec{r}_{PaCa}$	displacement vector, left caster pin to point C_a (m)
$\vec{r}_{PbCb}$	displacement vector, right caster pin to point C_b (m)
R_x	reaction at test cart support pin (N)
R_y	reaction at test cart support pin (N)
R_z	reaction at test cart support pin (N)
s	total wheelbase distance if caster trail is zero (m)
s_1	perpendicular distance from front wheels to c.g. (m)
s_2	perpendicular distance, caster pins to c.g. (m)
t	time (s), or half width of load transfer model (m)
T	period of torsional pendulum (sec)
t_1	lateral distance from c.g. to left caster pin (m)
t_2	lateral distance from c.g. to right caster pin (m)
u	displacement in body fixed $\hat{c}_1$ direction (m)
$\dot{u}$	velocity in body fixed $\hat{c}_1$ direction (m/s)
$\ddot{u}$	acceleration in body fixed $\hat{c}_1$ direction (m/s^2)
v	displacement in body fixed $\hat{c}_2$ direction (m)

$\dot{v}$	velocity in body fixed $\hat{c}_2$ direction (m/s)
$\ddot{v}$	acceleration in body fixed $\hat{c}_2$ direction (m/s^2)
$\vec{V}$	absolute velocity or body fixed reference frame (m/s)
$\dot{\vec{V}}$	absolute acceleration of body fixed frame (m/s^2)
$\vec{V}_A$	velocity of left caster contact point (m/s)
$\vec{V}_B$	velocity of right caster contact point (m/s)
$\vec{V}_D$	velocity of left front wheel contact point (m/s)
$\vec{V}_E$	velocity of right front wheel contact point (m/s)
W	total vehicle weight (N)
W_f	weight on front wheels of vehicle
W_r	weight on rear wheels of vehicle
x	lateral body fixed axis in $\hat{c}_1$ direction
X	lateral tire axis, or global reference frame axis
x_c	distance from test cart axle to test cart c.g. (m)
y	longitudinal body fixed axis in $\hat{c}_2$ direction
Y	longitudinal tire axis or global reference frame axis
z	vertical body fixed axis through c.g.
Z	vertical tire axis, or vertical axis through c.g.
α	slip angle of rolling tire (deg or rad)
α_A	slip angle of left caster wheel (rad)
α_B	slip angle of right caster wheel (rad)
α_D	slip angle of left front tire (rad)
α_E	slip angle of right front tire (rad)
α_f	slip angle of front tires, zero width model (rad)
α_r	slip angle of rear tires, zero width model (rad)
β	angle between right caster and $\hat{c}_1$ axis (deg or rad)
$\dot{\beta}$	angular velocity of right caster (rad/s)
$\ddot{\beta}$	angular acceleration of right caster (rad/s^2)

γ	camber angle (deg or rad)
δ	time step (sec)
ε	normal force offset distance (m)
η	angle between left caster and $\hat{c}_1$ axis (deg or rad)
$\dot{\eta}$	angular velocity of left caster (rad/s)
$\ddot{\eta}$	angular acceleration of left caster (rad/s^2)
θ	angular orientation (yaw) of wheelchair (deg or rad)
$\dot{\theta}$	angular velocity (yaw velocity) of wheelchair (rad/s)
$\ddot{\theta}$	angular acceleration of wheelchair (rad/s^2)
λ	exponential time constant (1/s)
ϕ	roll angle (rad), also test cart angle in Figure A-2
Ω	angular velocity of rolling wheel (rad/s)

CHAPTER 1

INTRODUCTION

The problem of controlling an unstable vehicle is not a recent development. For example, it has been known for some time that aircraft equipped with a castered tail wheel experience steering difficulty while taxiing. These planes require tail rudder control and wheel braking in order to maintain a straight path. Wheelchairs that have their pivoting caster wheels in the rear experience very similar handling problems. Aircraft and wheelchairs that have their caster wheels in front are always directionally stable. The reasons for this will be outlined in this chapter.

There are several motivations for studying the directional control problem associated with rear caster wheelchairs. Although less popular than conventional front caster wheelchairs, rear caster wheelchairs continue to exist because of several inherent advantages.

Electric wheelchairs often use rear casters because of the ease with which obstacles such as a curb can be negotiated. It is often desirable to use front wheel drive on an electric wheelchair. When this is done, it is also necessary to use rear casters. Other considerations sometimes make rear casters desirable for manual wheelchairs. For example, it is sometimes necessary to place restraining leg cushions at the front of a wheelchair. These cushions can be large and bulky, and hence may interfere with the normal pivoting of conventional front casters. Persons who own rear caster wheelchairs generally find them easier to maneuver close to an object such as a counter or table. Aside from these reasons, some users will purchase a rear caster wheelchair simply because it is what they are accustomed to.

Steering instabilities caused by rear casters must be compensated for in order for the user to maintain a straight path. Electric wheelchairs that are unstable require much more manipulation of the joy stick. Unstable manual wheelchairs require additional physical exertion that some users may be unable to supply. Furthermore, when operated at high speeds or on uneven ground, rear caster wheelchairs are often uncontrollable and may even be considered dangerous. For these reasons, an understanding of the parameters related to the directional instability of rear caster wheelchairs is desirable.

Figure 1-1 shows a typical manual rear caster wheelchair. The wheelchair shown is an Everest and Jennings "Premier" rear caster wheelchair. This chair was manufactured approximately 15 years ago (1972), but similar models are currently available.

DESCRIPTION OF THE DIRECTIONAL INSTABILITY PROBLEM

Directional stability is generally defined as the ability of a vehicle to stabilize its motion against external disturbances. A vehicle is considered to be directionally stable if it returns to a steady state of

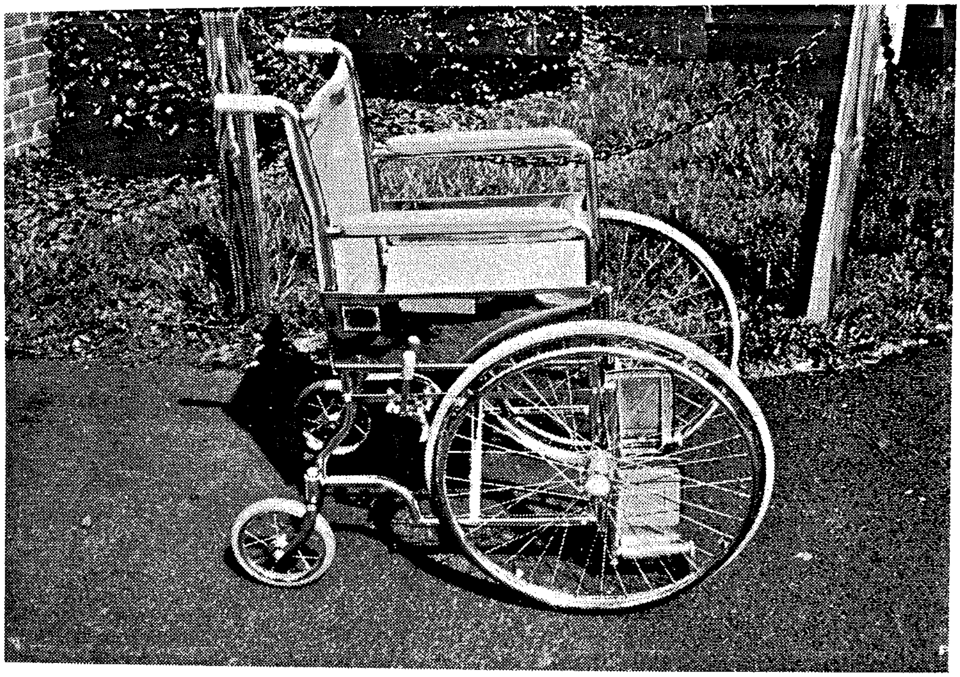

Figure 1-1 Everest and Jennings Premier Rear Caster Wheelchair

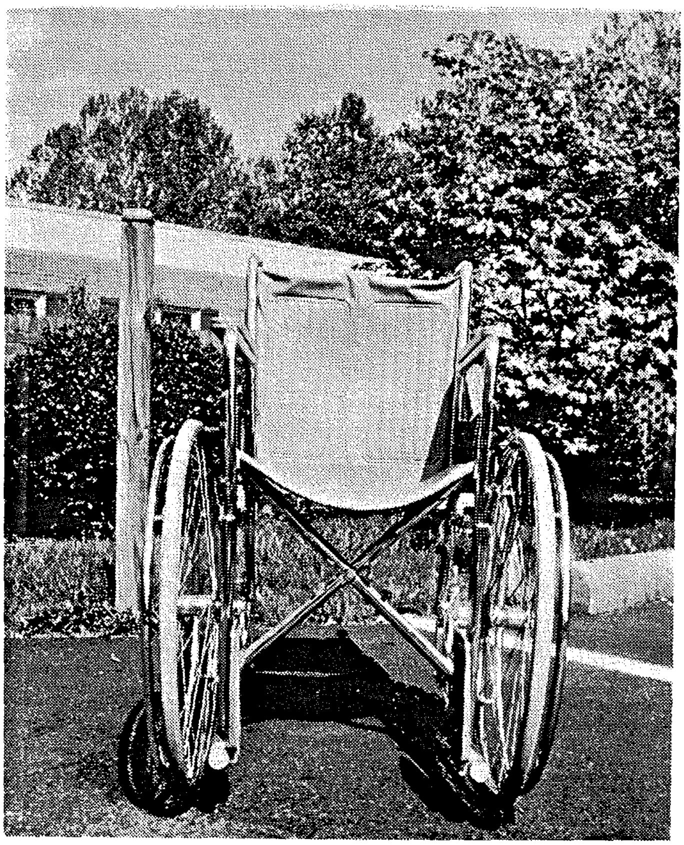

Figure 1-1 Continued

motion within a finite time after a disturbance is removed. Directionally unstable vehicles diverge more and more from the original line of motion even after the disturbance is removed. This diverging continues until either a course correction is made, or until ground looping occurs in which the vehicle totally reverses its direction of motion.

A fundamental description of the control problem associated with rear caster wheelchairs was first published in 1986 by Kauzlarich and Thacker. [1.1] The investigation that is the topic of this thesis grew from their original analysis. Kauzlarich and Thacker showed that when a wheelchair is displaced from its line of motion by a jolting force, such as a bump in the road, it experiences a twisting moment about the center of gravity. This moment is due to lateral road forces that develop at the tire-road interface.

Figure 1-2 shows a conventional front caster wheelchair that has been displaced from the intended direction of motion by an angle θ. For reasons to be given later, the lateral road force at the tires is referred to as the cornering force, F_y. In the simplest analysis, the road force is the same at each tire, and the resulting moment about the center of gravity is $2s_1F_y$. The distance s_1 is measured perpendicularly from the fixed wheels to the center of gravity. Because the lateral road force acts behind the center of gravity for a front caster wheelchair, the resulting moment tends to return the chair to a state of steady straight line motion. Thus, the moment is said to have a stabilizing effect.

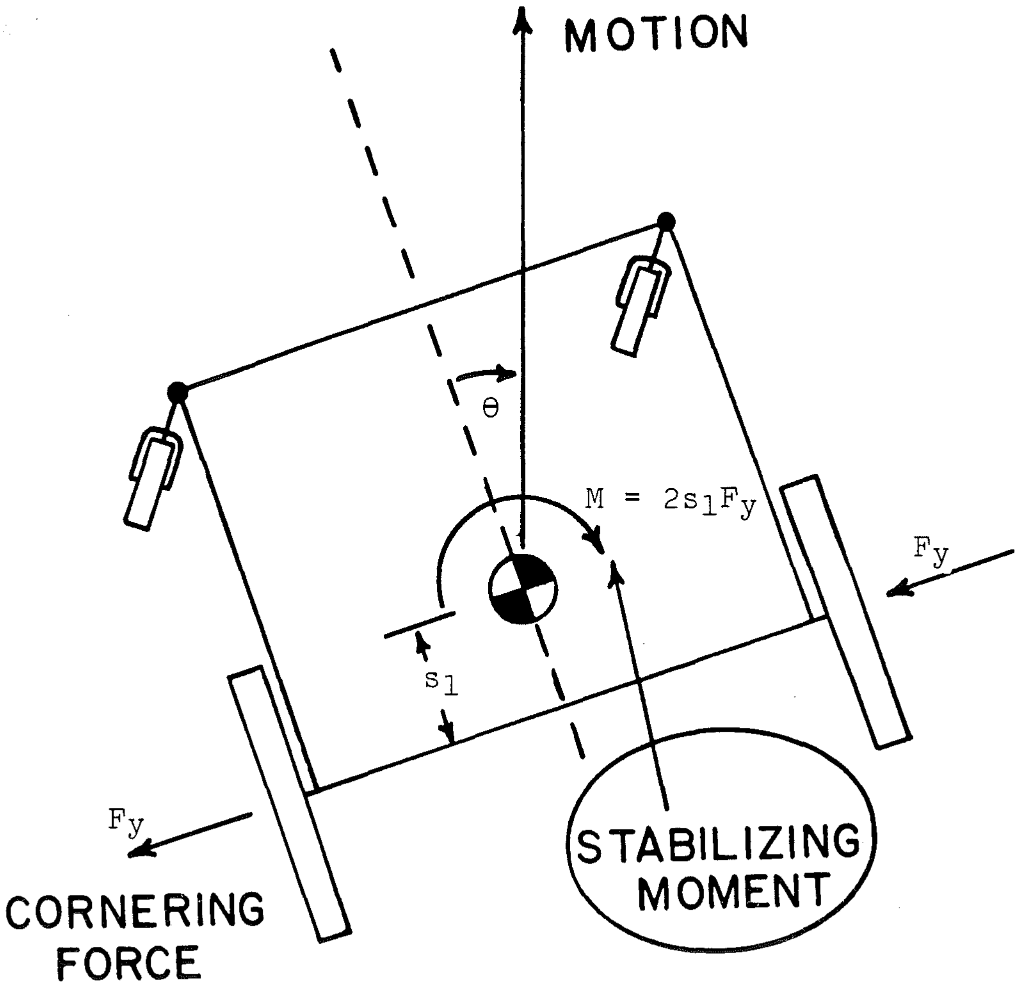

Figure 1-2 Stabilizing Moment For a Conventional Front Caster Wheelchair

Figure 1-3 depicts a similar situation for a rear caster wheelchair that has been displaced from its line of motion. In this case, the lateral road forces act ahead of the center of gravity. As a result, the moment about the center of gravity causes the wheelchair to rotate even further away from the desired directional heading. For this reason, the moment is referred to as destabilizing.

It is clear from this simple description that reducing the distance s_1 will reduce the destabilizing moment and make the rear caster wheelchair easier to control. Furthermore, it is clear that a knowledge of the lateral road force, F_y, is necessary for a complete analysis of the instability problem.

PROJECT DESCRIPTION

The purpose of this thesis project was to gain an understanding of the parameters that do or do not affect the directional stability of rear caster wheelchairs. A primary goal was to determine which of these parameters, if any, might be altered so as to significantly reduce the directional instability problem. Thus it became desirable to develop a computer model capable of simulating wheelchair motion and examining the variables that affect stability. In pursuing this end, several secondary goals developed.

The first necessary task was to experimentally determine the characteristics of the road forces which act on a wheelchair tire. Forces that occur at the tire-road

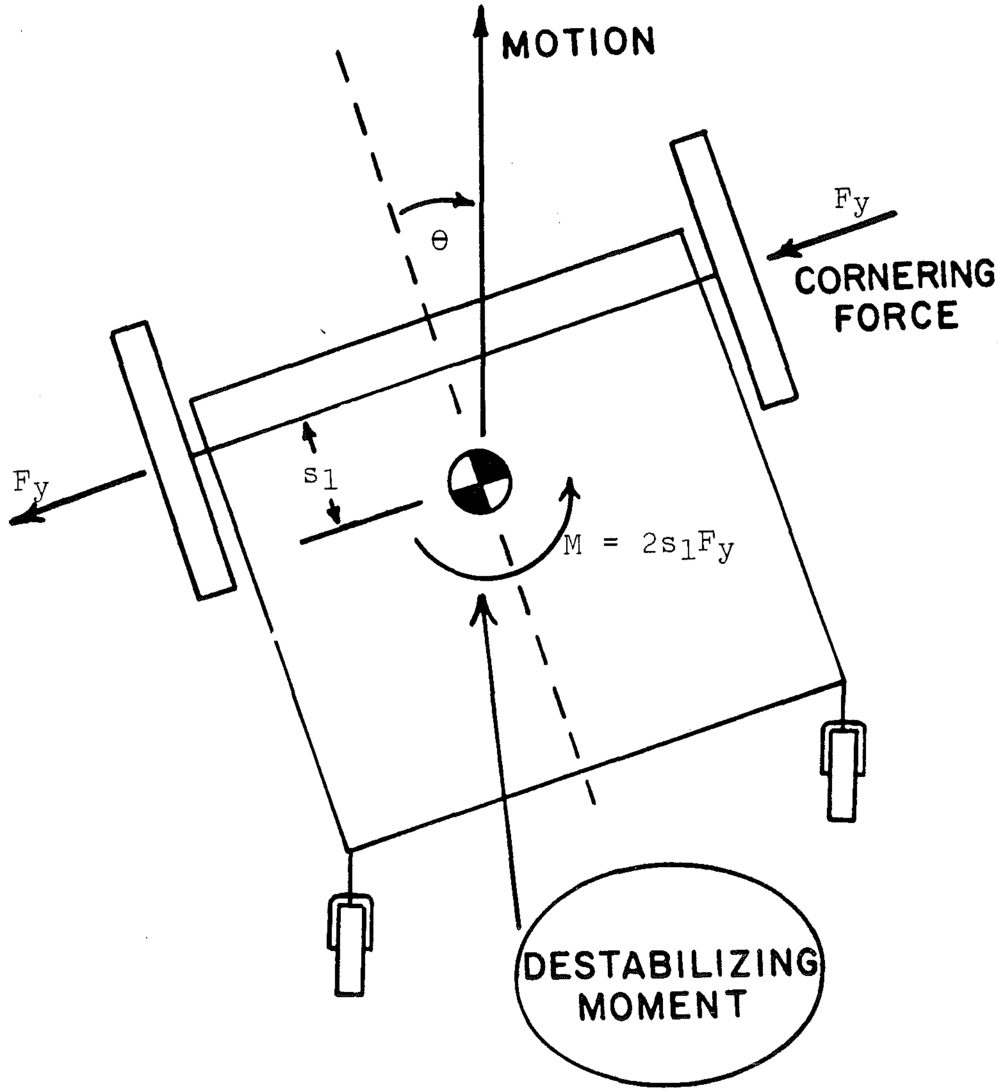

Figure 1-3 Destabilizing Moment For a Rear Caster Wheelchair

interface are by far the dominant forces governing the motion of any ground vehicle. A complete description of tire forces accounts for several variables. These include: vertical load, slip angle, camber angle, toe angle, and rolling resistance to name a few. All of these variables were considered as part of this work.

It was realized that some of these parameters might have only secondary effects on the steering characteristics of a wheelchair. However, in the interest of developing a complete and general model that might eventually be extended for other purposes, as many parameters as possible were included in the investigation. For example, although manual rear caster wheelchairs were the primary focus of this research, it might be desirable to eventually extend the study to include electric rear caster wheelchairs. Parameters that do not have an important influence on the stability of manual wheelchairs may play a more vital role in this case.

A simple tire model capable of predicting the ground forces on a wheelchair tire was developed. In addition, the complete equations of motion for a rear caster wheelchair were formulated. This was done with the goal in mind of eventually developing a simulation computer program.

The simulation model was developed for two primary reasons. The first of these was to determine if any parameters which have not been considered in the past, such as tire properties or width dimensions, have a significant influence on directional stability. The second reason for developing the simulation model was to gain a more quantitative description of the instability problem. For example, it was already known that moving the center of gravity forward will improve directional stability, but how significant is this improvement and how can it be quantified? A necessary requirement for the simulation model was that it accurately predict the inherent difference between front caster and rear caster wheelchairs.

Users of rear caster wheelchairs commonly observe that the directional control problem worsens at higher forward speeds. A goal of this work was to determine the speed at which a typical rear caster wheelchair becomes uncontrollable. An additional goal was to delineate the conditions under which a rear caster wheelchair should or should not be used. Based upon results from the simulation model, perhaps design recommendations could be made that will lead to improved stability.

With these goals in mind, the effect on directional stability of varying several different parameters was studied. The Everest and Jennings wheelchair shown in Figure 1 was used as the starting point for this investigation. Important parameters such as geometric dimensions and total mass were assumed to be typical for this chair.

OUTLINE OF THESIS TEXT

The text of this thesis is roughly separated into two parts. Part one includes Chapters 2 through 4 which discuss the force characteristics of rolling tires. Chapter 2 gives a complete description of the forces and moments that act on a wheelchair tire. The important and unimportant forces are defined. Chapter 3 presents the results of experimental testing which was done to determine the magnitude of wheelchair tire forces as a function of several variables. Finally, Chapter 4 gives a simple method for predicting wheelchair tire forces.

Once the important wheelchair tire forces have been described, the second part of the thesis considers the actual stability problem. Chapter 5 presents a simplified model of wheelchair motion. This model distinguishes the important parameters which are related to directional stability. The simplified model is able to predict the effect on stability of varying several parameters. It is unable however, to predict actual wheelchair motion or to determine quantitatively how much certain parameters affect stability.

Chapter 6 develops the complete equations of motion for a rear caster wheelchair. The primary assumption is that the wheelchair is restricted to planar motion. However, a quasi-static method which accounts for roll effects is developed. Chapter 7 describes a computer program which can be used to simulate the motion of a freely rolling wheelchair. The computer program utilizes the tire force characteristics described in Chapters 1 through 3 along with the equations of motion developed in Chapter 6.

After all of this groundwork has been given, Chapter 8 gives the results of several simulations of wheelchair motion. Methods by which the wheelchair model and the simulation program were verified are discussed. Results for both conventional front caster wheelchairs and rear caster wheelchairs are considered. The effect of several design variables on directional stability are examined. Finally, in Chapter 9 some conclusions are drawn with regard to how much the instability problem of rear caster wheelchairs can be improved.

CHAPTER 2

MECHANICS OF ELASTIC TIRES

This chapter presents a description of the ground forces that act on a rolling wheelchair tire. Literature related to the mechanics of wheelchair tires is almost non-existent, with the possible exception being articles pertaining to rolling resistance. Thus, the material in this chapter is adapted primarily from literature which concerns automobile tires. It will be shown in the next chapter that wheelchair tires exhibit many characteristics similar to those found for both automobile tires and for aircraft tires.

MOTIVATION FOR STUDYING TIRE FORCES

Numerous authors have pointed out the fact that aside from gravitational and aerodynamic forces, the only forces which influence the motion of a ground vehicle are applied at the tire-ground interface. Therefore, it is natural to assume that a basic knowledge of the ground forces that act on wheelchair tires is desirable. Nordeen and Cortese state that, "An understanding of the relations between tire operating conditions and the resulting forces and moments is a prerequisite to studies of vehicle dynamics." [2.1] Wong asserts that an understanding of tire forces is "essential to the study of the performance characteristics, ride quality, and handling behavior of ground vehicles." [2.2] Finally, Ellis writes, "When vehicle control and stability are studied, it is natural to start with the pneumatic tyre". [2.3]

These quotations were all written with automobiles or other large ground vehicles in mind. They are given here to illustrate the importance given to tire properties in most of the literature relating to vehicle dynamics. At the outset of this study, which concerns the stability of rear caster wheelchairs, it was assumed that tire properties would be very important. The simplified analysis by Kauzlarich and Thacker mentioned in Chapter 1 indicates that the magnitude of the lateral tire force is of primary importance. For these reasons, an extensive examination of several different wheelchair tires was undertaken.

It will be shown in later chapters that although tire selection does affect the handling characteristics of a rear caster wheelchair, its effect is only moderate in comparison to other variables. Nevertheless, a discussion of wheelchair tire forces is still relevant for several reasons. A knowledge of tire forces is necessary in order to simulate the motion of a wheelchair even when parameters other than tire selection are being considered. Methods are needed to predict typical tire forces for any given state of wheelchair motion.

In addition, some understanding of tire mechanics is fundamental to an understanding of wheelchair motion. Usual discussions of rolling generally assume a perfectly rigid wheel which does not deform. A perfectly rigid wheel can only have a velocity component which is parallel to the plane of the wheel. An elastic wheel on the other hand, will not exactly follow the laws of rolling typically developed for rigid wheels. A major difference is that elastic tires can deform. This elastic nature allows small velocity components which are not parallel to the wheel plane even though no slipping may occur. In simple terms, it is possible for an elastic tire to have a "sideways" component of velocity. A description of the forces that can act on an elastic tire as it rolls and deforms allows for a basic understanding of tire properties as related to wheelchair motion. More importantly, if a means for predicting wheelchair tire forces can be obtained, the differential equations of wheelchair motion can be solved as a means of examining the problem of directional stability.

TIRE FORCES AND MOMENTS

Figure 2-1 shows the axis system which is most commonly used as a reference for the definition of various tire forces and moments. This system is recommended by the Society of Automotive Engineers and is described in detail by Wong. [2.2]

First, notice the two angles associated with the rolling tire. These are the camber angle ,γ, and the slip angle ,α. The camber angle is the angle between the wheel plane and the plane formed by the X and Z axes. This angle may be zero, but in the case of wheelchairs, camber is often present because many wheelchair users adjust their wheels

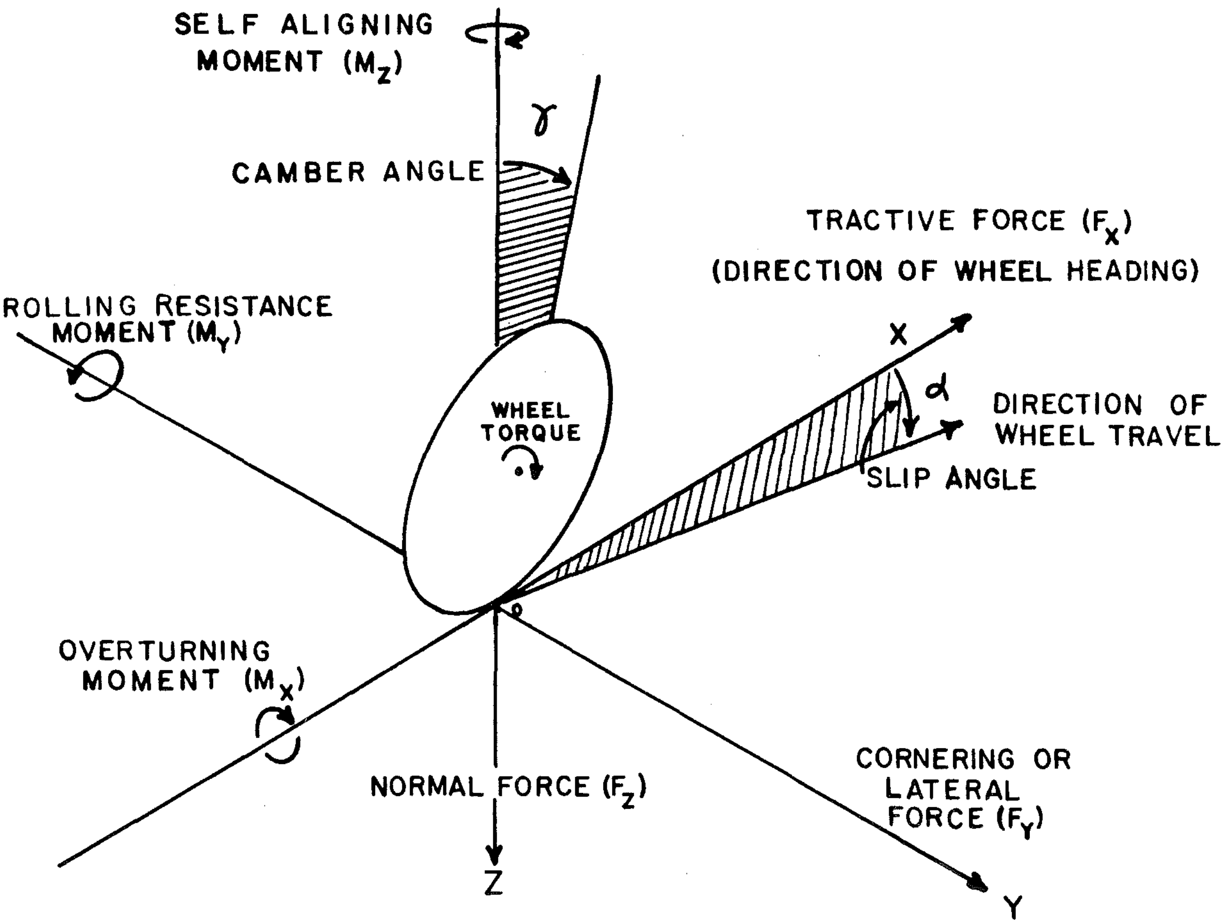

Figure 2-1 Tire Forces and Moments

inward at the top in order to obtain a firm and comfortable grip. The slip angle is the angle between the wheel plane's heading and the actual direction of wheel travel. A slip angle results whenever the wheel has a nonzero velocity component along its Y axis. The term slip angle is not meant to suggest that the wheel is slipping or sliding with respect to the ground. The elastic nature of the rolling tire allows small velocities perpendicular to the wheel heading without sliding.

Note that the X, Y, and Z axes shown are fixed in the rolling wheel. If the wheel rotates, these axes rotate with it. It is especially important to distinguish references to X and Y directions in this local axis system, from references to X and Y in a fixed reference frame (an inertial reference frame) which does not move or rotate. More will be said concerning reference frames in future chapters.

For the most general case, six quantities are required to completely describe the force system acting on a tire. These include three forces and three moments as shown in Figure 2-1. Reference [2.1] gives a complete description of these six quantities. There are three components of road force that act on the rolling tire:

(1) F_x is the longitudinal or "tractive force" acting on the tire by the road in the plane of the road and parallel to the direction of the wheel's heading. The direction of wheel heading is defined by the intersection of the wheel plane with the road plane. Wheel torques are converted into

propelling tractive forces through friction between the tire and the ground. In addition, some tractive force is always necessary to overcome a wheel's natural rolling resistance.

(2) F_y is termed the lateral force and it is the component of the road force acting at a right angle with respect to the wheel heading. If the slip angle is not zero, an elastic tire deforms slightly as it is forced to roll along an unnatural path. This deformation results in the lateral force between the tire and the ground. The lateral force resists the tendency for sliding of the wheel, and it always acts in a direction which is opposite the Y axis velocity component.

(3) Normal force F_z is the component of road force which acts in the negative Z direction or normal to the plane of the road. A vehicle's weight is supported by the sum of the normal forces acting on each wheel.

The three moments mentioned previously, M_x, M_y and M_z, are referred to respectively as the overturning moment, rolling resistance moment, and aligning torque. These moments result from the fact the lines of action for each of the forces F_x, F_y, and F_z do not necessarily pass directly through the origin shown in Figure 2-1. This can be better understood by examining the sketch shown in Figure 2-2.

Figure 2-2 is based upon experimental observation, and it depicts the deformation (exaggerated) of the tread band and contact region of a tire subjected to a constant slip angle. [2.4] Most tire models separate the contact region

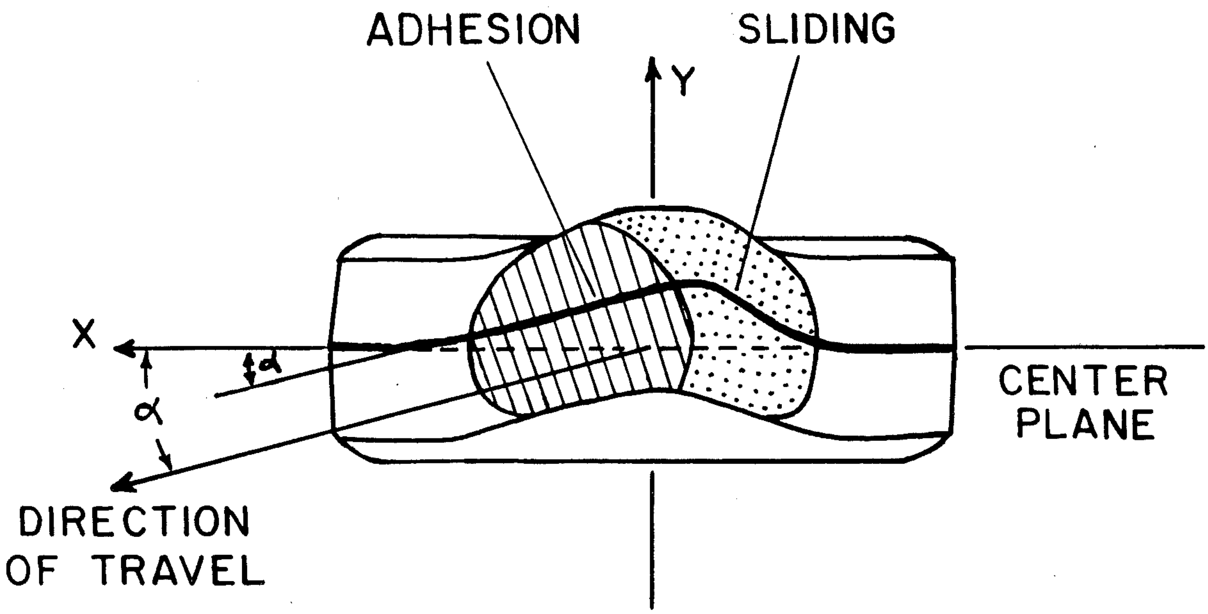

Figure 2-2 Cornering Tire Deformation

of a rolling tire into two general areas: a sliding region and an adhesion region. By observing tires on a glass surface, it is seen that in the adhesion area, the tread deformation is parallel to the direction of travel. The line which separates the adhesion region from the sliding region occurs at the point where the elastic force due to deformation exceeds the available tire-road friction force. At this point, the tread begins to slide back to its normal undeformed position.

As shown in Figure 2-2, the maximum deflection of the tread band occurs at a point slightly behind the Y axis and thus F_y is offset longitudinally by some small distance. The product of lateral force F_y and its offset distance defines the self aligning torque M_z. Similarly, as a result of tire distortion, the center of normal pressure is shifted slightly forward and to one side of the wheel plane. This shift in the center of normal pressure results in the rolling resistance and overturning moments. Figure 2-3 shows a greatly exaggerated diagram of the longitudinal and lateral force offsets which create the three tire moments.

Before examining tire properties in detail, it was necessary to assess which of the six possible tire forces and moments are relevant to wheelchair motion. Fortunately not all six quantities are equally important. The two main wheels of a wheelchair are constrained against rotation about either the X axis or the Z axis. They cannot overturn or pivot. Only rotation about the axle is permitted.

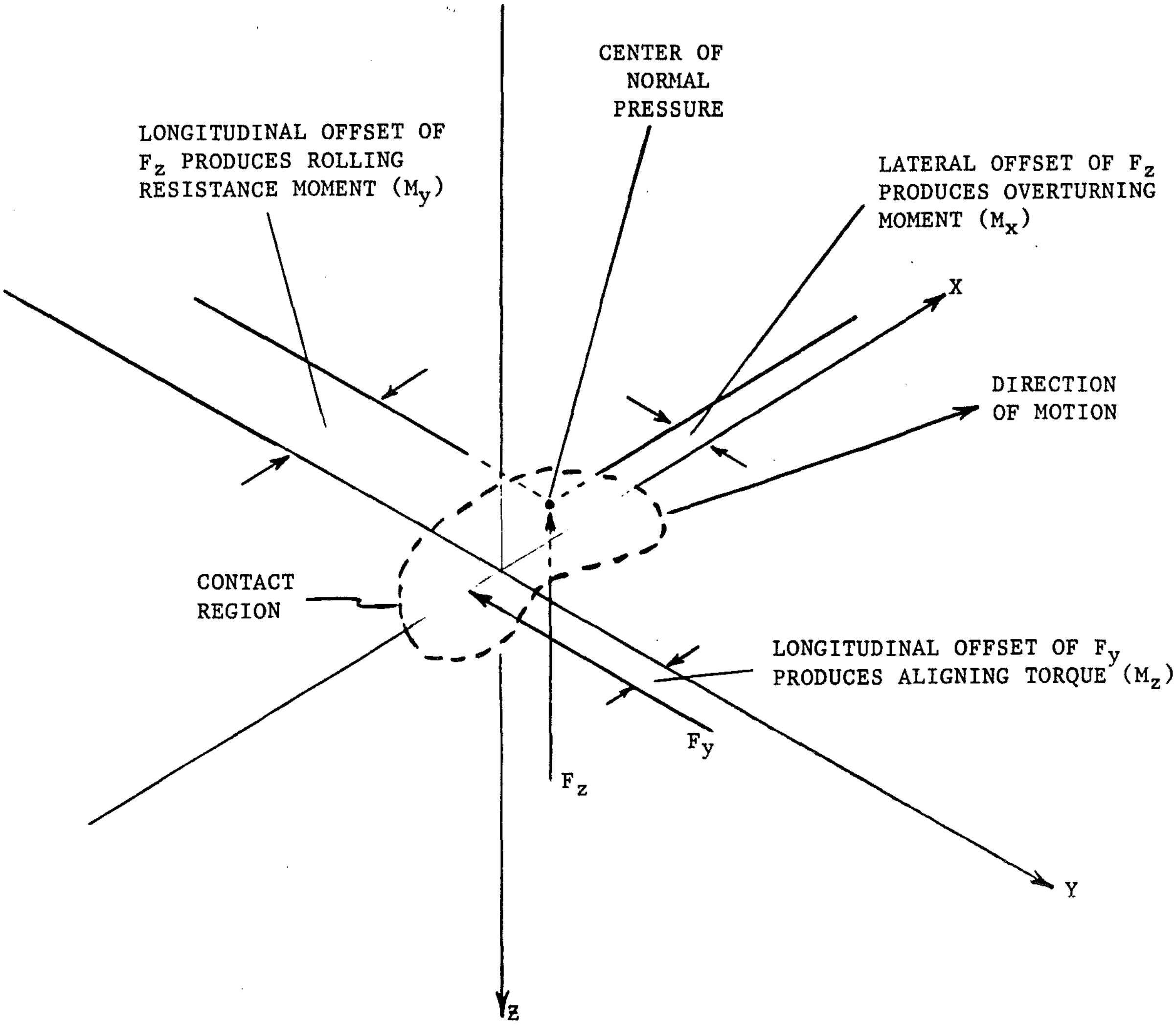

Figure 2-3 Tire Force Offset Distances

The caster wheels are also constrained from overturning about their own X axis. Although the casters are free to rotate about a vertical axis, this rotation does not occur about the Z axis shown in Figure 2-1 or Figure 2-3, but instead occurs about the caster pivot pin which is some distance away from the point where the caster contacts the ground. The distance from the point where the caster contacts the ground to the caster pivot point, rather than the relatively small offset distance of F_y, is therefore of primary importance. Any slight offset of the lateral force F_y will create only negligible differences in the overall wheelchair motion. Also, because the contact regions associated with wheelchair tires are small when compared to automobile tires, it is reasonable to expect that the offset distances will be less important.

As a result of these considerations the problem is reduced to one in which three forces (F_x, F_y and F_z) and one moment ,M_y, act on each of the four wheelchair tires. Each of these will now be discussed at greater length. It is emphasized that assumptions similar to those just described have been proven adequate for the analysis of vehicles much more complicated than a wheelchair. (see for example [2.5] which makes similar assumptions for a two degree of freedom treatment of automobile stability)

SLIP ANGLE AND CORNERING FORCE

Pure rolling of an elastic wheel refers to rolling motion which is confined only to the longitudinal (X) direction. If the wheel is forced to deviate from its direction of pure rolling, a slip angle and lateral force necessarily develop. The existence of a lateral force is made possible by the elastic forces of tire particles which, as they pass the ground contact region, are forced to travel sideways in addition to their rolling progression. [2.6] This is represented by the tread band which was illustrated in Figure 2-2.

When no camber angle is present, the lateral force is due solely to the presence of the slip angle α. In this instance, the lateral force is commonly referred to as the "cornering force". This term arises from the fact that lateral cornering forces supply the centripetal force required for a vehicle to negotiate a curved path. Thus, although lateral forces on the main wheels of a rear caster wheelchair may have a destabilizing effect as discussed in Chapter 1, some lateral force is necessary whenever directional changes are initiated.

Because lateral tire force is inevitably responsible for the deviation of a vehicle from a direct course, whether it be desirable or undesirable, it is almost universally regarded as the most important of all the tire forces and moments. [2.7] In the most general case, cornering force can be regarded as a function of as many as eleven independent variables. [2.4] However, when a vehicle is constrained to make only moderate course changes on a level surface, it is found that the primary variables which affect cornering force are normal load and slip angle. Other possible factors which may have some influence on cornering force are forward speed and inflation pressure. The effect that each of these variables has on the magnitude of cornering force was examined experimentally for several different wheelchair tires. The results of this testing and a comparison to similar results found in the literature for other types of tires are presented in the next chapter.

CAMBER FORCE

As was mentioned before, the term cornering force is reserved to describe the lateral force exerted on a tire when no camber angle is present. Cornering force is thus due only to the slip angle which results from the lateral component of tire velocity. If a camber angle is present, the total lateral force on a rolling tire is considered to consist of two components: a cornering force component which is due solely to the presence of the slip angle α, and a camber force component which is due to the presence of the camber angle γ.

Figure 2-4 shows a cambered wheel which is inclined at some angle γ with respect to the Z axis. An unconstrained wheel which is free to roll would revolve around the center of curvature (point O) as shown. However, when fixed to a vehicle, a cambered wheel is generally forced to roll along a straight path. As a result, a lateral force toward the center of curvature develops. This is the camber force just referred to. The total lateral force F_Y acting on a tire is

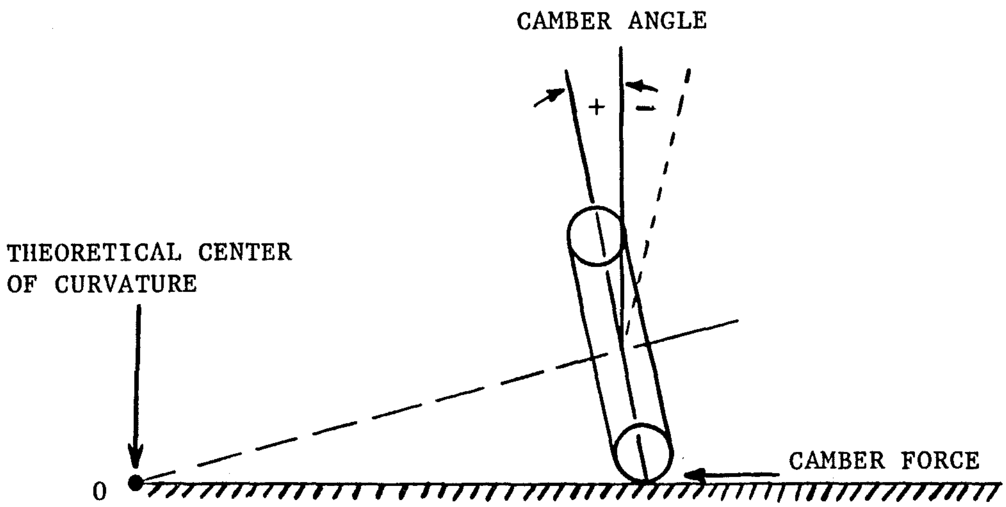

Figure 2-4 The Cambered Wheel

the sum of the cornering force and the camber force. The camber force can either add to or subtract from the cornering force depending on whether or not the camber inclination is toward or away from the direction of lateral wheel motion. Results of camber force tests for wheelchair tires will be discussed in Chapter 3.

ROLLING RESISTANCE

Rolling resistance is one of the few properties that has been investigated fairly extensively for wheelchair tires. At constant speed, a rolling tire requires a horizontal force P at the wheel center in order to overcome the rolling resistance. This force along with the other forces on the wheel are shown in Figure 2-5 where F_z is the normal load carried by the tire, r is the height of the wheel axle above the ground, Ω is the angular velocity of the wheel, and F_r is the rolling resistance force. [2.8]

Note again that the normal force is offset ahead of the contact center by some amount ε producing the rolling resistance moment M_y. Summing forces and moments in Figure 2-5 results in the following conditions for rolling with constant translational and rotational velocity.

$$\begin{aligned} F_r &= P \\ F_r r &= F_z \varepsilon \end{aligned} \qquad (2\text{-}1)$$

From the above it follows that if the force P required to maintain a constant forward velocity is known, both the force F_r and the offset distance ε can be found. More

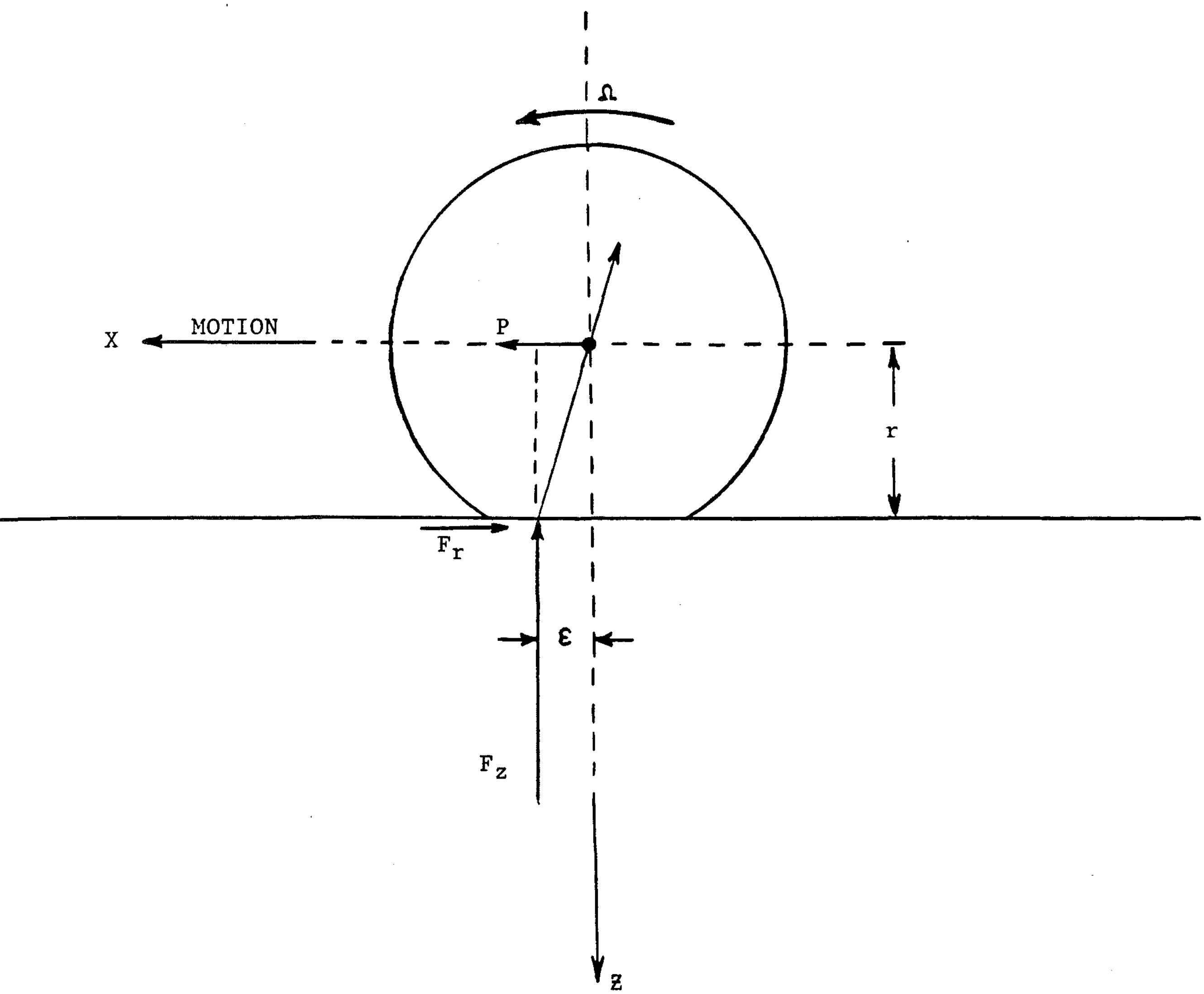

Figure 2-5 Rolling Resistance of Free Rolling Tire

importantly, if no other tractive forces exist in the X direction, the force F_r in Figure 2-5 completely represents the longitudinal force F_x which was described in association with Figure 2-1. In other words, the rolling resistance moment M_y can be incorporated into the tractive force F_x at the tire-road interface. Because of the reasoning just given, rolling resistance can be treated as a force for the purposes of investigating wheelchair motion. However, it should be noted that this force is almost entirely the consequence of hysteretic energy losses due to deformation of the tire during travel. [2.8] For a complete analysis of rolling resistance and a discussion of a hysteresis loss theory for predicting the rolling resistance of wheelchair tires, the reader should refer to Kauzlarich and Thacker. [2.9,2.10] The results of rolling resistance tests made for this work are presented in the next chapter along with results for the other tire forces.

TOE ANGLE

There is an additional angle which is sometimes referred to with regard to the tires of a vehicle. The angle between a rolling wheel and the longitudinal axis of the vehicle to which it is a part is often called the toe angle. A pair of wheels is said to be toed in when the transverse distance between the two wheels at the front of the two wheel planes is less than it is at the rear. The presence of a toe angle means that during straight line motion the wheel plane never coincides with the direction of travel. In other words, toe-in or toe-out forces the wheel to continually travel with a nonzero slip angle. Thus, a toe angle is in actuality no different than the slip angle which has already been discussed, except that in this case the slip angle is always present, even during simple forward motion. The continual lateral forces, F_y which develop from high toe angles are generally undesirable because they result in excessive tire wear and a greatly increased total force acting opposite the direction of wheel motion. [2.6]

In summary, the force system acting on a rolling wheelchair tire has been reduced to one which includes three forces. These are: a longitudinal force F_x which neglects input torques and includes the rolling resistance of the tire, a lateral force F_y which may include a cornering force due to the presence of a lateral component of wheel velocity (a slip angle) and a camber force due to wheel inclination, and finally a normal force F_z. Chapter 3 will discuss experimental results which illustrate those factors which determine the magnitude of F_x and F_y as well as their relationship to the normal force F_z.

CHAPTER 3

EXPERIMENTALLY DETERMINED TIRE FORCES

Chapter 2 presented an overview of the three ground forces which are important to a study of wheelchair motion. The concepts of slip angle, camber angle, toe angle, and rolling resistance were discussed. This chapter will discuss the results of testing which was done to determine what factors influence the magnitude of wheelchair tire forces. Each of the tire forces and tire angles discussed in Chapter 1 will be considered. Results from the literature for elastic tires in general will be compared to experimental results for several different types of wheelchair tires. This chapter does not discuss how the experimental tire data which was collected can be used to predict tire forces and examine directional stability. Methods of doing this and comparisons of different tires are described in Chapter 4.

METHOD USED TO DETERMINE WHEELCHAIR TIRE FORCES

There are several different types of experimental apparatus which can be used to assess the mechanical properties of a rolling tire. These include drum-type testers, moving flat bed testers, towed vehicle testers, and moving treadmill belts. [3.1] Because a variable speed treadmill was readily available, this type of test machine was used for the investigation of wheelchair tire forces. The treadmill has the advantages that it is easy to use and that it allows virtually continuous sustained operation.

The main disadvantage of using a treadmill is the fact that the tires being tested can only be subjected to simulated operating conditions. Furthermore, the treadmill does not allow any versatility with regard to test surface material. A treadmill belt may not be representative of the surfaces commonly encountered by wheelchair users.

During the course of this research two methods were used to examine wheelchair tire forces using a belt treadmill. The initial method is depicted in Figure 3-1 which shows a schematic of the treadmill and a test cart. The test cart takes the place of an actual wheelchair allowing for easy adjustment of several different variables. The test cart is designed such that known loads can be applied directly over the rear axle. Adjustments can be made in order to give the wheels on the test cart any desired angle of camber or toe. In addition, the test cart has a second axle position (not shown in the figure) which enables the small caster wheels of a wheelchair to be mounted. This allows data to be collected for the ground forces exerted on all four wheels of a typical wheelchair.

The test cart is rotated at the forward support shown in Figure 3-1 in order to give each of the tires a known slip angle α. A load cell mounted along the side of the treadmill is attached at the axle of the left test cart wheel. This load cell measures the side force necessary to restrain lateral motion of the wheelchair while it is held at the fixed angle. Neglecting other forces on the test

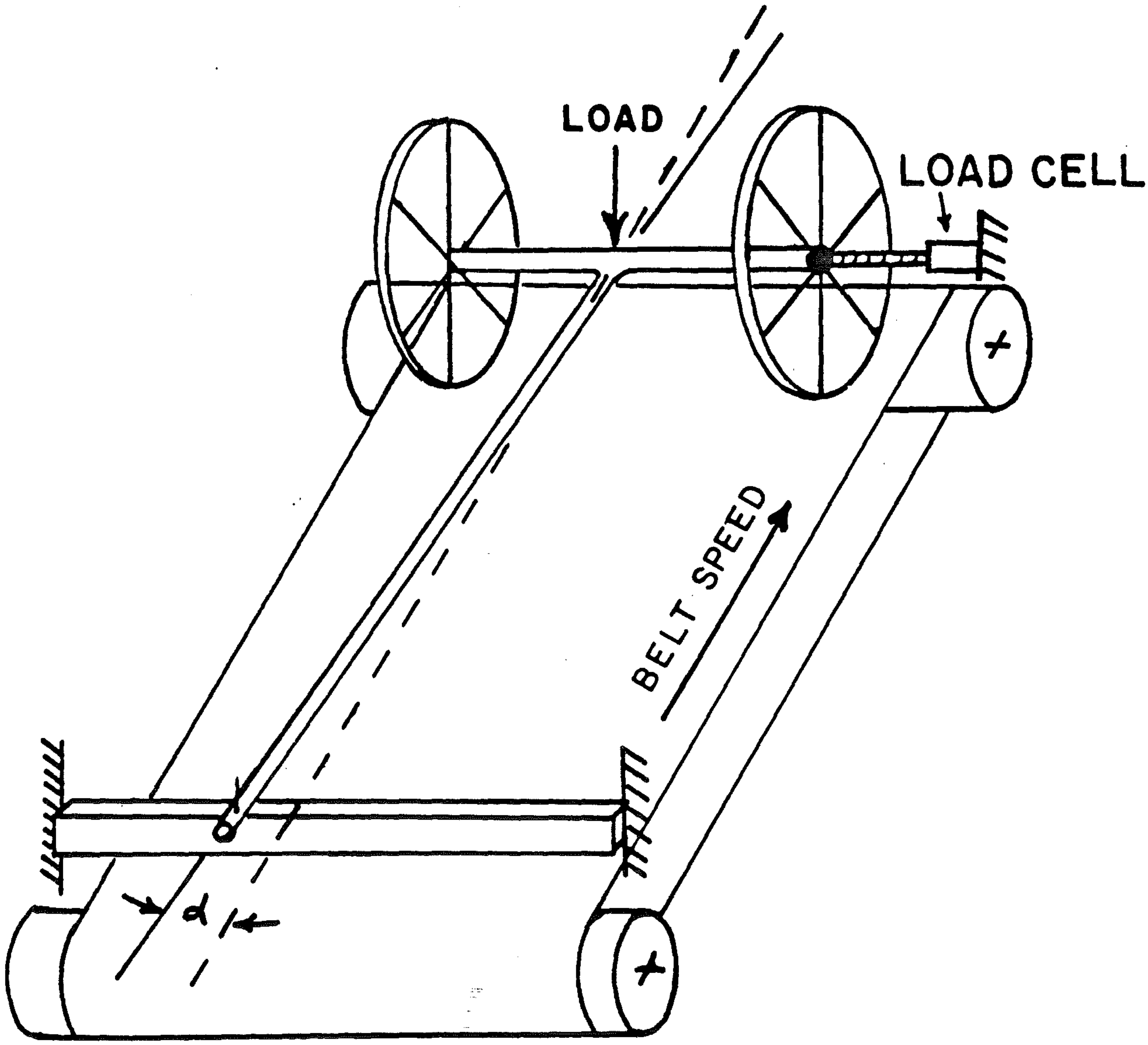

Figure 3-1   Sketch of Treadmill and Test Cart

cart, which are small for small slip angles, the force measured by the load cell is approximately equal to the sum of the lateral forces exerted on each of the fixed wheels.

A problem with the test method shown in Figure 3-1 is that the force exerted by the load cell constraint does more than simply restrain lateral motion. This restraining force also creates a twisting moment about the longitudinal axis which tends to rotate the test cart toward the load cell side of the treadmill. This results in a lateral load transfer such that there is a significant difference in the normal force carried by each of the two tires. This is highly undesirable if it is necessary to isolate the lateral and normal force exerted on a single wheel. It is not correct to simply divide the total force measured by the load cell in half, and then set that value equal to the force on each tire.

An eventual goal of the research related to tire forces was to use the data collected as part of a computer program to simulate wheelchair motion and examine directional stability. In order to simulate wheelchair motion properly, it is necessary to predict the force exerted on a single wheelchair tire given that tire's current slip angle and other conditions. For this reason, the test cart was modified from what is shown in Figure 3-1 such that one wheelchair tire at a time could be tested.

In order to do this, the right test cart wheel was removed and replaced with a vertical cable. If the cable is kept in the vertical position as the test cart is rotated, it will not contribute any lateral force, but instead will only help to support the test cart weight. The support cable was attached to a block and tackle on a rolling support such that both its length and its vertical orientation were readily adjustable. The tendency of the test cart to rotate when subjected to large lateral forces could then be compensated simply by changing the length (and hence the tension) in this cable. In other words, for each test case the support cable was kept vertical and was adjusted to a length so as to keep the test cart level.

Appendix A gives the details of the test cart including the static equations which are used to calculate the normal force F_z and the lateral force F_y from a measured value of side force at the load cell.

Several preliminary tests were conducted before the test apparatus was modified to accommodate only one wheel. These early tests were useful in that they provided insight as to what variables have an important influence on lateral force and what variables do not. For example, these first tests showed that speed and inflation pressure do not have a significant effect on cornering force in the case of wheelchair tires. Thus when it came time to design a slightly more sophisticated test method, these two variables did not have to be reconsidered.

The remainder of this chapter presents tire force findings for seven different wheelchair tires. (five main wheels and two caster wheels) Results obtained by using the test cart with two wheels are presented for rolling resistance to show the effect of speed and inflation pressure on lateral cornering force. All other test results were obtained by using the modified test cart setup in which the ground forces on a single wheel could be isolated. The reader is again referred to Appendix A for the details of the test cart apparatus and for a more complete description of how the tire force data presented in this chapter was obtained.

DESCRIPTION OF TIRES TESTED

The force characteristics of seven different wheelchair tires were tested. Five of these were 24 inch (70 cm) diameter wheels which are generally used as the primary tires on manual wheelchairs. The other two tires tested were caster wheels with diameters of approximately 8 inches (20 cm) each. Because this work focuses on the directional stability of manual rear caster wheelchairs, no tires representative of typical electric wheelchairs were tested. The tires which were tested are identified and described in Table 3-1. The selection of tires provided a fairly good representation of the many different tires which are available, while at the same time keeping the number of tires to be tested at a manageable number. Of the 24 inch tires tested, two were pneumatic tires and three were airless solid or semisolid. The two caster wheels tested were both airless, one being of the solid rubber type and the other being constructed of polyurethane. For the remainder of this text, the specific tire types will generally be referred to by the abbreviations given in Table 3-1.

TABLE 3-1

IDENTIFICATION OF TIRES TESTED

ABBREV	TIRE	Description/Nominal Size
AG	Unknown Airless Solid Rubber	Fits Schwinn Rims #4418 24" x 1 1/4"
EJP	Everest and Jennings Pneumatic	4" Silver Hub-Spoked 24"x1 3/8"x1 1/4",60-70psi
SS	Silver Star Pneumatic	Spoked,Gumwall,No-More Flats Innertube, 24"x1 1/4",75psi
IM	Invacare Mag-Spider Web	Polyurethane Grey Airless, Vee Tread, 24"x1 1/8"
EJA	Everest and Jennings Airless	Solid Grey Rubber old style, 24"x 3/4"
ER	Essem Rubber Caster	Solid Rubber 7 3/4" x 1 1/8"
PU	Unknown	Orange Polyurethane 7 3/4" x 1 1/8"

TYPICAL CORNERING FORCE VS. SLIP ANGLE CURVES

As stated earlier, the lateral cornering force is the primary force of interest for an examination of wheelchair motion. Because this force will be the most important force present when the equations of wheelchair motion are formulated, a knowledge of its magnitude is desirable.

Figure 3-2 shows a typical plot of cornering force as a

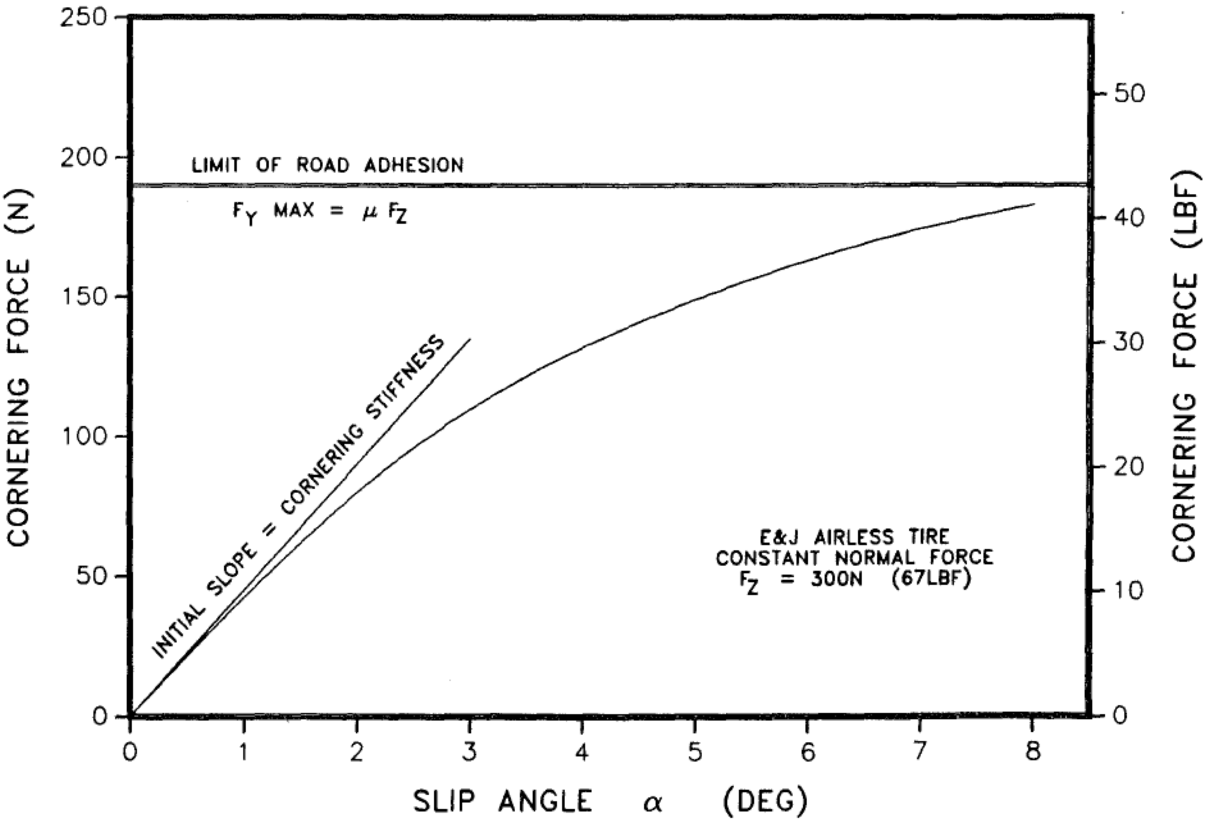

Figure 3-2 Typical Cornering Force Versus Slip Angle Curve at Constant Normal Force

function of slip angle for a single wheelchair tire. [2.6] For small angles of side slip, the cornering force increases linearly with an increase in slip angle. For slip angles greater than approximately two degrees, the cornering force begins to increase at a lower rate, and it reaches a maximum value when the tire begins to slide laterally. At the point where sliding begins, the peak cornering force is determined by the product ($\mu \times F_z$), where μ is referred to as the peak coefficient of road adhesion. The peak coefficient of road adhesion may be as much as 25% higher than the sliding coefficient of road adhesion which governs the cornering force after sliding has begun. [2.1]

As a basis for comparing different tires, the parameter 'cornering stiffness' is often used. Cornering stiffness is defined as the initial slope of the cornering force versus slip angle curve as shown in Figure 3-2, and is usually denoted by the symbol C_α. Thus, for the linear region of the cornering force versus slip angle curve, the cornering force F_y is given by:

$$F_y = C_\alpha \alpha \tag{3-1}$$

Smaller cornering stiffness values correspond to lower cornering forces for any given slip angle.

THE EFFECT OF NORMAL FORCE

The primary variable affecting cornering stiffness is the vertical load, F_z, on the tire. Typical results showing the effect of normal load on cornering force for an automobile tire are shown in Figure 3-3. [2.8] This figure is presented to illustrate the relationship between vertical load and cornering force, as well as to provide some means of comparing results for wheelchair tires to those found in the literature for other tire types. As one would expect, the cornering force generally increases as the normal load is increased. However, the relationship between cornering force and vertical load is nonlinear. It is important to note that in Figure 3-3 and throughout this text the term normal load (or vertical load) refers to the normal force F_z acting on the tire at the tire-road interface, and not to the laden weight of the vehicle.

Using the treadmill and test cart curves such as the one shown in Figure 3-3 were obtained for the seven different wheelchair tires. Each tire was rotated to fixed slip angles ranging from one to eight degrees with respect to the motion of the treadmill belt. In each case, this was repeated for six different known weights of the test cart resulting in 48 data points for each tire. These weights ranged from 365 Newtons (82 lbf) to 1010 Newtons (227 lbf) with an increment between loads of 129 N (29 lbf). The weight was varied by using steel blocks of known mass which could be placed in a wooden holder mounted over the test cart axle. For each load, the force necessary to keep the test cart at a fixed angle α was measured by the load cell. The cornering force, F_y, and the corresponding normal force, F_z acting at the tire-belt interface were then

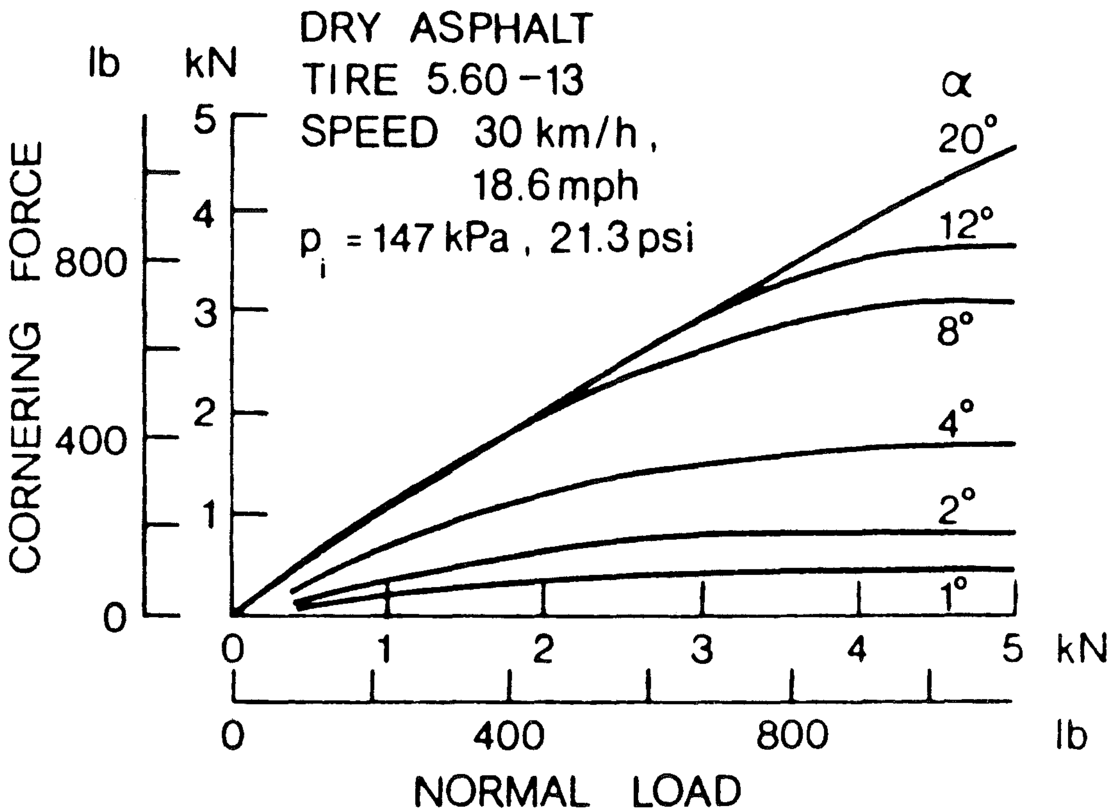

Figure 3-3 Typical Cornering Force Versus Normal Force Curves for Automobile Tires

calculated using the equations given in Appendix A.

The results for this series of tests are presented in Figures 3-4a through 3-4g. Note on each figure that eight curves are given corresponding to eight constant slip angles, α. In each case the belt speed is .75m/s (1.7mph), and the camber and toe angles are zero. It is very notable that all of the tires exhibit characteristic curves similar to the one shown in Figure 3-3 for automobile tires. This is encouraging because up to this point it has only been assumed that wheelchair tires exhibit tire force properties similar to those that have been described from the automobile literature.

Observe that each cornering force vs. normal force curve has six data points corresponding to the six known loads which were placed on the test cart. Note also that as the slip angle increases from one to eight degrees, the value of F_z for any one of the six data points (known test cart loads) increases slightly. This is shown on Figure 3-4a, where a series of slanting dashed lines has been placed through data points associated with a constant load on the test cart. It can be seen that even though the load on the test cart is constant along each of the slanting lines, the normal force F_z acting on the tire increases linearly as the slip angle is increased. This is due to the lateral load transfer caused by the tendency of the cart to rotate which was discussed in the first part of this chapter. The reason for the linear increase in F_z is discussed

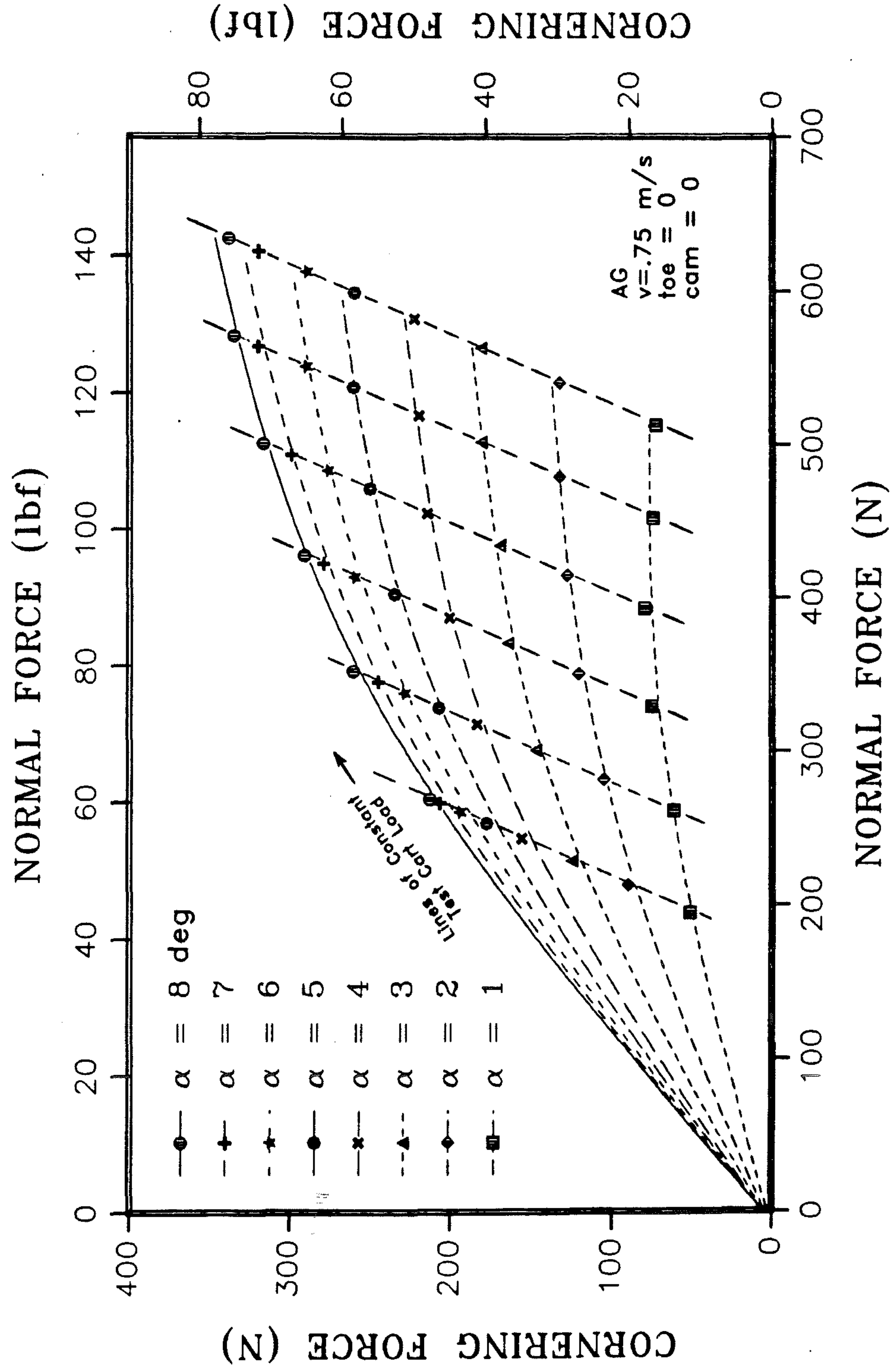

Figure 3-4a Cornering Force vs. Normal Force Curves at Constant Slip Angle (tire type AG)

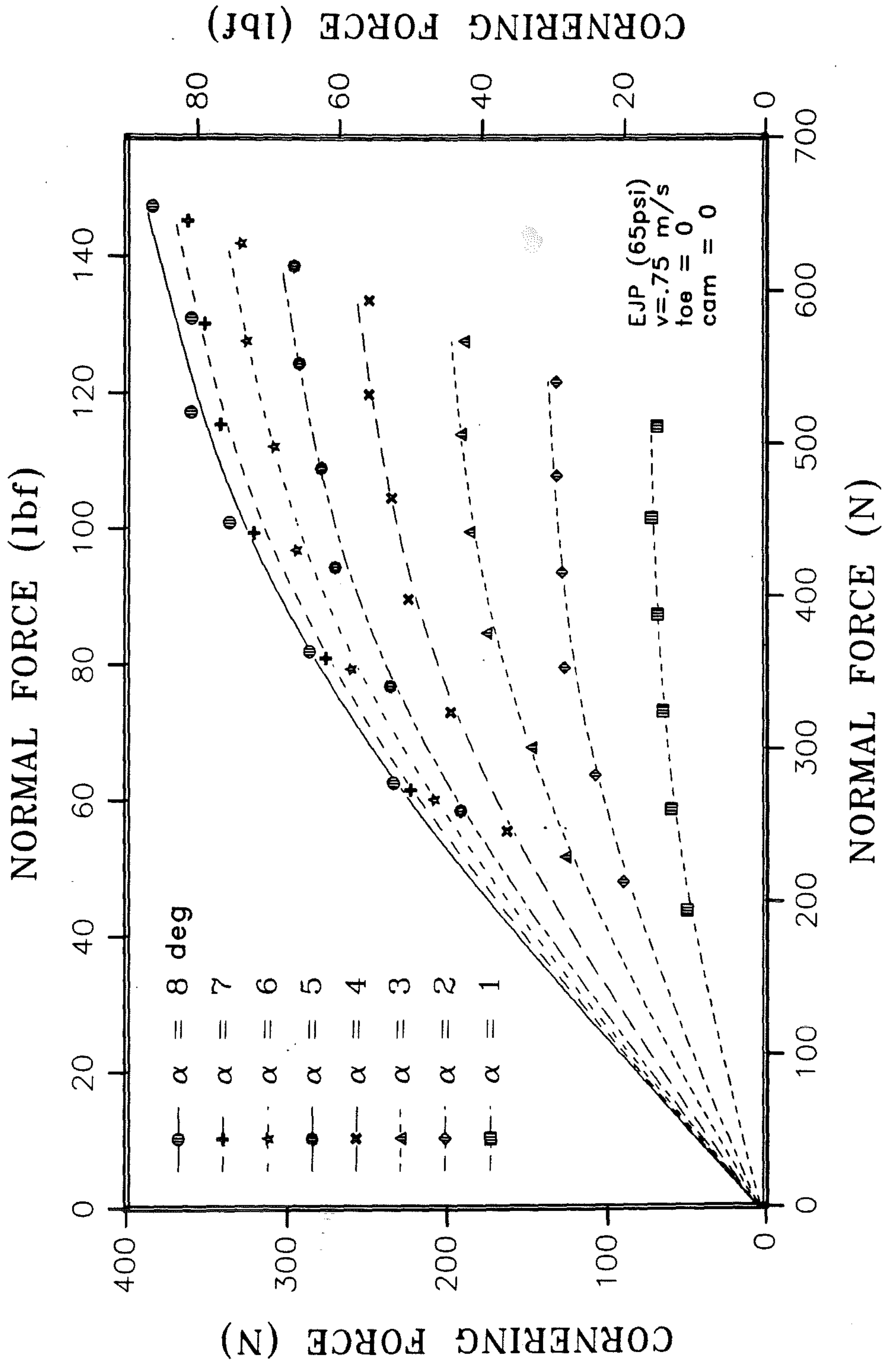

Figure 3-4b Cornering Force vs. Normal Force Curves at Constant Slip Angle (tire type EJP)

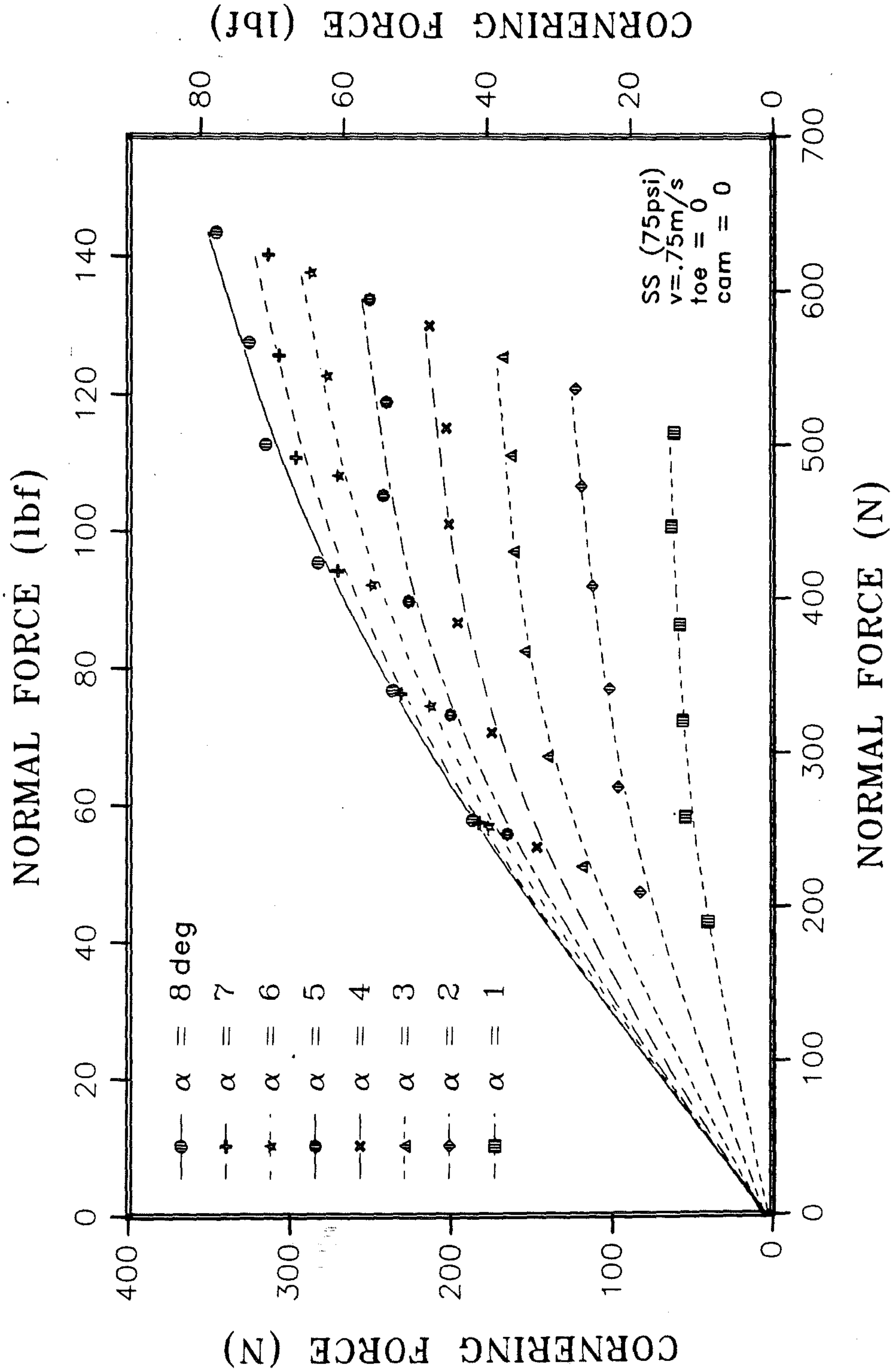

Figure 3-4c Cornering Force vs. Normal Force Curves at Constant Slip Angle (tire type SS)

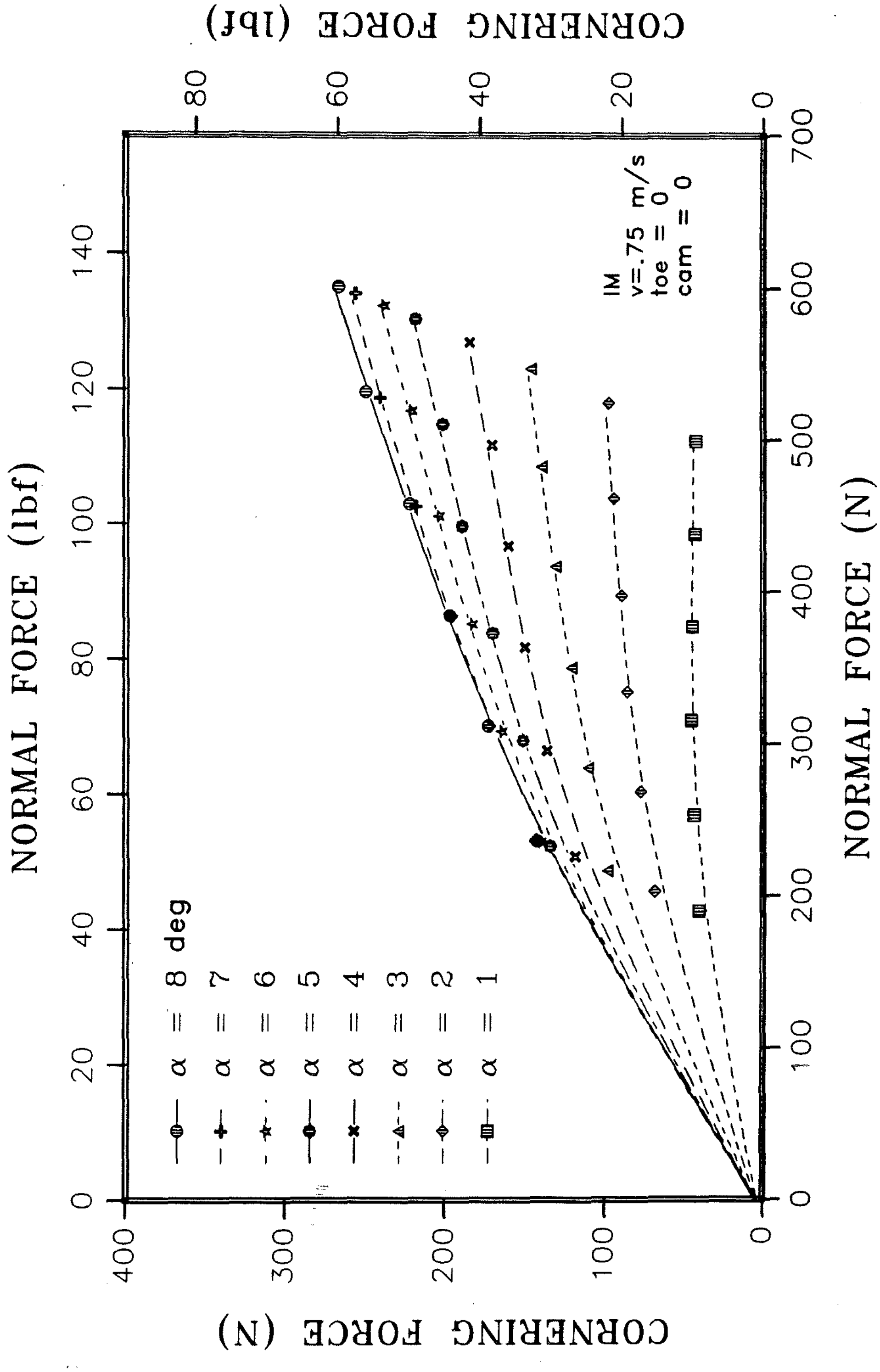

Figure 3-4d Cornering Force vs. Normal Force Curves at Constant Slip Angle (tire type IM)

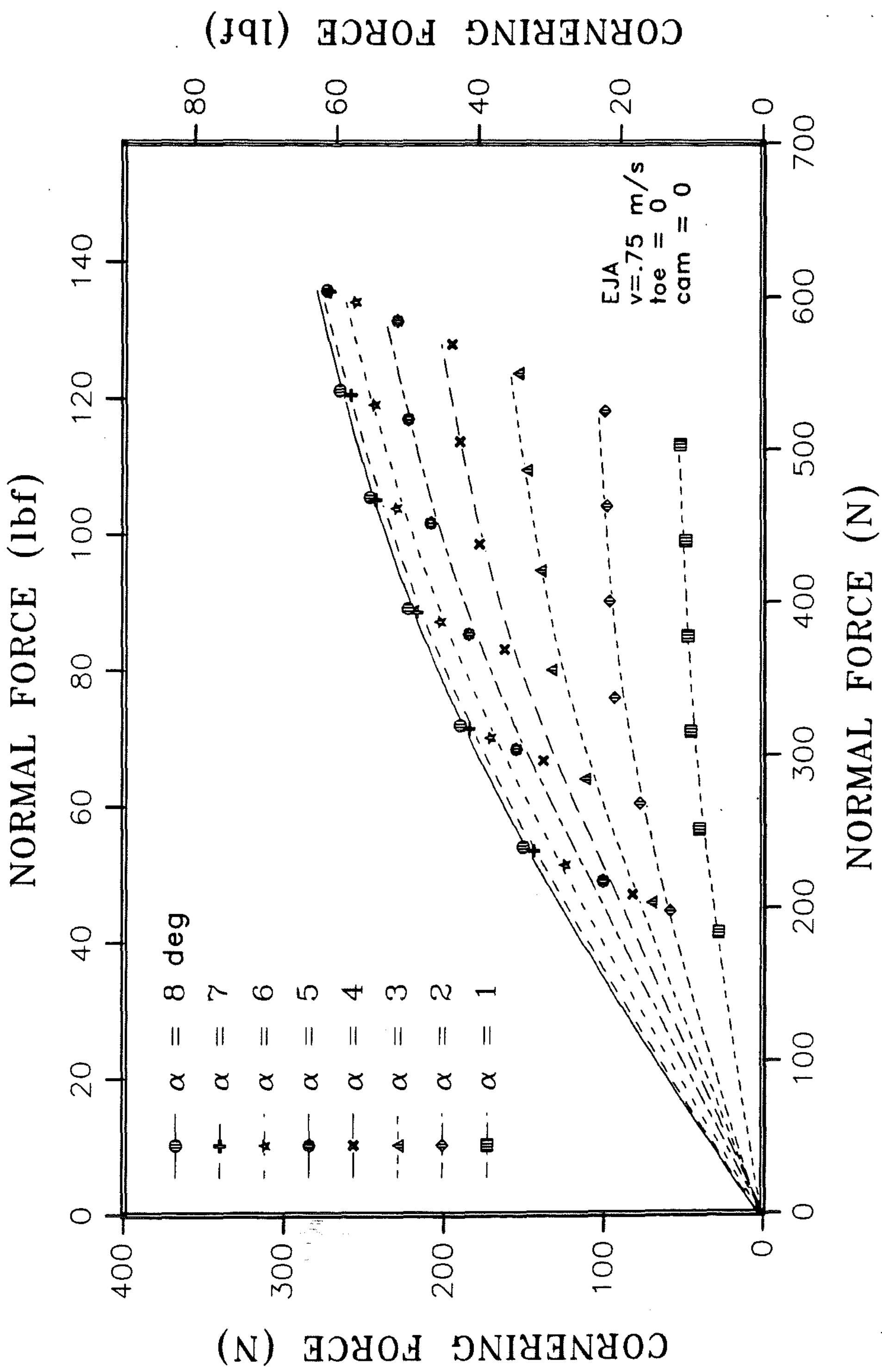

Figure 3-4e Cornering Force vs. Normal Force Curves at Constant Slip Angle (tire type EJA)

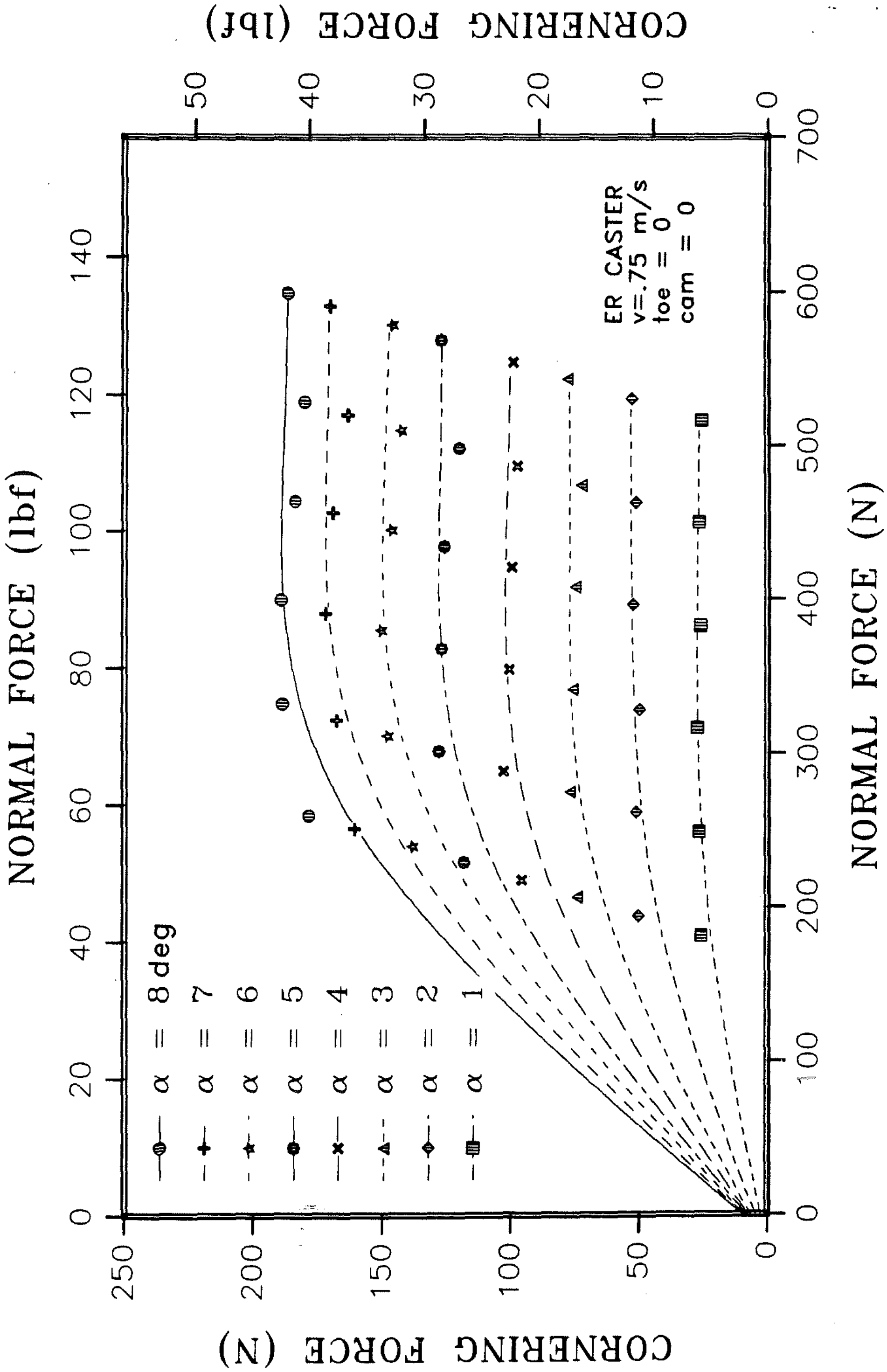

Figure 3-4f Cornering Force vs. Normal Force Curves at Constant Slip Angle (ER caster)

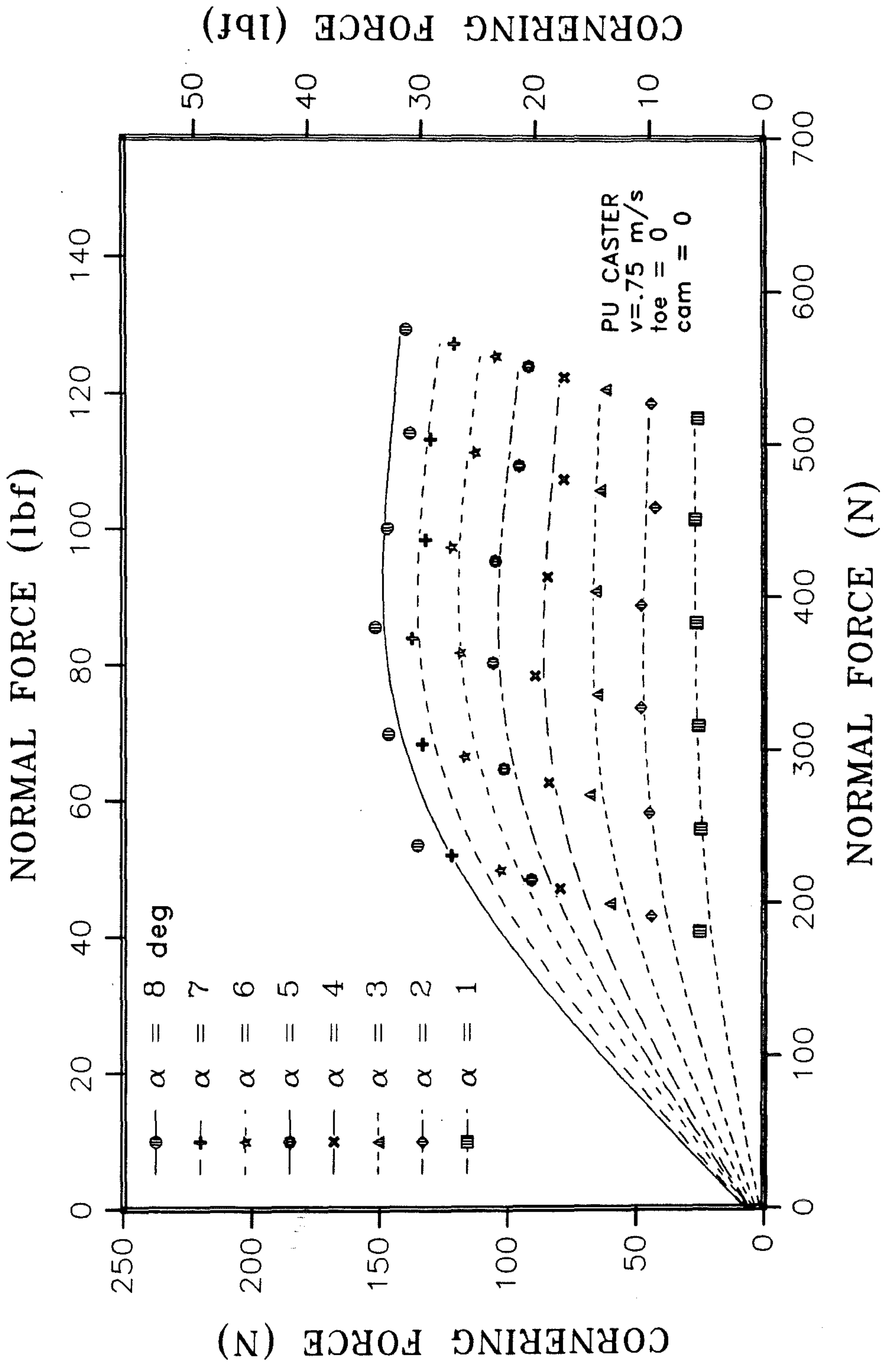

Figure 3-4g Cornering Force vs. Normal Force Curves at Constant Slip Angle (PU caster)

in Appendix A where the equations for calculating F_y and F_z are given. The point here is that F_z cannot be assumed constant simply because the load on the test cart has not changed.

Because the normal force F_z is different for each data point collected using the test cart, it is not possible to directly use the raw data to construct curves such as the one shown in Figure 3-2. The reader may question how the curve in Figure 3-2 was obtained since it shows cornering force versus slip angle for a constant normal force F_z on an Everest and Jennings airless wheelchair tire. A simple method by which the raw data shown in Figures 3-4a through 3-4g can be reduced to cornering force versus slip angle curves like the one in Figure 3-2 is presented in Chapter 4.. Doing this allows for the determination of cornering stiffness for each tire and for an easier comparison of different tires.

A close examination of the figures shows that the tires are arranged approximately from highest to lowest cornering force magnitude for any given slip angle and normal force. For example, the AG tires (Figure 3-4a) experience a higher cornering force than the SS tires (Figure 3-4c) for a particular value of α and F_z. Thus one would expect the AG tires to have a higher value of cornering stiffness than the SS tires. In later chapters, the effect of cornering stiffness on the directional control of rear caster wheelchairs will be considered.

The scales on the axes are the same for each of

Figures 3-4a through 3-4g except for the last two graphs which are for the two caster wheels (ER) and (PU). Note that although the caster wheel curves appear to exhibit the same trend as the curves for the other tires, the values for cornering force are almost at their maximum even for the lowest values of F_z that could be obtained with the test cart. In fact, at the higher slip angle values it can be seen that the caster wheel curves begin to decrease slightly with increasing normal force. This decrease indicates the onset of slipping and a corresponding reduction in the road adhesion capability of the tires. This is in contrast to the curves for the five 24 inch wheels where a maximum value of cornering force was never reached.

THE EFFECT OF FORWARD SPEED.

Now that the basic nature of cornering force has been described and several typical curves have been shown, it is interesting to examine some of the factors other than normal load which might have an effect on the cornering force magnitude. It was stated at the beginning of this chapter that several treadmill tests were conducted before the test cart was modified so that single tires rather than tire pairs could be examined. This section and the next will present results from the "two wheel" tests which demonstrate the effects of speed and inflation pressure on lateral tire force. These tests were quite conclusive and were in very good agreement with the literature. As a result, for these two series of tests only, the testing was not repeated with the modified "single wheel" test cart.

Figures 3-5a through 3-5e show the effect of varying the treadmill belt speed on the total lateral force exerted on a pair of fixed wheels which have been rotated to some angle α. Each of the five 24 inch tires (AG,SS,EJP,IM, and EJA) were tested at three different belt speeds. These speeds were .42, .83, and 1.4 meters per second. A constant load of 534N (120lbf) was placed on the test cart for each test speed, and the total lateral force per tire pair was measured using the load cell. As before, this was done for slip angles ranging from one to eight degrees. The total weight of 120 pounds was chosen because it is a reasonable value for the total weight carried by the main wheels of a wheelchair belonging to a user who weighs 130 - 170 pounds. Again it is noted that for these tests two wheels were placed on the test cart, and thus only the total lateral force on each pair of tires is plotted. Other than this, the varying speed curves are very similar to the slip angle versus cornering force curve shown in Figure 3-2. Although the normal force F_z and the cornering force F_y on each tire alone cannot be obtained from this data, the results do show a definite trend with regard to the effect of forward speed on cornering force.

Figures 3-5a through 3-5e clearly show that the effect of speed on lateral tire force for any given slip angle is almost negligible. This is somewhat surprising because intuitively one might expect the cornering force to increase

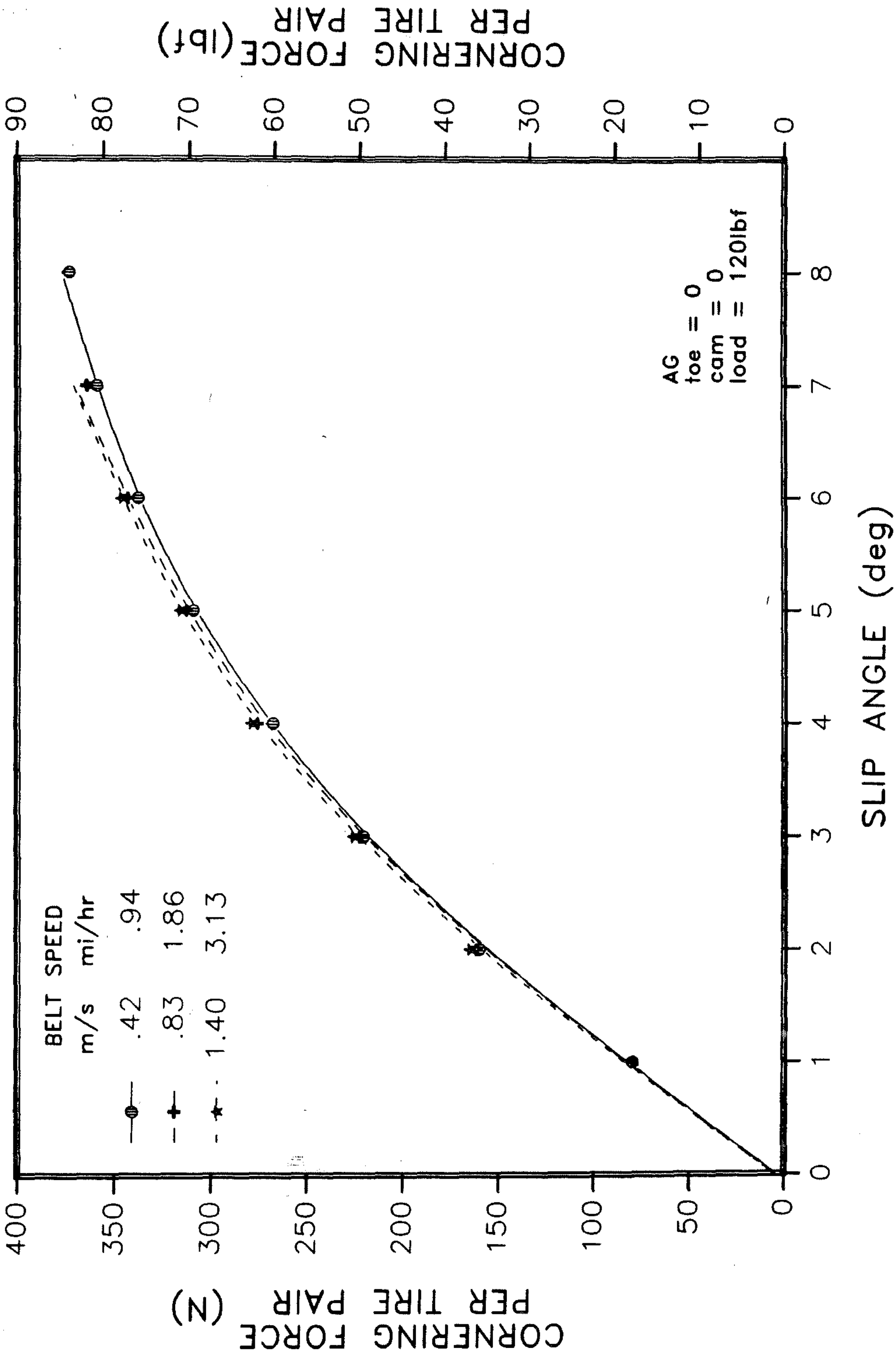

Figure 3-5a Cornering Force Per Tire Pair vs. Slip Angle, Effect of Belt Speed (AG tires)

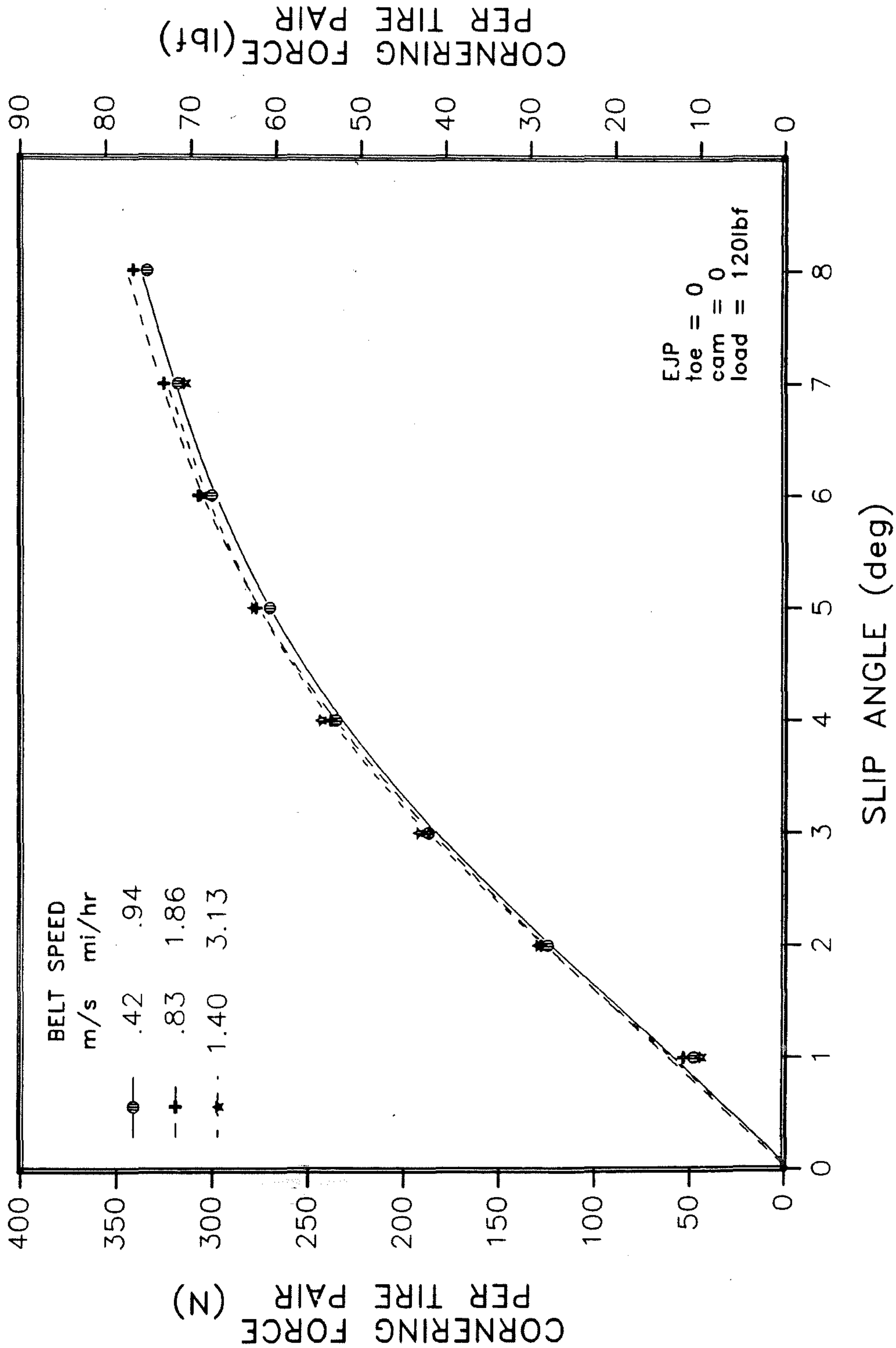

Figure 3-5b Cornering Force Per Tire Pair vs. Slip Angle, Effect of Belt Speed (EJP tires)

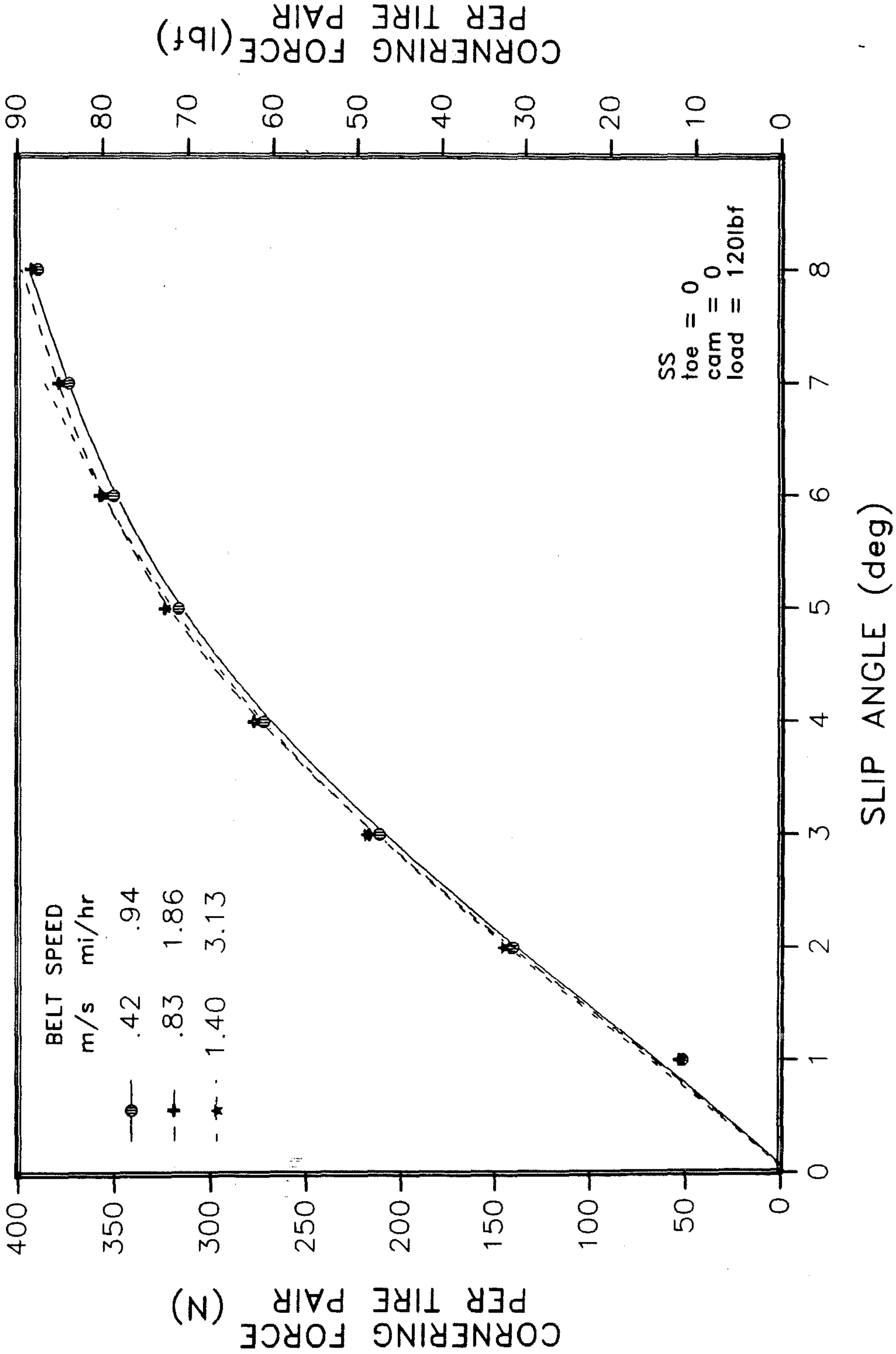

Figure 3-5c Cornering Force Per Tire Pair vs. Slip Angle, Effect of Belt Speed (SS tires)

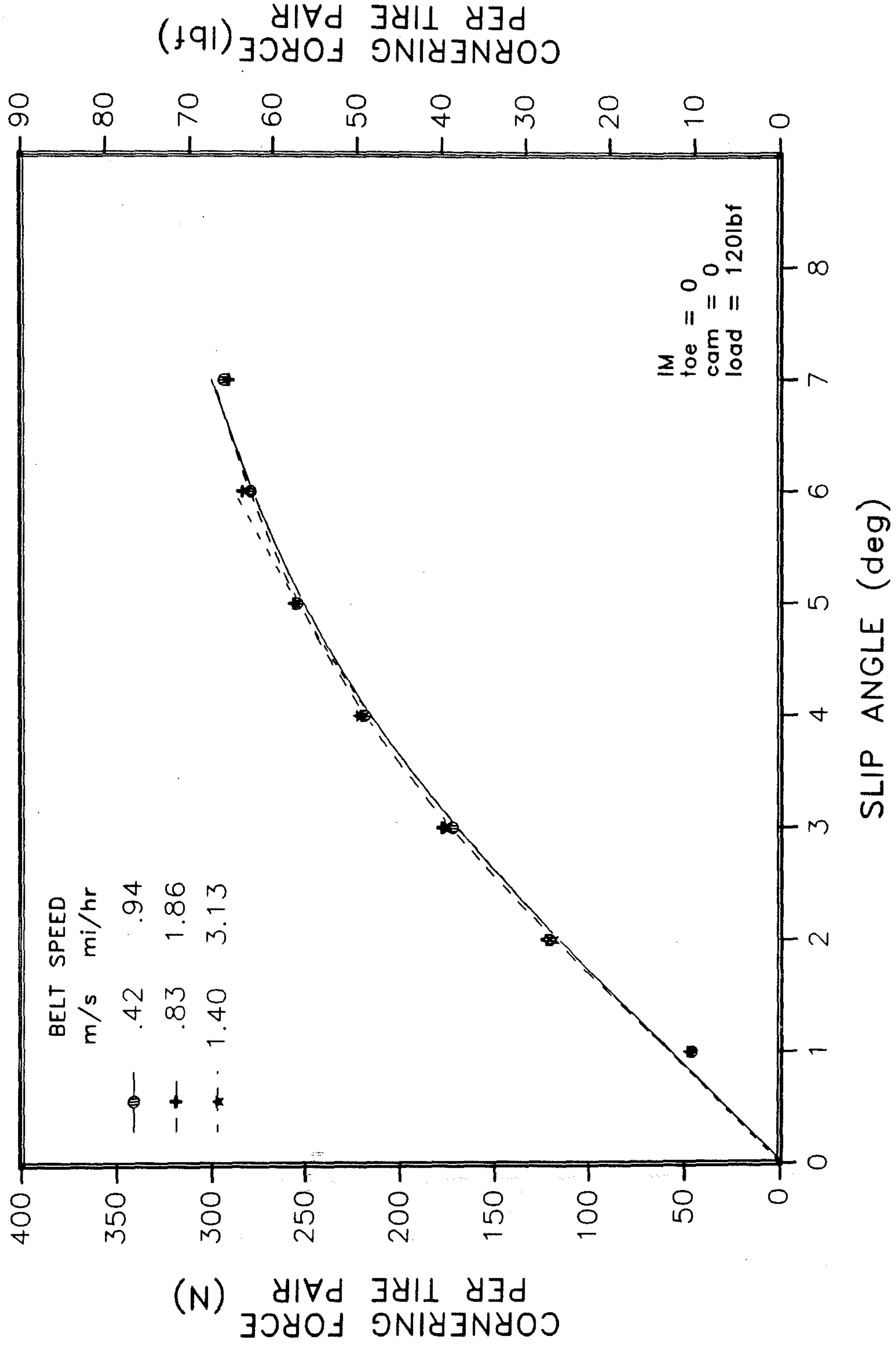

Figure 3-5d Cornering Force Per Tire Pair vs. Slip Angle, Effect of Belt Speed (IM tires)

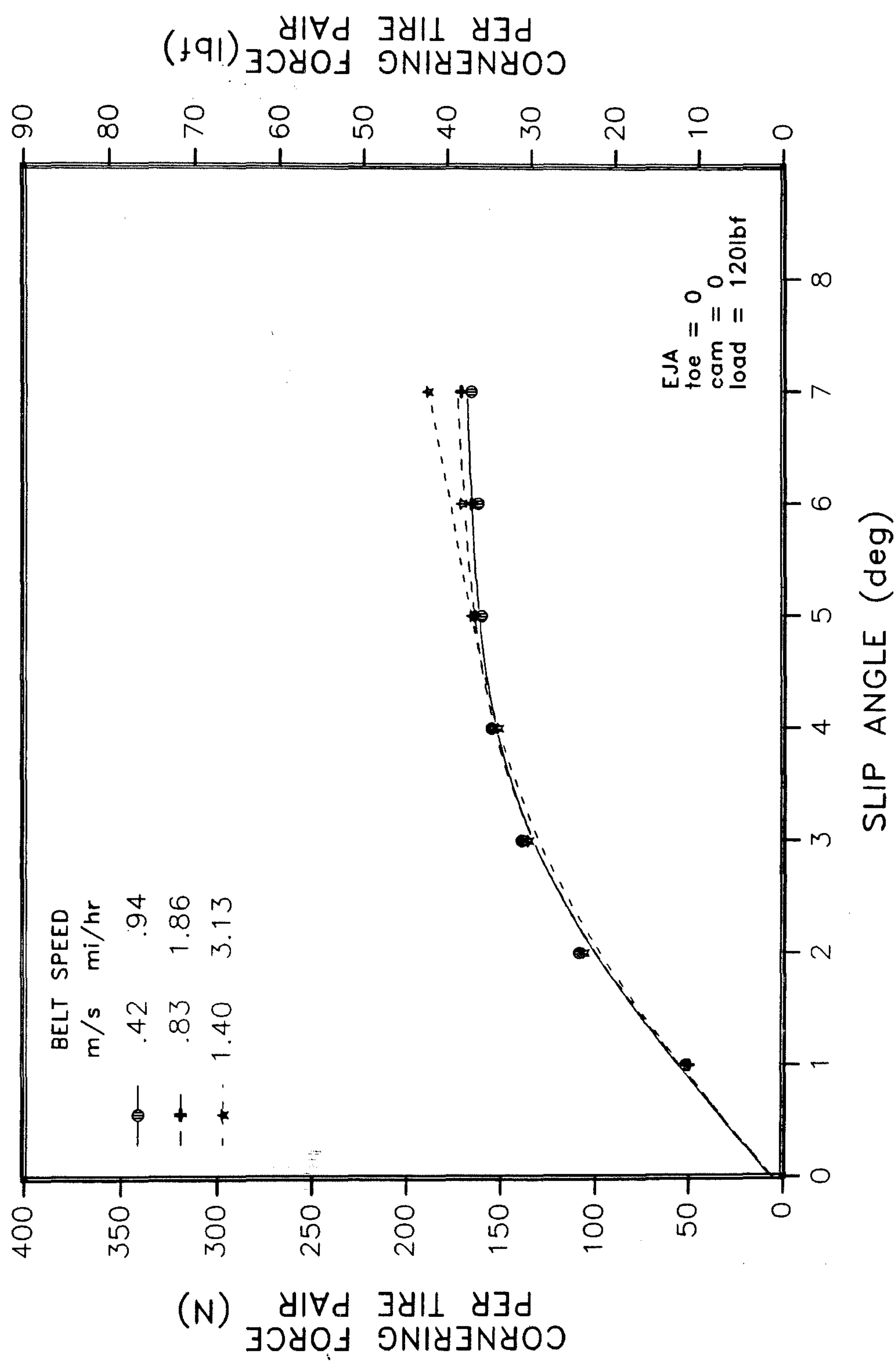

Figure 3-5e Cornering Force Per Tire Pair vs. Slip Angle, Effect of Belt Speed (EJA tires)

as forward speed increases. However, this result is consistent with similar findings for both automobile and aircraft tires. Results of investigations to determine the effect of test speed on automobile tire lateral forces have shown that approximately a tenfold increase in test speed is required to obtain only an 8 to 9 percent increase in lateral force for a given slip angle. [3.2] Similar studies relating to aircraft tires have shown that cornering force is almost entirely independent of rolling velocity even for speeds approaching 100 miles per hour (160 km/hr). [3.3]

The reason for these results is that the development of a lateral force by a rolling tire is essentially controlled by the elastic properties of the tire and the manner in which the contact area is laid on the road. Thus the speed of rolling should have little or no effect on the value of lateral force. [2.3]

In light of the fact that the eventual goal of studying tire forces is to use the data collected as part of an investigation of wheelchair directional stability, the independence of lateral tire force and forward speed is a very useful result. This will make the task of predicting tire forces for any given state of wheelchair motion much easier.

THE EFFECT OF INFLATION PRESSURE

The two pneumatic tire types (SS and EJP) were tested to investigate the effect of inflation pressure on cornering force. Turning to the literature for expected trends is somewhat less useful in this case as different authors seem to disagree. Taborek states that higher inflation pressures result in an increase in tire side-wall stiffness which in turn leads to an increase in cornering stiffness. [2.6] However, Ellis argues that overinflation does not affect cornering force because any increase in sidewall stiffness is offset by a corresponding decrease in the size of the contact region with the ground. [2.3] Most authors do seem to agree however that changes in inflation pressure have at the most only moderate effects on tire lateral force.

Figures 3-6a and 3-6b show the effect of varied inflation pressure on the total lateral force exerted on a pair of pneumatic wheelchair tires. As was the case for the varied belt speed tests, these results are for the test cart with two wheels. Again the total weight of the test cart is a constant 120 lbf for each curve shown. These figures indicate that for moderate changes in inflation pressure, there is virtually no change in the total cornering force per tire pair. For pressures which are much lower than the rated pressure (-50% or more), a slight decrease in cornering force is apparent at large slip angles. For small slip angles (less than 3 degrees) changes in cornering force are less obvious. Because no definitive effect of inflation pressure on cornering force was observed for the pneumatic tires tested, especially for small slip angles and moderate changes in pressure, inflation pressure was disregarded as an important wheelchair tire force variable.

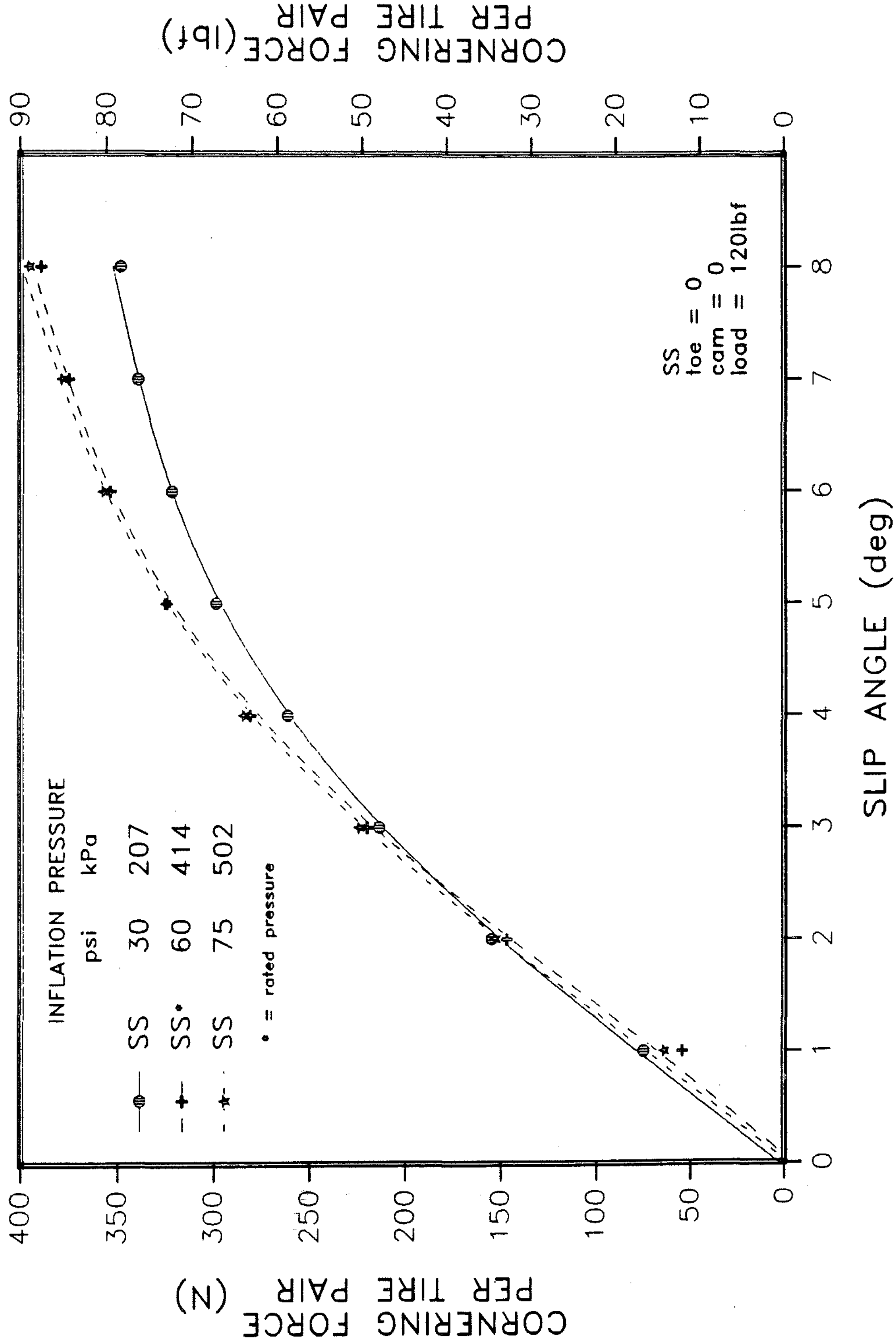

Figure 3-6a Cornering Force Per Tire Pair vs. Slip Angle, Effect of Inflation Pressure (SS tires)

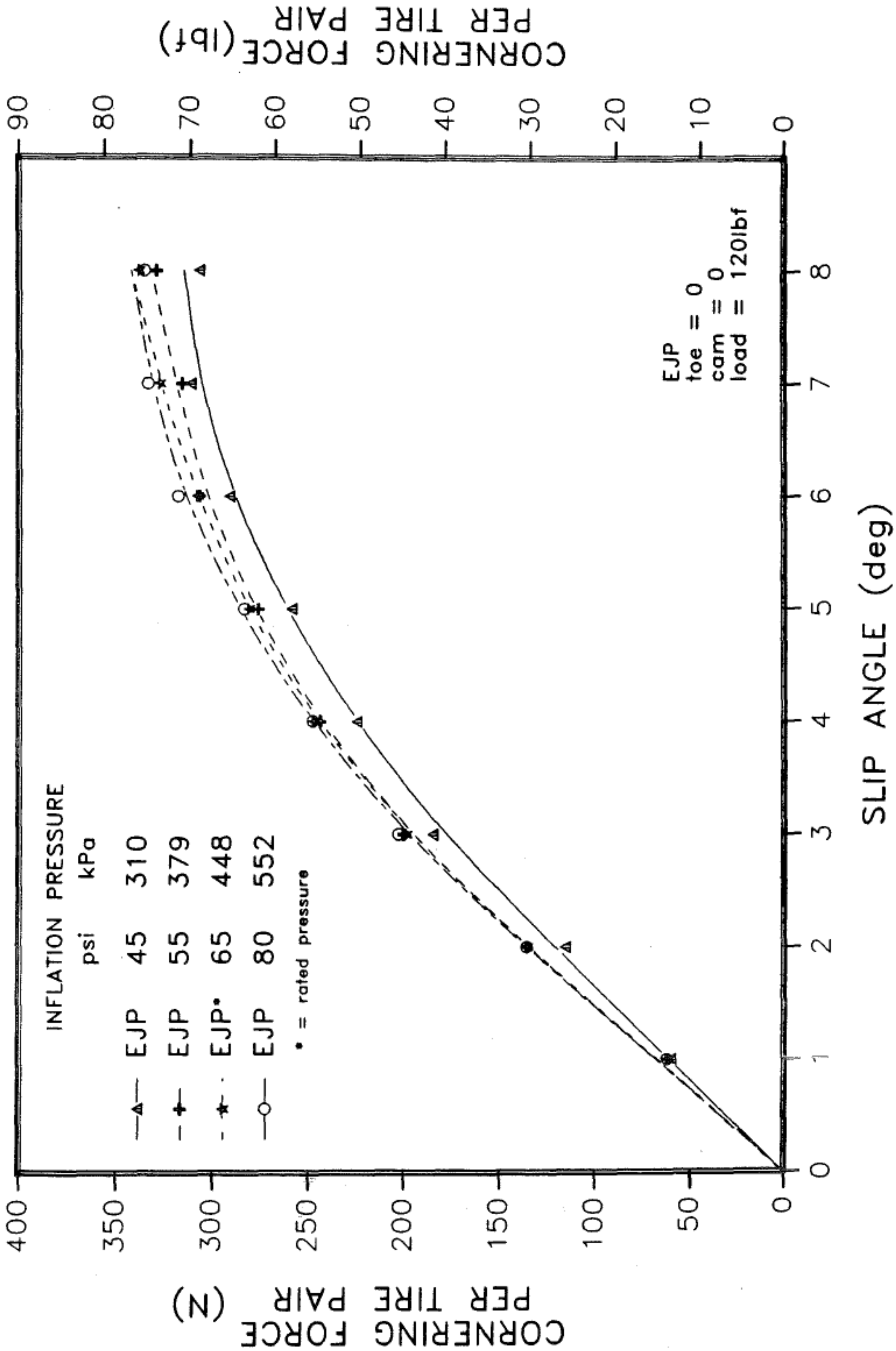

Figure 3-6b Cornering Force Per Tire Pair vs. Slip Angle, Effect of Inflation Pressure (EJP tires)

EFFECT OF CAMBER ANGLE

The basic concept of the cambered wheel was described in Chapter 2. A rolling wheel that is inclined at some angle with respect to the X-Z plane (see Figure 2-1) develops a lateral road force which acts in the same direction as the direction of inclination. Camber force was measured for the five 24 inch wheel chair tires described in Table 3-1. This was done in a manner similar to that used for the cornering force tests already discussed. The tires were tested individually using the single wheel test cart and vertical cable apparatus already described. This was done for each tire adjusted to camber angles of +2, +5, and +8 degrees.

Note that a positive camber angle for the test cart corresponds to tilting the single left wheel inward by a specified number of degrees. This corresponds to what is normally the case for wheelchair users. For each camber angle, the total lateral force developed was measured for the same six test cart weights given earlier. (365N to 1010N at 129N increments) For the camber tests however, the longitudinal axis of the test cart was kept parallel to the motion of the treadmill belt. In other words, the test cart was positioned to maintain a zero degree slip angle at the tire-belt interface. Recall that camber force is considered independent of cornering force which results from nonzero slip angles.

Figures 3-7a to 3-7e show camber force as a function of

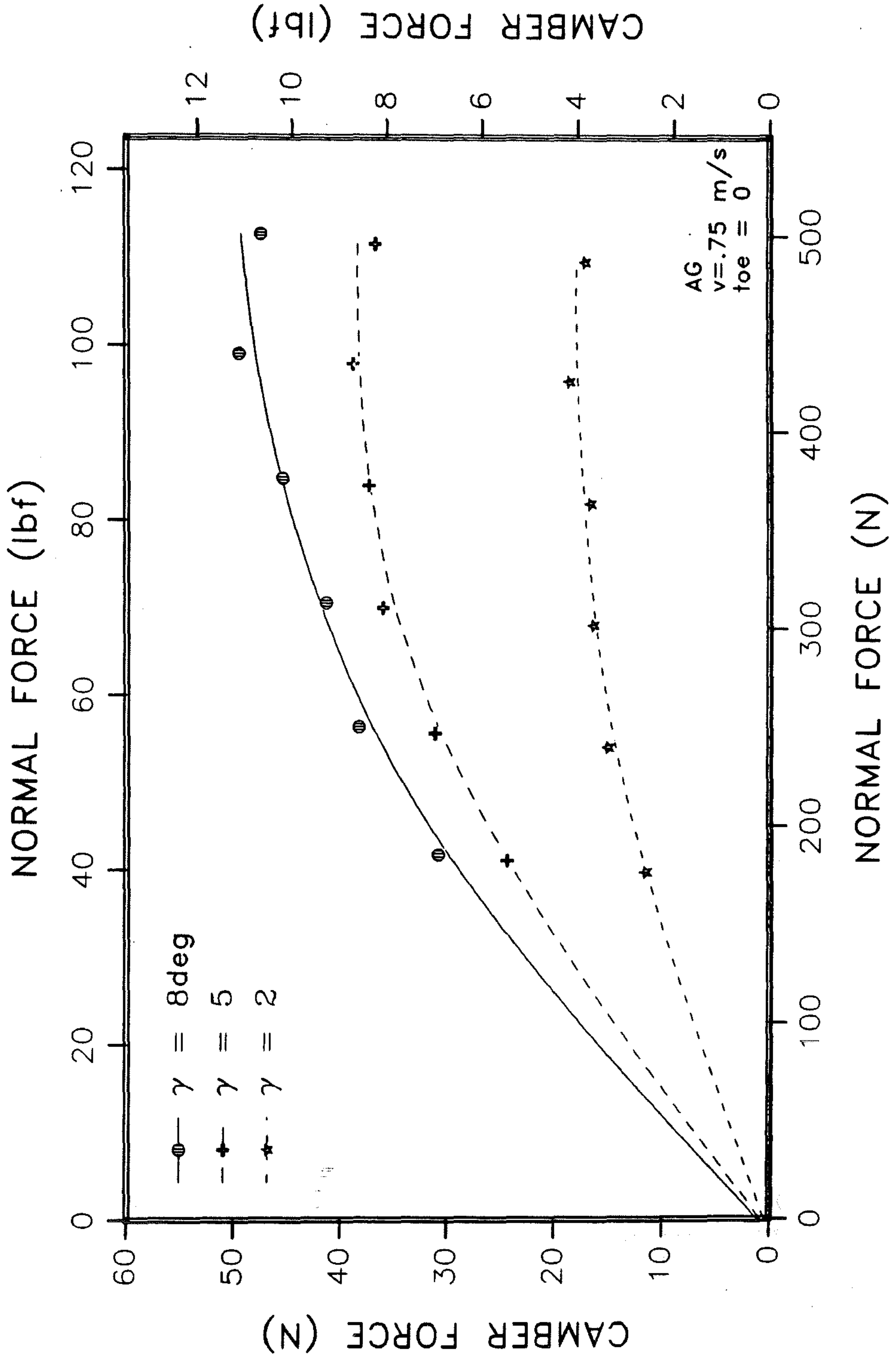

Figure 3-7a Camber Force vs. Normal Force (AG tire)

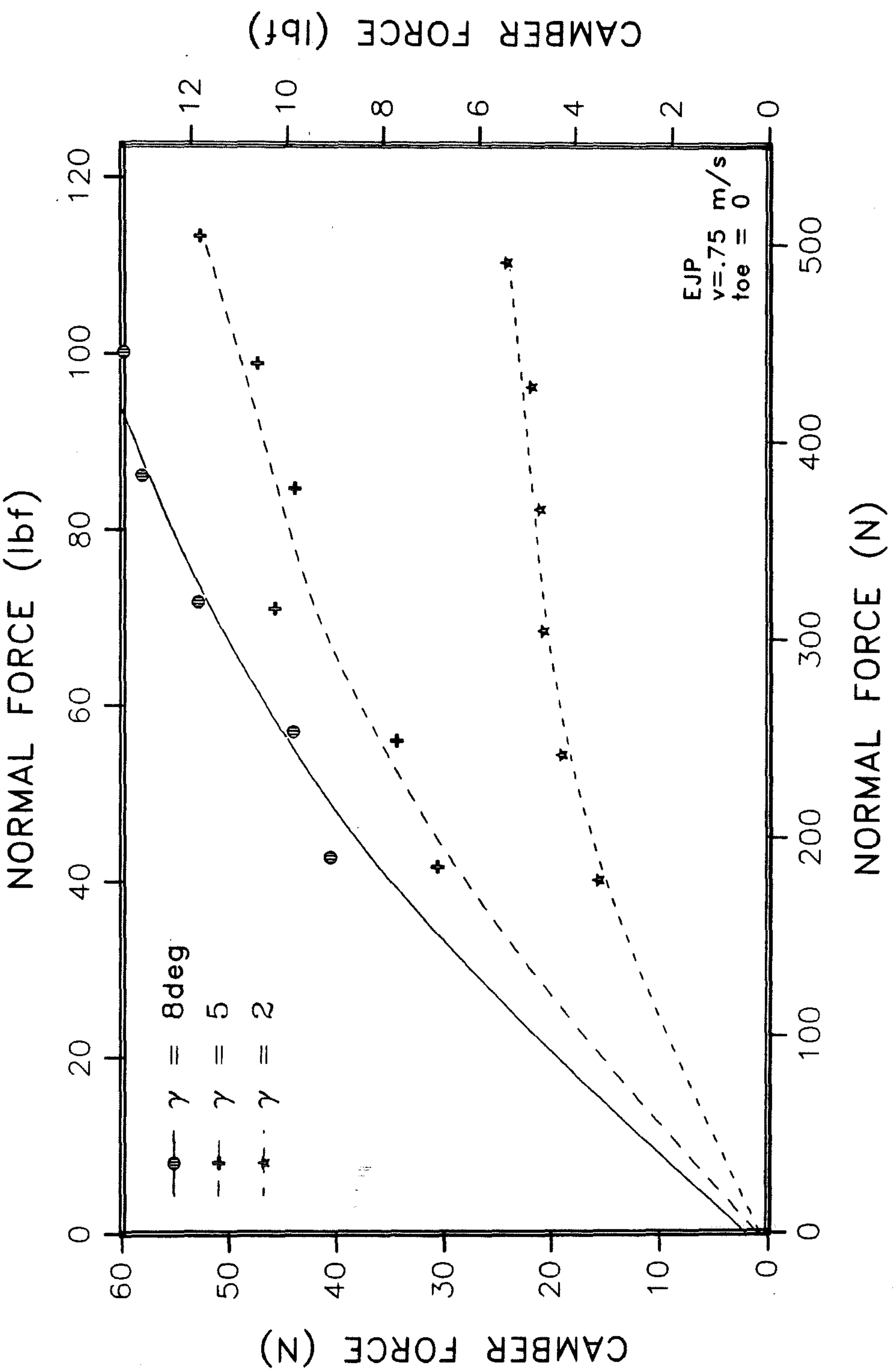

Figure 3-7b Camber Force vs. Normal Force (EJP tire)

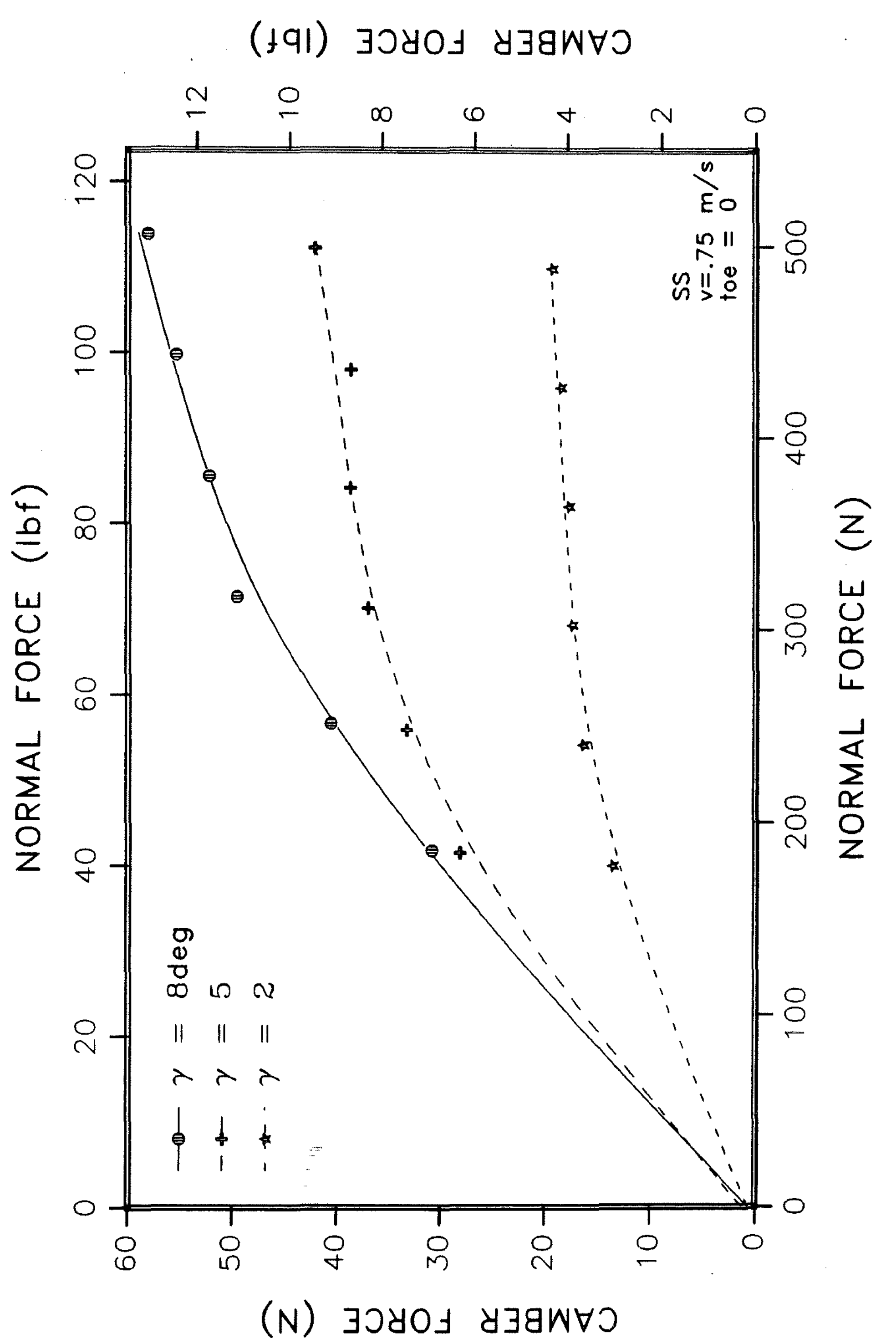

Figure 3-7c Camber Force vs. Normal Force (SS tire)

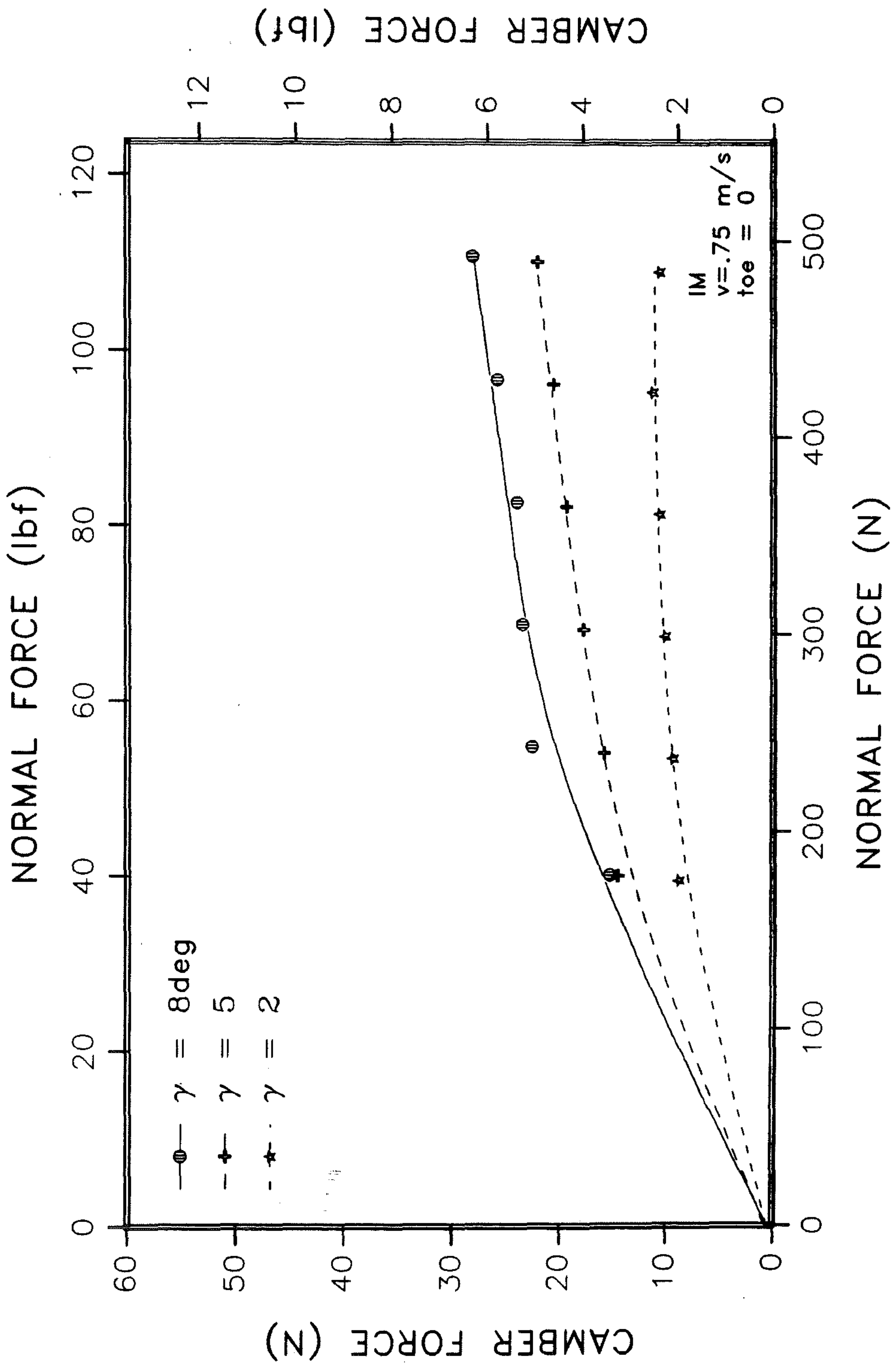

Figure 3-7d Camber Force vs. Normal Force (IM tire)

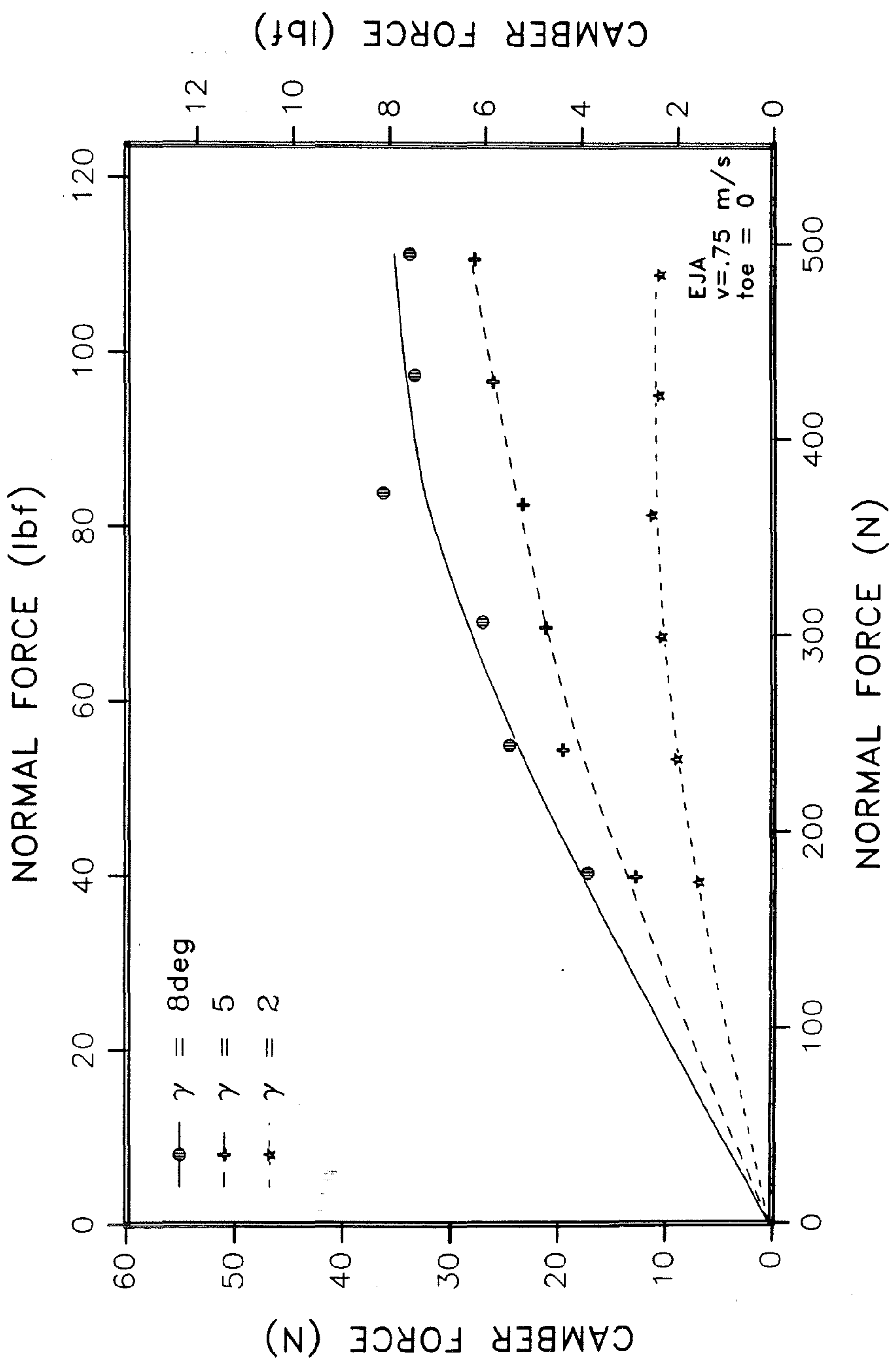

Figure 3-7e Camber Force vs. Normal Force (EJA tire)

normal force for each of the five 24 inch tires at the three camber angles tested. The F_z values for each data point were calculated using the single wheel test cart equations in Appendix A. Not surprisingly, the magnitude of the camber force is relatively small when compared to cornering force. For example, the AG tires develop a maximum lateral camber force of about 50N (11 lbf) at a camber angle of 8 degrees and a normal force F_z of 500N (110 lbf). However, at a slip angle of 8 degrees and normal force of 500N the same tires experience a lateral cornering force of approximately 300N (67 lbf) which is six times larger.

Studies of automobile and aircraft tires have shown that camber force is generally about one-fifth the value of cornering force for an equivalent slip angle and normal force. [2.2] It is shown in Chapter 4 that for the wheelchair tires tested, camber force values are found to range from 1/5 to 1/8 the value of cornering force

ROLLING RESISTANCE OF WHEELCHAIR TIRES

The remaining tire force which has not been considered is the longitudinal force F_x. In Chapter 2 the concept of rolling resistance was discussed in its simplest form. There it was stated that rolling resistance could be treated simply as a force for the purposes of investigating wheelchair motion. Rolling resistance data was collected for six of the seven wheelchair tires listed in Table 3-1. Because rolling resistance was measured using tire pairs, while only one of the PU type casters was available, rolling resistance data was not collected for this tire.

Fortunately rolling resistance on the treadmill surface is fairly easy to measure. To do this the load cell is mounted at the forward end of the test cart instead of at the left wheel axle as shown in Figure 3-1. The load cell is linked to the forward support rod of the test cart, and it measures the force required to restrain the cart as the treadmill belt moves under it at constant velocity. As was the case for camber force, this was done with the test cart parallel to the direction of belt motion so that the slip angles at each tire were both zero. When this is done, the total longitudinal force F_x exerted on the two wheels is approximately equal to the restraining force measured by the load cell. The word approximately is used because as it turns out, some small corrections must be made to account for moments and the fact that the center of gravity of the test cart is not directly over its rear axle.

Figure 3-8 shows the rolling resistance data for the wheelchair tires tested as a function of normal force F_z. In keeping with the tire force and axis system described in Chapter 2, the rolling resistance force is labeled as longitudinal force F_x. Again, because propelling and braking forces are being neglected for this analysis, the longitudinal force and rolling resistance force can be regarded as identical.

Figure 3-8 indicates also that the increase in longitudinal force varies nearly linearly with an increase in

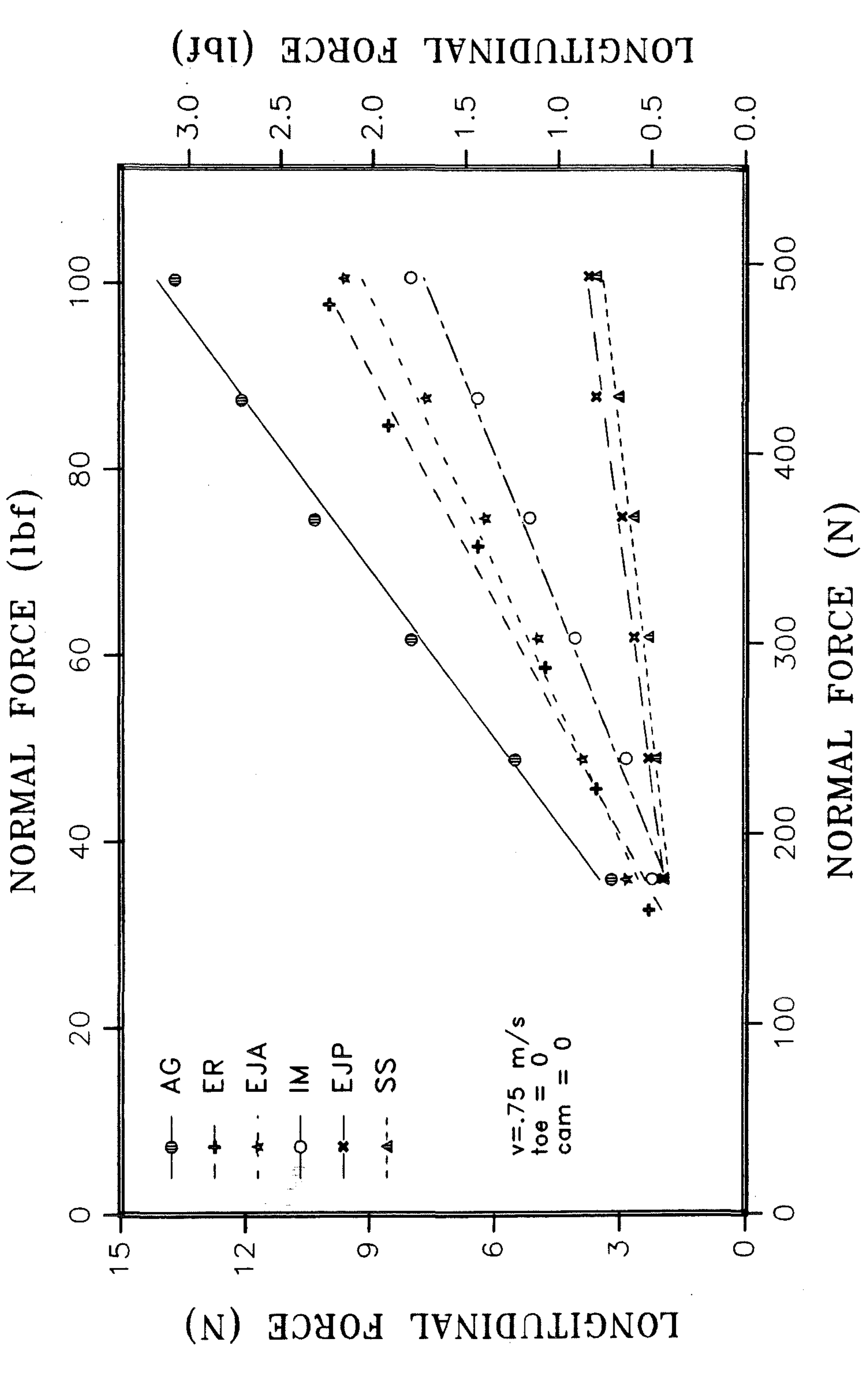

Figure 3-8 Longitudinal Force vs. Normal Force for Six Different Tires

normal force F_z. The ratio of longitudinal rolling resistance force to normal force is generally defined as the coefficient of rolling resistance f_r. Referring back to equation (2-1) and the diagram of the rolling wheel that was presented there, one sees that f_r is also equal to the ratio of normal force offset, ε, to axle height r. Putting this all together and remembering that rolling resistance force $F_r = F_x$, gives:

$$f_r = \varepsilon / r = F_r/F_z = F_x/F_z \tag{3-2}$$

In Figure 3-8, f_r is simply the slope of the longitudinal force vs. normal force curve. The coefficients of rolling resistance as found by performing a least squares fit on the data for the six wheelchair tires tested are given in Table 3-2.

TABLE 3-2: COEFFICIENTS OF ROLLING RESISTANCE

Tire	f_r
AG	.034
SS	.0050
EJP	.0058
IM	.018
EJA	.021
ER	.025

It is clear from Figure 3-8 that the solid rubber tires (AG, ER, and EJA) have considerably higher coefficients of rolling resistance than the polyurethane tire (IM) or the two pneumatic tires (EJP and SS). This is consistent with both theoretical and experimental results presented by Kauzlarich and Thacker. [2.9,2.10]

A remaining question with regard to rolling resistance concerns the effect of a nonzero slip angle. Various studies have shown that the effect of slip angle on the total longitudinal force in the wheel plane is very slight even for angles as high as 10 degrees. [2.8] This might be confusing because it may seem that a tire which is forced to roll in a direction which is not parallel to its wheel plane will experience a greatly increased rolling resistance. However, recall that a wheel which rolls at a slip angle α experiences a cornering force F_y and a longitudinal force F_x. It has already been shown that cornering force increases with increasing slip angle. Figure 2-1 showed the forces F_x and F_y acting on a wheel rolling at a fixed slip angle. Rolling resistance has been defined as the total longitudinal force in the wheel plane. This is vastly different than defining rolling resistance as the resultant force in the direction of wheel motion, because the direction of wheel motion does not lie in the wheel plane if the slip angle is not zero. Examining Figure 2-1 shows that the resultant force acting in the direction of motion is:

$$\text{Force in Direction of Motion} = F_x\cos(\alpha) + F_y\sin(\alpha) \qquad (3\text{-}3)$$

Thus as the slip angle increases, it is the lateral force F_y which has a component $F_y\sin(\alpha)$ acting against the direction of motion which creates the increased resistance to motion, and not an increase in the force F_x acting parallel to the wheel plane. While an increase in slip angle does make forward motion more difficult (this is the problem mentioned with regard to toe-in or toe-out), it does not correspond to a significant change in the longitudinal force F_x.

As a concluding remark with regard to rolling resistance, it is noted that Thacker has presented evidence that wheelchair tire rolling resistance force is very nearly independent of speed. [2.9] This is in contrast to several rolling resistance models used for automobile tires which express rolling resistance force as a function of speed. [2.9] In addition, it was shown by Thacker that for camber angles of 2, 5, and 10 degrees (inward for both wheels), rolling resistance is not significantly affected.

This chapter has presented the raw data from several different treadmill tests designed to examine wheelchair tire forces. The primary variable affecting lateral cornering force has been shown to be the normal force F_z acting on the tire from the ground. Both the literature and the treadmill testing indicate that forward speed and inflation pressure have small effects on cornering force and thus may be neglected for wheelchair tires. Data has been presented which will allow the inclusion of camber force and rolling resistance into the final mathematical formulation of wheelchair motion. Chapter 4 will demonstrate how the raw data in this chapter can be used to predict the forces acting on a wheelchair tire during any given state of motion. Once this is done, the wheelchair equations of motion can be solved and the problem of directional stability can be examined.

CHAPTER 4

EMPIRICALLY PREDICTING WHEELCHAIR TIRE FORCES

Thus far, a description has been given of the basic tire forces which are important to wheelchair motion. In Chapter 2 these forces were defined, while in Chapter 3 treadmill data was presented which gives some idea of the major factors which affect the magnitude of both the lateral force F_y and the longitudinal force F_x. Although an investigation of wheelchair tire force characteristics was in itself a goal of this research, the final aim was to use the data collected as part of an investigation of rear caster wheelchair instability. This chapter will explain a simple method for using the cornering force versus normal force curves given in Figures 3-4a to 3-4g to predict the lateral force on a wheelchair tire.

Of course, it is possible to simply look at the graphs and obtain an estimate of the cornering force F_y if the slip angle and normal force are known. In order to incorporate the data into a simulation of wheelchair motion, however, a more mathematical method of using the raw tire force data is needed. This chapter will also discuss a method of determining cornering stiffness, C_α. It will be shown later that estimates of the cornering stiffness for two casters and two main tires of a wheelchair can be used to help verify the computer program which has been developed to simulate wheelchair motion. Values of cornering stiffness can also be used to compare different tire types.

USING TREADMILL DATA TO REPRESENT OTHER SURFACES

As the transition from measured tire force values on a treadmill to predicted values for all surfaces is made, the legitimate question arises as to how valid this process will be. Because the treadmill surface is not very representative of other surfaces such as concrete or tile, one might expect that the tire forces measured by using the treadmill are not very valuable when considering wheelchair tires on other surfaces. However, it has already been discussed that lateral cornering force is due primarily to elastic effects produced by the tire tread band. Engineers at Ford Motor Company have shown that for small slip angles, lateral force is almost exclusively controlled by elastic tire properties and is practically independent of the road surface. [4.1] Thus, it is reasonable to expect that the cornering force data collected from the treadmill is representative of many surfaces provided that the limit of sliding is not reached. Note that for large slip angles near the onset of sliding, the road surface will play a much larger role.

Unfortunately, similar arguments to those above cannot be made with regard to the longitudinal rolling resistance force F_x. Rolling resistance force is unquestionably quite different for different surfaces such as grass, carpet, or floor tile. However, if values of the coefficient of rolling resistance f_r are available for these different surfaces, they can be easily substituted for those obtained with the treadmill.

The possible variations of tire forces depend upon an almost endless number of parameters. Even the very act of testing the tires can create a test-induced wear that tends to increase measured road force values. [4.2] Similarly it is impossible to test every conceivable tire type. For this reason the best that can be expected from treadmill data is to obtain reasonable estimates for values of cornering force, camber force, and rolling resistance for one surface and one particular group of tires. A good simulation model will then allow each of these estimates to be perturbed in various ways in order to simulate hypothetical conditions and tire types that cannot or have not been directly tested.

POSSIBLE METHODS FOR PREDICTING TIRE FORCES

After some time is spent reviewing the literature pertaining to the force characteristics of various tires, it becomes quite obvious that one could spend a lifetime doing research in this field. Primarily because of its extreme flexibility, the tire is very unique and does not easily lend itself to conventional analysis. Although a great deal of tire performance data has been collected, the process of developing theories which accurately predict tire forces is still in the early stages. [2.4] This is quite surprising considering the amount of time and effort that has gone into tire research and development.

Mathematical models which do exist for describing the cornering behavior of elastic tires are almost universally either empirical or semi-empirical. Nearly all current tire models are based mainly on the knowledge of experimentally determined tire characteristics, and thus in contrast to a true analytic tire model, generally ignore the actual tire structure. Usually the tire is represented as a series of components such as springs and masses designed expressly for the purpose of simulating known test data. These components often bear little or no resemblance to a real tire. [2.4] Perhaps the development of an accurate theoretical model for wheelchair tires would be easier to accomplish than has been the case for automobile or aircraft tires, but it is safe to say that at the present time such a model does not exist.

Because the purpose of this research was to examine important tire forces as related to the problem of directional stability, and not to develop a theoretical model to predict such forces, the simplest method possible for representing the experimental test cart data was chosen. This method is entirely empirical but is ideally suited for use as a software component in the computer simulation of vehicle response.

EMPIRICAL PREDICTIONS OF CORNERING FORCE

The method of describing tire lateral force which will be used here is very similar to a method presented by D. L. Nordeen of General Motors Corporation, and it is one of the primary methods used by GM's Engineering Mechanics

Department when studying vehicle handling. [4.3] It might be noted that Nordeen makes most of the same assumptions concerning cornering force, slip angle, and normal force which are being used for the analysis of wheelchair motion.

It has already been shown in Chapter 3 that most wheelchair tire forces can be represented by graphs of the forces as functions of vertical load. This is not however, an extremely useful form for representing tire data. In order to simulate continuous wheelchair motion, point by point computations must be performed. The raw data cannot be directly interpreted for application to a particular wheelchair. [2.7]

Turning attention once again to the graphs in Figures 3-4a to 3-4g, a method is required which will express lateral cornering force F_y as a function of normal force F_z at constant slip angle α. The method described by Nordeen is to simply represent this relationship by a third-degree polynomial as follows:

$$F_y = aF_z + bF_z^2 + cF_z^3 \qquad (4\text{-}1)$$

where a,b,c are constants which depend on the slip angle

F_z = normal force on tire

F_y = lateral cornering force

For each of the curves shown in Figures 3-4a through 3-4g values for the constants a,b, and c were determined by using a computer program which provides a polynomial best fit to a given set of data points using the method of least squares. [4.3] Correlation coefficients for the best fit curves were generally higher than .98 indicating good fits with the experimental data. Because treadmill data was collected for 8 slip angles, 24 constants (3x8) were computed for each tire. The computer program actually computed the best fit 3rd order polynomial having four terms where the fourth term is an additional constant indicating that the best fit in the least squares sense does not pass through the origin. Because for simulation purposes it is desirable to have zero cornering force F_y when the normal load F_z is zero, this fourth constant or residual at $F_z = 0$ was eliminated. This has a negligible effect on the overall approximation because all of the curves in Figures 3-4a through 3-4g very nearly pass through the origin. The largest residuals at $F_z = 0$ for all of the curves in Figures 3-4a through 3-4g were approximately 1N (.22 lbf) and most were even less than this value. Appendix B gives the treadmill load cell data used to plot the curves in Chapter 3 along with the corresponding polynomial coefficients a, b, and c. The discarded residuals and the correlation coefficients are also given.

Once the coefficients a, b, and c in equation (4-1) are known for a particular tire, it is possible to construct cornering force versus slip angle curves at constant normal force such as the one shown in Figure 3-2. F_z can be arbitrarily chosen to be some value and then the coefficients a,b, and c for a given slip angle can be used to compute the lateral cornering force F_y. This is desirable because curves such as the one shown in Figure 3-2 allow an estimation of the initial slope or cornering stiffness C_α for a given tire. As was stated before, cornering stiffness values can be used to compare different tires and to help verify the simulation program used to model wheelchair motion. The method of using the empirical coefficients as part of a computer program will be discussed later. It should be noted that even this method is somewhat restricted, because the constants a,b, and c can only be determined for the slip angles which were tested (1-8 degrees). A means for using equation (4-1) to obtain approximate values of F_y for *non-integer angles will be discussed later along with other simulation techniques.

DETERMINING CORNERING STIFFNESS

For each of the seven wheelchair tires tested, the empirical constants a,b, and c corresponding to the best fit for the curves shown in Figures 3-4a through 3-4g were determined. Again, these are listed in Appendix B. Equation (4-1) was then used to predict values of cornering force F_y for six constant values of normal force F_z. The constant F_z values chosen were 75N, 150N, 225N, 300N, 375N, and 450N. The cornering force versus slip angle curves (at constant normal force) which resulted from using equation (4-1) are shown in Figures 4-1a through 4-1g. It is emphasized that these figures do not represent new data, but instead represent the data shown in Figures 3-4a through 3-4g in a slightly different way. Also note that the data points shown represent interpolated values of F_y which were

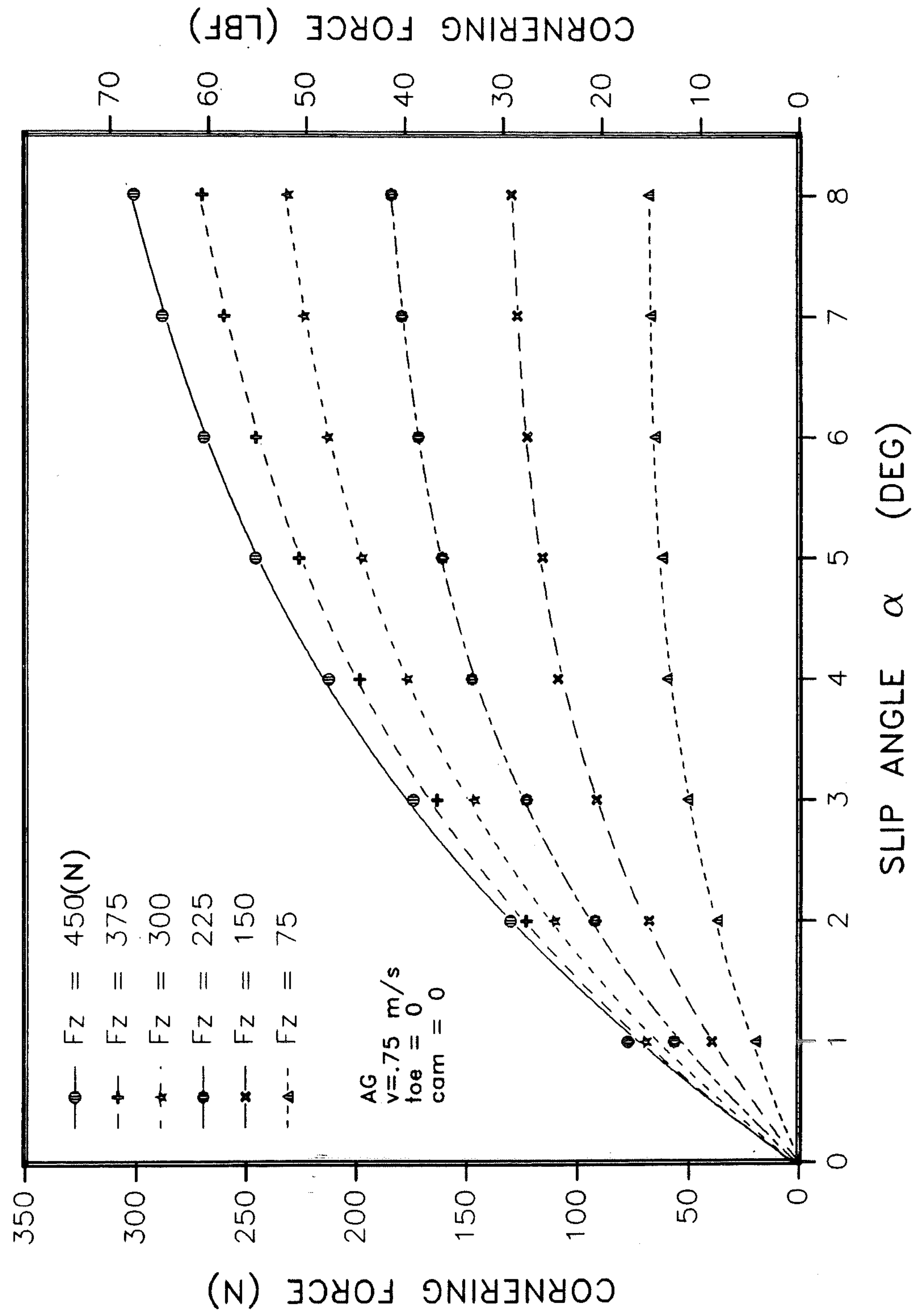

Figure 4-1a Interpolated Cornering Force vs. Slip Angle Curves at Constant Normal Force (AG tire)

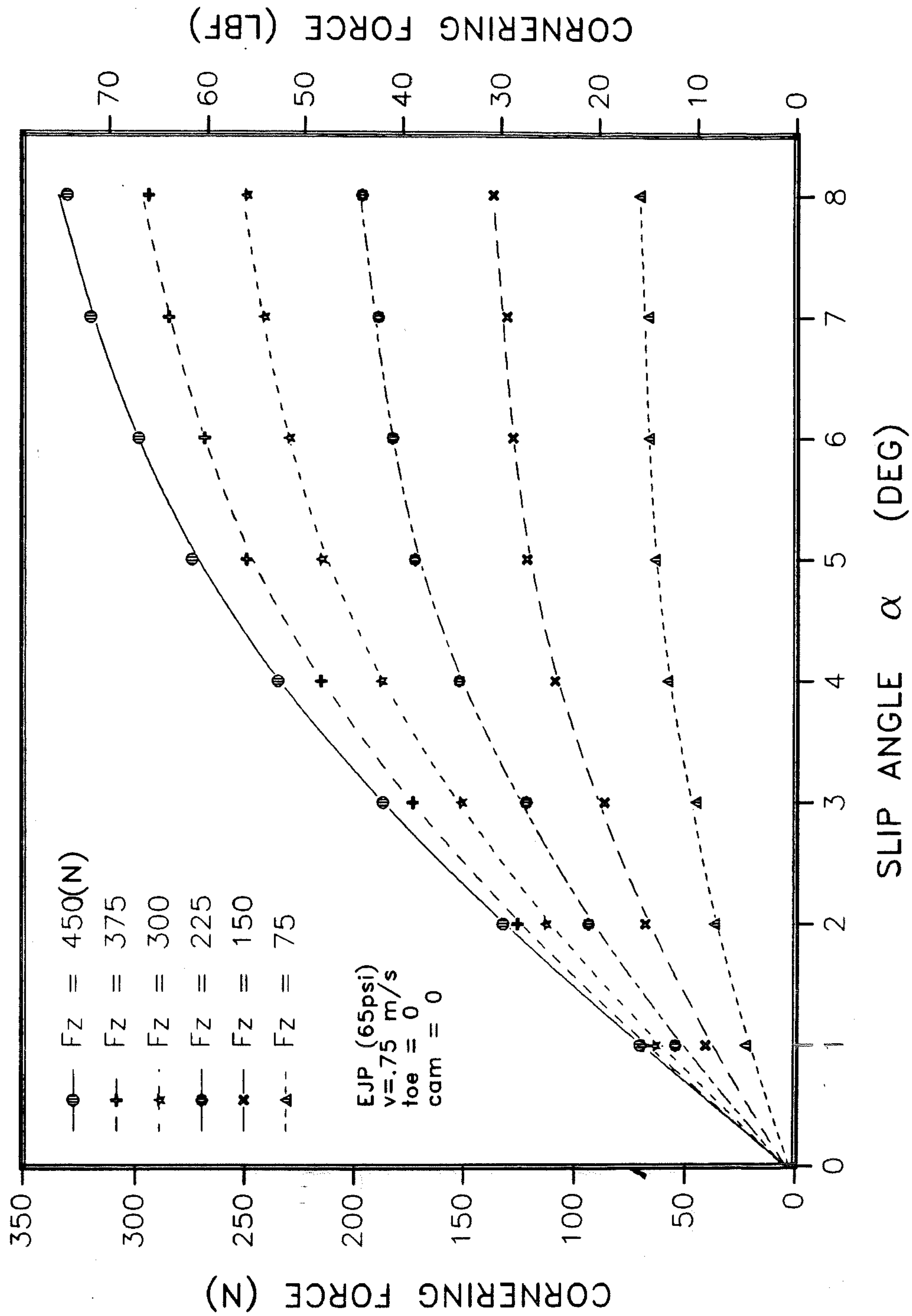

Figure 4-1b Interpolated Cornering Force vs. Slip Angle Curves at Constant Normal Force (EJP tire)

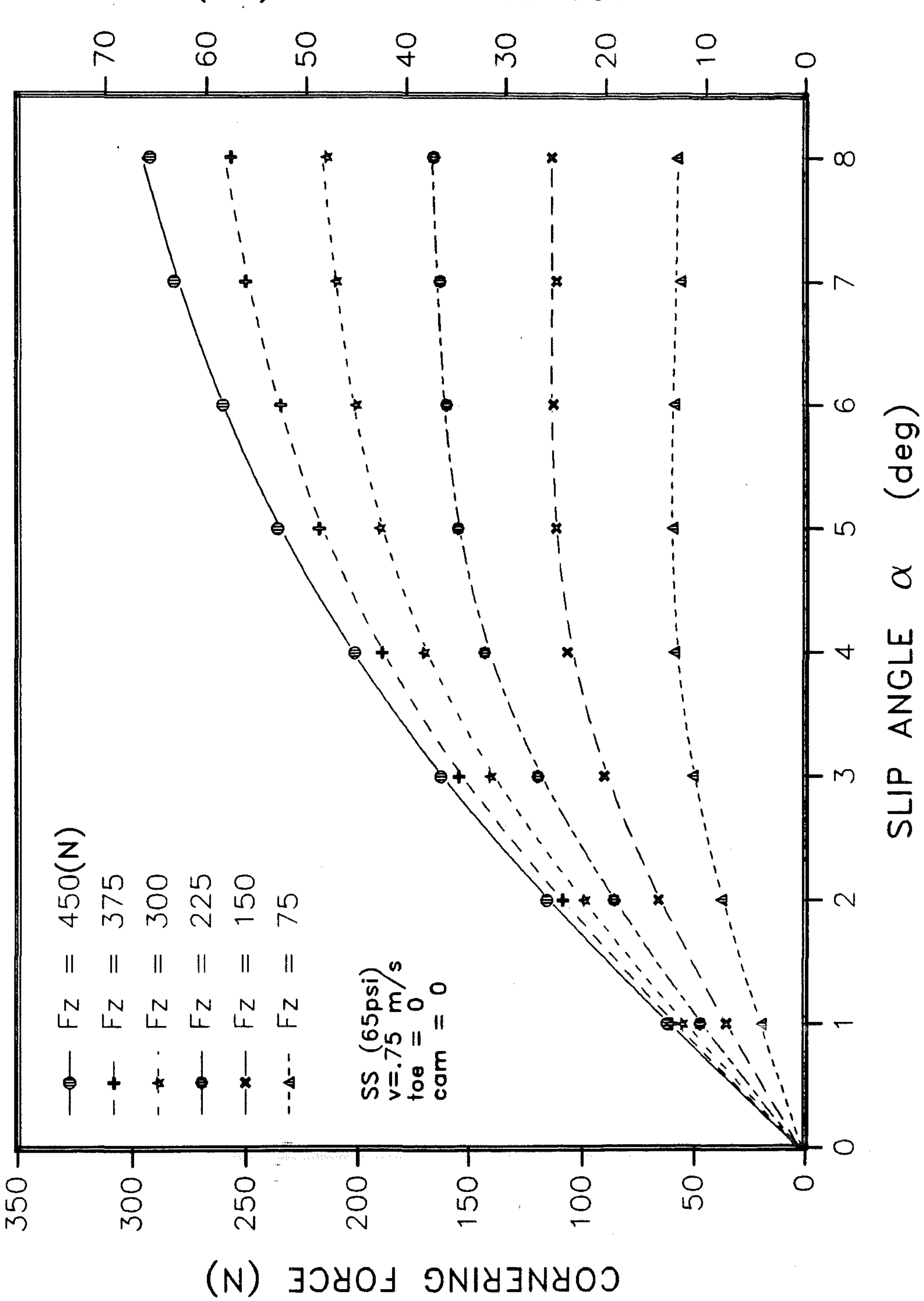

Figure 4-1c Interpolated Cornering Force vs. Slip Angle Curves at Constant Normal Force (SS tire)

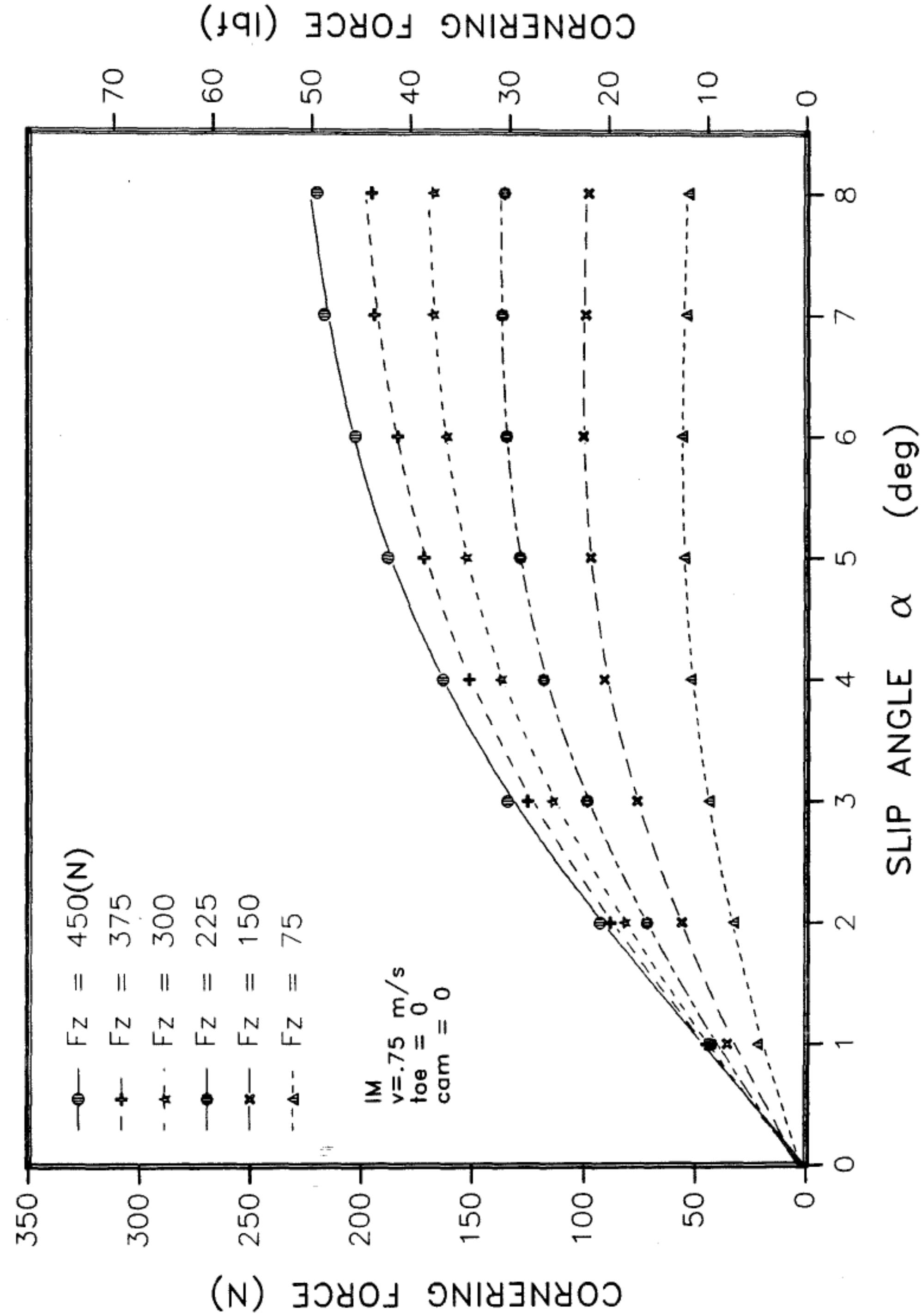

Figure 4-1d Interpolated Cornering Force vs. Slip Angle Curves at Constant Normal Force (IM tire)

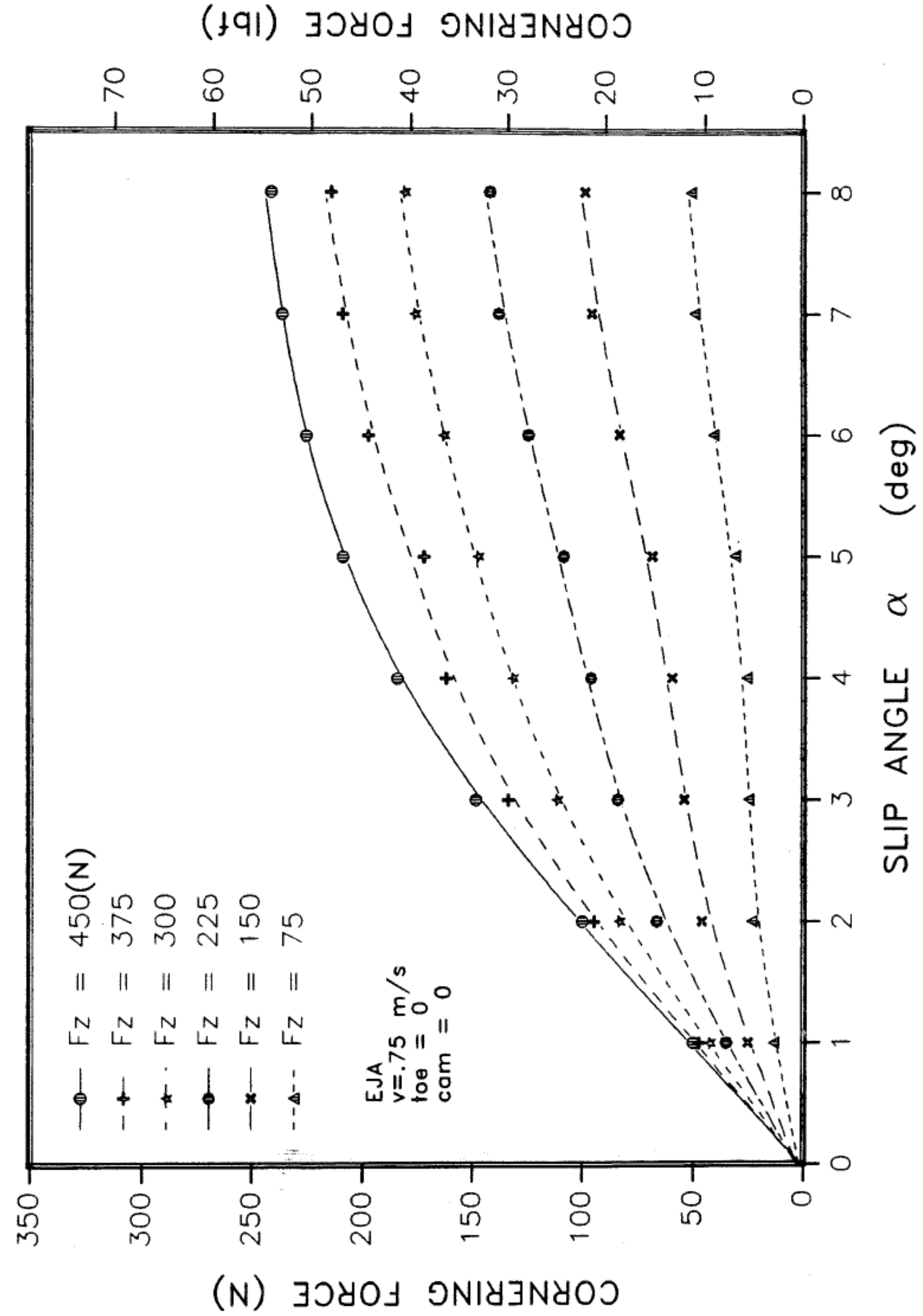

Figure 4-1e Interpolated Cornering Force vs. Slip Angle Curves at Constant Normal Force (EJA tire)

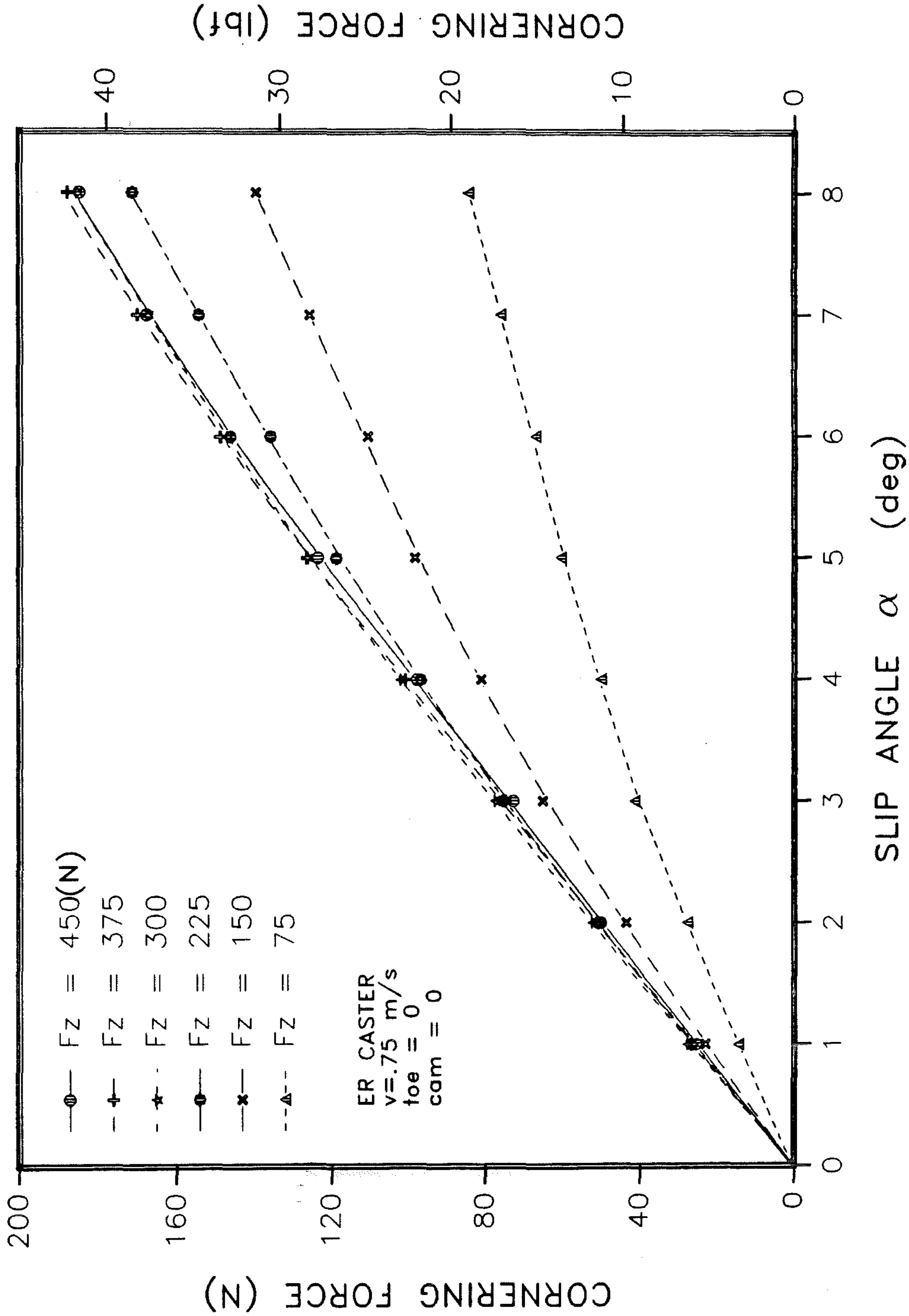

Figure 4-1f Interpolated Cornering Force vs. Slip Angle Curves at Constant Normal Force (ER caster)

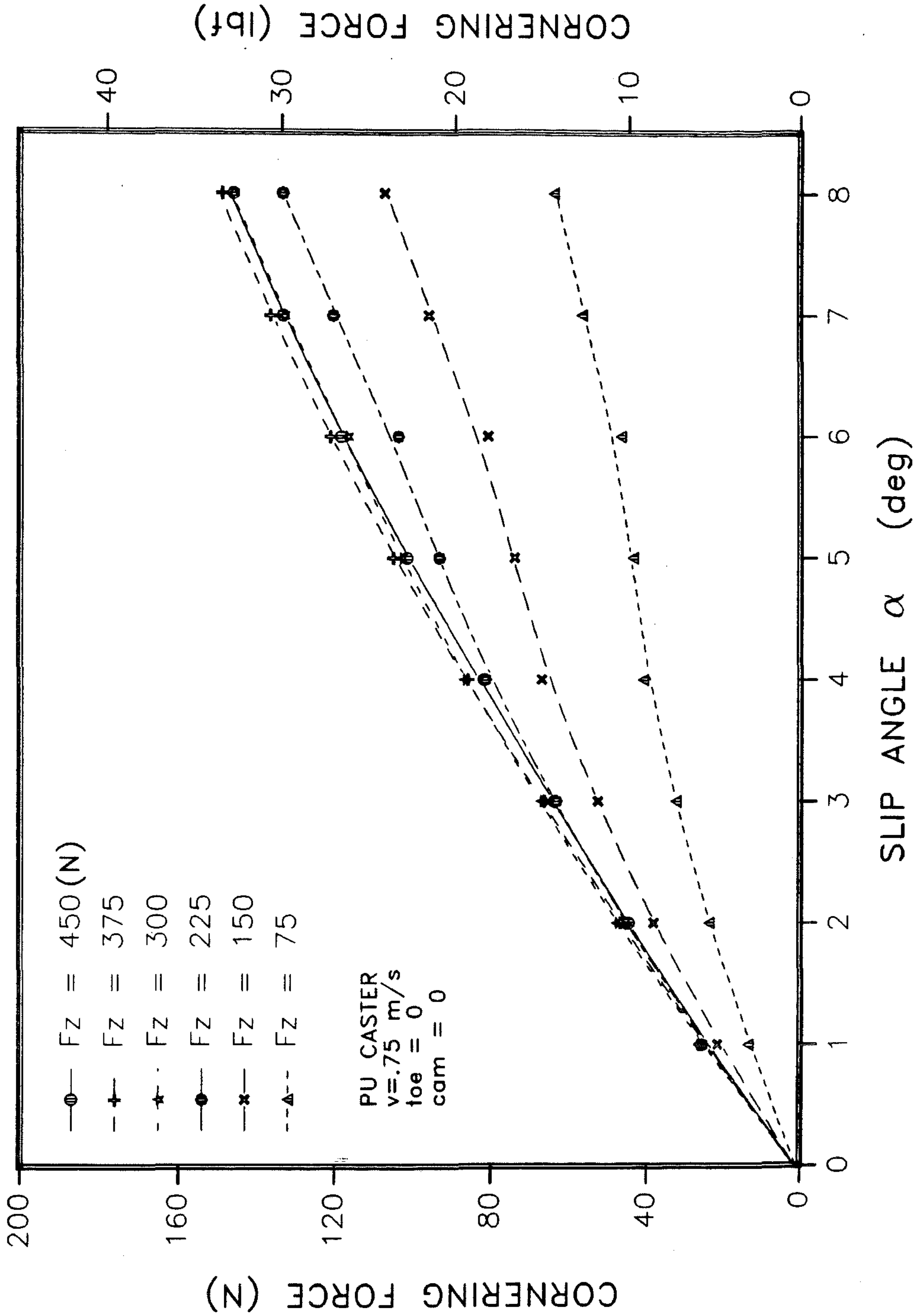

Figure 4-1g Interpolated Cornering Force vs. Slip Angle Curves at Constant Normal Force (PU caster)

obtained using equation (4-1) and the empirical constants which were derived from the test cart data.

Figures 4-1a through 4-1g are more useful than the graphs which were shown in Chapter 3. These curves are identical to the cornering force versus slip angle curve shown in Figure 3-2, and the initial slope of any one of the curves gives the cornering stiffness C_α for a particular tire at a particular value of normal force. The individual graphs are arranged in decreasing order according to the cornering stiffnesses of the tires. Observe that the linear region of the curves depends on the value of F_z, with higher values of F_z corresponding to larger linear regions. Also note that for the two caster wheels (ER) and (PU), after the normal force reaches about 225 N, further increases in F_z do not result in further increases in cornering force.

If the assumption is made that each of the curves shown in Figures 4-1 are linear for slip angles up to at least one degree, the cornering stiffness of each tire for each value of normal force can be estimated as the slope of each curve from zero to one degree. Examination of the figures shows the the assumption of linearity from 0 to 1 degree is best for high values of F_z. Table 4-1 shows the values of cornering stiffness obtained for each tire.

Table 4-1 provides an easy means for comparing the cornering stiffnesses of the different tires at different loads. Using Table 4-1 it is possible to construct a set of curves of cornering stiffness versus normal force for all seven tire types on a single graph. This is shown in Figure 4-2. Using this figure, it is possible to anticipate which tire will develop the largest cornering force F_y when subjected to small slip angles for a known normal force.

TABLE 4-1

VALUES FOR CORNERING STIFFNESS (C_α)

(normal force F_z)

Tire	75N	150N	225N	300N	375N	450N
AG	20.3*	39.7	56.6	69.6	77.1	77.4
EJP	22.8	40.8	54.4	63.7	69.0	70.5
SS	20.0	35.7	47.3	55.3	60.0	61.9
IM	22.1	35.7	42.8	45.2	44.8	43.4
EJA	13.6	25.4	35.1	42.5	47.6	50.2
ER	14.7	23.2	26.9	27.6	26.7	25.7
PU	13.7	21.7	25.6	26.6	26.3	25.9

* All cornering stiffness values have units (N/deg)

The normal force exerted on a pair of wheelchair tires is determined largely by the user's weight and the location of the center of gravity. Figure 4-2 shows that if the normal force is less than approximately 150 Newtons, there is not much difference between the AG, EJP, SS, or IM, tires, while the EJA, ER, and PU tires exhibit significantly lower cornering stiffnesses. For normal forces above 150 N the legend lists the tires in order of decreasing cornering stiffness. This is true for all but the IM and EJA tires for normal force values greater than about 330N.

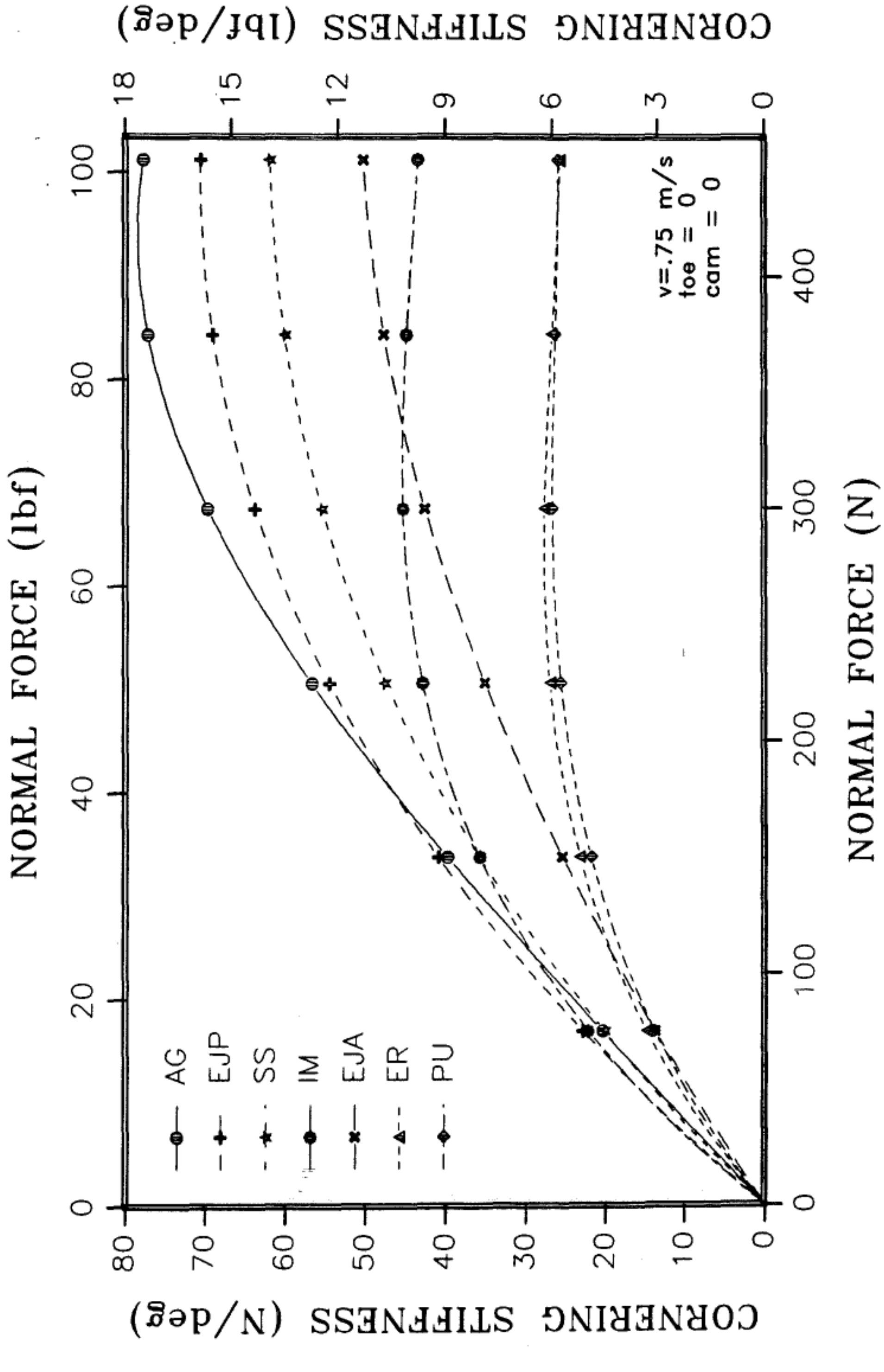

Figure 4-2 Cornering Stiffness vs. Normal Force for Seven Wheelchair Tires

The implication of Figure 4-2 is that some improvement in the directional stability of rear caster wheelchairs might be obtained by selecting the tire that will minimize the cornering stiffness and hence the destabilizing force on the main wheels for a given slip angle. Typical normal forces for the main wheels of a rear caster wheelchair are in the range 100 N to 250 N. Figure 4-2 then indicates that for a rear caster wheelchair, the EJA tires should produce the least amount of directional instability. The extent to which this is true is discussed later in this text.

EMPIRICAL RELATIONSHIP BETWEEN CAMBER AND CORNERING FORCE

It was stated earlier that studies of automobile tires have found the camber force at some camber angle, γ, to be on the order of 1/5 the cornering force developed at an equivalent slip angle α, assuming the normal force F_z is the same. It would be useful if a similar relationship could be determined for wheelchair tires.

To do this, empirical constants were determined for each of the camber force vs. normal force curves shown in Figures 3-7a through 3-7e. This was done in the same manner as was done for cornering force resulting in three constants a, b, and c such that camber force could be predicted as a function of F_z using a third order polynomial like the one in equation 4-1. Having determined a, b, and c the expected value of cornering force was computed for the same six values of normal force used previously to construct Figures

4-1a through 4-1g (75N, 150N, 225N, 300N, 375N, and 450N). By plotting the empirically predicted values of cornering force and camber force for the same F_z values and for the same camber or slip angles it is possible to obtain an approximate relationship between the two forces. This has been done in Figure 4-3 where camber force is plotted on the horizontal axis, cornering force is plotted on the vertical axis, and m is the slope of the best fit line relating camber force to cornering force for a given tire. It is emphasized that the data points shown were computed using empirical constants determined from the data in Figures 3-4 and 3-7. The data points are for the six F_z values just given and for $\alpha = \gamma = 2$, 5, or 8 degrees.

Figure 4-3 indicates that for equivalent angles of camber and slip and for the same value of F_z, camber force ranges from about 1/5 to 1/8 the value of cornering force. This is not totally in agreement with the literature pertaining to automobile tires but is reasonable. Figure 4-3 allows a good estimate of camber force for a given camber angle simply by using the empirical constants for cornering force. For the purposes of modeling camber force when simulating wheelchair motion, the inverse of the slopes, m, in Figure 4-3 will be referred to as camber coefficients, f_c. Then for any given angle of camber

$$\text{Camber Force} = 1/m(F_y) = f_c F_y \qquad (4\text{-}2)$$

where the F_y is computed for the equivalent slip angle α and normal force using equation (4-1).

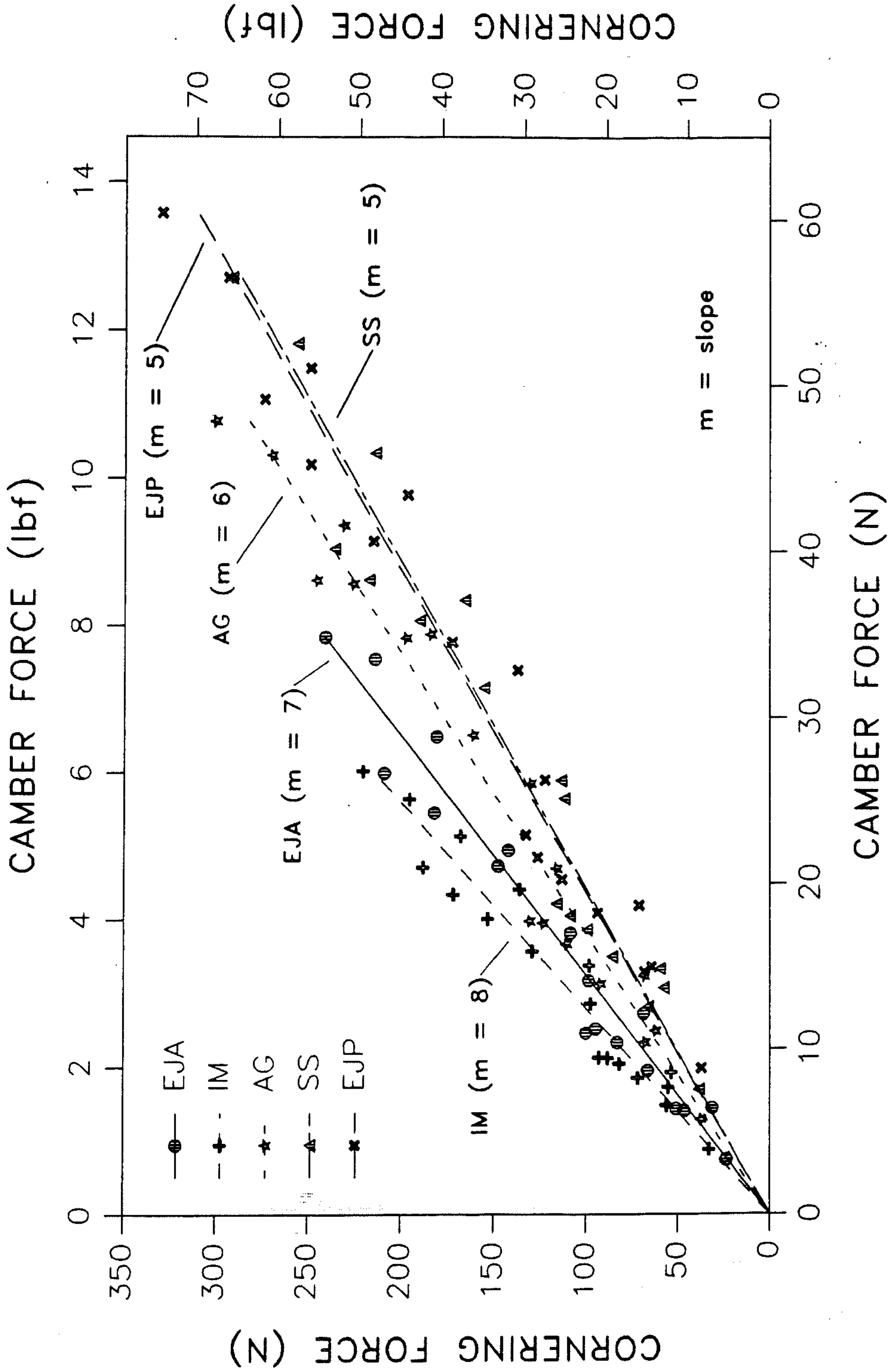

Figure 4-3 Empirical Relationship Between Cornering Force and Camber Force

EMPIRICALLY PREDICTING ROLLING RESISTANCE FORCE

The rolling resistance force F_x can be computed for a given value of normal force F_z by using the coefficients of rolling resistance given in Table 3-2 along with equation (3-2). Looking at Figure 3-8, however, one observes that the longitudinal force curves do not necessarily pass through the origin if a strictly linear best fit is chosen. For the purposes of predicting rolling resistance force with a computer program, it is desirable to ensure that the rolling resistance force approaches zero as the normal force becomes small. This avoids physically unrealizable situations where the rolling resistance might act in the same direction as the direction of wheelchair motion. For this reason, third order polynomials will also be used to calculate rolling resistance when a simulation program is formulated. The interested reader is again referred to Appendix B where the treadmill results and empirical constants used for cornering force, camber force, and rolling resistance are given.

In conclusion, this chapter has been used to present a simple yet effective way to represent the tire force data which was collected using the treadmill and test cart. The empirical methods which have been described are easily adaptable to a computer simulation. Certainly no claim can be made that a theoretical approach has been taken in accomplishing this. As stated earlier, the tire relationships presented in this chapter are entirely empirical.

From one point of view, this entirely empirical approach is quite primitive. However, the basic characteristics of wheelchair tire force behavior and a method of modeling this behavior for the purpose of investigating wheelchair motion has been outlined. Even an extremely detailed investigation of wheelchair tire properties might not lead to much improvement with regard to the accuracy with which tire forces can be predicted. This is one reason why empirical methods are still very popular within the automotive industry. Later chapters in this text will present arguments indicating that a detailed and time consuming investigation of the elastic force producing properties of wheelchair tires is probably not warranted if a desire to improve directional stability is the only motivation for such a study. The question as to whether or not such a study would be valuable in and of itself is open to debate.

CHAPTER 5

A SIMPLIFIED ANALYSIS OF THE DYNAMICS AND LATERAL STABILITY OF GROUND VEHICLES

Now that the important wheelchair tire forces have been defined, it is possible to begin an investigation of the directional stability problem associated with rear caster wheelchairs. This chapter will present a simple model which can be used to demonstrate how variables such as cornering stiffness and center of gravity position affect the directional stability of a ground vehicle. The important frames of reference relevant to vehicle motion will be introduced along with the major variables which will be used to describe wheelchair motion. As with earlier chapters, most of the discussion in this chapter and the next will be motivated by previous studies relating to automobiles or airplanes.

In searching the literature pertaining to directional stability, one finds almost exclusively work which describes the requirements for designing a stable vehicle or for making an already stable vehicle more stable. Virtually no mention can be found of how to deal with or improve an inherently unstable vehicle such as a rear caster wheelchair. The unstable situation is generally termed undesirable and is simply discarded from discussion. This chapter will demonstrate why rear caster wheelchairs are extremely directionally unstable, and why options for improving the problem may be very limited.

THE ZERO WIDTH VEHICLE

The most basic analysis begins by assuming that the wheelchair or vehicle is symmetric about its longitudinal axis. It is assumed that no lateral load transfer can take place. In other words, there is no roll degree of freedom. Furthermore, all four wheels of the vehicle are assumed to be locked against turning about their vertical axes, although it is emphasized that this does not mean that the vehicle cannot deviate from a straight path. This would only be true if the wheels were perfectly rigid. If the wheels are allowed to develop lateral velocity components as described in previous chapters, changes of direction may occur even if the wheels are locked.

To further simplify the analysis, it is assumed that the four wheeled vehicle can be adequately represented by what is referred to as the "zero width" vehicle or "bicycle model". This model places all four wheels on the center line of the vehicle as shown in Figure 5-1. It will be shown that some very interesting conclusions can be derived by considering this simple model. [5.1] This type of analysis was first presented by Rocard and has since become well known by those who frequently study vehicle dynamics. [5.2] To this author's knowledge no such analysis has been done with wheelchairs as the specific type of vehicle in mind. This chapter will draw upon Rocard's original text as well as some more recent publications. [5.1,5.2,2.2,2.3]

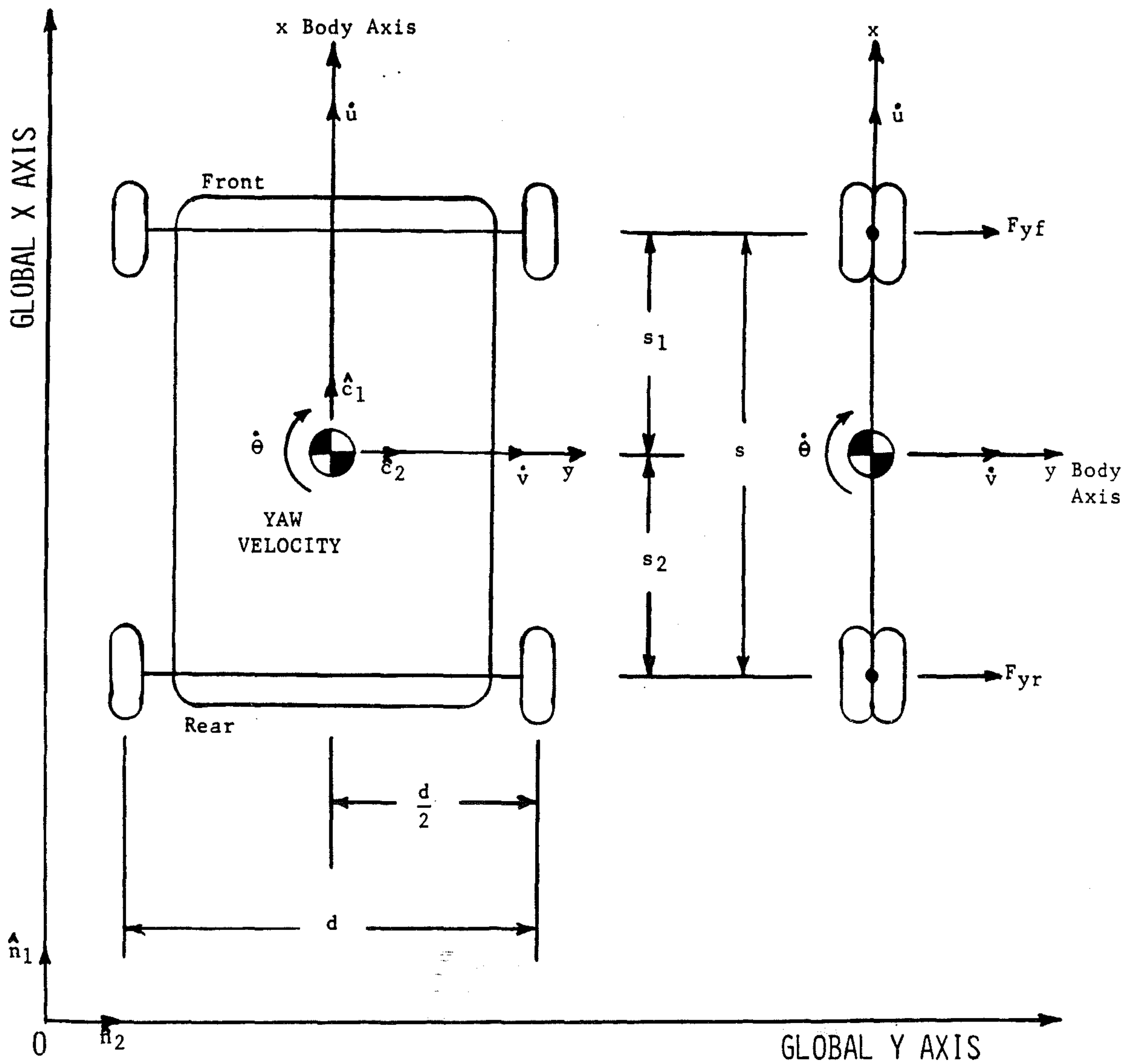

Figure 5-1 The Zero Width Vehicle Model

Figure 5-1 deserves careful attention because it contains variables and information that will be referred to for the remainder of the text. On the left side of the figure is the original four wheeled vehicle and on the right side is the simplified equivalent. The important dimensions as shown are s, s_1 and s_2 where: s is the total wheelbase distance, s_1 is the distance from the front wheels to the center of gravity, and s_2 is the distance from the rear wheels to the center of gravity. The width dimension, d, in the figure is ignored because of the zero width assumption. The zero width wheelchair is assumed to have two identical wheels in the front and two identical wheels in the rear, although the front and rear wheels may be different from each other.

Rolling resistance is ignored so that the only tire force developed is a lateral cornering force denoted as F_{yf} for the front wheels and as F_{yr} for the rear wheels. As discussed in earlier chapters, the magnitude of cornering force depends primarily upon slip angle and normal force.

There are two important axis systems or reference frames shown in Figure 5-1. The first of these is the global X-Y reference frame. This frame is fixed in space and does not move with the vehicle. The second reference frame is a body fixed reference frame which both moves and rotates with the vehicle. The body fixed or local x axis lies along the longitudinal axis of the vehicle, while the body fixed y axis lies along the lateral axis of the vehicle. The variables $\dot{u}$ and $\dot{v}$ represent velocities along the body fixed x and y axis. Finally, $\dot{\theta}$ represents the angular velocity (or yaw velocity) of the vehicle about a vertical axis through the vehicle's center of mass. The corresponding displacement and acceleration kinematic variables are represented by $(u,\ddot{u},v,\ddot{v},\theta,\ddot{\theta})$.

EQUATIONS OF MOTION IN THE BODY FIXED REFERENCE FRAME

Because the global X-Y reference frame is fixed in space, it is commonly referred to as an inertial reference frame. On the other hand, due to the fact that the body fixed reference frame can move and rotate with the vehicle, it is often called an accelerating or non-inertial reference frame.

It is convenient to use the body fixed axis system when formulating the wheelchair equations of motion for two reasons. First of all, using the body fixed axes eliminates the need for coordinate transformations of the tire forces from the body fixed reference frame to the global reference frame. More importantly, the mass moments of inertia of the vehicle are constant with respect to the body fixed axis system. This is not true with respect to the inertial reference frame. With respect to the global X-Y system, the moments of inertia continually change as the vehicle changes direction. [2.2]

There is however a disadvantage associated with using the body fixed axis system when formulating the equations of motion. Specifically, Newton's laws are not valid in a non-inertial reference frame. With respect to the body fixed axes, the acceleration of the center of mass is not equal to the ratio of total force on the vehicle to the vehicle's mass. For the unfamiliar reader, Tipler gives a good discussion of non-inertial reference frames. [5.3]

To formulate the equations of wheelchair motion it will be necessary to express the acceleration of the center of mass using the body fixed reference frame. These equations are generally given without derivation in the literature, but some explanation will be provided here.

Consider the two reference frames shown in Figure 5-1. As shown, $\hat{n}_1$ and $\hat{n}_2$ are unit vectors corresponding to the X and Y directions in the inertial reference frame, while $\hat{c}_1$ and $\hat{c}_2$ are unit vectors in the directions of the body fixed x and y axes. The absolute velocity is $(\vec{V})$ where:

$$\vec{V} = \dot{u}\hat{c}_1 + \dot{v}\hat{c}_2 \qquad (5\text{-}1)$$

Because the body fixed reference frame can rotate, the unit vectors $\hat{c}_1$ and $\hat{c}_2$ are not constant and hence the absolute acceleration found by taking the derivative of equation (5-1) is:

$$\dot{\vec{V}} = \ddot{u}\hat{c}_1 + \dot{u}\dot{\hat{c}}_1 + \ddot{v}\hat{c}_2 + \dot{v}\dot{\hat{c}}_2 \qquad (5\text{-}2)$$

It is well known that the absolute time rate of change of a unit vector in a rotating reference frame is equal to the cross product of the unit vector and the angular velocity of the rotating frame. [5.4] In this case the angular velocity is in the positive $\hat{c}_3$ direction and (5-2) becomes:

$$\dot{\vec{V}} = \ddot{u}\hat{c}_1 + \dot{u}(\dot{\vec{\theta}} \times \hat{c}_1) + \ddot{v}\hat{c}_2 + \dot{v}(\dot{\vec{\theta}} \times \hat{c}_2)$$

or $$\dot{\vec{V}} = (\ddot{u} - \dot{\theta}\dot{v})\hat{c}_1 + (\ddot{v} + \dot{\theta}\dot{u})\hat{c}_2 \tag{5-3}$$

Considering the $\hat{c}_1$ and $\hat{c}_2$ components of acceleration in equation (5-3), the basic equations of motion for a rotating vehicle using the body fixed reference frame are

$$\sum F_x = m(\ddot{u} - \dot{\theta}\dot{v}) \tag{5-4a}$$

$$\sum F_y = m(\ddot{v} + \dot{\theta}\dot{u}) \tag{5-4b}$$

$$\sum M_z = I_z\ddot{\theta} \tag{5-4c}$$

where the subscripts x and y refer to directions in the body fixed reference frame. For this simplified analysis there are no forces in the x direction and $\dot{u}$ is constant. In equations (5-4) m is the total mass of the vehicle and I_z is the mass moment of inertia about a vertical axis passing through the center of mass. Note that the third equation is valid in either the body fixed or the inertial reference frame, and that products of inertia can be ignored because planar motion is assumed. [5.5]

For the zero width vehicle in Figure 5-1 the motion will be restricted to small slip angles so that equation (3-1) can be used to find the forces on the two front and two rear wheels:

$$F_{yf} = -2C_{\alpha f}\alpha_f \tag{5-5a}$$

$$F_{yr} = -2C_{\alpha r}\alpha_r \tag{5-5b}$$

where again the subscripts refer to the front and rear tires respectively and the negative signs result from the fact that the cornering forces must act in a direction which is opposite the initial lateral velocity $\dot{v}$. It must be noted that the units for slip angle in equation (5-5a) or (5-5b) are radians, and the units for cornering stiffness are N/rad or lbf/rad.

Recall from Chapter 2 that the slip angle ,α, is defined as the angle between the wheel plane's heading and the actual direction of travel (Figure 2-1). For the zero width vehicle, due to its angular rotation both the front and rear wheels have velocity components in both the $\hat{c}_1$ and $\hat{c}_2$ directions.

$$\text{velocity front} = \dot{u}\hat{c}_1 + (\dot{v} + \dot{\theta}s_1)\hat{c}_2 \tag{5-6a}$$

$$\text{velocity rear} = \dot{u}\hat{c}_1 + (\dot{v} - \dot{\theta}s_2)\hat{c}_2 \tag{5-6b}$$

An expression for the slip angle α is found by examining Figure 5-2 which shows the orientation of the lateral and longitudinal velocity components.

$$\tan(\alpha) \cong \alpha = \frac{\text{lateral velocity component}}{\text{longitudinal velocity component}} \tag{5-7}$$

Then using equations (5-6a) and (5-6b) in equation (5-7), where the longitudinal velocity components are in the c_1 direction and the lateral components are in the c_2 direction, gives the following relationships for the front and rear wheels respectively.

$$\alpha_f = \frac{\dot{v} + \dot{\theta}s_1}{\dot{u}} \tag{5-8a}$$

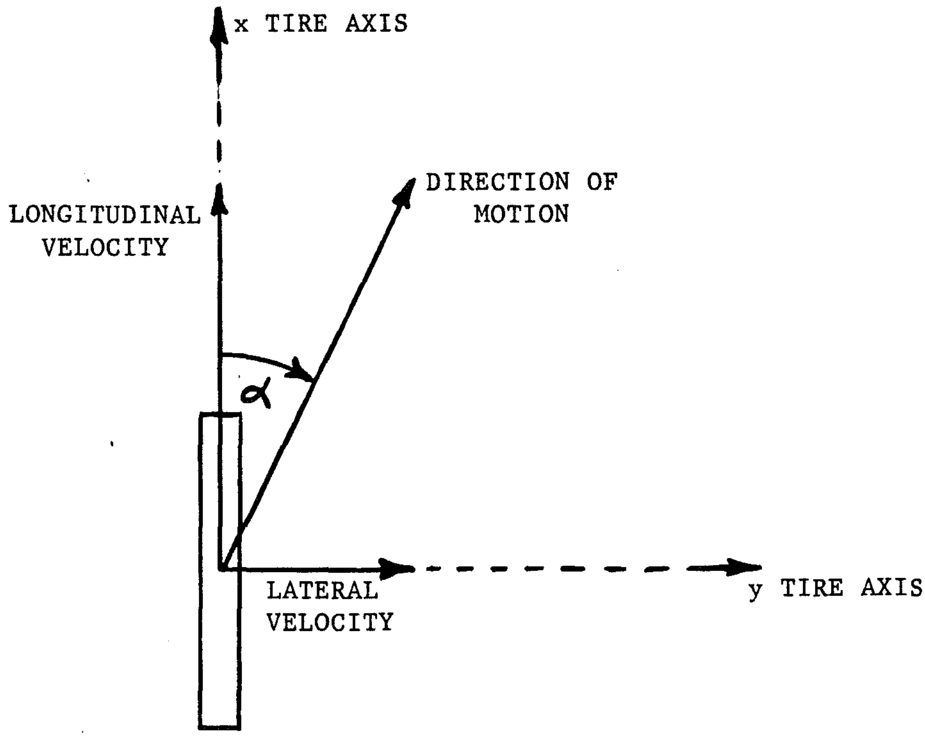

Figure 5-2 Lateral and Longitudinal Velocity Components for a Rolling Tire

$$\alpha_r = \frac{\dot{v} - \dot{\theta}s_2}{\dot{u}} \tag{5-8b}$$

Substituting equation (5-8) into equation (5-5) and then using equations (5-4b) and (5-4c) results in the following differential equations of motion for the zero width vehicle.

$$m\ddot{v} + \left[m\dot{u} + \frac{2C_{\alpha f}s_1 - 2C_{\alpha r}s_2}{\dot{u}}\right]\dot{\theta} + \left[\frac{2C_{\alpha f} + 2C_{\alpha r}}{\dot{u}}\right]\dot{v} = 0 \tag{5-9a}$$

$$I_z\ddot{\theta} + \left[\frac{2C_{\alpha f}s_1^2 + 2C_{\alpha r}s_2^2}{\dot{u}}\right]\dot{\theta} + \left[\frac{2C_{\alpha f}s_1 - 2C_{\alpha r}s_2}{\dot{u}}\right]\dot{v} = 0 \tag{5-9b}$$

APPLYING THE ROUTH-HURWITZ CRITERION

In Chapter 1 it was stated that a vehicle is considered directionally stable if it returns to a steady state of motion within some finite time after being subjected to a disturbance. The advantage of the zero width model is that the resulting differential equations (5-9) form a set of linear differential equations with constant coefficients. If the vehicle is subjected to a disturbance, after the disturbance is removed, both the yaw and lateral velocities will vary with time exponentially. [2.2] Thus, both $\dot{\theta}$ and $\dot{v}$ will have solutions of the form $e^{\lambda t}$, and the stability of the system will depend on the coefficient λ. [2.3] If λ is positive and real, the motion of the system will be unstable and diverge to infinity. If λ is negative and real the system will be stable. Finally, complex values of λ

correspond to oscillatory solutions to the differential equations. By assuming solutions for the yaw velocity, $\dot{\theta}$, and lateral velocity $\dot{v}$ of the forms:

$$\dot{v} = A_1 e^{\lambda t} \tag{5-10a}$$

$$\dot{\theta} = A_2 e^{\lambda t} \tag{5-10b}$$

it can be shown that the differential equations (5-9a) and (5-9b) have the following characteristic equation: [2.1]

$$\lambda^2 + \left(\frac{a_1 I_z + a_4 m}{I_z m}\right)\lambda + \left(\frac{a_1 a_4 - a_2 a_3}{I_z m}\right) = 0 \tag{5-11}$$

where the constants a_1, a_2, a_3, and a_4 are given by:

$$a_1 = \frac{2C_{\alpha f} + 2C_{\alpha r}}{\dot{u}} \tag{5-12a}$$

$$a_2 = m\dot{u} + \frac{2C_{\alpha f} s_1 - 2C_{\alpha r} s_2}{\dot{u}} \tag{5-12b}$$

$$a_3 = \frac{2C_{\alpha f} s_1 - 2C_{\alpha r} s_2}{\dot{u}} \tag{5-12c}$$

$$a_4 = \frac{2C_{\alpha f} s_1^2 + 2C_{\alpha r} s_2^2}{\dot{u}} \tag{5-12d}$$

The Routh-Hurwitz stability criterion states that a necessary condition for stability is that all of the coefficients of the characteristic equation must be positive. If the characteristic equation is quadratic, this condition is not only necessary, but is also a sufficient criterion for stability. [5.2]

Looking at the coefficient of the first order term in equation (5-11) it is clear that because s_1, s_2, m, I_z, C_α, and $\dot{u}$ are always positive, this term can never become negative. Before examining the conditions under which the zeroth order coefficient may become negative, note that if W is the total weight of the vehicle or wheelchair, then

$$W = mg \tag{5-13a}$$

$$W_r = Ws_1/2s \tag{5-13b}$$

$$W_f = Ws_2/2s \tag{5-13c}$$

where the portions of the total weight carried by the front and rear wheels, W_r and W_f, are found from statics. In equation (5-11) the zeroth order coefficient will be positive if the term $(a_1a_4 - a_2a_3)$ is greater than zero. Using (5-13), (5-12), and a fair amount of algebra, the condition that this term be positive results in

$$\frac{\dot{u}^2}{g}\left(\frac{W_f}{C_{\alpha f}} - \frac{W_r}{C_{\alpha r}}\right) + s > 0 \tag{5-14}$$

Equation (5-14) expresses the condition for the lateral stability of a ground vehicle. From this condition it is clear that the important parameters which determine stability are the position of the center of gravity, the total wheelbase distance, the cornering stiffness of the front and rear tires, and the forward speed. It is notable that the condition for stability does not depend upon the total vehicle weight W or the mass moment of inertia I_z.

If the condition for directional stability defined by equation (5-14) is rearranged, it is possible to define a condition for the forward speed at which a given vehicle will be directionally stable.

The condition is

$$\dot{u} < \sqrt{\frac{-gs}{k_{us}}} \tag{5-15}$$

where
$$k_{us} = \left(\frac{W_f}{C_{\alpha f}} - \frac{W_r}{C_{\alpha r}}\right) \tag{5-16}$$

Equation (5-15) defines the critical speed, above which a four wheeled vehicle will exhibit directional instability. The parameter k_{us} in equation (5-16) is commonly referred to as the understeer coefficient for reasons which will be discussed in the last section of this chapter. [5.1]

Note first that if k_{us} is positive, equation (5-14) is always satisfied. This means that the vehicle is stable at any speed, and in fact the critical speed defined by equation (5-15) is undefined. The critical speed in this instance is $\dot{u} = \infty$. The understeer coefficient can be written in slightly different form as follows:

$$k_{us} = \frac{W_f C_{\alpha r} - W_r C_{\alpha f}}{C_{\alpha f} C_{\alpha r}} \tag{5-17a}$$

or using (5-13)
$$k_{us} = \frac{W(s_2 C_{\alpha r} - s_1 C_{\alpha f})}{2 s C_{\alpha f} C_{\alpha r}} \tag{5-17b}$$

It can be seen by examining the numerator in (5-17b) that the condition under which k_{us} always be positive is that the product of the distance of the rear wheels from the center of gravity and the cornering stiffness of the rear tires must be greater than the product of the distance of the front wheels from the center of gravity and the cornering stiffness of the front tires. This condition is stated as a theorem for stability by Rocard. [5.2]

A special case results if the front and rear cornering stiffnesses are approximately equal. This might occur for an electric wheelchair that has four identical wheels, but would not occur for typical manual wheelchairs. When $C_{\alpha f} = C_{\alpha r}$, Rocard's theorem implies that in order to ensure directional stability s_2 must be greater than s_1 which is equivalent to stating that the center of gravity must lie in the front half of the wheelchair. Implications of the stability conditions for manual front caster and rear caster wheelchairs will now be considered.

IMPLICATIONS FOR WHEELCHAIRS

The ideas which have been presented thus far are completely general and might be applied to any type of vehicle. It will now be shown that front caster and rear caster wheelchairs are two special cases which can be illustrated by examining the condition for stability, equation (5-14), and the critical speed equation (5-15).

When considering wheelchair motion, it is now important to deviate slightly from the original assumption that all four wheels are locked against turning. Although it is possible to lock all four wheels of an automobile in place by holding the steering wheel in a set position, this can not be done with manual front caster or rear caster wheelchairs. For manual wheelchairs in particular, the caster wheels are completely free to pivot about the caster pins. The only resistance to motion of the casters is provided by friction. This is equivalent to stating that the caster wheels will only sustain very small lateral cornering forces. For the purposes of the zero width model, the effects of this can be considered by assuming that the "effective" cornering stiffness of the caster wheels is very small.

Case One: Front Caster Wheelchair

For a front caster wheelchair it is the front wheels which are free to pivot, and thus the effective value of $C_{\alpha f}$ is very small. Examination of (5-16) then shows that k_{us} is always positive because the term $W_f/C_{\alpha f}$ will be very large. Thus the conventional front caster wheelchair is stable at all speeds as previously discussed. This is a well known and expected result.

Case Two: Rear Caster Wheelchair

If the pivoting caster wheels are at the rear of the wheelchair, then it is the rear cornering stiffness that becomes effectively very small. If $C_{\alpha r}$ approaches zero, the coefficient k_{us} in (5-16) is a negative number with very large magnitude. The left hand side of equation (5-14), which must be positive for directional stability, approaches $-\infty$. Thus, if the rear casters are considered to offer zero resistance to turning, the rear caster wheelchair is in a sense infinitely unstable. In this case, the critical speed obtained from equation (5-16) will approach zero, indicating that a rear caster wheelchair will be unstable at any speed.

In actuality the resistance of the caster wheels to turning is not zero but instead is only very small. The implication of this is that there is some speed, small as it may be, below which rear caster wheelchairs will be directionally stable. This speed cannot be determined using the simplified zero width model because there is no way to determine the effective cornering stiffness of the pivoting casters. Because the model assumes that all four wheels are locked against turning, the pivoting casters can only be considered in a qualitative sense as just described. A more detailed analysis of caster effects must be accomplished by using a more sophisticated model.

Given that rear caster wheelchairs are virtually always directionally unstable, the primary consideration then becomes a question of what can be done to reduce the stability problem. If the assumption is made that $C_{\alpha r}$ is very small so that the magnitude of $W_r/C_{\alpha r}$ is much greater than the magnitude of $W_f/C_{\alpha f}$, then the stability condition given in equation (5-14) becomes for rear caster wheelchairs

$$\frac{-\dot{u}^2 W_r}{C_{\alpha r}} + s > 0 \qquad (5\text{-}18)$$

Because $C_{\alpha r}$ is very small, this condition will only be satisfied for very low forward velocities. This is consistent with observation, where users of rear caster wheelchairs report the most difficulty when trying to maneuver at higher speeds. Unless $\dot{u}$ is small, the first term in equation (5-18) will be extremely negative, and the rear caster wheelchair will be directionally unstable. The degree to which the left side of equation (5-18) is negative is a measure of how unstable a given wheelchair or vehicle will be. Because the velocity $\dot{u}$ is raised to the second power, it is clear that directional stability is highly sensitive to forward speed. Note that this is somewhat surprising because it was shown in Chapter 2 that the magnitude of the destabilizing cornering force is nearly independent of speed. It can also be seen from equation (5-18) that the degree of instability can be minimized by increasing the total wheelbase distance s or by reducing the amount of weight on the rear wheels, W_r. This later statement is equivalent to stating that the center of gravity should be moved as far forward as possible, a result which is consistent with the simplified analysis of Kauzlarich and Thacker described in Chapter 1.

A useful but discouraging conclusion can be proposed as a result of examining the zero width model. Because equation (5-18) will yield extremely negative values for nearly all center of gravity positions, and because the wheelbase term in (5-18), s, is much smaller than the velocity dependent term, it may be the case that even fairly drastic design changes will not lead to a significant increase in directional stability. Since the zero width model cannot predict actual wheelchair motion, this conclusion can only be proven or disproven by using a more sophisticated model.

THE ZERO WIDTH MODEL AS A VERIFICATION TOOL

It has already been stated that one goal of this research is to develop a computer program capable of simulating wheelchair motion and examining directional stability for various initial conditions. For any complex program the problem of verification is always present. How can one be sure that the motion predicted by the simulation program is reasonable? The zero width model provides one good means for such verification. The simplified analysis of this chapter cannot be used to predict actual critical speeds for wheelchairs because it began by assuming that all four tires are locked against turning. However, an interesting result is obtained if one assumes the unrealistic case where all four wheels of a wheelchair are locked.

It will be shown later that for a typical rear caster wheelchair with all four wheels locked, equation (5-15) predicts a critical speed close to 123 m/sec (27 mph). This is obviously out of the range of operating speeds for manual wheelchairs and has no practical significance. However, any simulation program for modeling wheelchair motion should be able to approximately predict this value of critical speed for the hypothetical case where the caster wheels are locked against turning. This is an excellent tool which will be discussed again when program verification is considered in more detail.

An additional prediction about wheelchair motion results by again considering the understeer coefficient k_{us} defined by equation (5-16). The terms understeer and oversteer were originally defined in reference to the path of motion of a vehicle which is acted upon by a side force at the center of gravity. [2.3] Figure 5-3 shows the directional responses of neutral steer, understeer, and oversteer vehicles subjected to such a side force.

A front caster wheelchair corresponds to a positive value of k_{us} as described previously. A vehicle having k_{us} greater than zero is said to exhibit understeer. When such a vehicle is subjected to a side force as shown in Figure 5-3, the lateral force generated by the rear tires is greater than that generated by the front tires. As a result, the front tires tend to "give way" and a front caster wheelchair will turn away from the side force as in Figure 5-3.

If K_{us} is less than zero, the opposite situation results. This is the case for a rear caster wheelchair where the lateral force generated by the front tires is greater than that generated by the rear tires. In this case, the rear wheels will tend to rotate about the center of mass and the wheelchair will follow the oversteer path

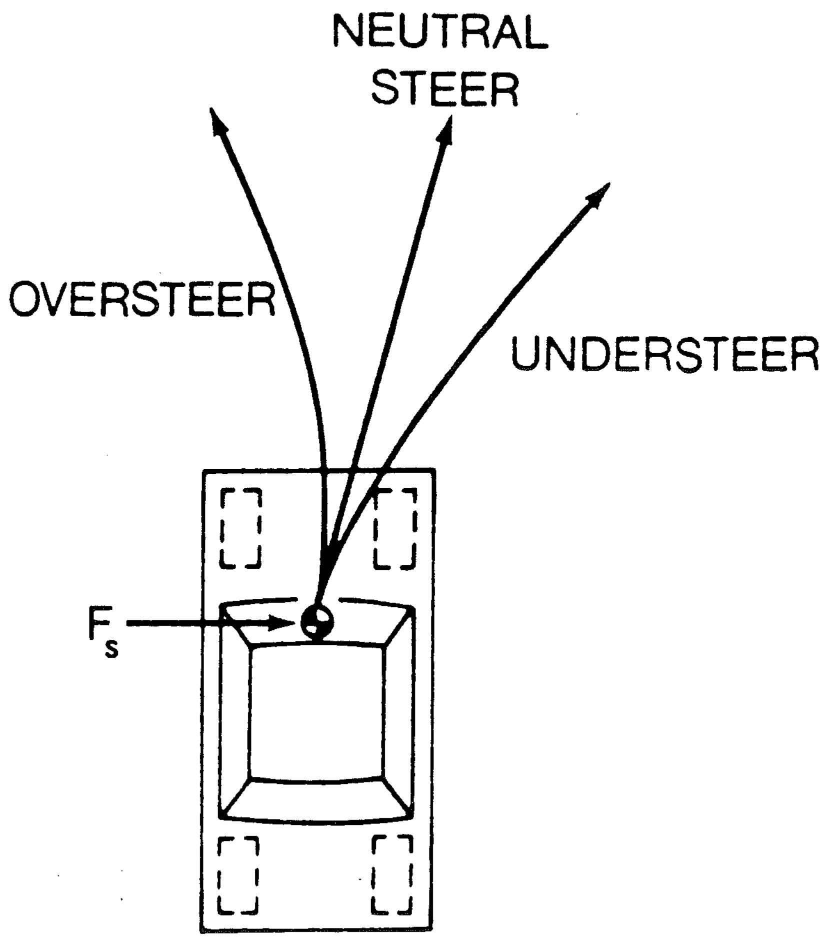

Figure 5-3 Expected Trajectories for Vehicles Exhibiting Understeer and Oversteer

shown in Figure 5-3. The motion paths illustrated by Figure 5-3 are easily visualized by imagining the response of a stationary manual wheelchair which is pushed from the side. Although the understeer and oversteer directional response paths say nothing quantitative about wheelchair motion, they do provide a qualitative prediction that must be in agreement with the results of any simulation computer program.

In the last chapter of this thesis, the application of a side force at the center of gravity will be used as the initial disturbance tending to make a wheelchair deviate from a desired directional heading. A measure of stability will be the response of a given wheelchair after the application of this disturbance. By examining the computer simulated responses of both front and rear caster wheelchairs, and comparing to the response paths shown in Figure 5-3, it will at least be possible to determine whether or not the correct type of motion is predicted.

CHAPTER 6

DESCRIBING PLANAR WHEELCHAIR MOTION IN MORE DETAIL

To begin this chapter, it is worthwhile to summarize what has been done up to this point. In Chapters 1-3 the important wheelchair tire forces were described, and some simple empirical methods for predicting these tire forces were given. This was essential because it is impossible to solve the equations of wheelchair motion without some knowledge of the forces that act on the tires. Chapter 4 developed the general form of the equations of motion using a set of body fixed axes moving with the wheelchair (equation 5-4). The simplified zero width model was used to identify the key variables which are relevant to directional stability, and to gain some insight with respect to why rear caster wheelchairs are especially unstable. The simplified model however, cannot predict actual wheelchair motion, nor does it allow an extensive examination of the parameters which affect stability.

There are still two major hurdles to be overcome before a more detailed analysis can be performed. First of all, the complete equations of motion which take into account width dimensions and pivoting of the casters must be formulated. Secondly, a computer program to solve the equations of motion, and to include the effects of variables such as camber angle, toe angle, caster friction, and lateral load transfer, must be written and verified.

At this point, no conclusion can be made with regard to whether or not a more sophisticated model will lead to ways to significantly reduce the directional instability problem associated with rear caster wheelchairs. Although rear caster wheelchairs are the primary focus, it is a goal of this work to present methods and models which are also applicable to front caster wheelchairs, electric wheelchairs, three wheeled wheelchairs, etc. For this reason it is desirable to create a model that is as general as possible while at the same time being fairly manageable.

THE COMPLETE WHEELCHAIR MODEL

The basic model which will be used to simulate wheelchair motion is shown in Figure 6-1. For this analysis, planar motion will be assumed. Pitch and roll effects will not appear in the final equations of motion. However, a quasi-static method for accounting for lateral load transfer will be incorporated. This will be described later in this chapter. Five degrees of freedom are assumed corresponding to translation and rotation of the center of mass and to rotation of each of the caster wheels. These are represented by u, v, θ, η, and β in the figure.

In an attempt to make the following discussion as clear as possible, the model shown in Figure 6-1 utilizes several of the symbols and concepts which were developed for the zero width model in Chapter 5. First note that the body fixed axes ($\hat{c}_1$, $\hat{c}_2$, and $\hat{c}_3$) are the same. Again, these correspond to the body fixed x, y and z axes. The inertial

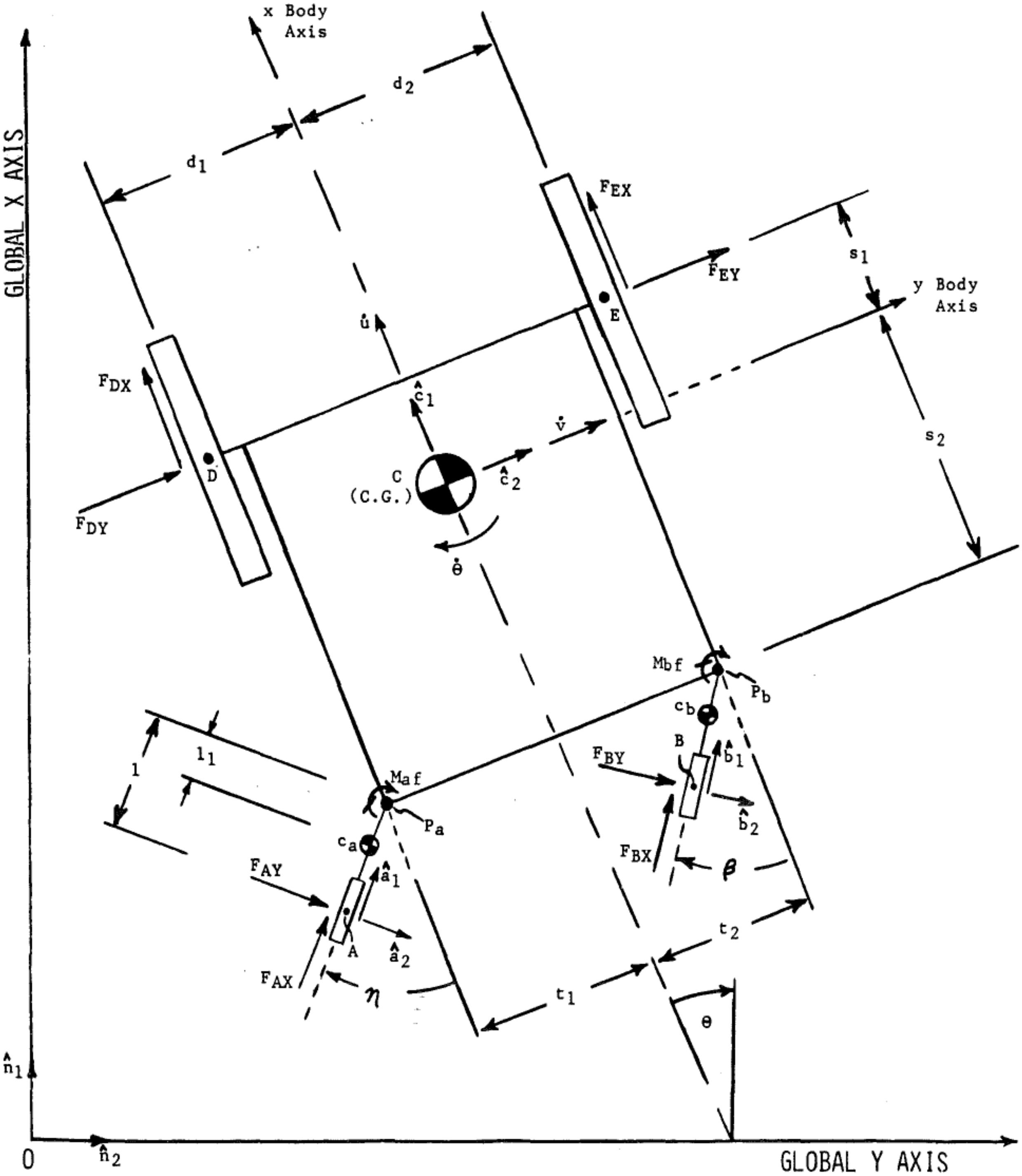

Figure 6-1 A Complete Wheelchair Model

or global reference frame corresponding to the fixed X and Y axes are also the same. The unit vectors $\hat{n}_1$ and $\hat{n}_2$ indicate global directions as before. Note that the model is drawn to depict a rear caster wheelchair. This is not a restriction however, as it will be shown that the same model can be used to investigate the motion of front caster wheelchairs.

There are two additional reference frames that were not present for the zero width model. These are represented by the unit vectors $\hat{a}_1, \hat{a}_2$ and $\hat{b}_1, \hat{b}_2$ which describe directions in two local reference frames fixed within the two pivoting caster wheels. For this model, the letters A, B, D, and E correspond to the contact points of the four tires as shown. Similarly, the letter C corresponds to the wheelchair-user center of gravity. Note that the unit vectors fixed in the caster wheels correspond to the x and y tire axes as shown in Figure 2-1. C_a and C_b indicate the centers of gravity of the two caster assemblies. P_a and P_b indicate the two pins about which casters A and B pivot.

In Figure 6-1 the symbol F represents force, and appropriate subscripts are used to indicate which tire a particular force is acting on and the tire axis along which the force acts. For example, F_{AX} represents the longitudinal road force acting on caster A and F_{AY} represents the lateral road force. M_{af} and M_{bf} are frictional moments which act at the caster pins and tend to resist rotation of the caster wheels.

The symbolic dimensions of the model are shown on the figure. In a manner similar to what was done for the zero width model, s_1 represents the distance from the front wheel contact points to the center of gravity, while s_2 represents the distance from the caster pins to the center of gravity. Note that in this case the total wheelbase distance is not s as was the case with the zero width model, but instead is $s_1 + s_2 + l$ where l is the caster trail distance. For a complete description of every symbol shown in Figure 6-1, refer to the list of symbols that precedes the text.

Finally, $\dot{u}$ and $\dot{v}$ are again used as the kinematic variables in the body fixed x and y directions. Angular displacement of the entire wheelchair with respect to the global X-Y axes is represented by θ. θ is positive in the $\hat{c}_3$ direction (clockwise rotation as shown in Figure 6-1.) Angular displacement of the individual casters with respect to the wheelchair frame will be measured by the angles η and β as shown. These are also positive clockwise.

It has not been assumed that the wheelchair is symmetric about the center of gravity. The tire forces at each wheel will be calculated individually. This is why it was stated in earlier chapters that a knowledge of the forces acting on a single wheelchair tire is desirable. Note that the forces shown on the tires in Figure 6-1 are not constant, but instead vary depending on the state of motion of the wheelchair at a given instant in time. The tire forces depend on load, slip angle, and other variables as discussed in Chapters 1 through 3.

Although this model is able to account for variations of several different parameters, it is certainly not all inclusive. Because the model assumes that the chair and user are lumped together as one mass, it will not be able to account for shifts in the user's weight as the wheelchair moves. Furthermore, it is important to remember that the normal loads and slip angles allowed for each tire will be limited to the ranges for which experimental tire data was collected. This means that excessive loads or types of motion that result in large lateral wheel velocities and large slip angles will not be allowable.

DERIVING THE EQUATIONS OF MOTION

The equations of motion for the wheelchair and user system will be derived in terms of the variables shown in Figure 6-1. It will be shown later how the actual magnitude of the varying tire forces are determined and implemented. The reader who is not interested in the details of this derivation may skip directly to the end of this section where the final equations of motion are summarized in Table 6-1.

When deriving the equations of motion, several coordinate transformations relating the reference frames shown in Figure 6-1 will be useful. They are given below.

$$\hat{c}_1 = \cos(\theta)\hat{n}_1 + \sin(\theta)\hat{n}_2 \tag{6-1a}$$

$$\hat{c}_2 = -\sin(\theta)\hat{n}_1 + \cos(\theta)\hat{n}_2 \tag{6-1b}$$

$$\hat{a}_1 = \cos(\eta)\hat{c}_1 + \sin(\eta)\hat{c}_2 \tag{6-1c}$$

$$\hat{a}_2 = -\sin(\eta)\hat{c}_1 + \cos(\eta)\hat{c}_2 \tag{6-1d}$$

$$\hat{b}_1 = \cos(\beta)\hat{c}_1 + \sin(\beta)\hat{c}_2 \tag{6-1e}$$

$$\hat{b}_2 = -\sin(\beta)\hat{c}_1 + \cos(\beta)\hat{c}_2 \tag{6-1f}$$

also note $\hat{n}_3 = \hat{c}_3 = \hat{a}_3 = \hat{b}_3$

Using equation (6-1c) through (6-1f) and Figure 6-1, the total force acting on the wheelchair, $\vec{F}_C$, can be written as:

$$\vec{F}_C = \left\{ \begin{array}{l} F_{DX} + F_{EX} + F_{AX}\cos(\eta) - F_{AY}\sin(\eta) \\ + F_{BX}\cos(\beta) - F_{BY}\sin(\beta) \end{array} \right\} \hat{c}_1 + \left\{ \begin{array}{l} F_{DY} + F_{EY} + F_{AX}\sin(\eta) + F_{AY}\cos(\eta) \\ + F_{BX}\sin(\beta) + F_{BY}\cos(\beta) \end{array} \right\} \hat{c}_2 \tag{6-2}$$

Summing moments about a the center of gravity results in the following expression for the total moment ($\vec{M}_C$) acting on the wheelchair-user system:

$$\vec{M}_C = \left\{ \begin{array}{l} (F_{DX}d_1 - F_{EX}d_2) + (F_{DY} + F_{EY})s_1 \\ + F_{AX}\{t_1\cos(\eta) - s_2\sin(\eta)\} \\ - F_{AY}\{t_1\sin(\eta) + s_2\cos(\eta) + 1\} \\ - F_{BX}\{t_2\cos(\beta) + s_2\sin(\beta)\} \\ + F_{BY}\{t_2\sin(\beta) - s_2\cos(\beta) - 1\} \end{array} \right\} \hat{c}_3 \tag{6-3}$$

Equations (6-2) and (6-3) can be used to obtain expressions for $\ddot{u}$, $\ddot{v}$, and $\ddot{\theta}$. This is done using the equations of motion for the body fixed reference frame (5-4a through 5-4c) given in Chapter 5. This yields

$$\ddot{u} = \frac{\sum F_x}{m} + \dot{\theta}\dot{v} \tag{6-4}$$

$$\ddot{v} = \frac{\sum F_y}{m} - \dot{\theta}\dot{u} \qquad (6\text{-}5)$$

$$\ddot{\theta} = \frac{\sum M_c}{I_z} \qquad (6\text{-}6)$$

where $\sum F_x$ = the lateral or $\hat{c}_1$ component of equation (6-2)

$\sum F_y$ = the longitudinal or $\hat{c}_2$ component of equation (6-2)

I_z = the mass moment of inertia of the wheelchair-user system about a vertical axis through the c.g.

Equations (6-4) through (6-6) are written in their final form in Table 6-1 which summarizes the equations of motion.

Although the equations of motion just given are adequate for obtaining expressions for $\ddot{u}$, $\ddot{v}$, and $\ddot{\theta}$, they cannot be used to determine the motion of the individual casters. In order to completely describe all 5 degrees of freedom of the model shown in Figure 6-1, it is necessary to formulate expressions for the angular accelerations of the caster wheels, $\ddot{\eta}$ and $\ddot{\beta}$. One way to do this is to sum moments about the center of gravity of each of the casters. However, this is not a straight forward procedure because it involves determining the unknown reaction forces at the caster pins. A simpler method of determining $\ddot{\eta}$ and $\ddot{\beta}$ is to sum moments about the caster pins themselves, and in so doing eliminate the unknown reaction forces. The price to be paid for doing this is that the angular acceleration is no longer simply the sum of the moments divided by the mass moment of inertia. This will be illustrated next where an expression for the angular acceleration of caster A will be determined.

The expression which relates the resultant moment on caster A to the angular acceleration of caster A is: [5.5]

$$\vec{M}_{Pa} = I_{zP}(\ddot{\eta})\hat{c}_3 + \vec{r}_{PaCa} \times m_c\vec{a}_{Pa} \qquad (6\text{-}7)$$

where: $\vec{M}_{Pa}$ = sum of moments on caster A about it pivot point

I_{zP} = moment of inertia of caster wheels about a vertical axis passing through their pivot points

$\vec{r}_{PaCa}$ = displacement vector directed from the pivot point Pa to the caster center of gravity C_a

m_c = mass of the caster assemblies

$\vec{a}_{Pa}$ = acceleration of point P_a relative to the caster center of gravity

Note that this type of subscript notation will be used throughout this section. Again, the reader is referred to the list of symbols for clarification of any variables for which the meaning is not clear. To evaluate (6-7) some additional expressions must be formulated. The reader is advised that the next several steps are all for the purpose of solving for $\ddot{\eta}$ in equation (6-7). The acceleration of pin P_a is related to the acceleration of the wheelchair center of mass as follows:

$$\vec{a}_{Pa} = \vec{a}_c + \vec{\ddot{\theta}} \times \vec{r}_{cPa} + \vec{\dot{\theta}} \times (\vec{\dot{\theta}} \times \vec{r}_{cPa}) \qquad (6\text{-}8)$$

where $\vec{a}_c$ = the acceleration of the wheelchair center of mass as observed in the body fixed reference frame

and $\vec{r}_{cPa}$ = displacement vector from the wheelchair center of gravity to pin P_a

Specifically, $\vec{r}_{cPa} = -s_2\hat{c}_1 - t_1\hat{c}_2$ (6-9)

Then, substituting (6-9) into (6-8) gives:

$$\vec{a}_{Pa} = \vec{a}_c + (\ddot{\theta}t_1 + \dot{\theta}^2 s_2)\hat{c}_1 - (\ddot{\theta}s_2 - \dot{\theta}^2 t_1)\hat{c}_2 \quad (6\text{-}10)$$

Using equation 6-2 to obtain an expression for $\vec{a}_c$, along with equation (6-10) results in the following expression for the term $m_c\vec{a}_{Pa}$ in equation (6-7),

$$m_c\vec{a}_{Pa} = \frac{m_c}{m}\left\{\begin{array}{l} F_{DX} + F_{EX} + F_{AX}\cos(\eta) - \\ F_{AY}\sin(\eta) + F_{BX}\cos(\beta) - \\ F_{BY}\sin(\beta) + m(\ddot{\theta}t_1+\dot{\theta}^2 s_2) \end{array}\right\}\hat{c}_1$$
$$+ \frac{m_c}{m}\left\{\begin{array}{l} F_{DY} + F_{EY} + F_{AX}\sin(\eta) + \\ F_{AY}\cos(\eta) + F_{BX}\sin(\beta) + \\ F_{BY}\cos(\beta) - m(\ddot{\theta}s_2-\dot{\theta}^2 t_1) \end{array}\right\}\hat{c}_2 \quad (6\text{-}11)$$

Next, an inspection of Figure 6-1 shows that

$$\vec{r}_{PaCa} = -l_1\hat{a}_1$$

or using (6-1) $\vec{r}_{PaCa} = -l_1\cos(\eta)\hat{c}_1 - l_1\sin(\eta)\hat{c}_2$ (6-12)

Before continuing, note that equation (6-7), the one that contains $\ddot{\eta}$ for which we are trying solve, can be written as follows:

$$\ddot{\eta}\hat{c}_3 = \frac{\vec{M}_{Pa} - (\vec{r}_{PaCa} \times m_c\vec{a}_{Pa})}{I_{zP}}\hat{c}_3 \quad (6\text{-}13)$$

Also, the resultant moment ($\vec{M}_{Pa}$) acting on caster A about the caster pin P_a is:

$$\vec{M}_{Pa} = (M_{af} - F_{AY}l)\hat{c}_3 \quad (6\text{-}14)$$

Equation (6-14) is the first term in the numerator on the right hand side of equation (6-13). The cross product term in equation (6-13) can be evaluated using (6-12) and (6-11). When doing this the following identities are employed:

$$\cos^2 x \; + \; \sin^2 x \; = \; 1 \tag{6-15a}$$

$$\cos(x)\sin(y) - \sin(x)\cos(y) = \sin(y-x) \tag{6-15b}$$

$$\sin(x)\sin(y) + \cos(x)\cos(y) = \cos(y-x) \tag{6-15c}$$

The final result for $\ddot{\eta}$ after much manipulation is

$$\ddot{\eta} = \frac{l_1 m_c}{I_z p m} \times \left\{ \begin{array}{l} M_{af}\left(\dfrac{m}{l_1 m_c}\right) + F_{AY}\left(1 - \dfrac{lm}{l_1 m_c}\right) \\ - F_{BX}\sin(\eta-\beta) + F_{BY}\cos(\eta-\beta) \\ + (F_{DY} + F_{EY})\cos(\eta) \\ - (F_{DX} + F_{EX})\sin(\eta) \\ - m\ddot{\theta}\{t_1\sin(\eta) + s_2\cos(\eta)\} \\ + m\dot{\theta}^2\{t_1\cos(\eta) - s_2\sin(\eta)\} \end{array} \right\} \tag{6-16}$$

The procedure used to find an expression for $\ddot{\beta}$ is exactly analogous to that just used to obtain equation (6-16). When finding $\ddot{\beta}$ however, moments are summed about caster pin P_b rather than P_a, and the displacement vectors, $\vec{r}$, used in obtaining equation (6-16) are not be the same.

Table 6-1 summarizes the equations of motion for the five variables $\ddot{u}$, $\ddot{v}$, $\ddot{\theta}$,$\ddot{\eta}$, and $\ddot{\beta}$. The equations are non-linear, coupled, second order differential equations. As a result, only numerical solutions are feasible. Again, all of the forces appearing in Table 6-1 vary with time and must be treated accordingly.

TABLE 6-1

WHEELCHAIR EQUATIONS OF MOTION

$$\ddot{u} = \frac{1}{m}\left[\begin{array}{l} F_{DX} + F_{EX} + F_{AX}\cos(\eta) - F_{AY}\sin(\eta) \\ + F_{BX}\cos(\beta) - F_{BY}\sin(\beta) \end{array}\right] + \dot{\theta}\dot{v} \tag{6-17}$$

$$\ddot{v} = \frac{1}{m}\left[\begin{array}{l} F_{DY} + F_{EY} + F_{AX}\sin(\eta) + F_{AY}\cos(\eta) \\ + F_{BX}\sin(\beta) + F_{BY}\cos(\beta) \end{array}\right] - \dot{\theta}\dot{u} \tag{6-18}$$

$$\ddot{\theta} = \frac{1}{I_z}\left\{\begin{array}{l} (F_{DX}d_1 - F_{EX}d_2) + (F_{DY} + F_{EY})s_1 \\ + F_{AX}\{t_1\cos(\eta) - s_2\sin(\eta)\} \\ - F_{AY}\{t_1\sin(\eta) + s_2\cos(\eta) + l\} \\ - F_{BX}\{t_2\cos(\beta) + s_2\sin(\beta)\} \\ + F_{BY}\{t_2\sin(\beta) - s_2\cos(\beta) - l\} \end{array}\right\} \tag{6-19}$$

$$\ddot{\eta} = \frac{l_1 m_c}{I_z p m}\left\{\begin{array}{l} M_{af}\left(\frac{m}{l_1 m_c}\right) + F_{AY}\left(1 - \frac{lm}{l_1 m_c}\right) \\ - F_{BX}\sin(\eta-\beta) + F_{BY}\cos(\eta-\beta) \\ + (F_{DY} + F_{EY})\cos(\eta) \\ - (F_{DX} + F_{EX})\sin(\eta) \\ - m\ddot{\theta}\{t_1\sin(\eta) + s_2\cos(\eta)\} \\ + m\dot{\theta}^2\{t_1\cos(\eta) - s_2\sin(\eta)\} \end{array}\right\} \tag{6-20}$$

$$\ddot{\beta} = \frac{l_1 m_c}{I_z p m}\left\{\begin{array}{l} M_{bf}\left(\frac{m}{l_1 m_c}\right) + F_{BY}\left(1 - \frac{lm}{l_1 m_c}\right) \\ + F_{AX}\sin(\eta-\beta) + F_{AY}\cos(\eta-\beta) \\ + (F_{DY} + F_{EY})\cos(\beta) \\ - (F_{DX} + F_{EX})\sin(\beta) \\ + m\ddot{\theta}\{t_2\sin(\beta) - s_2\cos(\beta)\} \\ - m\dot{\theta}^2\{t_2\cos(\beta) + s_2\sin(\beta)\} \end{array}\right\} \tag{6-21}$$

DETERMINING THE SLIP ANGLE AT EACH TIRE

Recall that cornering force F_y is primarily a function of normal force and slip angle. Therefore, in order to compute the magnitudes of the F_y forces in the equations of motion given in Table 6-1 it will be necessary to determine both the slip angle and the normal force at each of the four wheelchair tires at any instant in time. This section describes how the slip angles can be determined. The next section discusses how the normal force at each tire can be found using a quasi-static approximation.

The basic equation for the slip angle α of any rolling tire was given in equation (5-7). In order to determine the magnitude of α both the lateral and longitudinal velocity components of each tire must be known. This requires determining the $\hat{c}_1$ and $\hat{c}_2$ components of velocity for tires D and E in Figure 6-1, the $\hat{a}_1$ and $\hat{a}_2$ components of velocity for tire A, and the $\hat{b}_1$ and $\hat{b}_2$ components of velocity for tire B.

The vector velocity of points A, B, D, and E are given by:

$$\vec{V}_D = (\dot{u} + \dot{\theta}d_1)\hat{c}_1 + (\dot{v} + \dot{\theta}s_1)\hat{c}_2 \tag{6-17a}$$

$$\vec{V}_E = (\dot{u} - \dot{\theta}d_2)\hat{c}_1 + (\dot{v} + \dot{\theta}s_1)\hat{c}_2 \tag{6-17b}$$

$$\begin{aligned}\vec{V}_A = &\begin{bmatrix} \dot{u}\cos(\eta) + \dot{v}\sin(\eta) + \dot{\theta}t_1\cos(\eta) \\ - \dot{\theta}s_2\sin(\eta) \end{bmatrix} \hat{a}_1 \\ - &\begin{bmatrix} \dot{u}\sin(\eta) - \dot{v}\cos(\eta) + \dot{\theta}t_1\sin(\eta) \\ + \dot{\theta}s_2\cos(\eta) + (\dot{\eta})l \end{bmatrix} \hat{a}_2\end{aligned} \tag{6-17c}$$

$$\vec{V}_B = \begin{bmatrix} \dot{u}\cos(\beta) + \dot{v}\sin(\beta) - \dot{\theta}t_2\cos(\beta) \\ - \dot{\theta}s_2\sin(\beta) \end{bmatrix} \hat{b}_1 - \begin{bmatrix} \dot{u}\sin(\beta) - \dot{v}\cos(\beta) - \dot{\theta}t_2\sin(\beta) \\ + \dot{\theta}s_2\cos(\beta) + (\dot{\beta})l \end{bmatrix} \hat{b}_2 \qquad (6\text{-}17d)$$

Then using equation (5-7), the instantaneous magnitude of the slip angle for each of the four wheelchair tires is:

$$\alpha_D = \tan^{-1}\left(\frac{\dot{v} + \dot{\theta}s_1}{\dot{u} + \dot{\theta}d_1}\right) \qquad (6\text{-}18a)$$

$$\alpha_E = \tan^{-1}\left(\frac{\dot{v} + \dot{\theta}s_1}{\dot{u} - \dot{\theta}d_2}\right) \qquad (6\text{-}18b)$$

$$\alpha_A = \tan^{-1}\left(\frac{\dot{u}\sin(\eta)-\dot{v}\cos(\eta)+\dot{\theta}t_1\sin(\eta)+\dot{\theta}s_2\cos(\eta)+\dot{\eta}l}{\dot{u}\cos(\eta)+\dot{v}\sin(\eta)+\dot{\theta}t_1\cos(\eta)-\dot{\theta}s_2\sin(\eta)}\right) \qquad (6\text{-}18c)$$

$$\alpha_B = \tan^{-1}\left(\frac{-\dot{u}\sin(\beta)+\dot{v}\cos(\beta)+\dot{\theta}t_2\sin(\beta)-\dot{\theta}s_2\cos(\beta)-\dot{\beta}l}{\dot{u}\cos(\beta)+\dot{v}\sin(\beta)-\dot{\theta}t_2\cos(\beta)-\dot{\theta}s_2\sin(\beta)}\right) \qquad (6\text{-}18d)$$

Equations (6-18a) through (6-18d) can be used to find the slip angle at each wheelchair tire provided that the instantaneous value of the other kinematic variables are known. The term instantaneous is used because the forces, slip angles, and other variables will all be transient as a wheelchair moves along a given path. The next chapter will explain how equations (6-18) are actually incorporated into a computer program which simulates wheelchair motion.

A QUASI-STATIC METHOD TO ACCOUNT FOR LATERAL LOAD TRANSFER

As a vehicle travels along a curved path, the normal force on each of the wheels is in general different. In particular, the two wheels at the outer radius of a turn experience a greater normal force than the two wheels at the inner radius. It was shown in Chapter 2 that lateral cornering force is significantly affected by the magnitude of the normal force on a given tire.

Because the relationship between normal force and cornering force is nonlinear, the transfer of load from the inside wheels to the outside wheels during a turning maneuver tends to reduce the total lateral force developed by a pair of tires. This can be understood by examining Figure 6-2. The curve shown in Figure 6-2 shows normal force versus cornering force at constant slip angle, and it is identical to the curves that were presented in Figures 3-4a through 3-4g. Consider a pair of tires, each of which develops cornering force F_y when subjected to a constant slip angle α. If lateral load transfer is neglected, the total lateral force developed by this pair of tires will be equal to $2F_y$. However, as the pair of wheels negotiates a turn, the normal force on the inside wheel will be reduced to F_{zi}, while the normal force on the outside wheel will be increased to F_{zo}. Due to the nonlinear nature of the cornering force curve, the total cornering force developed by the two tires ($F_{yi} + F_{yo}$) will be less than 2_{Fy} as shown in Figure 6-2. [2.2,4.3]

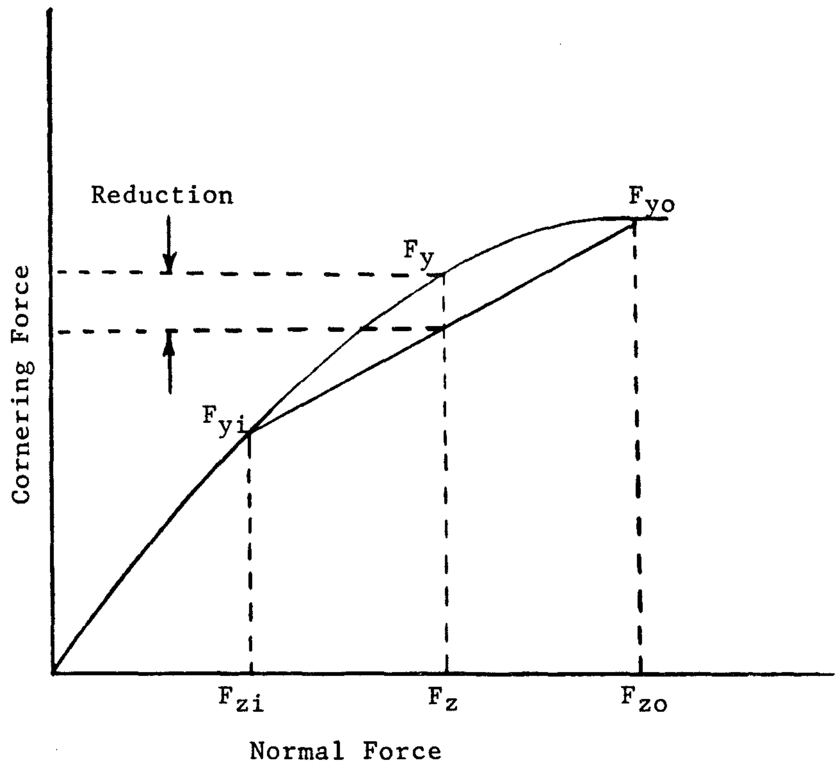

Figure 6-2 Reduction in Total Cornering Force due to Lateral Load Transfer

Dugoff, Fancher, and Segel present one method for accounting for lateral load transfer when simulating vehicle dynamics. [6.1] Their approach utilizes the vehicle geometry shown in Figure 6-3. Most of the symbols shown in the figure have been previously defined. In Figure 6-3, h is the height of the vehicle center of gravity and t is the lateral distance to each tire contact point. Note that the model used by Dugoff, Fancher, and Segel assumes that the lateral distance to each tire contact point is the same, and that there is no caster trail distance. By comparing Figure 6-1 with Figure 6-3, it can be seen that their model is a special case of the rear caster wheelchair model given at the beginning of this chapter, with $t_1 = t_2 = d_1 = d_2 = t$, and $l = 0$. The vehicle geometry in Figure 6-3 was developed to represent an automobile and thus requires some modification. This section will first discuss the original geometry as presented by Dugoff, Fancher, and Segel, and then the necessary modifications will be considered.

The quasi-static approximation for lateral load transfer begins by assuming that the roll angle $\emptyset$ of the vehicle can be estimated as

$$\emptyset = \frac{-h \sum F_y}{k_f + k_r} \tag{6-19}$$

where k_f and k_r are referred to as the front and rear roll stiffnesses. The dimensions of k_f and k_r are n-m/rad or ft-lbf/rad.

Equation (6-19) simply states that the product of the

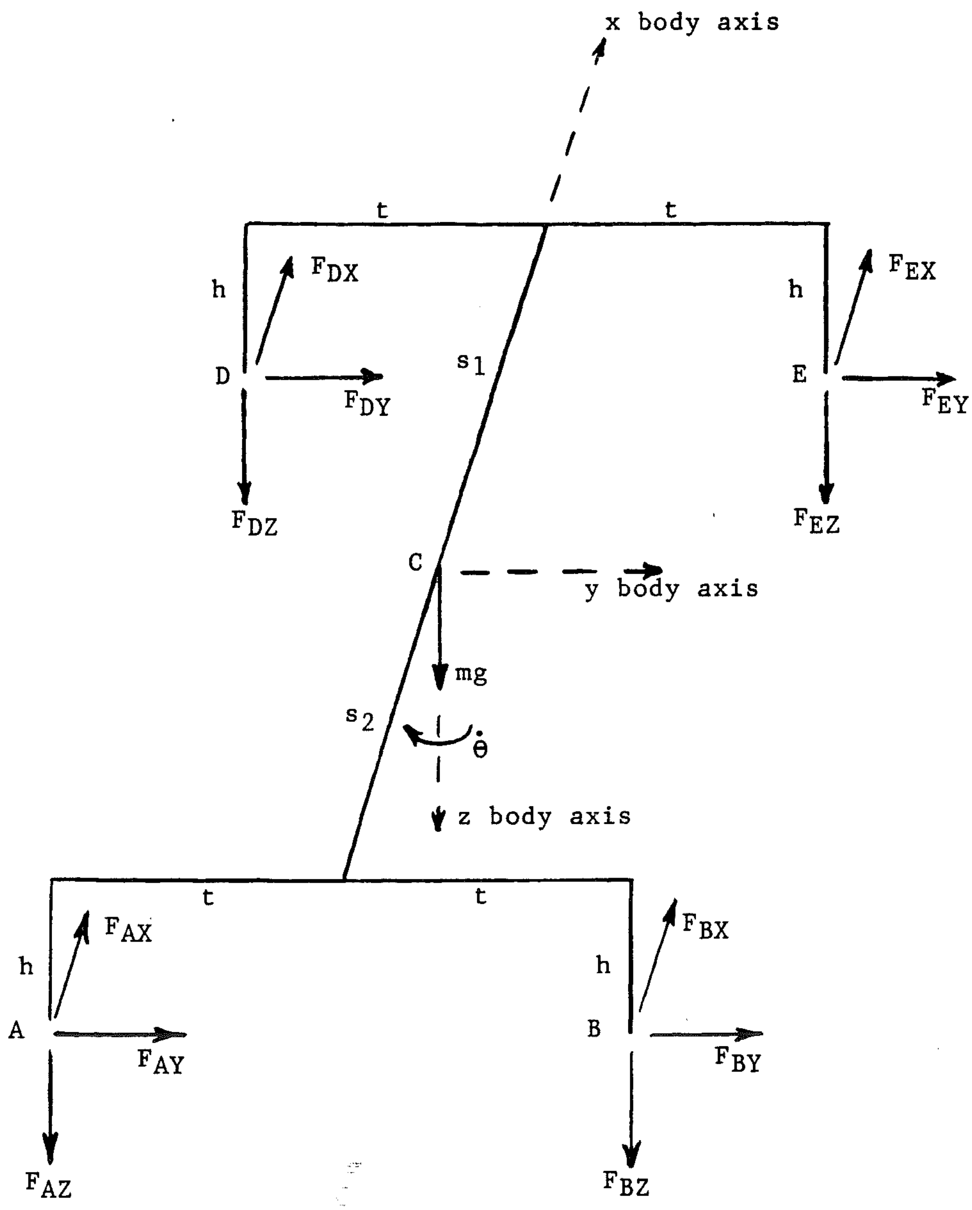

Figure 6-3 Vehicle Geometry Used to Account for the Lateral Load Transfer of Automobiles

total roll stiffness ($k_f + k_r$) and the roll angle ($\emptyset$) is equal to the total moment about the longitudinal (x) axis of the vehicle. A further assumption is made that the total load transfer has two components. The first component is due to the difference in the normal forces acting on the front tires. The difference in the front tire normal forces tends to roll the vehicle, but this tendency is counteracted by the front roll stiffness. The second component of lateral load transfer is produced by the difference in the normal forces at the rear tires. This difference is offset by the rear roll stiffness.

It is also assumed that the vehicle does not develop any velocity in the z direction, and that the vehicle can not rotate about its y axis. With these assumptions it is possible to write the following static equations:

$$F_{AZ}t - F_{BZ}t = -\sum F_y h\left(\frac{k_r}{k_f + k_r}\right) \tag{6-20a}$$

$$F_{DZ}t - F_{EZ}t = -\sum F_y h\left(\frac{k_f}{k_f + k_r}\right) \tag{6-20b}$$

$$F_{AZ} + F_{BZ} + F_{DZ} + F_{EZ} = -mg \tag{6-20c}$$

$$-F_{AZ}s_2 - F_{BZ}s_2 + F_{DZ}s_1 + F_{EZ}s_1 = \sum F_x h \tag{6-20d}$$

Using a system of equations such as this to account for lateral load transfer is referred to as a quasi-static method. This term results from the fact that a series of static equations are used to partially describe the behavior of a vehicle which is actually moving. Note that if equations (6-20a) and (6-20b) are added together the following equation results:

$$F_{AZ}t - F_{BZ}t + F_{DZ}t - F_{EZ}t = -\sum F_y h \qquad (6\text{-}21)$$

This is the same equation that results simply from summing moments about the x axis. However, equations (6-20c),(6-20d) and (6-21) alone do not form a determinate set of equations. Using equations (6-20a) through (6-20d) it is possible to simultaneously solve for the normal forces acting at each wheelchair tire. These are given by: [6.1]

$$F_{AZ} = -\frac{mg}{2}\left(\frac{s_1}{s_1+s_2}\right) - \frac{h\sum F_x}{2(s_1+s_2)} - \frac{k_r}{k_f+k_r}\left[\frac{h\sum F_y}{2t}\right] \qquad (6\text{-}22a)$$

$$F_{BZ} = -\frac{mg}{2}\left(\frac{s_1}{s_1+s_2}\right) - \frac{h\sum F_x}{2(s_1+s_2)} + \frac{k_r}{k_f+k_r}\left[\frac{h\sum F_y}{2t}\right] \qquad (6\text{-}22b)$$

$$F_{DZ} = -\frac{mg}{2}\left(\frac{s_2}{s_1+s_2}\right) + \frac{h\sum F_x}{2(s_1+s_2)} - \frac{k_f}{k_f+k_r}\left[\frac{h\sum F_y}{2t}\right] \qquad (6\text{-}22c)$$

$$F_{EZ} = -\frac{mg}{2}\left(\frac{s_2}{s_1+s_2}\right) + \frac{h\sum F_x}{2(s_1+s_2)} + \frac{k_f}{k_f+k_r}\left[\frac{h\sum F_y}{2t}\right] \qquad (6\text{-}22d)$$

Equation (6-22a) through (6-22d) make it possible to compute the normal force at each tire contact point. It is easily verified that if h = 0 (which is equivalent to neglecting load transfer), then the magnitudes of F_{AZ}, F_{BZ}, F_{DZ}, and F_{EZ} reduce to W_r and W_f as defined for the zero width model in Chapter 5. Specifically, if h = 0, then equations (6-22) give

$$F_{AZ} = F_{BZ} = \frac{-mg}{2}\left(\frac{s_1}{s_1+s_2}\right) = \frac{-Ws_1}{2s} = -W_r \qquad (6\text{-}23a)$$

$$F_{DZ} = F_{EZ} = \frac{-mg}{2}\left(\frac{s_2}{s_1+s_2}\right) = \frac{-Ws_2}{2s} = -W_f \qquad (6\text{-}23b)$$

Dugoff, Fancher, and Segel have shown that equations (6-22a) through (6-22d) provide a good approximation for the lateral load transfer effects associated with automobile motion. [6.1] In order to utilize this method, for the rear caster wheelchair model shown in Figure 6-1, some modification is necessary. For the rear caster wheelchair model the lateral and longitudinal distances of each tire contact point from the center of gravity are not all equal to t as was shown in Figure 6-3.

The necessary modification is made fairly easy by referring to Figure 6-1 and introducing the following definitions:

longitudinal distance to contact point A = $a_x = s_2 + l\cos(\eta)$ (6-24a)

longitudinal distance to contact point B = $b_x = s_2 + l\cos(\beta)$ (6-24b)

lateral distance to contact point A = $a_y = t_1 + l\sin(\eta)$ (6-24c)

lateral distance to contact point B = $b_y = t_2 - l\sin(\beta)$ (6-24d)

Using these definitions and again again assuming a height h for the center of gravity, the static equations for the wheelchair model shown in Figure 6-1 are

$$F_{AZ}a_y - F_{BZ}b_y = -\sum F_y h\left(\frac{k_r}{k_f + k_r}\right) \tag{6-25a}$$

$$F_{DZ}d_1 - F_{EZ}d_2 = -\sum F_y h\left(\frac{k_f}{k_f + k_r}\right) \tag{6-25b}$$

$$F_{AZ} + F_{BZ} + F_{DZ} + F_{EZ} = -mg \tag{6-25c}$$

$$-F_{AZ}a_x - F_{BZ}b_x + F_{DZ}s_1 + F_{EZ}s_1 = \sum F_x h \tag{6-25d}$$

These equations are identical to those given in equations (6-20) except for the variable changes introduced by referring to Figure 6-1 for the distances to the tire contact points.

In principle, it is possible to use (6-25) to solve for F_{AZ}, F_{BZ}, F_{DZ}, and F_{EZ} explicitly and obtain equations similar to those given in equations (6-20). In practice however, this becomes an algebraic nightmare due to the presence of four unequal width variables rather than a single value, t, as was the case before. A more useful technique for finding the normal forces at each tire using equation (6-25) is a sequential solution which is ideally suited for computer programming purposes. The solution proceeds as follows:

For convenience define:

$$C_1 = \frac{k_r}{k_f + k_r} \tag{6-26a}$$

and
$$C_2 = \frac{k_f}{k_f + k_r} \tag{6-26b}$$

Then the normal forces can be found in the following sequence:

$$F_{BZ} = \frac{\sum F_y h C_1 (s_1 + a_x) - \sum F_x h a_y - mgs_1 a_y}{s_1(a_y + b_y) + a_y b_x + a_x b_y} \tag{6-27a}$$

$$F_{EZ} = \frac{F_{BZ}(b_x + a_x b_y / a_y) + \sum F_y h (C_2 s_1 / d_1 - C_1 a_x / a_y) + \sum F_x h}{s_1(1 + d_2/d_1)} \tag{6-27b}$$

$$F_{DZ} = F_{EZ}\frac{d_2}{d_1} - \sum F_y \frac{hC_2}{d_1} \tag{6-27c}$$

$$F_{AZ} = F_{BZ}\frac{b_y}{a_y} - \sum F_y \frac{hC_1}{a_y} \tag{6-27d}$$

Equations (6-27a) through (6-27d) must be solved in the order given. They are easily adapted to a computer program. Note that in these equations, F_x and F_y are found for the wheelchair model using the longitudinal (c_1) and lateral (c_2) components of equation (6-2) as explained previously.

Finally, before equations (6-27) can actually be used, some estimate of the front and rear roll coefficients is necessary. In practice, only the ratio k_f/k_r must be known. This ratio will be defined as

$$k = \text{Roll Coefficient} = k_f/k_r \tag{6-28}$$

Or in words,

$$k = \frac{\text{Resistance of Front of Wheelchair to Roll}}{\text{Resistance of Rear of Wheelchair to Roll}} \tag{6-29}$$

Then the constants C_1 and C_2 which appear in equations (6-27) and were defined in (6-26) become simply

$$C_1 = \frac{1}{k + 1} \tag{6-30a}$$

$$C_2 = \frac{k}{k + 1} \tag{6-30b}$$

The final result of this manipulation is that given the total tire force acting on the wheelchair along its body fixed x and y axis, it is possible to compute the normal forces at each tire and account for lateral load transfer if the single parameter k can be estimated.

A value for k for wheelchairs was not experimentally determined as part of this research. For automobiles, k generally has a value in the range 2.0 - 3.0. [6.1,6.2] For the purposes of investigating wheelchair motion, an initial value of k = 1.0 was assumed. This is equivalent to assuming that the tendency of the front of the wheelchair to resist roll is equal to that of the rear of the wheelchair. As will be discussed in the next chapter, the computer program which was written to simulate wheelchair motion allows the user to vary the input value of k. This makes it possible to observe whether or not a value of k different than 1.0 has a significant effect on the resulting motion. The effect of varying k and of lateral load transfer in general is discussed again in Chapter 8.

CHAPTER 7

A COMPUTER PROGRAM TO SIMULATE WHEELCHAIR MOTION

Most of the basic concepts which are required for an investigation of wheelchair directional instability have now been discussed. In Chapter 4, a simple means of empirically determining wheelchair tire forces was presented. These tire forces are primarily a function of normal force F_z and slip angle α. In Chapter 6, the equations of motion were formulated, and equations for determining both the normal force and the slip angle at each of the four wheelchair tires were given. Fundamentally, this is all that is necessary in order to determine the directional response of a rear caster or front caster wheelchair.

This chapter will outline the method by which all of the ideas discussed up to this point can actually be implemented as part of a computer program which simulates wheelchair motion. In principle, the method is very straightforward. The purpose of this chapter is to describe the steps used by the actual computer program in a qualitative way, while referring to the actual computer code as little as possible. While doing this, it will often be necessary to refer to ideas or equations which were given in earlier chapters. It is in the formulation of the simulation program that all of the material previously presented comes together to allow an investigation of the parameters that affect directional stability.

BLOCK DIAGRAM OF THE SIMULATION PROGRAM

The basic method which will be used to simulate wheelchair motion is adapted from a simulation model described by Dugoff, Fancher and Segel. [6.1] Their model is intended for the study of automobile dynamics and therefore includes many parameters that are unimportant to wheelchair motion. For example, aerodynamic drag and steering system dynamics can be excluded from a study of wheelchair motion.

Figure 7-1 shows a block diagram of the wheelchair motion simulation program. The diagram begins in the upper left corner where the initial conditions are defined. Omitting the details for a moment, the basic simulation method proceeds as follows:

1) The initial state of motion and other necessary parameters are defined.

2) The current values for forward velocity and angular velocity (yaw velocity) are used to compute the slip angle at each wheelchair tire. The current normal force (F_z) at each tire is found from the current values of the longitudinal forces (F_x) and lateral forces (F_y).

3) Using the current value of normal force and the newly calculated slip angles from step 2, it is possible to determine new values for the lateral and longitudinal forces acting on each tire.

4) The forces at each tire are input into the equations of motion, which are in turn used to calculate the instantaneous accelerations ($\ddot{u}$, $\ddot{v}$, and $\ddot{\theta}$) of the wheelchair.

5) The instantaneous accelerations are assumed constant over a single iteration or time step. A single iteration is one

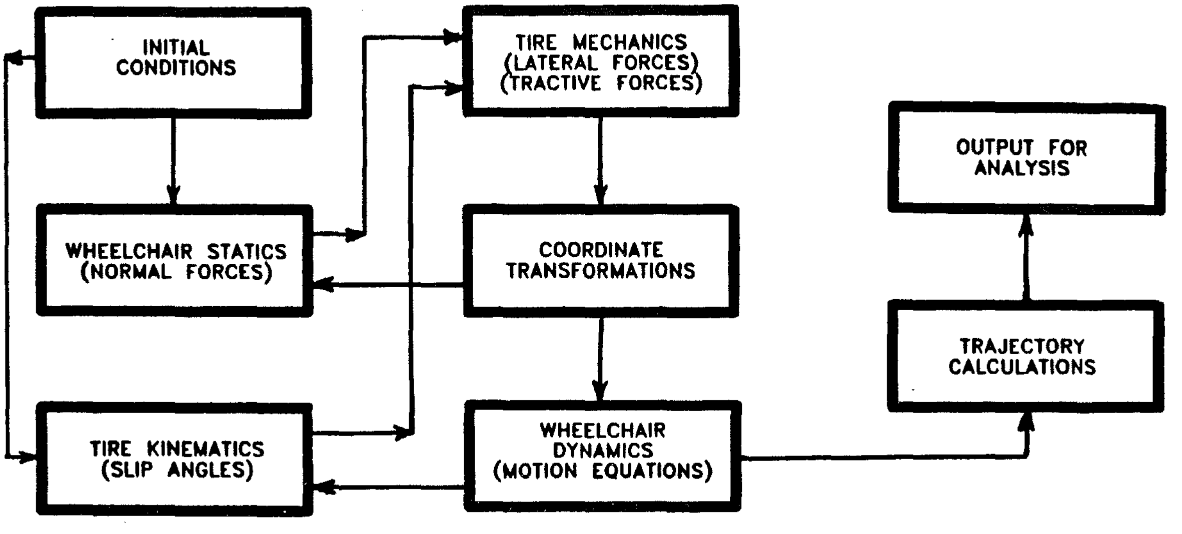

Figure 7-1 Block Diagram of Wheelchair Motion Simulation Program

pass through the block diagram in Figure 6-1. The values of acceleration are used to update the current position and velocity of the wheelchair.

6) The new position, velocity, and acceleration are printed as output for later analysis. The new lateral and longitudinal tire forces found in step 3 and the updated forward and angular velocity found in step 5 are used as input to step 2 so that new normal forces and slip angles can be calculated. At this point, a second iteration has begun.

This process of iteratively calculating forces and then updating kinematic variables is repeated over many time steps. The iteration continues until a specified time limit has elapsed.

The discussion which follows will elaborate on each of these steps. Again, this is meant to be a qualitative discussion which describes how the simulation program works. The actual computer code is contained in the program WCHAIR which is listed in Appendix C. There, the program is documented and specific variables are listed and defined. As just mentioned, the next several sections of this chapter will elaborate upon the block diagram in Figure 7-1. In order to provide some correlation with the actual computer code in Appendix C, each heading for the remaining sections will contain in parenthesis the name the Fortran 77 subroutine which corresponds to what is discussed under that heading. The results from various simulation cases are discussed in Chapter 8.

SPECIFYING INITIAL CONDITIONS

(Subroutine SETUP)

As just mentioned, the actual simulation program is entitled WCHAIR. Program WCHAIR is a partially interactive code written in FORTRAN 77. The program allows for the investigation of wheelchair motion in response to a variety of initial conditions. Almost all of these initial conditions can be specified by the user at the start of a particular simulation run. The specifiable initial conditions have default values which will be given in Chapter 8. Thus, it is unnecessary to redefine all of the initial conditions each time the program is run.

Program WCHAIR allows for the specification of all of the geometric wheelchair variables shown in Figure 6-1. These are d_1, d_2, s_1, s_2, l_1, l, t_1, and t_2. Also, the center of gravity height h can be specified. Thus, the effect of center of gravity position, caster trail distance, etc. can be easily examined.

In addition to geometric variables, mass and inertia properties may be varied. These include the mass moments of inertia of the wheelchair and user, I_z, and the mass moment of inertia of the caster wheels, I_{zp}, as defined in Chapter 6. Of course, the actual wheelchair-user mass and the mass of the casters, m and m_c, can also be varied.

The amount of friction at the caster pins is specified by providing values for M_{af} and M_{bf}. These were also defined in Chapter 6 and are shown in Figure 6-1.

The camber angle and toe angle for the main wheels have a default value of zero, but this can be changed by the user. When specifying a camber angle, the user must also give a camber coefficient as defined in equation 4-2. Recall that the camber coefficient relates the camber force for a given camber angle and normal force, to the cornering force at an equivalent slip angle and normal force.

Program WCHAIR allows the selection of five different primary wheelchair tire types. These correspond to the five 24 inch tires which were tested on the treadmill and are listed in Table 3-1. Because both of the caster wheels which were tested on the treadmill exhibited similar force characteristics, the user cannot select different caster wheels. However, the program does allow the user to play 'what if' by specifying tire and caster characteristics which do not correspond to any of the tires tested on the treadmill. The method for doing this will be described later in this chapter.

The roll coefficient as defined in Chapter 6 has a default value of 1.0 which can also be modified by the user. The meaning of choosing 1.0 for the roll coefficient was discussed earlier in Chapter 6.

Because program WCHAIR predicts the directional response of a wheelchair by using an iterative technique, it is desirable to have some control over the time step used for each iteration. At the start of the program, the user can specify TTOTAL, TSTEP, and PINT,

where:

TTOTAL	=	total real time for the motion to be simulated
TSTEP	=	time step for each iteration
PINT	=	time interval between successive print outs of output variables

The user may also specify whether or not all variables are printed as output or only a few key variables are printed. This is done by specifying the variable PRCTRL as described in the program documentation (Appendix C).

The user also supplies an initial forward velocity ($\dot{u}$) to the wheelchair. The default value is .75 m/sec (1.7mph). This corresponds to .75 m/sec in a direction parallel to the $\hat{n}_1$ axis in Figure 6-1. In other words, the initial motion at time zero is straight ahead along the global X axis. The angle theta is initially zero. Any directional response is measured with respect to this initial configuration.

Finally, the user must specify an initial disturbance which will tend to make the wheelchair deviate from its straight line directional heading. Note that even the inherently unstable rear caster wheelchair will not deviate from a straight path unless some disturbance initiates this response.

There are three ways that the program allows an initial disturbance to be input to the wheelchair during a given simulation run. The first method is to specify an initial lateral force acting on the main wheels. The second method is to specify an initial lateral force acting at the center of gravity. These forces are specified as FTIMP (force at tires) and FCIMP (force at c.g.) respectively. Such disturbing forces might be caused by bumps in a road, cracks in a sidewalk, or a momentary shift in the user's weight. Because these forces are only momentary, a duration time must also be specified. This duration time is given as DUIMP (duration of impulse). When impulse forces are specified, they are simply added to the equations of motion as derived in Chapter 6 for all times less than DUIMP. For times greater than DUIMP, the impulse forces are removed.

The third method for supplying an initial disturbance to the wheelchair is to simply specify an initial lateral velocity ($\dot{v}$) along the $\hat{c}_2$ axis. This is equivalent to specifying an initial slip angle at all four wheelchair tires. For example if the initial longitudinal velocity is $\dot{u}$ = .75 m/sec, and an initial lateral velocity of $\dot{v}$ = .04 m/sec is specified, then equation (5-7) can be used to find that the initial slip angle at each tire is approximately 3 degrees. This initial slip angle will result in lateral forces at the tires that tend to make the wheelchair deviate from its original heading.

Most of the simulation trials that were actually done using program WCHAIR incorporated an initial impulse at the center of gravity as the initial disturbance. Reasons for this are discussed in Chapter 8.

Program WCHAIR uses a BLOCK DATA routine to initialize all variables. Thus, the default value for any particular value can be easily changed.

WHEELCHAIR STATICS

(Subroutine STATICS)

The statics portion of the computer program is used to calculate the normal force at each wheelchair tire. This is done using equations (6-27a) through (6-27d) as presented in Chapter 6. Because equations (6-27) require values for the lateral and longitudinal forces on each tire, the normal forces are calculated by using the lateral and longitudinal forces from the previous time step.

To illustrate this somewhat confusing point, assume that the time step for each iteration is 1 sec. At (t=0) the normal forces will be unknown. The normal forces at (t=1) will be calculated using the longitudinal and lateral forces which existed at (t=0). Similarly, the normal forces at (t=2) will be calculated from the longitudinal and lateral forces that were present at (t=1). This slight lag between the normal force and the other tire forces is insignificant for small time steps. The values for longitudinal and lateral force at (t=0) are assumed to be zero. Thus the wheelchair is assumed to be freely rolling, without the influence of any external forces, until the moment when a given simulation run begins.

When the normal force at each wheelchair tire is calculated, the program checks to make sure that no F_z value is greater than 450N. This ensures that the normal forces are within the range of the empirical coefficients used to predict tire forces using equation (4-1). The empirical coefficients were obtained from treadmill tests in which the normal force at one degree slip angle reached a maximum of about 475N. Meaningless values may result if the empirical coefficients are used to predict cornering force or rolling resistance for values of F_z which are out of the range of the original test cart data. Program WCHAIR prints warning messages for the first ten iterations in which F_z is out of the reliable range. After ten such messages, program execution is terminated.

TIRE KINEMATICS
(Subroutine SLIP)

This step in the simulation process corresponds to the calculation of the slip angles at each wheelchair tire. This is done by using equations (6-17) and (6-18) as given in Chapter 6. The slip angles are computed using the current values of the necessary variables ($\dot{u}$, $\dot{v}$, $\dot{\theta}$, $\dot{\eta}$, and $\dot{\beta}$). The program checks to ensure that no slip angle is greater than 8 degrees. Recall that 8 degrees was the largest slip angle for which cornering forces were determined using the treadmill and test cart. Warning messages are given for the first ten occurrences of a slip angle greater than 8 degrees. After ten messages, the program stops.

It should be noted that because of the restrictions on slip angle and normal force, it is unreasonable to expect program WCHAIR to simulate extreme types of motion. Extreme motion includes motion near the limit of sliding or tipping.

As a final detail with regard to how program WCHAIR calculates slip angles, it is pointed out that the program actually calculates the absolute value of the slip angle at each tire. Only the absolute value is necessary in order to determine the magnitudes of the tire forces F_x and F_y. To ensure that the tire forces act in the proper directions, F_x is always assigned a direction which opposes the direction of longitudinal wheel motion, while F_y is given a direction which opposes the lateral wheel velocity. These directions are actually assigned in the subroutine to be described next.

TIRE MECHANICS
(Subroutine MECHAN)

Once slip angles and normal forces have been determined for each tire, the lateral force and longitudinal force at each tire can be found. Because previous values of lateral and longitudinal force will always exist, these forces are not found for the first time, but instead are updated.

The lateral cornering force F_y and the longitudinal rolling resistance force F_x are found using equation (4-1). The necessary empirical constants for each tire (see Appendix B) are built into the program so that all the user must do is select a particular tire at the start of the program. Again, the force directions are assigned such that the tire forces always act opposite the lateral and longitudinal directions of wheel motion.

It was stated earlier that the program allows for hypothetical tire types which do not correspond to any of those tested on the test cart. This is done through the use of four modifying coefficients which scale forces calculated using equation (4-1) by some factor which is specified at the start of the program.

These modifying coefficients are termed TXMOD, TYMOD, CXMOD, and CYMOD in the computer program. Values for these coefficients may be specified at the start of the program. TXMOD and TYMOD allow for modification of the main wheel x and y tire forces, while CXMOD and CYMOD allow for modification of the caster wheel x and y tire forces. As an example, suppose TYMOD is specified as 1/2. Then the cornering force which is calculated for each of the main wheels will be scaled to 1/2 the value obtained from equation (4-1).

The modifying coefficients can be used to investigate the effect of doubling or halving the cornering force capability of a given tire. Note also that by choosing TXMOD and TYMOD to be zero, the longitudinal force on both the tires and the casters can be scaled to zero. In this manner, it is possible to examine wheelchair motion in the absence of rolling resistance. Reasons as to why this is sometimes desirable are given in Chapter 8.

It should be pointed out that Equation (4-1) can be used to calculate the cornering force on a given wheelchair tire only if two conditions are met:

(1) the normal force must be less than 450N as stated previously.

(2) the slip angle must be 0, 1, 2, 3, 4, 5, 6, 7, or 8 degrees. These are the slip angles that were used with the test cart, and they are the only slip angles for which the empirical constants a, b, and c exist for use with equation (4-1).

For non-integer slip angles, the value of cornering force must be interpolated. Subroutine MECHAN uses a linear interpolation to do this. This results in little error, as it is readily seen from Figures 4-1a through 4-1g that cornering force increases approximately linearly between any two integer values of slip angle.

During the tire mechanics step of Figure 7-1, if either the camber angle or the toe angle of the main wheels is not zero, subroutine MECHAN corrects for this. If a camber angle is present, a camber force is added to the total lateral force. The magnitude of the camber force is determined by using equation 4-2 along with the camber coefficients, f_c, found from Figure 4-3.

If the toe angle is not zero, program WCHAIR incorporates the toe angle into the current slip angle at each main wheel. Chapter 2 discussed the equivalence of toe angle and slip angle. For nonzero toe angles, the wheel plane is no longer parallel to the $\hat{c}_1$ direction. For this reason, the presence of toe requires that coordinate transformations be performed on the main wheel tire forces. These are straightforward and are listed in lines 735 through 738 of program WCHAIR, but will not be given here.

WHEELCHAIR DYNAMICS
(Subroutine DYNAM)

After the longitudinal and lateral forces have been found for each tire, the accelerations can be computed for a single time step. The accelerations are found using the equations of motion given in Table 6-1. A small detail is that the directions of the frictional caster moments M_{af} and M_{bf} must be calculated in a way such that these moments always oppose the direction of angular caster velocity. The coordinate transformation step shown in Figure 7-1 was actually incorporated into the equations of motion when they were derived in Chapter 6.

CALCULATING TRAJECTORY AND UPDATING VARIABLES
(Subroutine UPDATE)

Other than actually printing out variables for analysis, the process of calculating trajectories and updating variables is the last step performed for a single iteration of the program. As stated previously, the accelerations (angular and translational) are assumed constant over a single time step. This assumption is only valid if a small enough time step is chosen. In Chapter 8, it will be shown that .001 sec is approximately the largest time step which leads to a converging solution when using program WCHAIR.

In general, position and velocity must be found by integration. However, when constant acceleration is assumed over a single time step, δt, displacement and velocity can be computed using standard constant acceleration formulas. These are given below for the kinematic variables associated with the wheelchair model (Figure 6-1).

For updating the displacement variables:

$$u = u_o + \dot{u}_o\delta t + 1/2\ddot{u}(\delta t)^2 \qquad (7\text{-}1a)$$

$$v = v_o + \dot{v}_o\delta t + 1/2\ddot{v}(\delta t)^2 \qquad (7\text{-}1b)$$

$$\theta = \theta_o + \dot{\theta}_o\delta t + 1/2\ddot{\theta}(\delta t)^2 \qquad (7\text{-}1c)$$

$$\eta = \eta_o + \dot{\eta}_o\delta t + 1/2\ddot{\eta}(\delta t)^2 \qquad (7\text{-}1d)$$

$$\beta = \beta_o + \dot{\beta}_o\delta t + 1/2\ddot{\beta}(\delta t)^2 \qquad (7\text{-}1e)$$

For updating the velocity variables:

$$\dot{u} = \dot{u}_o + \ddot{u}\delta t \qquad (7\text{-}2a)$$

$$\dot{v} = \dot{v}_o + \ddot{v}\delta t \qquad (7\text{-}2b)$$

$$\dot{\theta} = \dot{\theta}_o + \ddot{\theta}\delta t \qquad (7\text{-}2c)$$

$$\dot{\eta} = \dot{\eta}_o + \ddot{\eta}\delta t \qquad (7\text{-}2d)$$

$$\dot{\beta} = \dot{\beta}_o + \ddot{\beta}\delta t \qquad (7\text{-}2e)$$

The variables on the left side of the equations are the updated variables and the subscript (o) indicates the value of the variable for the current time step. It is important that equations (7-1) be solved before equations (7-2). If this is not done, the current velocities will be updated and lost before the displacements are calculated.

The variables $u, \dot{u}, \ddot{u}, v, \dot{v}$, and $\ddot{v}$ all correspond to the body fixed reference frame described in Chapter 6. Thus their directions are along the $\hat{c}_1$ and $\hat{c}_2$ axes. In order to transform these variables into the global X - Y reference frame at any instant, the transformation equations given by (6-1a) and (6-1b) are used. Making this transformation, allows the wheelchair's position, velocity, and acceleration relative to the fixed X - Y axes to be recorded for the entire simulation time.

CHAPTER 8

SIMULATION RESULTS

All of the tools necessary for examining the parameters related to the directional stability of rear caster wheelchairs have now been developed. Tire forces and methods for their prediction have been described. The zero width model has given some insight with regard to the primary factors that affect directional stability. The full wheelchair equations of motion have been formulated. Finally, a computer program which utilizes the equations of motion for the purpose of simulating wheelchair motion has been described. It has taken a considerable amount of effort to reach this point, but it is now possible to look more closely at several design parameters that affect the directional control of rear caster wheelchairs.

The results of several motion simulations that were performed using program WCHAIR will be described in this chapter. The Everest and Jennings Premier rear caster wheelchair which was shown in Chapter 1 was used as a starting point for the investigation of the stability problem. The default values for many of the variables used in the computer program correspond to this wheelchair. These default values are given in this chapter. Also discussed is the problem of verifying the computer program. Simulation results for both rear caster and front caster wheelchairs are presented for this purpose. The choice of time step and the specification of initial conditions are considered.

Finally, several parameters that affect the degree of instability associated with rear caster wheelchairs will be examined. A particular set of initial conditions will be chosen as an "assumed reference case". It is believed that this reference case roughly corresponds to a critical degree of directional instability. Wheelchairs that exhibit more instability than the reference case will be considered to be uncontrollable and possibly even dangerous under certain conditions. The effect that varying different parameters has on directional stability will in part be determined by comparison to the reference case.

DEFAULT PARAMETERS

The default parameters for many of the variables used in program WCHAIR were chosen to correspond to the Everest and Jennings rear caster wheelchair shown in Figure 1-1. The reader is advised to refer to Figure 6-1 which shows the configuration of the important variables which will be given in this section. Most of the geometric dimensions were determined by directly measuring the Everest and Jennings wheelchair. These are shown in Figure 8-1. For the default case, it was assumed the center of gravity lies on the longitudinal axis of the wheelchair.

The longitudinal position of the center of gravity and the mass moments of inertia of the wheelchair/user and the caster assemblies had to be estimated. This was also true for the position of the caster assembly center of gravity

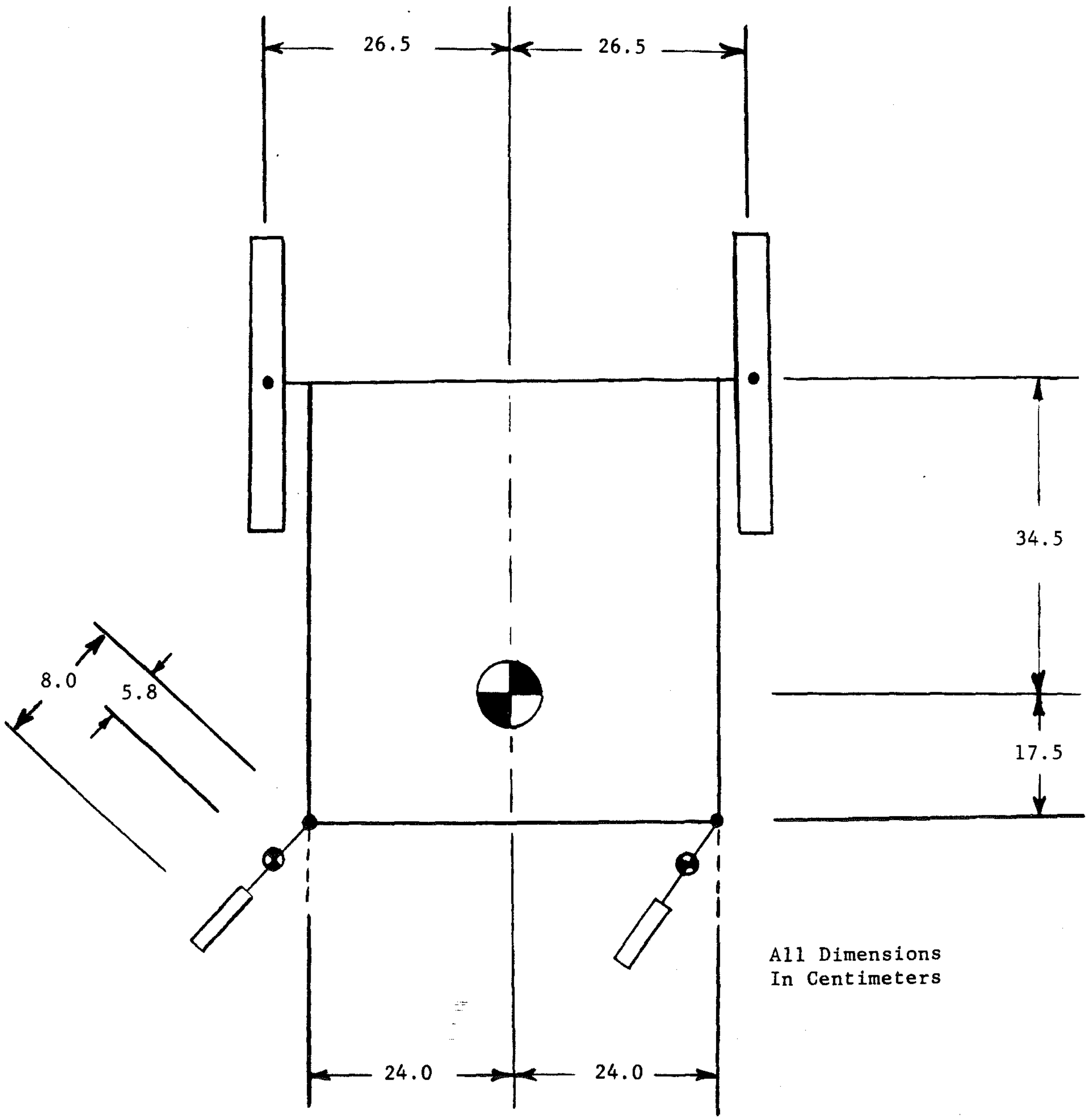

Figure 8-1 Geometric Dimensions of the Everest and Jennings Premiere Rear Caster Wheelchair

and for the frictional moments at the caster pins. Appendix D explains the methods used for determining each of these quantities. Because the Everest and Jennings rear caster wheelchair belonged to a local nursing home patient and was used daily, it was not possible to test this chair directly. Determining precise values was not considered important, as it is the effect of varying these different variables that is of interest.

As mentioned in Chapter 6, the default value for the roll coefficient was chosen to be 1.0. The camber angle and toe angle of the main wheels is zero unless specified otherwise. The initial forward velocity ($\dot{u}$) has a default value of .75 m/s in the positive global X direction. The initial lateral velocity ($\dot{v}$) has a default value of zero. For the rear caster model in Figure 6-1, the initial caster angles η and β are both zero. These are the default values, but other values can be specified at the start of program WCHAIR.

A total mass of 95 kg (209 lbf) is assumed. This corresponds to a 75 kg (165 lbf) user and a 20 kg (44 lbf) manual rear caster wheelchair. Assuming a user mass of 75 kg allows for the use of previously determined moment of inertia values for the ISO (International Organization for Standardization) 75 kg test dummy. (see Appendix D)

For reasons that will be explained in later sections of this chapter, the default values of the modifying coefficients TXMOD and CXMOD are set to zero. Thus, unless the program user specifies differently, program WCHAIR simulates motion without the presence of rolling resistance. Default values of TYMOD and CYMOD are 1.0. This means that there is no modification of the calculated lateral tire forces. The modifying coefficients were explained in Chapter 7.

As stated previously, many of the simulations to be discussed in this chapter utilized an initial impulse acting at the center of gravity as a disturbance to initiate instability. For this reason the default values of FCIMP and DUIMP are 40 N and .10 sec respectively. This corresponds to an initial lateral impulse at the center of gravity of 4 N-sec. The motivation behind choosing these values will be discussed shortly.

For the default case, a maximum time limit (TTOTAL) of 10 seconds is allowed for any single simulation run. The default time step is .001 sec. Output variables are printed every .20 sec.

A summary of all specifiable variables and their default values is given in Table 8-1. Again the reader is referred to Figure 6-1 and Chapter 7 where these variables are illustrated and defined. The list of symbols which precedes the text and the program listing in Appendix C also contains definitions for the variables in Table 8-1.

TABLE 8-1

SUMMARY OF DEFAULT VALUES FOR
SPECIFIABLE PARAMETERS USED BY PROGRAM WCHAIR

Geometry Related Variables
$d_1 = d_2 = 26.5$ cm (10.4 in)
$s_1 = s_2 = 34.5$ cm (13.6 in)
$t_1 = t_2 = 24.0$ cm (9.4 in)
$l_1 = 5.8$ cm (2.3 in)
$l = 8.0$ cm (3.1 in)
$h = 61.0$ cm (24.0 in)
$\eta = \beta = 0$ degrees
$\gamma = 0$ degrees
TOEANG = 0 degrees
Mass and Inertia Parameters
$m = 95.0$ kg (209 lbf)
$m_c = 1.2$ kg (2.6 lbf)
$I_z = 5.6$ kg-m^2 (4.1ft-lbf-sec^2)
$I_{zp} = 0.02$ kg-m^2 (.015 ft-lbf-sec^2)
Force Related Parameters
$M_{af} = M_{bf} = 0.10$ N-m (.88 in-lbf)
FCIMP = 40 N (9.0 lbf)
FTIMP = 0 N
DUIMP = 0.10 sec
TXMOD = CXMOD = 0
TYMOD = CYMOD = 1

YAW VELOCITY RESPONSE CURVES FOR TWO INITIAL DISTURBANCES

It has already been stated that the directional stability of a vehicle is concerned with its ability to stabilize its motion against external disturbances. Thus, in order to investigate the directional stability of a wheelchair, it is necessary to choose an initial disturbance which tends to make the wheelchair deviate from its original directional heading. It was discussed in Chapter 6, that upon being subjected to such an initial disturbance, an unstable vehicle will experience an exponentially increasing yaw velocity, $\dot{\theta}$. A stable vehicle will experience an exponentially decreasing yaw velocity.

One method of comparing the directional responses of different vehicles is by comparing the yaw velocity response of each vehicle upon being subjected to the same initial disturbance. This method is used in the automobile literature. [2.2,2.3] This section will explain the meaning of typical yaw velocity response curves, and will examine two initial disturbances that were considered as possible inputs for initiating directional instability.

Figure 8-2 shows the yaw velocity response curves for two different initial disturbances. These were obtained from program WCHAIR for the Everest and Jennings rear caster wheelchair. The figure shows yaw velocity, $\dot{\theta}$, on the vertical axis versus time on the horizontal axis. The meaning of the two curves shown in Figure 8-2 and an explanation of the two initial disturbances will now be given. Note that for

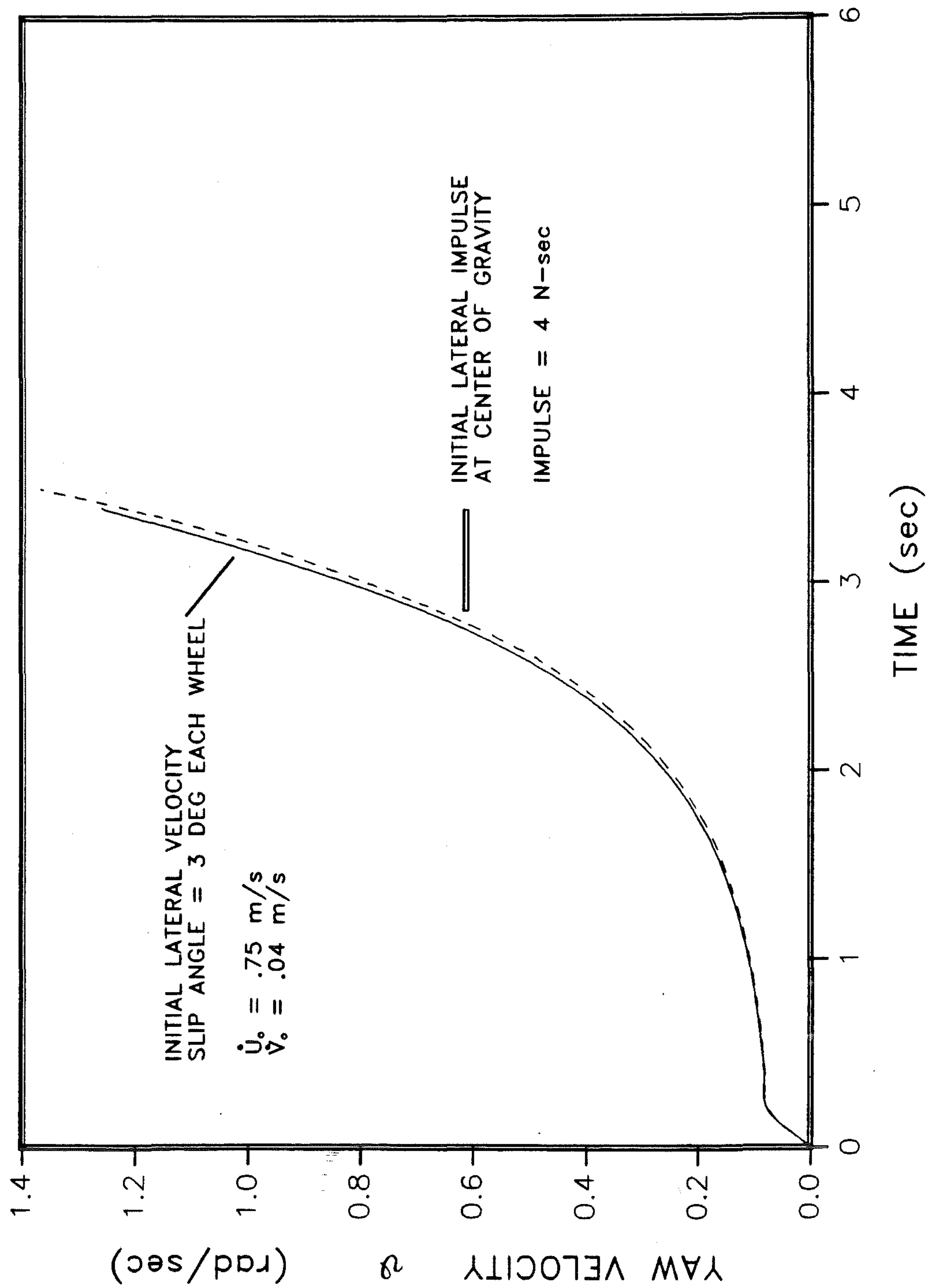

Figure 8-2 Typical Wheelchair Yaw Velocity Response Curves for Two Different Initial Disturbances

these curves and all others given in this chapter, unless specified otherwise, the tire type selected when using program WCHAIR was EJA (see Table 3-1). Recall that this tire exhibited the lowest cornering stiffness of the five 24 inch tires tested. The effect of selecting different tires is another topic in this chapter.

For time less than about 0.2 sec, there is a sharp increase in the rotational velocity of the wheelchair. This sharp increase corresponds to the initial disturbance used to cause a deviation from the original directional heading. For time greater than 0.2 sec but less than 2.0 sec, the yaw velocity slowly but gradually increases. After 2 seconds have elapsed, the directional instability becomes very apparent as the yaw velocity begins to increase rapidly.

Any point on the yaw velocity response curves represents the instantaneous rate at which the wheelchair is diverging from its directional heading. Note that the area under the yaw velocity curves represents the total angular displacement of the wheelchair, θ, with respect to its original heading. Similarly, the slope of the tangent to the yaw velocity curves at any point represents the instantaneous angular acceleration, $\ddot{\theta}$, of the wheelchair. This interpretation of the curves in Figure 8-2 is useful and is one motivation for plotting yaw velocity response.

The initial disturbance shown by the solid line in Figure 8-2 corresponds to an initial lateral wheelchair velocity of .04 m/s. As described in Chapter 7, this lateral velocity results in an initial slip angle of 3 degrees at each wheelchair tire. These slip angles produce lateral cornering forces that immediately begin to cause the wheelchair to deviate from its original course. It is commonly observed that a wheelchair may be displaced from its line of motion by several degrees due to a bump or other disturbance in the road.

Although it is reasonable to specify an initial lateral velocity for the wheelchair, there are some problems with this approach. When an initial velocity along the x body axis is specified, the lateral cornering force changes from zero to a fairly large value during only a single time step. The sum of the 4 lateral forces at each tire tends to tip the wheelchair, resulting in a large lateral load transfer. This often results in normal force values that are out of the allowable range.

An additional problem with specifying an initial lateral velocity results in cases where it is desirable to vary the forward velocity of the wheelchair, $\dot{u}$. In order to keep the slip angle constant, if the initial longitudinal velocity is changed, the initial lateral velocity must also be changed. This can be seen simply by examining equation (5-7). Changing the initial lateral velocity results in a shorter duration time for the initial large cornering forces at the tires, and thus produces a different yaw velocity response curve.

For the reasons just described, a second method for initially disturbing the wheelchair was chosen. Directional instability can be initiated by applying an initial lateral force at the center of gravity. The yaw velocity response of the Everest and Jennings wheelchair subjected to an initial lateral force of 40 N for a duration of .10 sec is shown by the dashed line in Figure 8-2. This is equivalent to an impulse of 4 N-sec. From Figure 8-2, it is clear that this impulse produces approximately the same yaw velocity response as the initial lateral velocity of .04 m/s. This is not an accident, as it was determined basically by trial and error that these two initial disturbances are equivalent. Note that the initial forward speed, $\dot{u}$, is .75 m/s for both curves in Figure 8-2. Using an initial lateral force at the center of gravity does not result in sharp and sudden lateral forces on the tires. It also has the advantage that the predicted directional response can be easily compared with those discussed in association with the understeer coefficient, k_{us}, given in Chapter 5 (see Figure 5-3).

The magnitudes of the two initial disturbances shown in Figure 8-2 are somewhat arbitrary. It is impossible to avoid making a somewhat arbitrary choice with regard to an initial disturbance. With this in mind, the important consideration is to choose a reasonable initial disturbance, and then to keep this disturbance constant while examining the effects on stability of varying other parameters. The two initial disturbances shown in Figure 8-2 are believed to be reasonable in magnitude, while at the same time producing a definitely unstable response.

The next section of this chapter will show the effect that forward speed has on the yaw velocity response curves. Following this, a reference case will be defined which can be used as a basis for comparison when other parameters are varied. For reasons to be given later, this reference case will be the same dashed curve shown in Figure 8-2.

THE EFFECT OF FORWARD SPEED ON DIRECTIONAL STABILITY

The analysis of the zero width vehicle presented in Chapter 5 showed that the degree of instability associated with a rear caster wheelchair should be very sensitive to forward speed. Using program WCHAIR, the yaw velocity response and angular displacement response of the Everest and Jennings rear caster wheelchair was determined for five different initial forward velocities. This was done using the same 4 N-sec impulse shown in Figure 8-2. The results for these two responses are shown in Figures 8-3a and 8-3b.

Figure 8-3a shows yaw velocity, $\dot{\theta}$, versus time for initial values of $\dot{u}_o$ ranging from .55 m/s to .95 m/s. This figure clearly shows that the degree of instability is highly dependent upon speed. The degree of instability is represented by the rate at which the yaw velocity increases. This is equivalent to the rate at which the wheelchair diverges from its original directional heading. As expected, as the forward speed decreases the stability of the wheelchair improves.

It appears from Figure 8-3a that for the case where $\dot{u}_o$ = .55 m/s, the yaw velocity is constant. However, the yaw

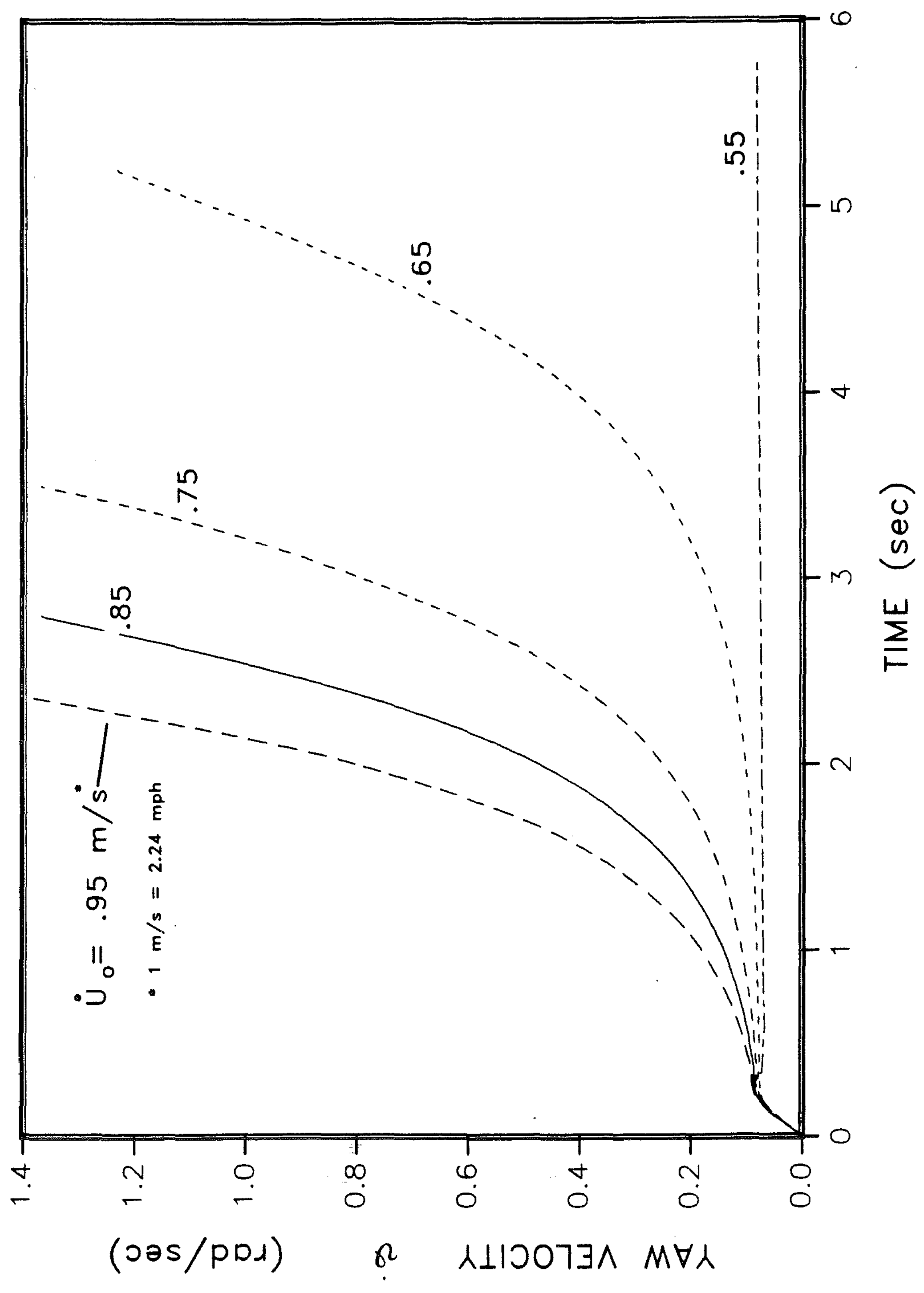

Figure 8-3a The Effect of Forward Speed on Yaw Velocity Response

velocity for this case is actually slowly increasing. If the graph were extended to show times greater than 6 seconds, a more rapid increase for this case would become obvious.

Figure 8-3b illustrates the correlation between yaw velocity response and total angular displacement. Clearly the more rapidly increasing yaw velocity curves correspond to more rapid increases in the total yaw angle. Figure 8-3b also shows that for the case where $\dot{u}_o$ = .55 m/s, the yaw angle increases at an approximately constant rate. Thus, this case still corresponds to directional instability because the wheelchair is steadily rotating away from its original heading.

Because the degree of instability is extremely dependent upon forward speed, rolling resistance was omitted for each of the simulations shown in Figures 8-3. Since propelling forces from the user are not included in the simulation model, the introduction of rolling resistance tends to decrease the longitudinal speed of the wheelchair fairly rapidly. This has an apparent stabilizing effect. If tires are selected which have a high rolling resistance, this effect becomes even more noticeable.

When examining parameters that affect directional stability, it is desirable to isolate the effects of actual wheelchair design changes from the effect of decreased speed due to rolling resistance. For this reason, rolling resistance was eliminated for the motion simulations presented in this chapter. This has the effect of keeping

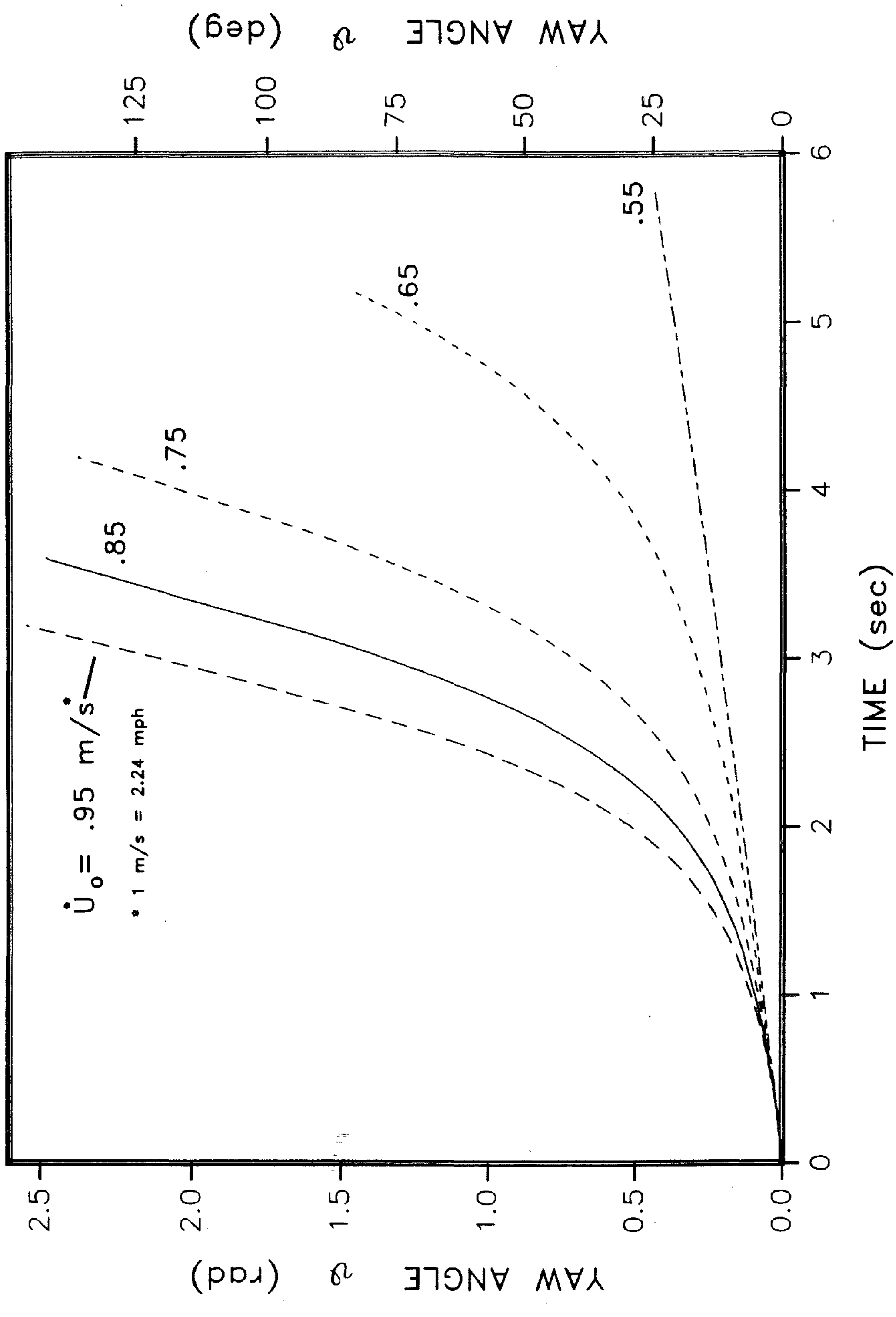

Figure 8-3b Increase in Yaw Angle vs. Time for Five Different Forward Speeds

the longitudinal speed of the wheelchair approximately constant. A wheelchair that is being propelled at constant speed or that is travelling down a slight incline might exhibit this type of motion. Rolling resistance is eliminated by specifying TXMOD and CXMOD in program WCHAIR equal to zero as discussed earlier in this chapter.

The next section of this chapter will present the results of several simulation tests that were used to verify the simulation computer program.

VERIFYING THE COMPUTER PROGRAM

Before examining several other parameters that may or may not have a significant effect on wheelchair stability, it is reasonable to question the reliability of the basic wheelchair model developed in Chapter 6, and of the computer program being used to implement the model. This section will discuss two methods that were used to gain confidence in the simulation model.

Method One: Comparing The Predicted Motion Responses for Front and Rear Caster Wheelchairs

The directional response of a vehicle subjected to a side force at the center of gravity was discussed with respect to the understeer coefficient, k_{us}, in Chapter 5. The predicted paths for an understeer vehicle (front caster wheelchair) and an oversteer vehicle (rear caster wheelchair) were shown in Figure 5-3. A first true test of the simulation model for wheelchair motion is whether or not it is able to clearly predict the different responses that are observed for front and rear caster wheelchairs. The model should be able to demonstrate the directional stability of front caster wheelchairs and the directional instability of rear caster wheelchairs.

Program WCHAIR was used to predict the trajectories of a front and rear caster wheelchair travelling forward with a speed of .75 m/s, each subjected to the same initial lateral impulse at the center of gravity. The rear caster wheelchair was the same Everest and Jennings model that has already been described. A front caster wheelchair can be easily simulated using program WCHAIR. By referring to Figure 6-1, it can be seen that a front caster wheelchair can be modelled using the rear caster model already formulated if the following initial conditions are specified:

$\eta = \beta = 180$ degrees

$\dot{u}_o$ = any negative value

s_1 and s_2 values are exchanged

Thus, by specifying $\dot{u}_o = -.75$ m/s and changing the default values of s_1 and s_2 to, $s_1 = .175$m, and $s_2 = .345$m, it is possible to simulate the motion of a front caster wheelchair. Note that specifying $\dot{u}_o$ as a negative number has no significance other than the fact that it causes the front caster wheelchair to travel in a forward direction. Figures 8-4a and 8-4b show the predicted trajectories for a rear caster wheelchair and a front caster wheelchair as

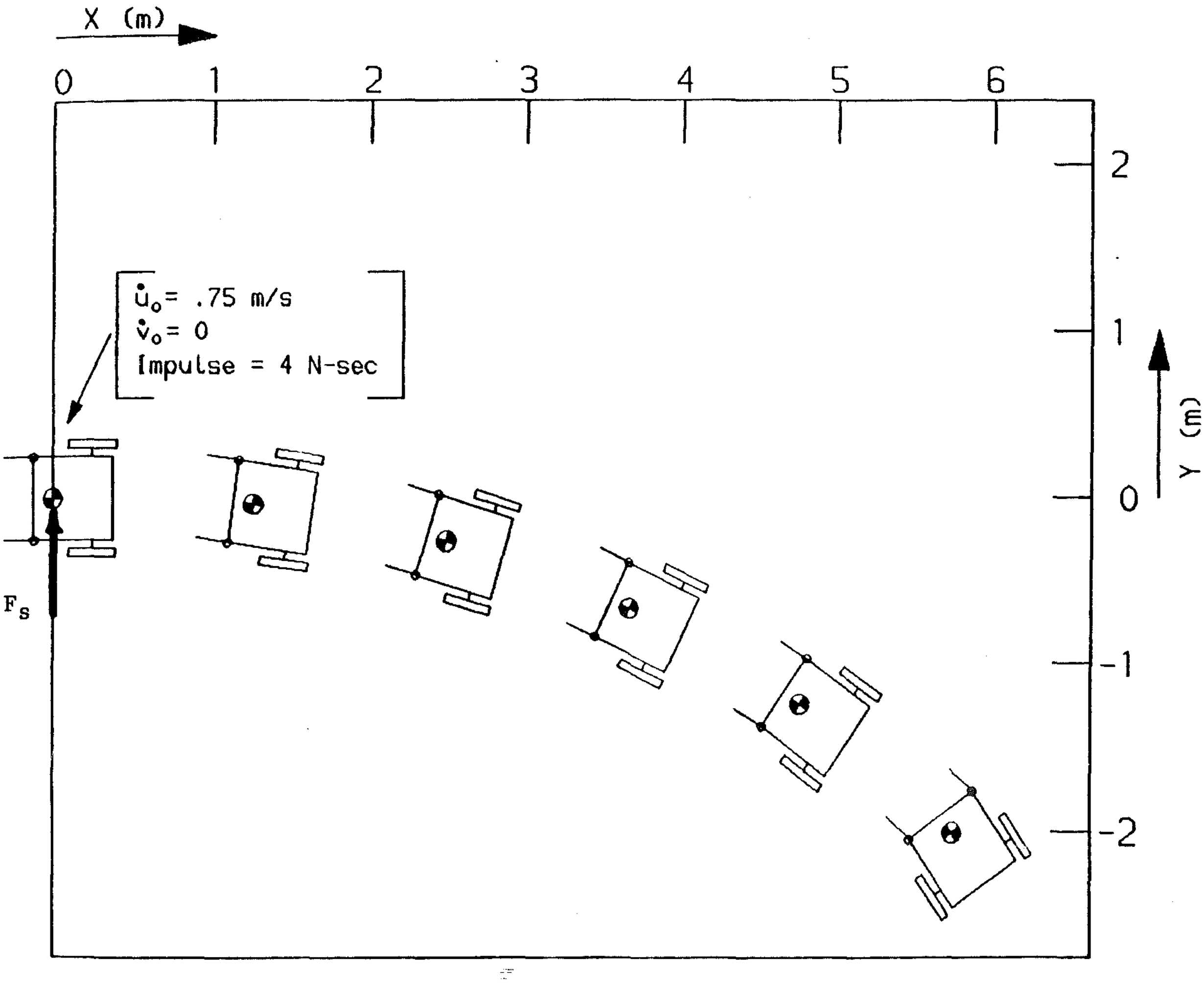

Figure 8-4a Predicted Trajectory For a Rear Caster Wheelchair Traveling at .75 m/s and Subjected to a Lateral Impulse at the Center of Gravity of 4 N-sec.

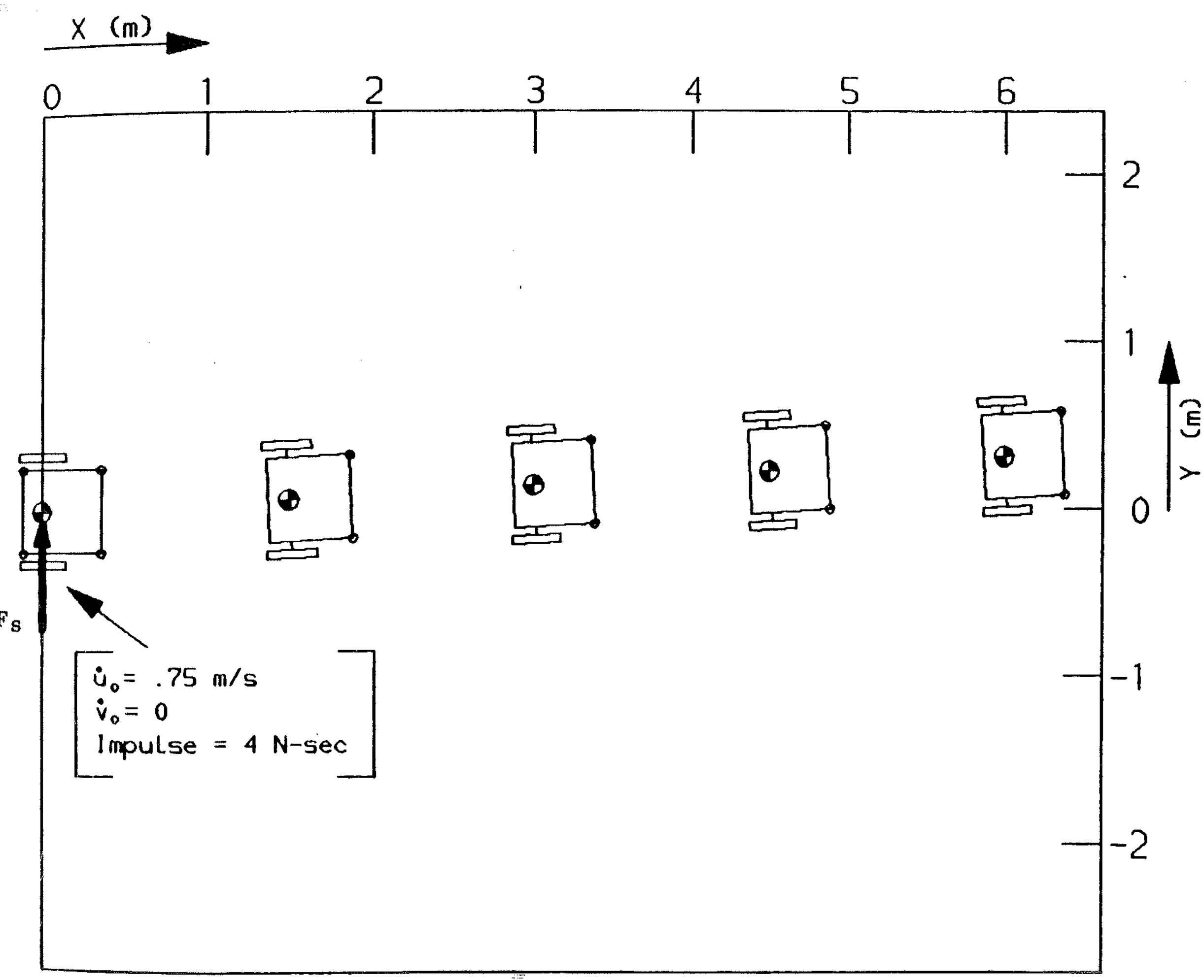

Figure 8-4b Predicted Trajectory for a Front Caster Wheelchair Traveling at .75 m/s and Subjected to a Lateral Impulse at the Center of Gravity of 4 N-sec.

obtained from the computer program. Both wheelchairs are initially moving forward with a speed of .75 m/s. At time = 0 the initial lateral side force, F_s, is imparted to both chairs as shown in the figures. The global X and Y position of each wheelchair and the angular orientation is shown at 1.0 second time intervals.

Figures 8-4a and 8-4b clearly show the different directional responses that are expected for the front and rear caster wheelchairs. The rear caster wheelchair continues to diverge more and more from its original heading even after the initial disturbance is removed. Note that the trajectory shown for the rear caster wheelchair in Figure 8-4a corresponds to the $\dot{u}_o$ = .75 m/s yaw velocity response curves already shown in Figures 8-2 and 8-3. Although the front caster wheelchair deviates from its original directional heading, it quickly returns to a state of steady straight-line motion after the side force is removed. As discussed in association with the understeer and oversteer paths shown in Figure 6-3, the rear caster wheelchair tends to rotate toward the initial lateral force, while the front caster wheelchair rotates away. From a qualitative point of view at least, the simulation model seems to predict reasonable motion.

Figure 8-5 shows several yaw velocity response curves. Three of these are for a front caster wheelchair, and one is for a rear caster wheelchair. Each of these curves again corresponds to an initial forward velocity of .75 m/s and an

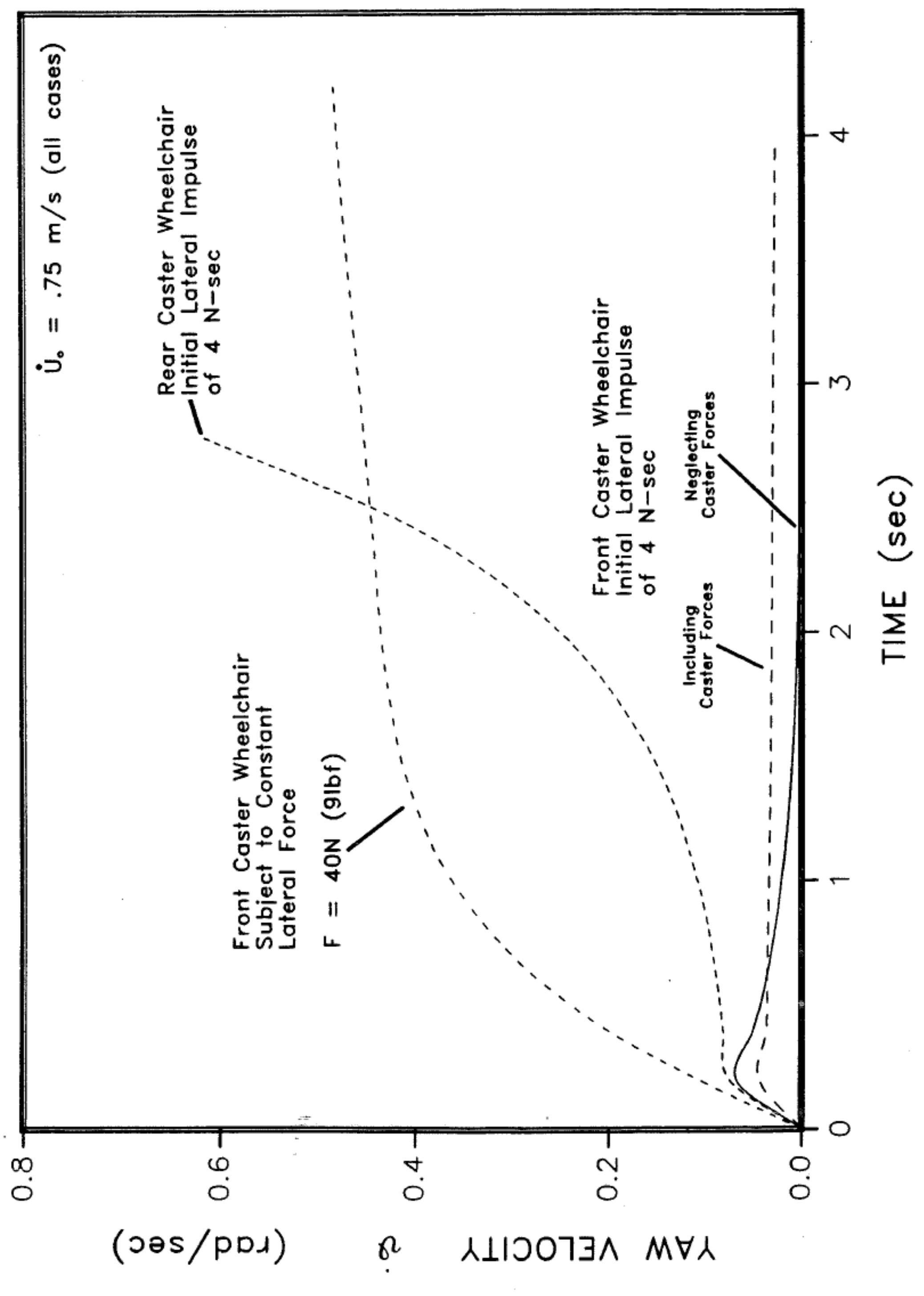

Figure 8-5 Comparing the Yaw Velocity Response Curves for a Front Caster and Rear Caster Wheelchair

initial lateral impulse of 4 N-sec. The two curves near the bottom of the figure show that the front caster wheelchair experiences a yaw velocity that initially increases, but quickly begins to decrease towards a steady state value. Note that if caster forces are neglected, the front caster wheelchair yaw velocity rapidly converges to zero after the initial disturbance is removed. When caster effects are included, the front caster wheelchair motion returns to a steady state more slowly. This is indicative of the small but noticeable lateral forces which are exerted on the caster wheels. For a front caster wheelchair, lateral forces on the caster wheels slightly negate the stabilizing effect of the rear wheel forces. Note that figure 8-4b corresponds to the solid yaw velocity curve shown at the very bottom of Figure 8-5.

Also shown in Figure 8-5 is a yaw velocity response curve for a front caster wheelchair which is subjected to a constant lateral force of 40 N at the center of gravity. This curve was obtained from program WCHAIR simply by specifying a large duration time, DUIMP, for the initial lateral force of 40 N. When subjected to this constant side force, the front caster wheelchair experiences a sharply increasing yaw velocity which soon begins to approach a constant value. The fact that the yaw velocity approaches a constant value indicates that the wheelchair approaches a state of steady turning motion. This type of predicted motion is identical to that predicted for automobiles which are subjected to a constant lateral side wind. [2.3]

Method Two: Comparing Predicted Versus Theoretical Critical Speeds for a Rear Caster Wheelchair with its Caster Wheels Locked Against Turning

A second method for testing the simulation computer program is by using the equation for critical speed that was given in Chapter 5 for the zero width model. Equation (5-15) can be used to predict the speed above which a rear caster wheelchair that has its wheels locked against turning will exhibit directional instability. Of course, permanently locking the wheels against turning would be highly undesirable for any wheelchair. However, considering such a hypothetical case provides a means for testing program WCHAIR against accepted theory.

This was done for the Everest and Jennings Premier rear caster wheelchair for the following initial conditions:

$$\begin{aligned} m &= 75 \text{ kg} \\ m_c &= 1.2 \text{ kg} \\ s_1 &= .345 \text{ m} \\ s_2 &= .255 \text{ m} \\ s &= .60 \text{ m} \end{aligned} \qquad (8\text{-}1)$$

Recall that s_2 for the zero width model is defined slightly differently than s_2 for the wheelchair model in Figure 6-1 and Figure 8-1. If the casters are locked, then the distance from the c.g. to the caster contact points, s_2 for the zero width model, is found from Figure 8-1 as .175m + .08m = .255m.

Using the values given in (8-1) and equations (5-13), the following approximate values are found for the total weight and for the weight carried by the each front and each rear wheel:

$$W = 748 \text{ N}$$
$$W_f = 159 \text{ N} \tag{8-2}$$
$$W_r = 215 \text{ N}$$

Next, by referring to Figure 4-2 it is possible to estimate the cornering stiffness for the two front tires (type EJA) and the two caster wheels (type ER). From the figure it is seen that for EJA tires at 159 N normal force and for ER casters at 215 N normal force, the cornering stiffness is approximately

$$C_{\alpha f} = C_{\alpha r} = 25 \text{ N/deg} = 1432 \text{ N/rad} \tag{8-3}$$

Substituting the values for CSf, CSr, Wf and Wr into equation (5-16) gives a value for the understeer coefficient of

$$k_{us} = -.04 \tag{8-4}$$

Finally, substituting this value, along with the value for s given in (8-1) allows for the calculation of the critical speed associated with the locked caster wheelchair. The critical speed is given by:

$$\dot{u}_{crit} = \sqrt{\frac{(-9.8\text{m/sec}^2)(.60\text{m})}{-.04}}$$

or $$\dot{u}_{crit} = 12 \text{ m/s} \tag{8-5}$$

Thus, the zero width model predicts that for speeds above 12 m/s (27 mph), the rear caster wheelchair will experience directional instability, even if the caster wheels are locked. Obviously this is a very high speed that has little or no practical significance. However, it can be used to check the simulation model.

In order to simulate a rear caster wheelchair with its caster wheels locked against turning, the mass moments of inertia of the caster wheels, I_{zp}, were assigned extremely high values. This has the effect of restraining the caster motion without changing the wheelchair mass.

Figure 8-6 shows the results of three simulations that were done using this method. The curves in Figure 8-6 are for initial forward speeds of 10.0, 11.25, and 12.5 m/s. It is obvious from the figure that a transition from stable to unstable motion occurs for a forward speed somewhere in the range of 11.25 to 12.5 m/sec. Thus, it is found that the value of critical speed predicted by the zero width model and the value predicted by the computer simulation are in very good agreement.

The preceding discussion has attempted to elaborate on the methods that were used to test the simulation program, and to gain confidence in the wheelchair motion that it predicts. It is believed that the arguments given in this section at least demonstrate that program WCHAIR predicts the proper trends for wheelchair motion subject to various initial conditions.

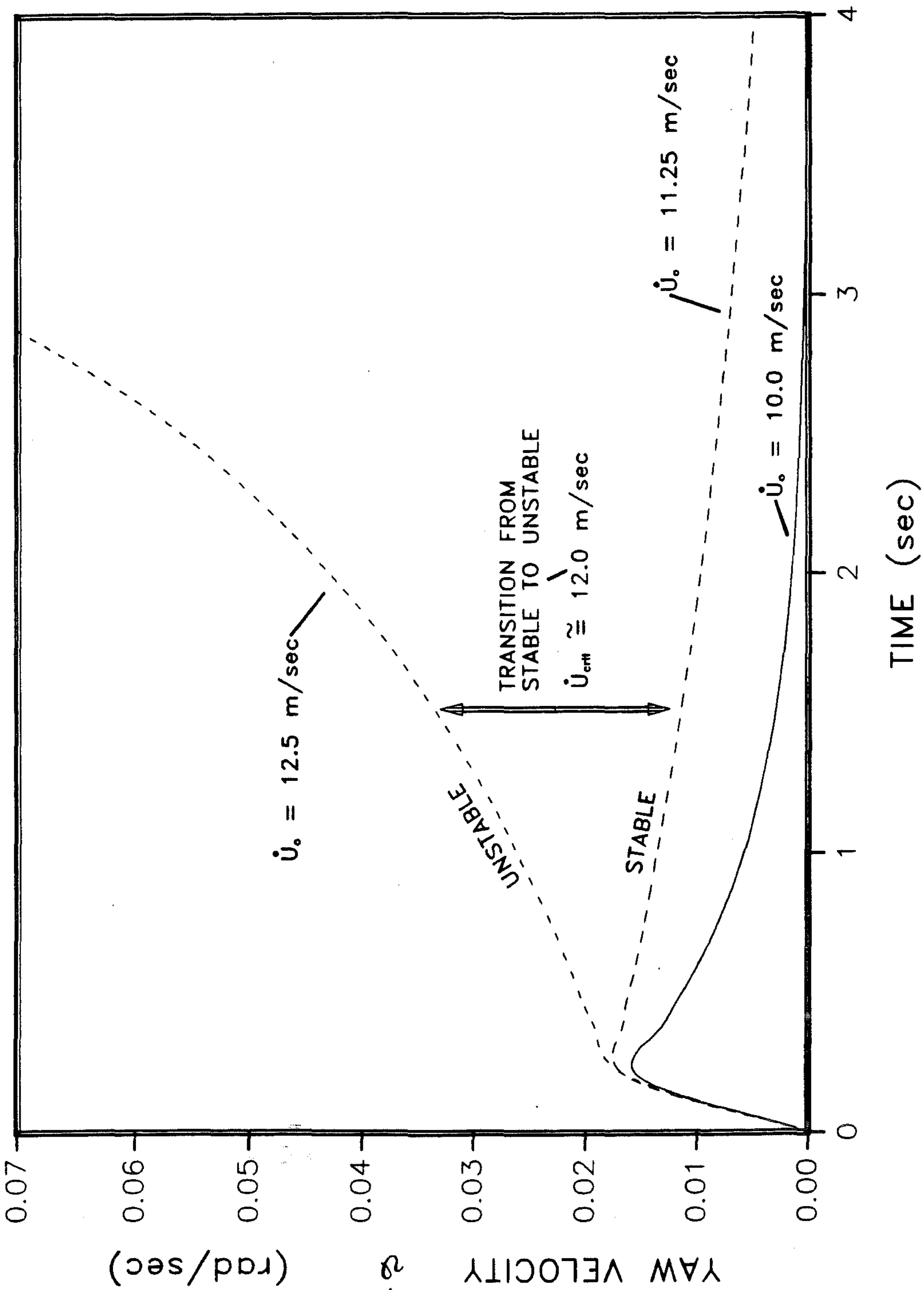

Figure 8-6 Predicted Critical Speed for a Rear Caster Wheelchair With its Casters Locked Against Turning

CHOOSING A TIME STEP

Because program WCHAIR uses an iterative solution technique, it is necessary to choose a time step that is small enough to ensure convergence to the best possible solution. On the other hand, it is highly desirable to choose the largest time step possible in order to reduce computation time and avoid round-off error. Figure 8-7 shows the effect of three different time steps on the yaw velocity response curve of a rear caster wheelchair. It is emphasized that all three curves in Figure 8-7 represent identical initial conditions. Each curve is for a wheelchair having an initial forward speed of .75 m/s subject to an initial lateral impulse of 4 N-sec.

Figure 8-7 supports the statement made earlier that a time step of .001 sec is approximately the largest time step which leads to a reliable solution. A time step of .01 sec is clearly too small, while it can be seen from the figure that little change in the response curve results from decreasing the time step to .0001 sec.

The necessary time step of .001 sec is quite small. One reason for this is the fact that the transient tire forces change very quickly. This is especially true for the caster wheels which are free to pivot. In order to model the wheelchair motion successfully, the caster wheels must be allowed to accelerate quite rapidly. A small time step is required to track this acceleration.

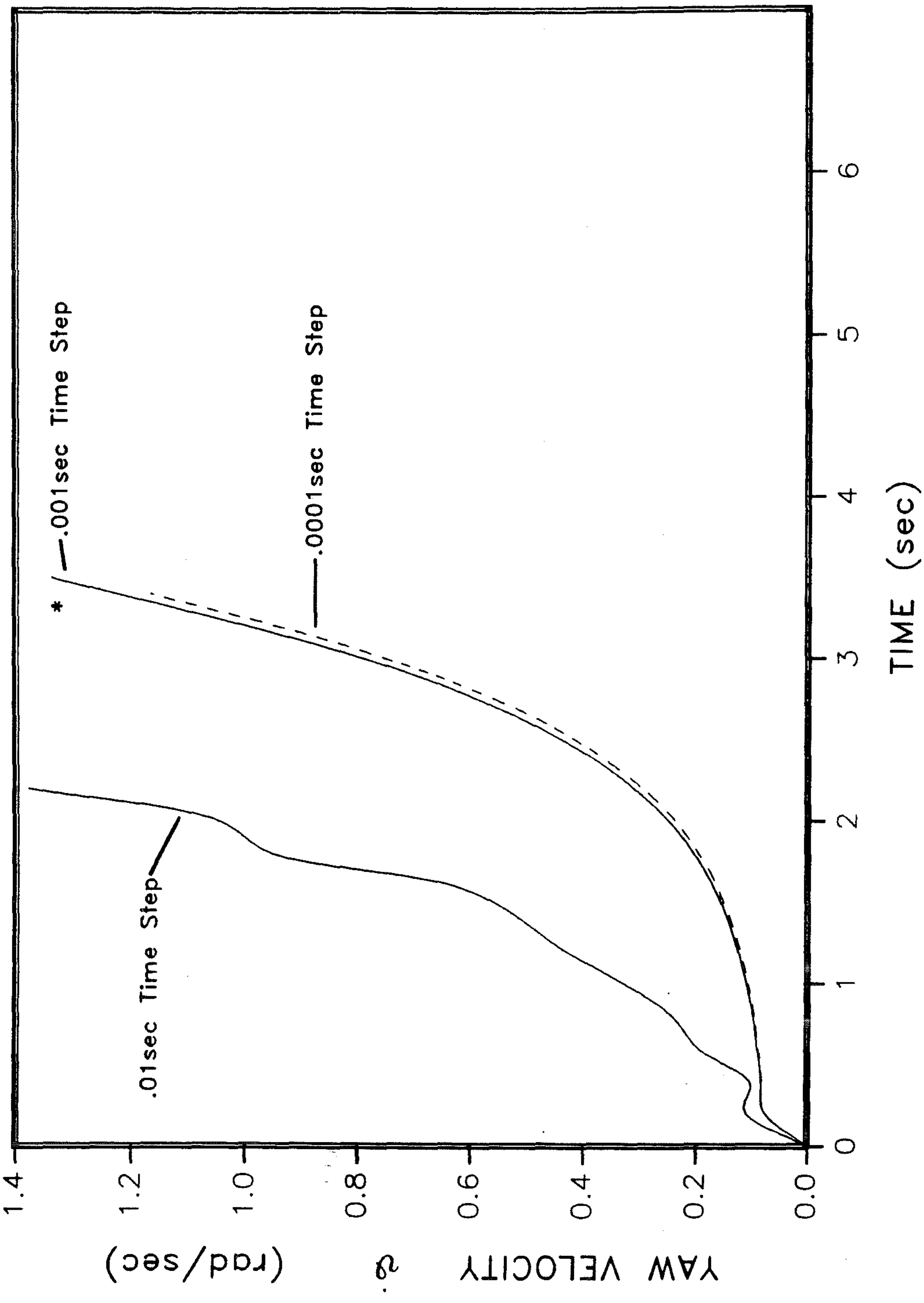

Figure 8-7 The Effect of Time Step on the Reliability of Results from Program WCHAIR

ASSUMING A REFERENCE CASE

In order to evaluate the effect on directional stability of varying any particular parameter, it is desirable to assume a reference yaw velocity response curve against which other responses can be compared. A motivation for assuming a particular reference case can be found by again examining Figure 8-3a. This figure showed five yaw velocity response curves for the Everest and Jennings Premier rear caster wheelchair subjected to an initial lateral impulse of 40 N-sec.

Consider the two cases shown in Figure 8-3a that represent the least amount of directional stability, namely $\dot{u}_o$ = .55 m/s and $\dot{u}_o$ = .65 m/s. Even though both of these curves do indicate a divergence from an initial directional heading, the rate of divergence is clearly slower than for the other three cases. For these two cases the wheelchair user would most likely have ample time to take corrective action which would return the wheelchair to its original heading. Of course the need to constantly make course corrections is an annoyance, but it appears that for these two cases the directional instability is controllable.

The three remaining curves in Figure 8-3a represent much more rapid increases in yaw velocity, $\dot{\theta}$. For the case with $\dot{u}_o$ = .75 m/sec for example, the yaw velocity increases to 1.0 rad/sec in slightly over 3 seconds. This is equivalent to a rotational velocity of approximately 60 degrees per second. The slope of the curve indicates that this value will increase sharply in a very short period of time.

By examining the curves in Figure 8-3a, it is possible to estimate an approximate maximum response time to each curve. The maximum response time is the maximum amount of time that the wheelchair user has to take corrective action before the yaw velocity response curve begins to sharply increase. The approximate maximum response times obtained simply by observing each of the curves in Figure 8-3a are listed in Table 8-2.

TABLE 8-2

ESTIMATED MAXIMUM RESPONSE TIMES
ASSOCIATED WITH FIGURE 8-3a

$\dot{u}_o$	t_{max}
.55 m/s	> 6 sec
.65 m/s	3.5 sec
.75 m/s	2 sec
.85 m/s	1.5 sec
.95 m/s	1 sec

It is emphasized that the values in Table 8-2 are only estimates which give some indication of how quickly the user must respond. It is reasonable to expect that if a wheelchair user does not take corrective action within the maximum response time, the resulting rapid increase in yaw velocity will be at best highly undesirable, and at worst quite dangerous.

When considering the ability of an individual to respond to an initial disturbance within a given time interval, it is important to think in terms of total response time rather than simple reaction time. Simple reaction time is defined as the shortest time between the moment a sensory receptor is stimulated and the time some body element reacts. [8.1]

Total response time, sometimes called complex reaction time, includes the additional time required for brain recognition time and decision making time. Simple reaction times to sensory inputs such as light or touch are generally in the range of 0.1 to 0.2 seconds. However, Woodson presents estimates indicating that the minimum complex reaction time is generally about 0.5 seconds, and may often be as long as 4.0 - 10.0 seconds. [8.1]

Complex reaction time is especially important if the user is not necessarily aware that a stimulus is about to occur. This is obviously the case for wheelchair users. If a wheelchair is disturbed by a bump or other obstacle in the road, there is a very good chance that it will take the user at least one or two seconds to take corrective action.

Based upon this reasoning, the $\dot{u}_o = .75$ m/s curve in Figure 8-3a with maximum response time of approximately 2.0 seconds was chosen as an assumed reference case. Figure 8-8 shows the assumed reference case plotted alone. The region to the right of this curve will be termed the controllable region, while the region to the left of the curve will be

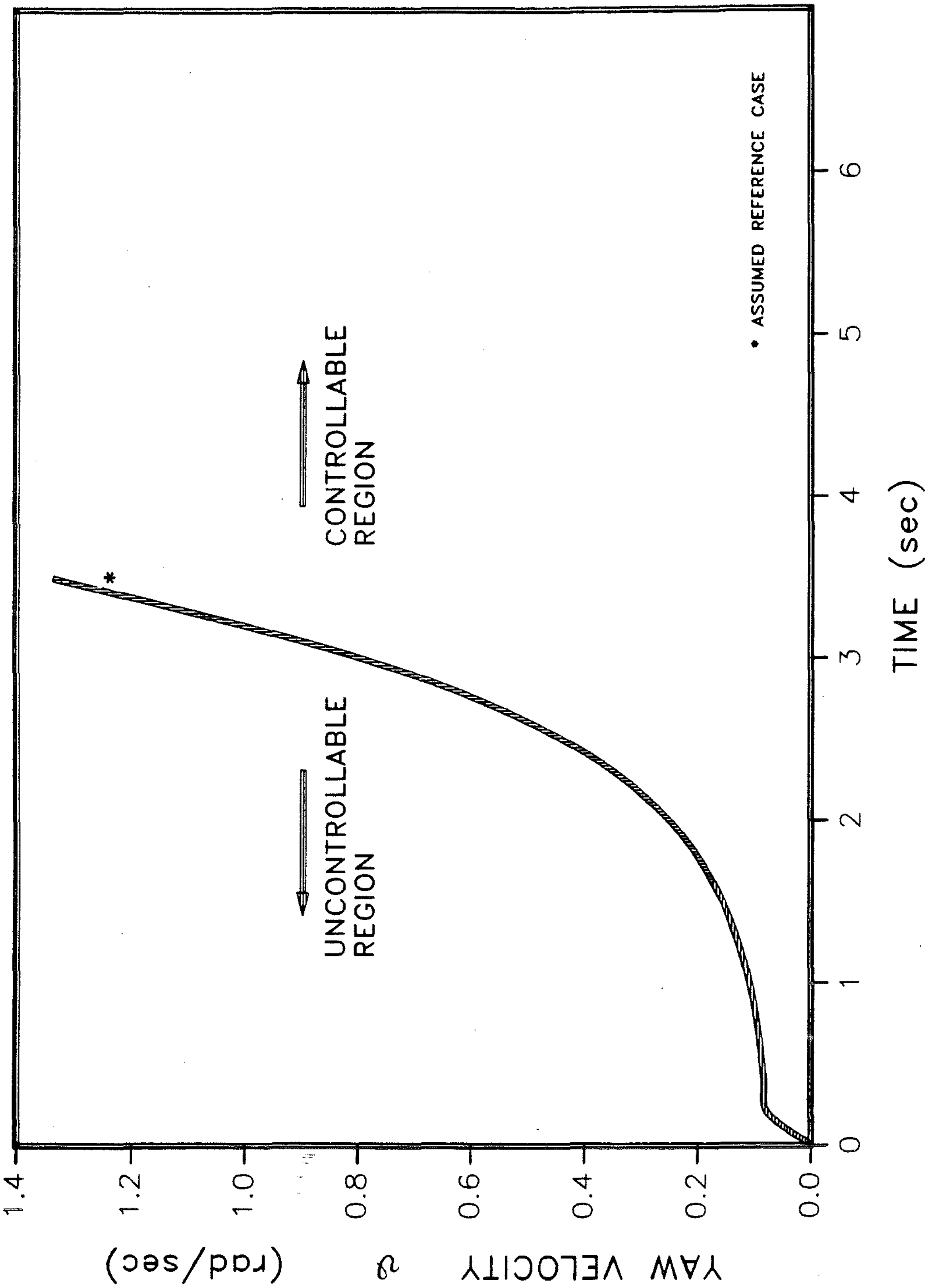

Figure 8-8 Assuming a Reference Case for the Purpose of Comparing the Effects of Different Parameters on Directional Stability

termed uncontrollable. The following assumptions with regard to the assumed reference case cannot be over emphasized:

1) The uncontrollable and controllable regions are defined as reasonable estimates only for the purpose of comparing the effects of varying other design parameters.

2) The assumed reference corresponds to one forward speed only (.75 m/s) , and one initial disturbance only (lateral impulse of 4 N-sec at c.g.) as discussed previously. When comparing other simulation results, these two initial conditions must be the same.

3) The assumed reference case is only representative of the Everest and Jennings Premier rear caster wheelchair, with default parameters as listed in Table 8-1, and EJA tires as the main wheels.

It is obviously impossible to examine all of the possible forward speeds and initial disturbances that could be used for an investigation of directional stability. It is believed that the curve in Figure 8-8 represents a typical yaw velocity response curve for a typical wheelchair subject to a typical initial disturbance while traveling at a typical forward velocity. Experimentally verifying these assumptions might be a focus for future work.

AN EXTENSIVE PARAMETRIC STUDY

Thus far this chapter has showed the results of several simulations. Several yaw velocity response curves have been presented, and an attempt has been made to define a reasonable reference case which separates uncontrollable from controllable directional instability. It is now possible to examine several other parameters.

This will be done by selecting a particular parameter which will be varied while all other variables are held constant. The effect of varying this parameter will be examined by comparing the new yaw velocity response curves with the assumed reference case. Thus, it is emphasized that for each of the figures remaining in this chapter, all of the initial conditions are identical to those associated with the reference case except for the varied parameter. This includes an initial forward velocity of .75 m/s and an initial lateral impulse of 4 N-sec at the center of gravity. Also, for each case the rear caster wheelchair has the default parameters given in Table 8-1. EJA tires are used for each simulation unless specified otherwise.

EFFECT OF CENTER OF GRAVITY POSITION

Of all the geometric variables for the rear caster wheelchair, the one most expected to have a significant effect on directional stability is the position of the center of gravity. The fact that this parameter is important was discussed in the original analysis by Kauzlarich and Thacker. [1.1]

Referring to Figure 6-1, the variables that determine center of gravity position are the distances s_1 and s_2. The effect of changing the center of gravity position while keeping all other variables constant can be determined by varying the following ratio:

$$RAT = \frac{s_1}{s_1 + s_2} \tag{8-6}$$

Where

s_1 = distance from front wheels to center of gravity

s_1+s_2 = total distance from front wheels to caster pins = constant

Thus, as s_1 is varied, s_2 will also be varied so as to keep the total distance between the front wheels and the caster pins constant.

For the default case s_1 = .345 m and s_2 = .175 m. This gives a value for the ratio in equation (8-6) of 0.66. The effect of varying this ratio on yaw velocity response is shown in Figure 8-9. As the center of gravity is moved forward, the ratio decreases, and as expected the degree of directional instability decreases. Even though Figure 8-9 does show the expected trend, there are still some interesting observations to be made.

The decrease in yaw velocity response as the center of gravity is moved forward appears to be fairly dramatic. Decreasing the ratio in equation (8-6) from .66 to .60, a decrease of 6%, produces only a slight change in the reference curve. However, moving the center of gravity forward only slightly more so that the ratio is .55 produces a very noticeable change in yaw velocity response. It appears that for ratios less than .55, the yaw velocity response curve will fall well into the controllable range.

To avoid confusion, it must be made clear that this

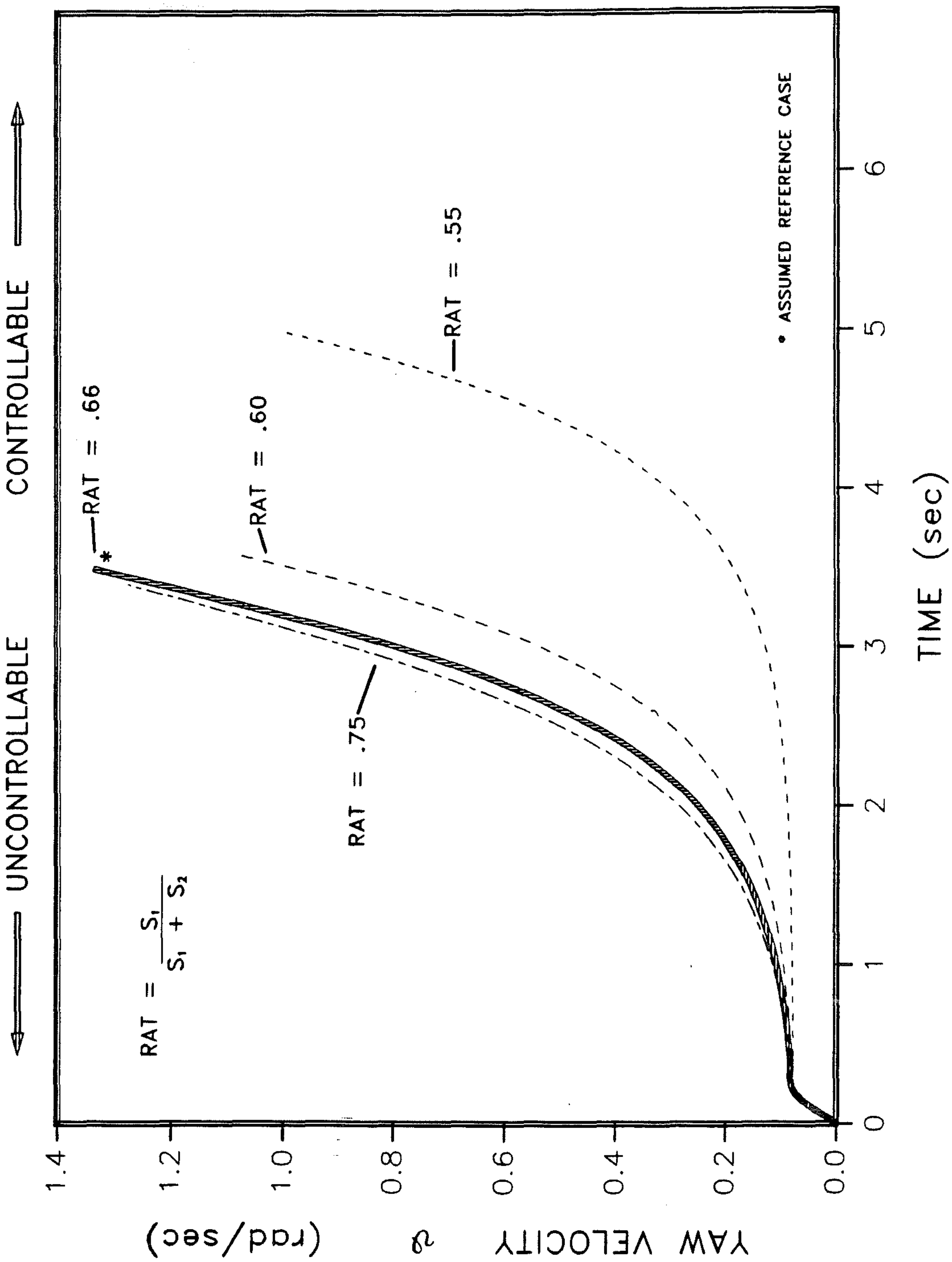

Figure 8-9 The Effect of Center of Gravity Position on Yaw Velocity Response

does not necessarily mean that reducing the ratio to .55 or some lower value produces a dramatic improvement in the overall directional stability of the wheelchair. It only indicates a significant improvement for the single value of initial forward speed that was assumed for the reference case. A measure of the improvement in overall stability can only be obtained by determining how much the initial forward speed can be increased while still keeping the yaw velocity response curve in the controllable range. This question will be examined in the next chapter.

There is a second interesting aspect of Figure 8-9. It is surprising that when the ratio in equation (8-6) is increased from .66 to .75, no appreciable change in yaw velocity response occurs. It appears that as the center of gravity is moved toward the caster wheels, a limiting yaw velocity response is reached. This limit is very near the assumed reference case. Figure 8-9 indicates that the transition from controllable to uncontrollable occurs over a narrow range of s_1 values.

EFFECT OF TOTAL ($s_1 + s_2$) DISTANCE

The second geometric parameter to be considered is the total distance, $s_1 + s_2$, separating the front wheel contact points from the caster pins (see Figure 6-1). This distance is analogous to the total wheelbase distance for the zero-width model discussed in Chapter 5. The zero-width model predicted that increasing the wheelbase distance should have a stabilizing effect.

Figure 8-10 shows yaw velocity response for 4 different values of $s_1 + s_2$. In this case the yaw velocity curves again follow the expected trend. Note that for these curves the total distance $s_1 + s_2$ is varied, but s_1 is kept constant. Of course this is equivalent to varying s_2 only.

The change in yaw velocity response does not vary in proportion to the change in $s_1 + s_2$. Decreasing the $s_1 + s_2$ distance from .52 m to .40 m moves the yaw response curve into the uncontrollable range. However, the change in yaw velocity response that results from increasing $s_1 + s_2$ from .52 m to .62 m is much more dramatic. The wheelchair clearly becomes more controllable. The sensitivity of yaw velocity to these parameters is illustrated by the fact increasing the $s_1 + s_2$ distance by only 2 cm, from .60 m to .62 m, has a significant effect on the resulting response.

For $s_1 + s_2$ greater than .62 m, the wheelchair appears to be very nearly stable under the assumed initial conditions. Again the transition from controllable to uncontrollable occurs over a narrow range of values.

EFFECT OF CASTER TRAIL DISTANCE

The measured caster trail distance, l, for the Everest and Jennings rear caster wheelchair was 8 cm. Figure 8-11 compares the results for two other l values, with the assumed reference case. Increasing l from 8 cm to 10 cm shifts the yaw velocity response curve into the

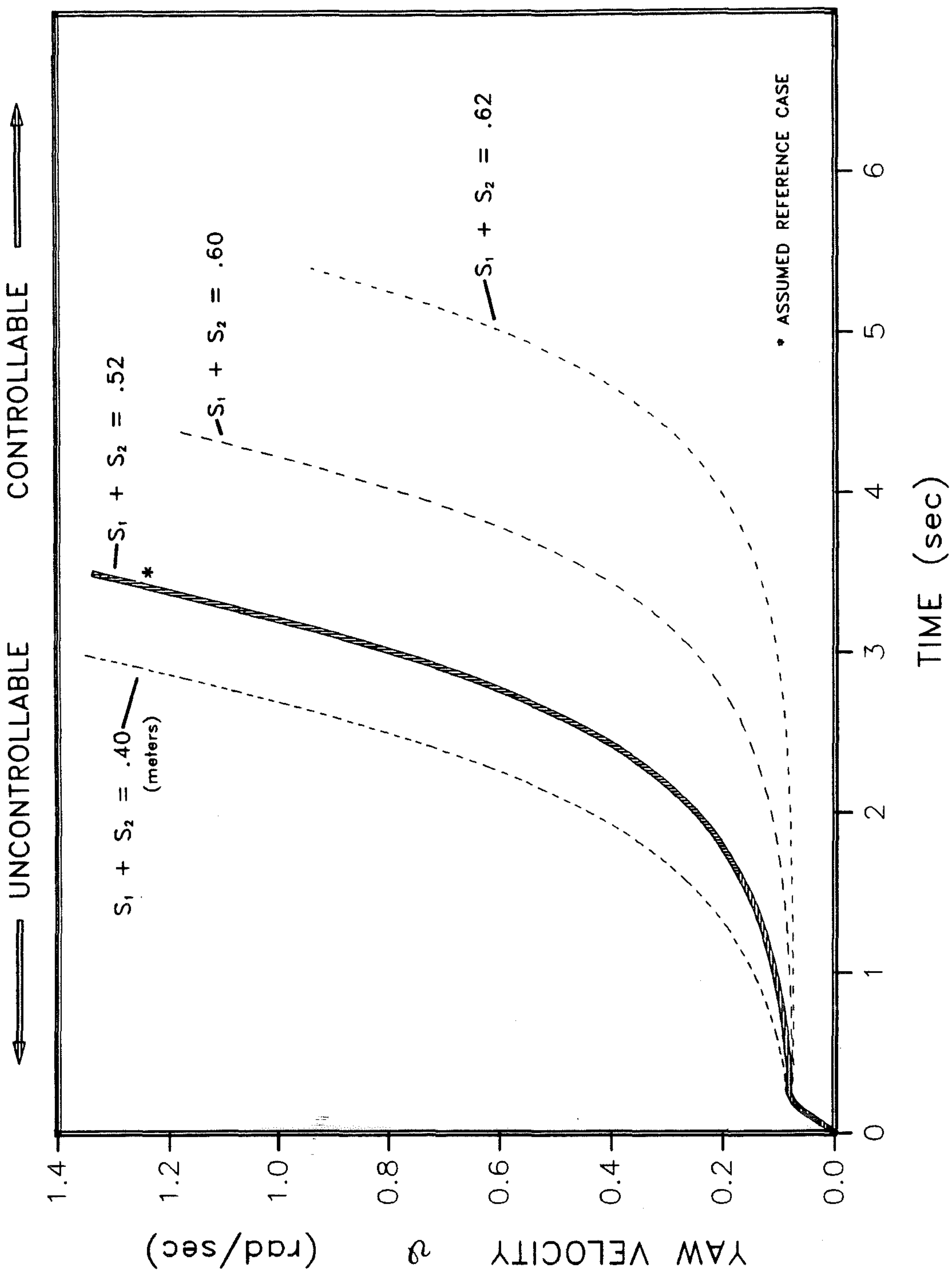

Figure 8-10 The Effect of Total ($s_1 + s_2$) Distance on Yaw Velocity Response

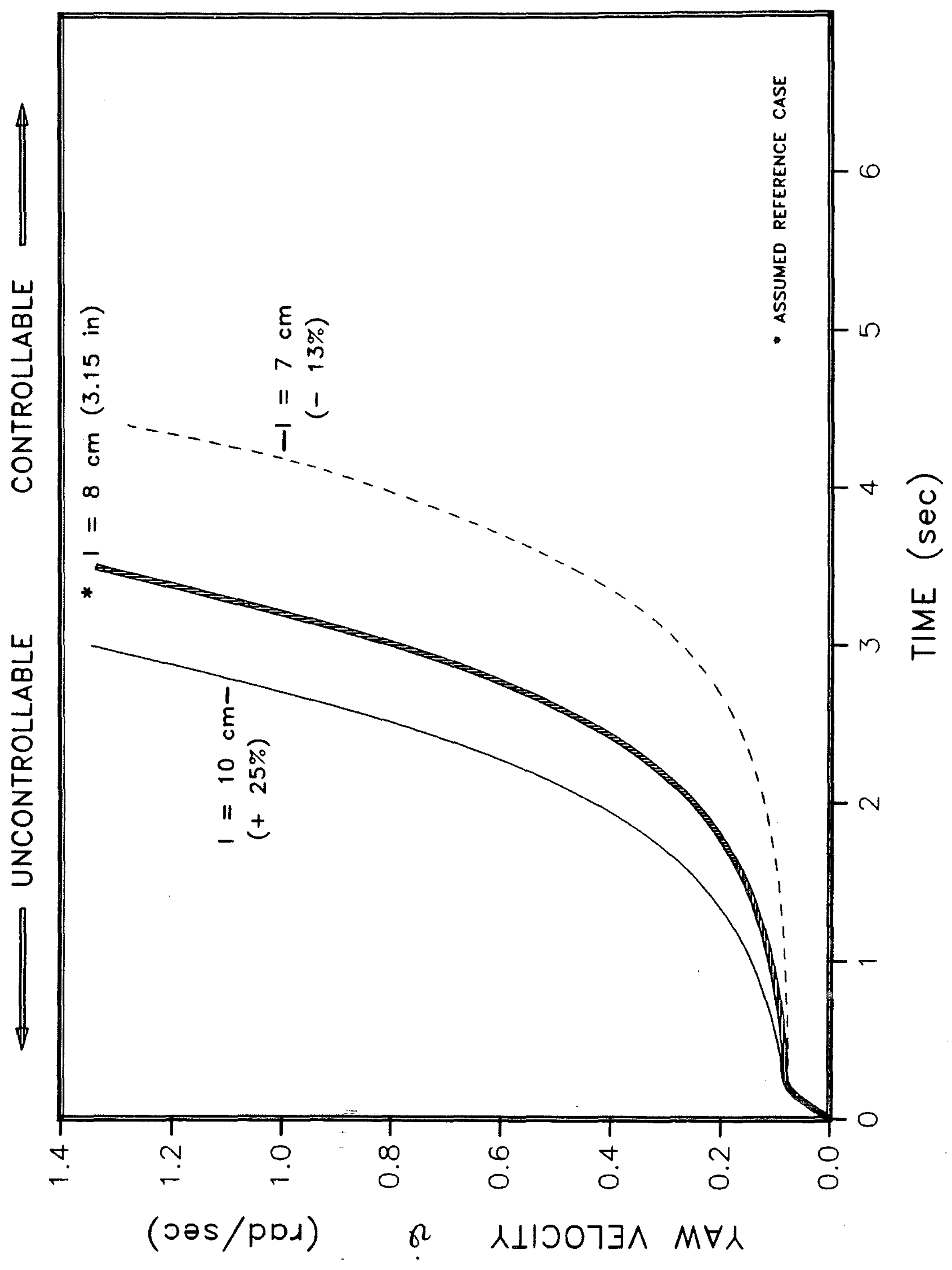

Figure 8-11 The Effect of Caster Trail Distance on Yaw Velocity Response

uncontrollable region. Decreasing l from 8 cm to 7 cm shifts the curve into the controllable region. For all three curves in Figure 8-11 the distance to the caster assembly center of gravity, l_1, is constant. Again it is observed that variations which tend to increase controllability produce the most significant changes in the yaw velocity response curve.

There is an obvious reason for the fact that decreasing the caster trail distance improves stability. As the caster trail distance is decreased, the effective moment arm for the lateral forces acting on the casters is decreased. This has the effect of making the casters more resistant to turning. This allows the caster wheels to sustain larger cornering forces. It has already been shown that stability always improves if the rear casters are made more resistant to turning. In principle, if the caster trail were zero, the moment arm for the lateral caster forces would be zero, and the casters would not turn. This would have the effect of locking the casters as discussed earlier.

Figure 8-11 suggests that some improvement in directional stability might be achieved by decreasing the caster trail distance. Unfortunately, it has been shown by Kauzlarich, Bruning, and Thacker that decreasing caster trail distance encourages the onset of caster wheel shimmy. [8.2] In addition, decreasing the caster trail distance will make it more difficult to turn the caster wheels even when this is the desired motion. The wheelchair will thus be less maneuverable.

For the reasons just given, it is clear that it is undesirable to decrease caster trail by an extreme amount. However, the value of 8 cm that was actually measured for the Everest and Jennings rear caster wheelchair seems to be unnecessarily large. It is common to find caster trail distances of only 4 cm to 6 cm for many front caster wheelchairs. Furthermore, Kauzlarich has designed a grooved dual tread caster wheel that tends to inhibit shimmy problems. [8.2] It is therefore reasonable to expect that, at least in some instances, slightly decreasing caster trail distance may be a means for reducing directional instability. The total improvement that can be obtained by combining such a decrease with changes in other parameters will be considered later in this chapter.

OTHER DIMENSIONAL PARAMETERS

Several other dimensional parameters were found to have little or no effect on the predicted yaw velocity response curve. Even though considerable effort was made to include width dimensions in the complete model, varying these parameters results in nearly negligible changes in the yaw velocity response curve. This was true for the width dimensions, d_1, d_2, t_1, and t_2 as well as the center of gravity height h. Similarly, placing the center of gravity in an off center position did not result in a significant deviation from the assumed reference curve.

These observations indicate that lateral load transfer is not an important effect for wheelchair motion under the initial conditions which are being considered. This conclusion is supported by the fact that varying the roll coefficient, k, also produced a negligible change in yaw velocity response.

From these observations, it is apparent that the zero width model is a better approximation than might be intuitively expected. The range of options for improving rear caster directional stability through dimensional changes appears to be limited to those already discussed.

EFFECT OF CASTER MASS

Aside from the caster trail distance, there are two other caster related parameters that influence directional stability. These are the caster mass and the frictional moments at the caster pins. This section will consider caster mass.

It is fairly obvious that increasing the mass of the caster assemblies should improve the controllability of a rear caster wheelchair. Increasing the caster mass has the same effect as increasing the caster trail in the sense that the pivoting motion of the casters is made more difficult. As a result, the casters will be able to withstand a greater lateral force. The increased lateral force on the casters helps to partially offset the destabilizing lateral force exerted on the front tires of the wheelchair.

The default value for the mass of the caster assemblies is 1.2 kg for the reference case. To test the influence of caster mass, m_c, on yaw velocity response, this value was increased first to 2.4 kg, and then to 3.6 kg. When increasing the mass of the caster assemblies, it is necessary to also increase the moment of inertia of the casters about the caster pins, I_{zp}. Because all geometric variables are constant, the increase in caster inertia will be roughly proportional to the increase in caster mass. This is at least a reasonable approximation for the purposes of a parametric study.

Figure 8-12 shows the effect of increasing the total caster mass m_c and the caster moment of inertia, I_{zp} by factors of two and three. As expected, these increases do tend to reduce the yaw velocity response. However, this reduction is not dramatic even for the 3 fold increase in caster mass and inertia. A 3.6 kg (7.8 lbm) caster wheel is well above the mass observed for most caster wheels. In fact, the mass of the 24 inch main wheelchair tires is generally on the order of only 2.7 kg (6 lbm). It is reasonable to conclude then, that caster mass has only a secondary influence on directional stability.

EFFECT OF FRICTION AT THE CASTER PINS

It will be shown in this section that yaw velocity response is quite sensitive to the amount of friction present at the caster pins. The assumed value for both M_{af} and M_{bf} was .10 N-m. These moments are a measure of how much torque it takes to rotate the caster wheels about their

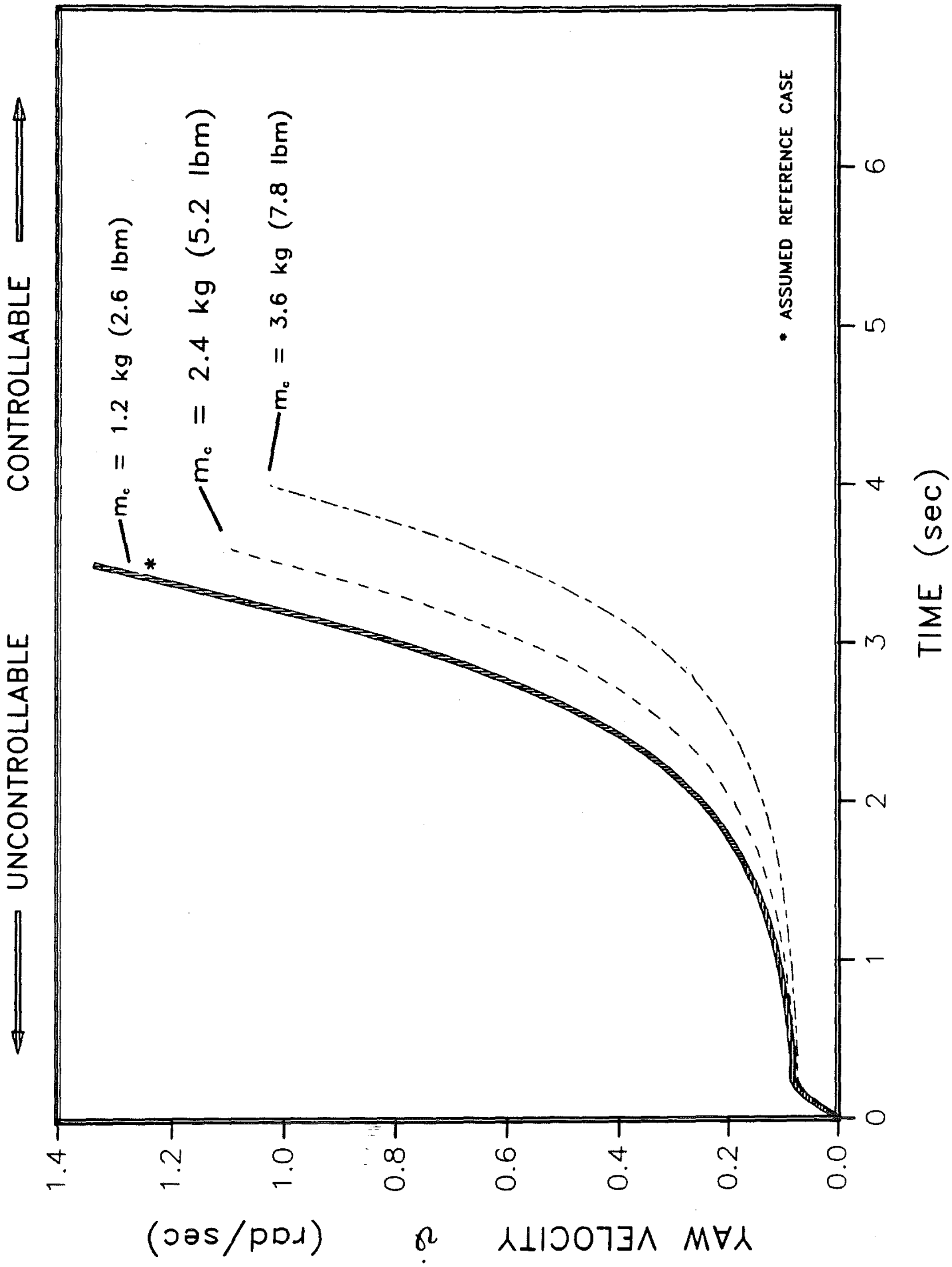

Figure 8-12 The Effect of Caster Mass on Yaw Velocity Response

pivot pins when no other forces are present.

The friction at the caster wheels can be varied by tightening or loosening the bolt which holds the caster in place. Many wheelchairs are adjusted such that the friction at the caster pins is for all practical purposes zero. Thus, the assumed value of 0.10 N-m should be considered an above average value. Zero caster friction is desirable for front caster wheelchairs, because less friction makes the wheelchair more maneuverable. However, for rear caster wheelchairs, a tolerable amount of caster friction can help to reduce the degree of directional instability.

The effect on yaw velocity response of varying the frictional moments, M_f, at the caster pins is shown in Figure 8-13. Note that M_{af} and M_{bf} are considered to have the same value M_f. The simulation results shown in the figure indicate that simply increasing the caster friction by 20% significantly improves the controllability of the wheelchair. The amount of time available for the user to make a course correction is essentially unlimited for the case where M_f = .12 N-m. It is interesting that increasing M_f from .115 N-m to .12 N-m, an increase of only 5 percent, sharply reduces the degree of instability.

It is again emphasized however, that this improvement is with respect to the reference case with $\dot{u}_o$ = .75 m/s. It is clear that increasing M_f to .12 N-m improves stability. This means that the wheelchair should be controllable at higher speeds if the caster friction is increased. The question of how much the forward speed might be increased is

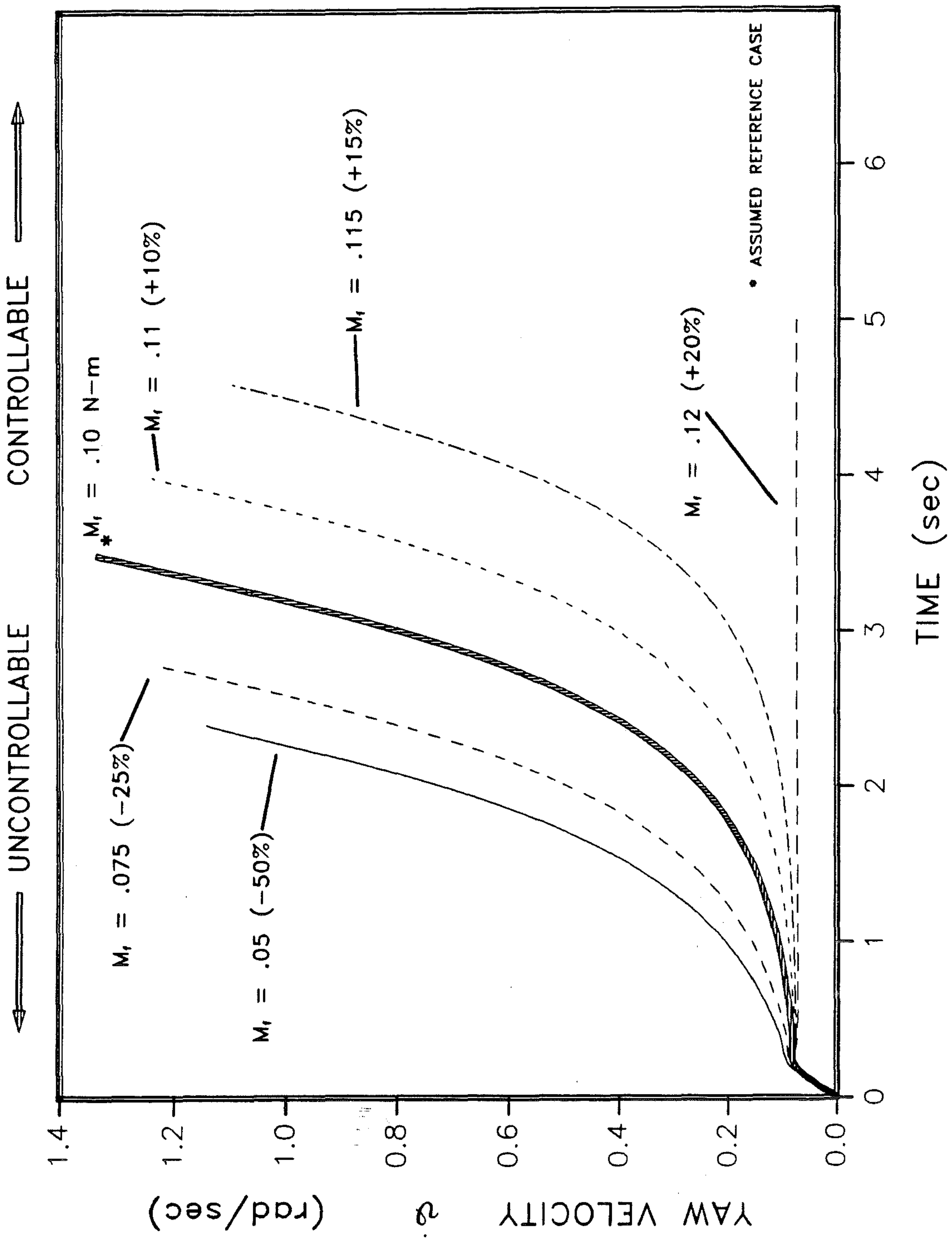

Figure 8-13 The Effect of Friction at the Caster Pins on Yaw Velocity Response

addressed later in the next chapter.

EFFECT OF TOTAL MASS AND INERTIA

Program WCHAIR predicts several interesting results with regard to the effect of varying the total mass and inertia of the wheelchair and user. Intuitively, one might expect that decreasing the mass and inertia of the wheelchair will increase the degree of directional instability. As the mass and inertia are decreased, the angular acceleration of the wheelchair for a given set of lateral forces will increase.

The conclusion that decreasing the mass and inertia of the wheelchair will worsen the instability problem assumes that the forces on the tires remain the same after the mass has been changed. However, as the mass of the wheelchair is decreased, the normal forces on the tires are also decreased. It has already been demonstrated that lower normal forces correspond to lower lateral cornering forces. As the cornering forces are decreased, the wheelchair becomes more stable.

Recall that the stability condition for a ground vehicle given in equation (5-14) was independent of the vehicle mass moment of inertia. The effect of increasing the total wheelchair/user mass can be determined by the stability condition for a rear caster wheelchair, equation (5-18).

From equation (5-18) it can be seen that as the total mass of the wheelchair and user is decreased, the value of W_r will also decrease. This of course assumes that the geometry of the wheelchair does not change. Because less weight will be carried by the rear wheels, the value of $C_{\alpha r}$ will also decrease. However, because the relationship between cornering stiffness and normal force is nonlinear, the decrease in $C_{\alpha r}$ will not be proportional to the decrease in W_r (see Figure 4-2). For example, if W_r is decreased by one half, $C_{\alpha r}$ will decrease by less than one half. The net result is that the left hand side of equation (5-18) will have a lower magnitude than before the total mass was decreased.

The default values for m and I_z for the Everest and Jennings wheelchair are 95 kg (chair and occupant) and 5.6 kg-m^2. To test the ideas just discussed, the total mass and inertia were each reduced by approximately 20%. The mass, m, was reduced to 75kg and I_z was reduced to 4.7 kg-m^2. Assuming the mass of the wheelchair itself is constant, this corresponds to a decrease in the user's mass of 20 kg (44 lbf).

The effect of reducing the mass and inertia on yaw velocity response is shown in Figure 8-14. It is called to the reader's attention that Figure 8-14 is slightly different than any of the previous graphs given in this chapter. The assumed reference case is plotted as usual. On each side of the reference case curve are yaw velocity curves for the decreased mass wheelchair and user. In obtaining each of these curves, the initial forward speed

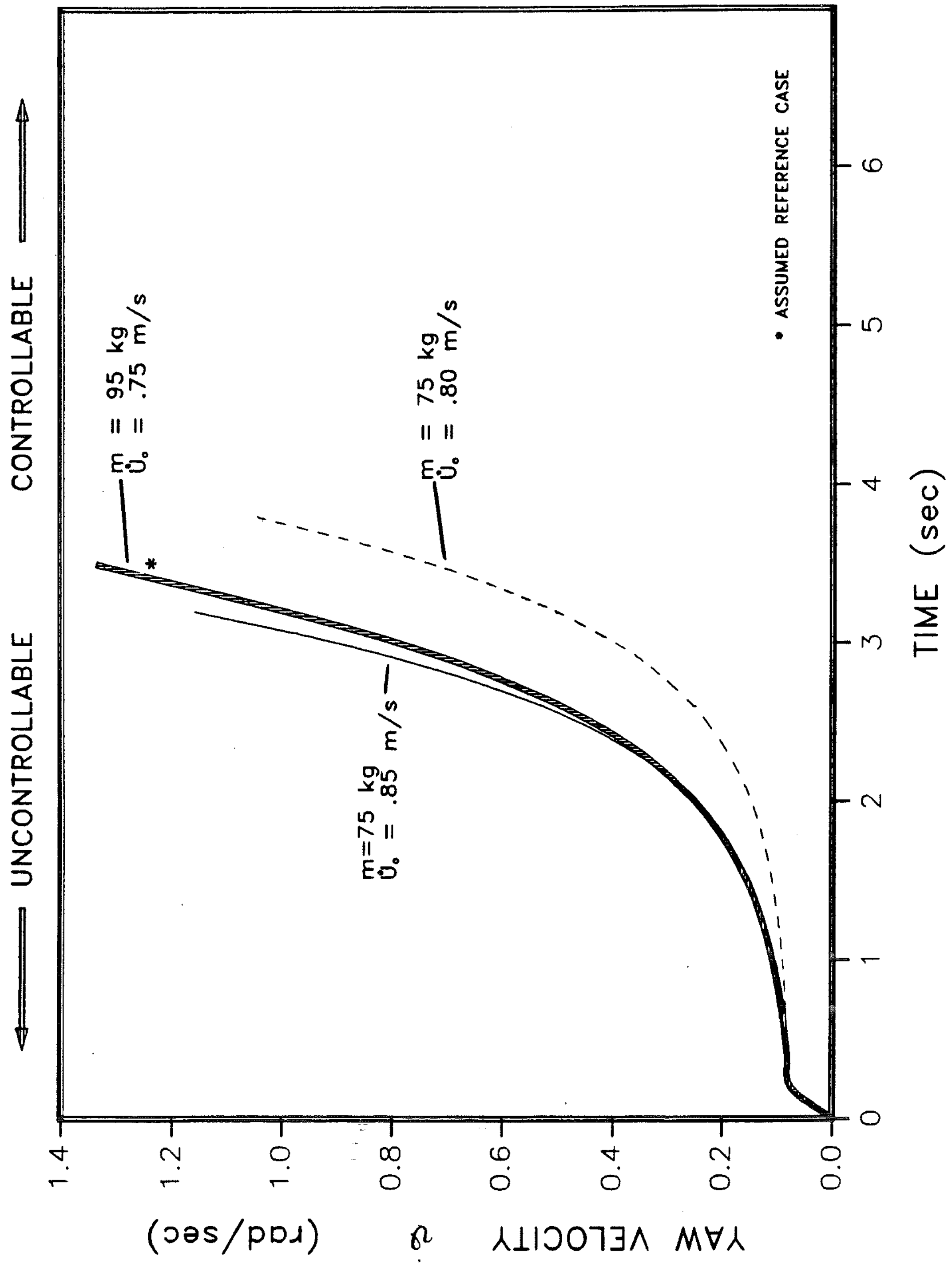

Figure 8-14 The Effect of Wheelchair/User Total Mass and Inertia on Yaw Velocity Response

has been increased slightly. From the figure, it is clear that the reduced mass wheelchair and user can travel at approximately .85 m/s before exhibiting the same directional instability as the original wheelchair. As a result of decreasing the mass and inertia, the directional stability of the wheelchair has improved. This result is somewhat surprising, but it is precisely what is predicted by the zero width model.

EFFECT OF TIRE SELECTION

As discussed earlier in this text, tire characteristics are generally considered very important to the handling qualities of a vehicle. The extensive tire study was carried out in part for the purpose of determining if tire selection significantly affects the directional stability of a rear caster wheelchair. It was hoped that the stability problem might be improved by considering tire design or selection.

The assumed reference case described earlier corresponds to type EJA tires as given in Table 3-1. Keeping all other parameters constant, four additional simulations were run where in each case a different tire was selected. Thus results were obtained for the AG, EJP, SS, and IM tires. These were compared with the assumed reference case. It was found that changing the tires had virtually no effect on the predicted yaw velocity response curve. When the yaw responses were plotted for each tire, all four of the new curves appeared identical to the reference case.

Recall that the reference case corresponds to an initial forward speed of .75 m/sec. In order to determine whether or not tire selection would have any effect at slower speeds, five additional simulation tests were performed. For these simulations, the initial forward speed was reduced to .62 m/s. Figure 8-15 shows the resulting yaw velocity response curves for all five tires.

As was the case with earlier curves, the yaw velocity gradually increases at first, and then increases very rapidly. The wheelchair slowly begins to drift away from its original heading. This slow drifting occurs for a period of time, and then the wheelchair begins to rapidly gain rotational velocity.

From Figure 8-15 it is observed that with respect to decreasing yaw velocity response, the tires are arranged in the order AG, EJP, SS, IM, EJA. Only the EJA tires significantly increase the time required for the wheelchair to become extremely unstable. These observations are precisely what would be expected from considering the cornering stiffnesses which were given for each tire in Figure 4-2. The load on each of the main tires is approximately 100 N for the assumed reference case. Looking at Figure 4-2, one finds that at this value of normal force, the AG, EJP, SS, and IM tires all have nearly the same cornering stiffness. Only the EJA tires in Figure 4-2 show a significantly lower cornering stiffness value. This

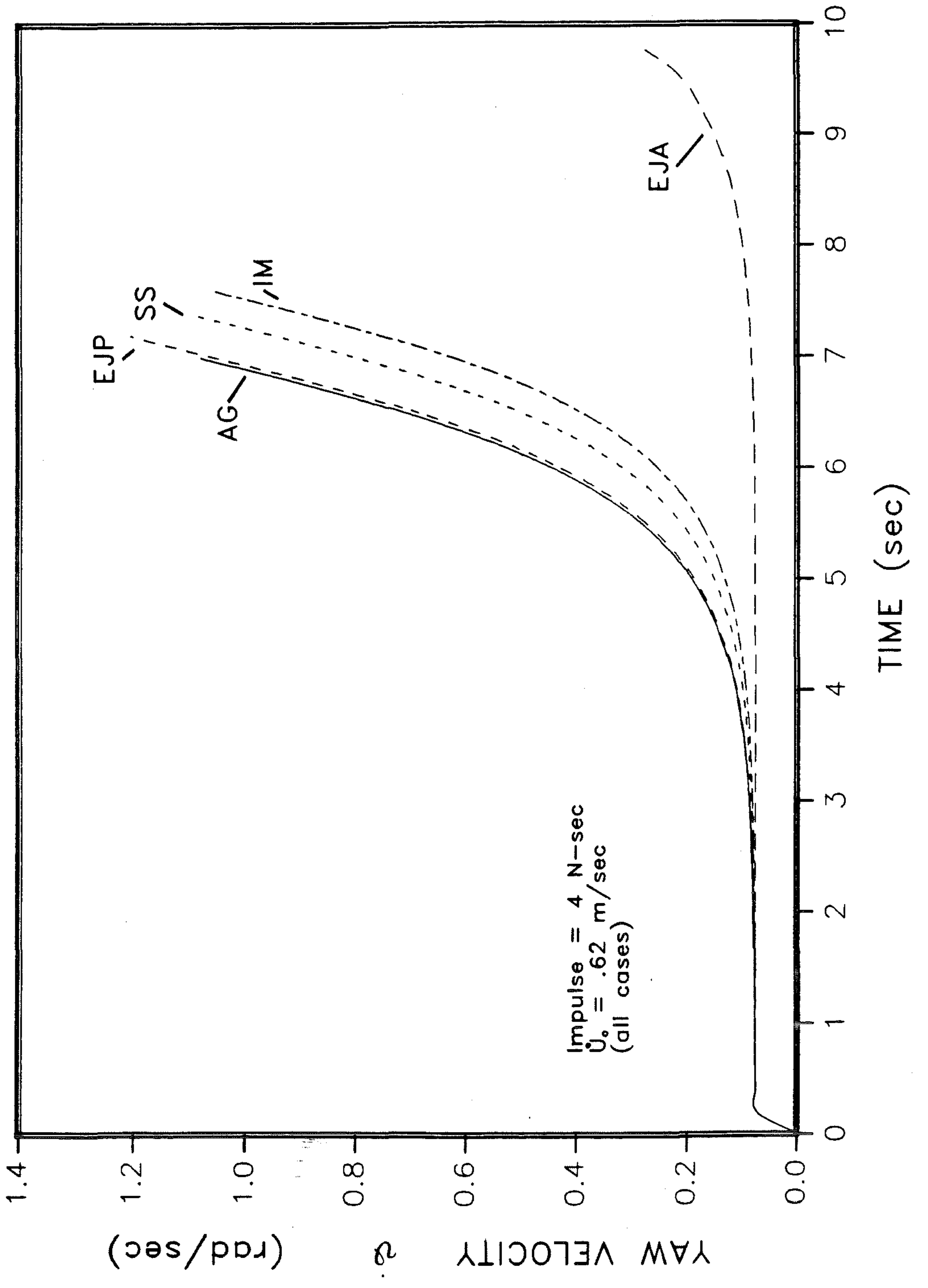

Figure 8-15 The Effect of Tire Selection on Yaw Velocity Response

observation agrees well with Figure 8-15.

The apparent conclusion is that tire selection cannot significantly change the control characteristics of the rear caster wheelchair when the motion is near the limit of extreme instability. However, selecting a tire with a low cornering stiffness does tend to decrease the rate at which the wheelchair slowly diverges to a state of uncontrolled motion.

EFFECT OF CAMBER AND TOE ANGLES

Several simulation tests were performed for camber angles of 2, 5, and 8 degrees. These corresponded to the same camber angles used for the treadmill and test cart testing. The results in every case showed that camber angle produces no noticeable change in the directional response of the wheelchair. This is consistent with the other results which have shown that the yaw velocity response is overwhelmingly dominated by the magnitude of the forward velocity and the geometry of the wheelchair.

It should be noted that for each simulation the wheels were cambered inward at the top by equal amounts. This means that two wheels develop lateral cambering forces which act in opposing directions. As a result, the forces on each wheel tend to negate each other. This is the primary reason behind the fact that camber angle does not significantly affect directional stability. Of course, it is possible to imagine cases where the camber angles are not equal, or even where one wheel is cambered inward and the other wheel is cambered outward (away from the user). These somewhat peculiar cases were not considered.

In addition to the camber angles just discussed, toe angles of one and two degrees were also considered. The simulation results indicated only that the presence of the toe angles significantly inhibited the forward motion of the wheelchair. Because the toe angles tended to reduce the forward speed of the wheelchair, they produced an apparent stabilizing effect.

As written, program WCHAIR can not propel the wheelchair so that a constant speed is maintained even though rolling resistance or toe angles are present. If both main wheels are toed in the same direction (inward or outward), the lateral forces on each tire resulting from the toe angle will act in opposite directions. As a result, they will tend to negate each other, and the directional response of the wheelchair will not change. Some authors have written that the directional stability of rear castered aircraft can be improved by slightly toeing out the main wheels. However, Stinton explains that this effect depends heavily upon lateral load transfer which occurs when airplane begins to travel along a curved path. [8.3] If the normal forces on both main tires are not the same, then the lateral forces will not be equal and opposite as just described. The results from program WCHAIR indicate that lateral load transfer is virtually insignificant, at least in the case of the Everest and Jennings rear caster wheelchair. For this reason, and because of the greatly increased resistance to rolling caused by toe angles, it is concluded that toe-out is not a desirable means for improving the directional stability of rear caster wheelchairs.

CHAPTER 9

RECOMMENDATIONS AND CONCLUSIONS

Based upon the simulation results given in Chapter 8, it is concluded that the two most important parameters affecting directional stability are the position of the center of gravity and the amount of friction at the caster pins. Unfortunately, these were the obvious parameters before this research was even begun. Although tire selection does influence directional stability, its effect is secondary when compared to other parameters.

Forward speed, caster friction, and geometry have such a dominant effect on the directional stability of manual rear caster wheelchairs, that modifications of any other parameter have virtually no effect. This is useful to know, but it makes the options for improving the directional stability problem very limited.

One contribution of this research is that improvements in directional stability can be somewhat quantified. The next section of this chapter will consider the improvement in directional stability that might be obtained for the Everest and Jennings wheelchair shown in Figure 1-1. Finally a list of conclusions that have resulted from this work will be presented and some recommendations for future work will be considered.

A REVISED WHEELCHAIR DESIGN

The basic dimensions of the Everest and Jennings rear caster wheelchair shown in Figure 1-1 were illustrated in Figure 8-1. Based upon the results given in Chapter 8 for yaw velocity response, it can now be concluded that from the standpoint of directional stability, the Everest and Jennings wheelchair is an extremely poor design.

Looking at Figure 1-1 one observes that the front axle of the Everest and Jennings wheelchair is located nearly as far forward as possible. This means that the distance from the center of gravity to the front wheels (s_1 =.345 m) is very large compared to what it might be. Placing the front wheels this far forward not only increases instability, it also makes it more difficult for the user to reach the handrim and propel the wheelchair.

It was shown in Chapter 8 that decreasing the caster trail distance, l, leads to an improvement in directional stability. The measured caster trail distance for the Everest and Jennings wheelchair is 8.0 cm. After measuring the caster trail distance for several other manual wheelchairs it was concluded that the value of 8.0 cm is quite large. In fact, not a single wheelchair could be found with a caster trail larger than 8.0 cm. It appears that at the time the Everest and Jennings wheelchair was designed, the engineers were either unaware of the factors that affect stability or were unconcerned with the problem.

A hypothetical revised design for the Everest and

Jennings wheelchair was considered in order to determine how much the directional stability could be improved. The geometric dimensions were modified in accordance with the trends given in Chapter 8. The caster trail was reduced from 8.0 cm to 6.0 cm. The front wheel axle was moved back so as to reduce the axle to center of gravity position from .345 cm to .245 cm. These dimensional changes for the Everest and Jennings wheelchair are shown in Figure 9-1, where both the original and the revised designs are shown.

Note that the total front wheel to caster pin distance, $s_1 + s_2$, has only been reduced by 5.0 cm even though the front wheels have been moved back a total of 10.0 cm. This was done simply by extending the caster pins behind the wheelchair as shown in Figure 9-1. Larger values for $s_1 + s_2$ correspond to greater stability. Thus it is desirable to keep this distance as large as possible even though the front wheels are moved back.

With these design changes implemented, the revised wheelchair should exhibit more directional stability. Recall that the original Everest and Jennings wheelchair was assumed to exhibit uncontrollable directional stability at forward speeds greater than .75 m/s. This was the assumed reference case described earlier for an initial lateral impulse of 4 N-sec. Several simulation tests were done to determine how much faster the revised wheelchair could travel before exhibiting the same degree of instability as the original design.

The results of these tests are shown in Figure 9-2.

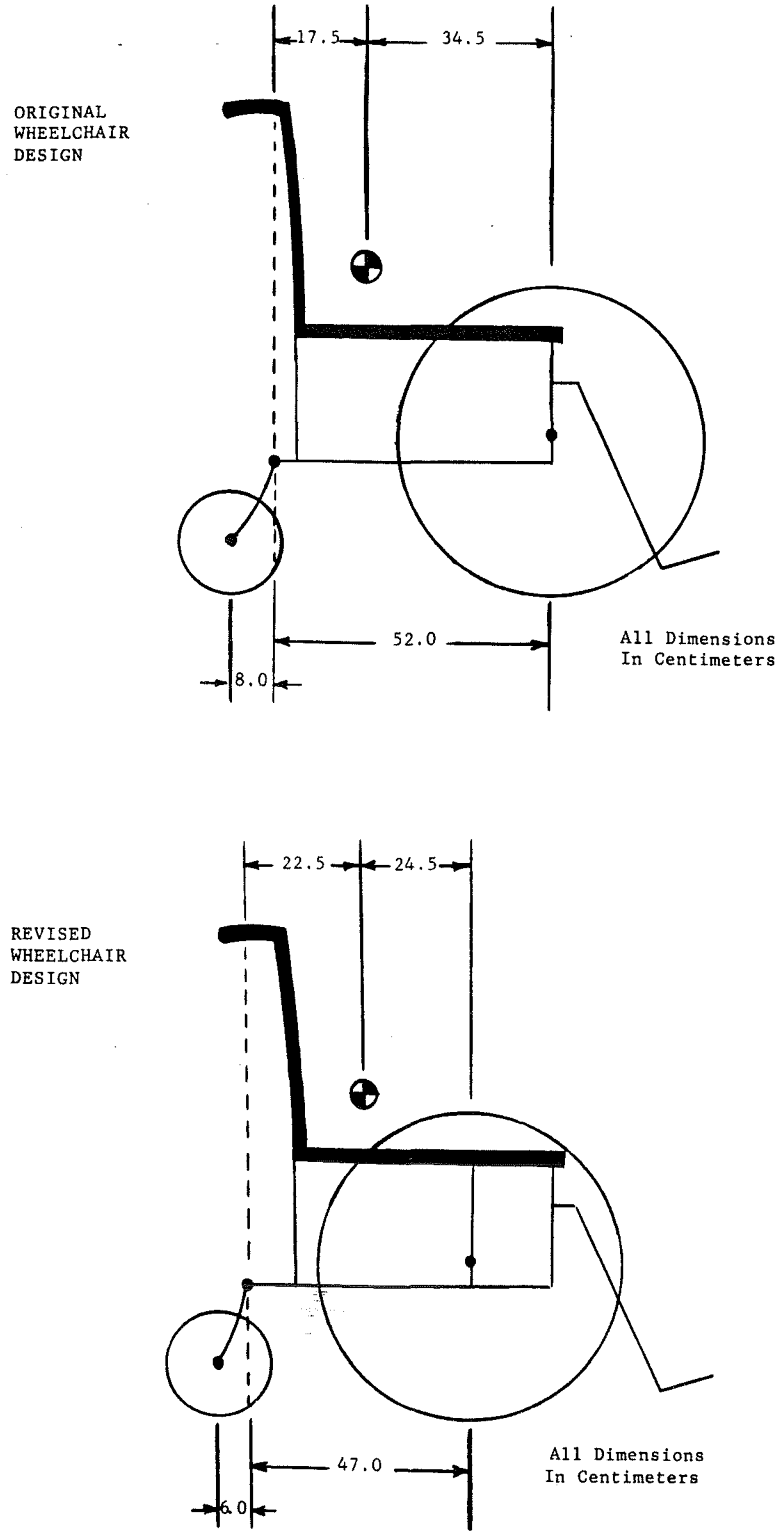

Figure 9-1 A Revised Design for the Everest and Jennings Rear Caster Wheelchair

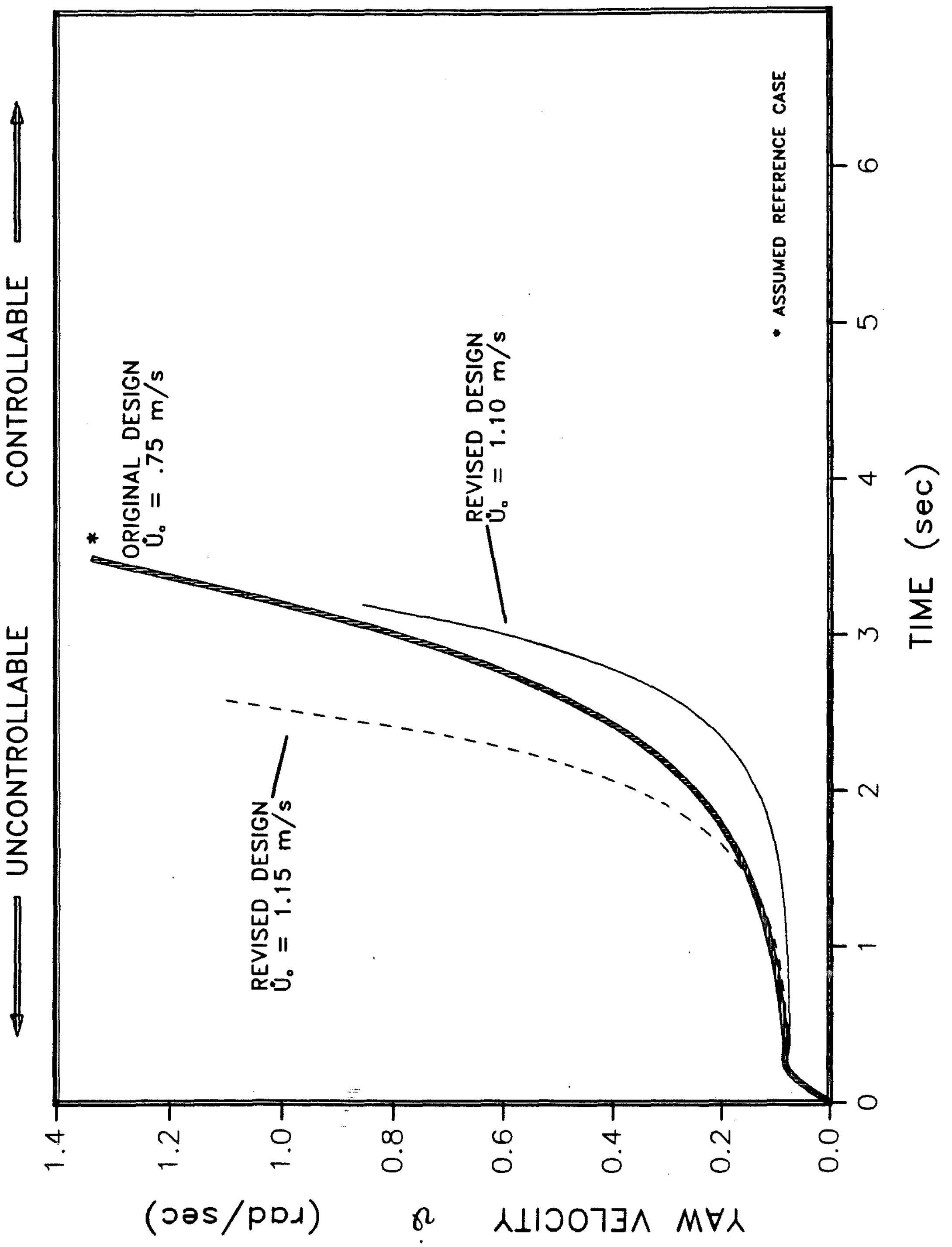

Figure 9-2 Increase in Controllable Speed Resulting from Geometric Design Changes of the Everest and Jennings Wheelchair

There are three curves in the figure. As usual, the assumed reference case corresponding the original design moving at .75 m/s is shown. Two additional curves are given for the revised design. Figure 9-2 shows that for a forward speed of 1.10 m/s the revised wheelchair is slightly more stable than the original design. However, when the speed is increased to 1.15 m/s, the new design is less stable than the original. Again the sensitivity of yaw velocity response to forward speed is apparent.

The key point is that the revised wheelchair can travel approximately .35 m/s (0.8 mph) faster than the original design before displaying the same instability. This is an increase in speed of 46% from the assumed uncontrollable curve with u_o = .75 m/s. Using this as a measure, the new wheelchair is 46% more stable than the original design.

Thus far, it has been assumed that the frictional moments at the caster pins for the revised design are unchanged. The default value for the assumed reference case was .10 N-m. Increasing this value should also improve stability. However, a large amount of caster friction is undesirable because the wheelchair becomes difficult to maneuver. Figure 9-3 shows the effect of increasing or decreasing the friction at the caster pins by 50%.

In the figure, all three curves are assumed to correspond to approximately the same degree of instability. The curves for the revised design were obtained by trial and error variation of the initial forward speed. The effect on

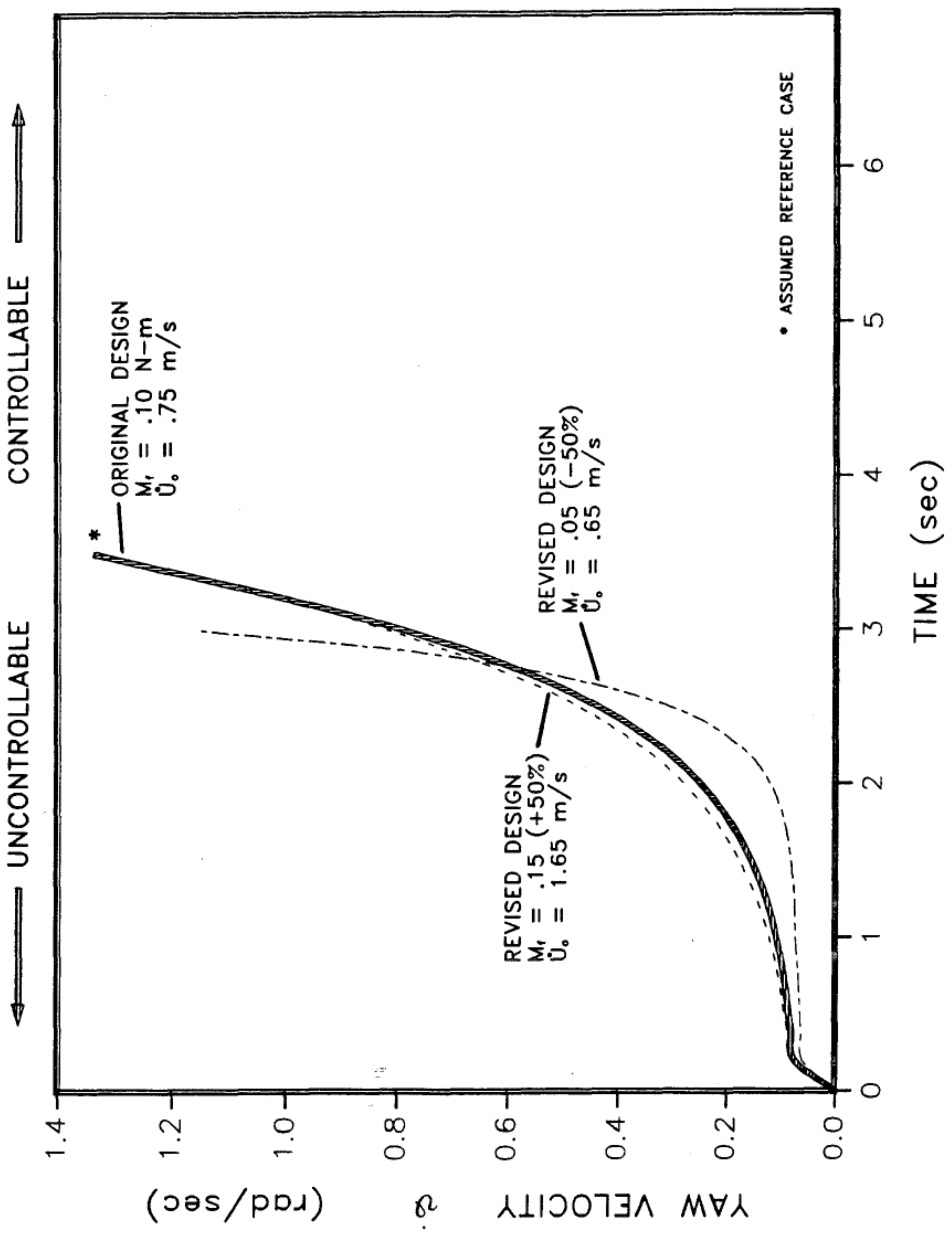

Figure 9-3 The Effect of Increasing or Decreasing Caster Friction on Controllable Speed

allowable forward speed that results from increasing or decreasing the caster friction by 50% is quite dramatic. In Figure 9-2, it was shown that the modified wheelchair could travel at a speed of 1.1 m/s before approaching the uncontrollable region. With the friction at the caster pins cut in half, this speed becomes .65 m/s, a decrease of 41%. Similarly, if the caster friction is increased by 50% the allowable forward speed increases to 1.65 m/s. This is an increase of 50% over the value of 1.1 m/s.

Figure 9-3 indicates that directional instability is roughly proportional to the amount of friction at the caster pins. In other words, doubling the amount of caster friction will approximately double the speed at which the wheelchair can travel before exhibiting the same amount of instability. Of course, the reader is reminded that these conclusions only apply for the initial lateral disturbance that was assumed throughout Chapter 8. Obviously a wheelchair subjected to a more severe disturbance could become uncontrollable at speeds slower than those given in Figure 9-2 and Figure 9-3.

CONCLUSIONS

There are several conclusions which have resulted from this research. Many of these are not favorable with regard to the prospect of improving rear caster wheelchair directional stability. These conclusions are listed next:

(1) The directional instability of rear caster wheelchairs

is strongly linked to the fact that the caster wheels are completely free to pivot. Unless some type of steering mechanism or locking device is implemented, manual rear caster wheelchairs will always be unstable, even at fairly low forward speeds.

(2) Directional stability can be improved significantly by moving the front wheels toward the user as far as possible.

(3) The distance between the front wheels and the caster pins should also be made as large as possible, within the constraints of other design parameters. This is equivalent to stating that the distance from the center of gravity to the caster pins should be as large as possible. Note, that to be consistent with (2) above, the distance between the front wheels and the caster pins should not be increased by moving the front wheels forward.

(4) The caster trail distance should be no more than five or six centimeters. Even smaller values might be feasible if the dual tread caster wheel recommended by Kauzlarich is used. [8.2] This caster wheel helps to reduce the problem of shimmy associated with short caster trail distances.

(5) Making these geometric changes can increase the controllable operating speed of a rear caster wheelchair by as much as 50%. This conclusion assumes that the results shown in Figure 9-2 are typical.

(6) Friction at the caster pins significantly improves a

wheelchair's directional stability. The amount of friction can be varied fairly easily by the user. From a directional stability point of view, the caster friction should be adjusted to the maximum tolerable amount. The tolerable amount of friction can be determined by trial and error, but a reasonable estimate is 0.3 N-m. This is about three times the value estimated for the Everest and Jennings wheelchair.

(7) Because rear caster wheelchairs are extremely unstable even at slow forward speeds, they should be used primarily indoors. If used outdoors, great care should be taken to avoid uneven ground or sharp inclines. Even a moderate incline may be dangerous, especially if the user has slightly impaired motor skills. If an incline must be negotiated, this should be done with assistance from another person. If speeds greater than approximately 2 m/s (4.5 mph) will be encountered, a rear caster wheelchair should not be used.

(8) Modifying secondary design variables such as camber angle, wheelchair width, or center of gravity height will not have a significant effect on wheelchair stability.

(9) Tire selection has a moderate influence on rear caster wheelchair handling characteristics. This influence is most noticeable at slower speeds. Tire selection should be based on ride and wear properties, although a tire with low cornering stiffness is best.

FUTURE WORK

Future research into the area of directional stability should be extended to include electric wheelchairs. Using rear casters on electric wheelchairs is more common than is the case for manual wheelchairs. Although electric wheelchairs can use automatic controls to maintain a straight path, it is still desirable to make them as stable as possible. Doing this will increase the speeds at which automatic controls can be effective.

Extending the stability study to include electric wheelchairs would require treadmill testing to determine the force characteristics of electric wheelchair tires. These tires come in a much wider range of shapes and sizes and might exhibit more variation than was found for manual wheelchair tires. This could result in tire selection being more important for electric wheelchairs.

Program WCHAIR might be used for determining the total motor torque required to stabilize an electric wheelchair against external disturbances. Because the computer program monitors the angular acceleration, $\ddot{\theta}$, of a wheelchair as it diverges from a desired path, it is possible to determine the total destabilizing moment acting on the wheelchair at any instant in time. Figure 9-4 shows the total destabilizing torque as a function of time for the assumed reference case that was used throughout Chapter 8. For an electric wheelchair, the motors must be able to generate a torque through the tires which at least offsets a curve like

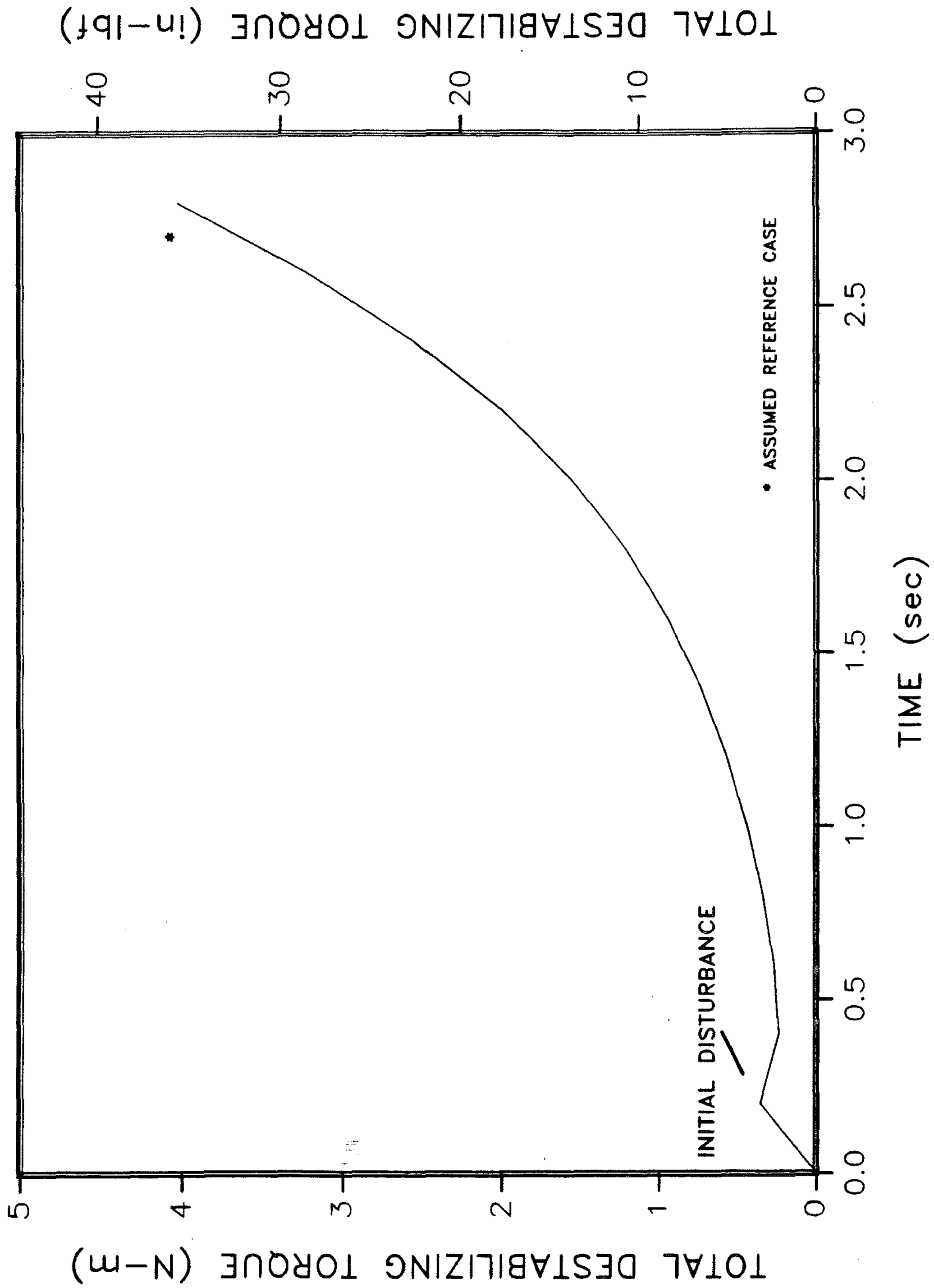

Figure 9-4 Using Program WCHAIR to Predict the Total Destabilizing Torque Exerted on a Wheelchair as a Function of Time

the one shown in Figure 9-4. If the total destabilizing torque produced by the lateral road forces becomes greater than the maximum tractive torque which can be generated by the motor, it will become impossible to return the wheelchair to a state of steady motion.

The equations of motion and computer program that were developed as part of this work can be easily extended for the purposes of examining other types of wheelchairs. The results of this research indicate that a more sophisticated model will probably not uncover any significant stability parameters that have not already been examined. In addition to electric wheelchairs, it might be of interest to examine three wheeled wheelchairs or other peculiar designs. The simulation program may also be useful for examining the handling characteristics of conventional front caster wheelchairs. Because the effects of lateral load transfer have been incorporated into the model, it would be possible to investigate more severe types of motion than those that have been considered in this thesis. It would be useful to modify the simulation program such that propelling forces from the user or input torques from a motor could be included.

Before extending the wheelchair model any further, it would be highly desirable to experimentally verify the results obtained from the simulation program. This could be done by instrumenting an actual rear caster wheelchair which is subjected to a known initial disturbance.

REFERENCES

[1.1] Kauzlarich, J.J. and Thacker, J.G., "Rear Caster Wheelchair Directional Instability," Proceedings of the RESNA 8th Annual Conference, Memphis, Tennessee, 1985, pp. 78-80.

[2.1] Nordeen, D.L., and Cortese, A.D., "Force and Moment Characteristics of Rolling Tires," SAE Reprint 713A, June 1963, and SAE Transactions, Vol. 72, 1964, pp. 325-337.

[2.2] Wong, J.Y., Theory of Ground Vehicles, John Wiley and Sons, New York, 1978.

[2.3] Ellis, J.R., Vehicle Dynamics, London Business Books Limited, London, 1969.

[2.4] Motor Vehicle Performance-Measurement and Prediction, Engineering Summer Conference, Univ of Michigan, 1973. DOT HS-015 952

[2.5] Hales, F.D., "Automobile Stability, Part III. A Two Degree of Freedom Mathematical Model Compensated for Roll Effects," Technical Memorandum 152, Stevens Institute of Technology, Hoboken, N.J., June 1986.

[2.6] Taborek, J.J., Mechanics of Vehicles, Penton Education Division, Cleveland, 1957. DOT HS-014 285

[2.7] Nordeen, D.L., "Analysis of Tire Lateral Forces and Interpretation of Experimental Tire Data," SAE Paper

670173, 1967.

[2.8] Clark, S.K. Ed., _Mechanics of Pneumatic Tires_, U.S. Department of Transportation, 1971. DOT HS-012 573

[2.9] Thacker, J.G., "Measurement of Wheelchair Rolling Resistance," Unpublished Report, University of Virginia Rehabilitation Engineering Center, Charlottesville, VA, 1984.

[2.10] Kauzlarich, J.J., and Thacker, J.G., "Wheelchair Tire Rolling Resistance and Fatigue," _Journal of Rehabilitation Research and Development_, Vol. 22, No. 3, July 1985, pp. 25-41.

[3.1] Dugoff, H., and Brown, B.J., "Measurement of Tire Shear Forces," SAE Paper 700092, 1970.

[3.2] Pottinger, M.G., Marshall, K.D., and Arnold, G.A., "Effects of Test Speed and Surface Curvature on Cornering Properties of Tires," SAE Paper 760029, 1976.

[3.3] Smiley, R.F. and Horne, W.B., "Mechanical Properties of Pneumatic Tires with Special Reference to Modern Aircraft Tires," NACA Technical Memo 4110, Washington, January 1958.

[4.1] Bergman, W., and Beauregard, C., "Transient Tire Properties," SAE Paper 740068, 1974.

[4.2] Fancher, P.S., Bernard, J.E., and Emery, L.H., "The Effects of Tire-in-Use Factors on Passenger Car Performance," Proceedings International Automobile Tire Conference, Toronto, Canada, 1974, pp. 113-120.

[4.3] The Right Stuffware, "Pwrstar", Numerical Curve Fitting Program, Version 1.02, 1986.

[5.1] Huston, J.C., Graves, B.J., and Johnson, D.B., "Three Wheeled Vehicle Dynamics," SAE Paper 820139, 1982.

[5.2] Rocard, Y., Dynamic Instability : Automobiles, Aircraft, and Suspension Bridges, Frederick Ungar Publishing Company, New York, 1957.

[5.3] Tipler, P.A., Physics, Worth Publishers Inc., New York, 1976.

[5.4] Greenwood, D.T., Principles of Dynamics, Prentice-Hall Inc., N.J., 1965.

[5.5] McGill, D.J., and King, W.W., Engineering Mechanics: An Introduction to Dynamics, PWS Publishers, Ca., 1984.

[6.1] Dugoff, H., Fancher, P.S., and Segel, L., "An Analysis of Tire Traction Properties and Their Influence on Vehicle Dynamic Performance," SAE Paper 700377, 1970.

[6.2] Segel, S.L., "On the Lateral Stability and Control of the Automobile as Influenced by the Dynamics of the

Steering System," Journal of Engineering for Industry, August 1966, pp. 283-295.

[8.1] Woodson, W.E., Human Factors Design Handbook, McGraw Hill, New York, 1981.

[8.2] Kauzlarich, J.J., Bruning, T., and Thacker, J.G., "Wheelchair Caster Shimmy and Turning Resistance," Journal of Rehabilitation Research and Development, Vol. 20, No. 2, July 1984, pp. 15-29.

[8.3] Stinton, D., The Design of The Aeroplane, Van Nostrand Reinhold Company, New York, 1983.

[D.1] Mochel, E.V., "Center of Gravity of Wheelchair and Dummy," Unpublished Document, University of Virginia Rehabilitation Engineering Center, Charlottesville, VA, May, 1986.

[D.2] Duffey, T.M., "Comparison of the Mass Moments of Inertia of an ISO Test Dummy to Those of an Anthropometric Dummy," Unpublished Report, University of Virginia Rehabilitation Engineering Center, Charlottesville, VA, 1984.

In addition to the references which were specifically cited in the thesis text, there are two extremely useful subject bibliographies which should be noted. These are published by the Department of Transportation and they contain abstracts, title listings, and author listings of literally hundreds of articles which pertain to tires and/or vehicle handling and stability. Subject bibliographies for several other subjects are also available, but only the two which were used for this thesis are given here.

[1] Vehicle Handling and Stability, a Subject Bibliography from Highway Safety Literature, DOT HS-805 045, SB-38, October, 1979.

[2] Tires, a Subject Bibliography from Highway Safety Literature, DOT HS-802 148, SB-14, March 1977.

APPENDIX A

DETAILS OF THE TREADMILL AND TEST CART

A basic description of the treadmill and test cart apparatus was given in Chapter 3. Figure 3-1 shows a sketch of the treadmill, test cart and load cell. As stated previously, the test cart was rotated to a fixed angle, α, and the force required to hold the test cart in the fixed position was measured using a load cell. In this appendix, a more complete description of how the load cell measurements were used to compute cornering force F_y as a function of normal force F_z (at constant slip angle) will be given.

Figure A-1 shows a sketch of the test cart and its associated forces and dimensions. Recall that for most of the cornering force tests, the right wheel of the test cart was removed and replaced by a vertical cable. This was described in Chapter 3. This cable is shown in Figure A-1. The dimensions of the test cart are:

d = test cart half width

r = radius of wheel

x_c = distance from axle to test cart c.g.

l = distance from axle to support pin

h = height of forward support rod

The important forces as shown in Figure A-1 are:

R_x = reaction at pin in X direction

R_y = reaction at pin in Y direction

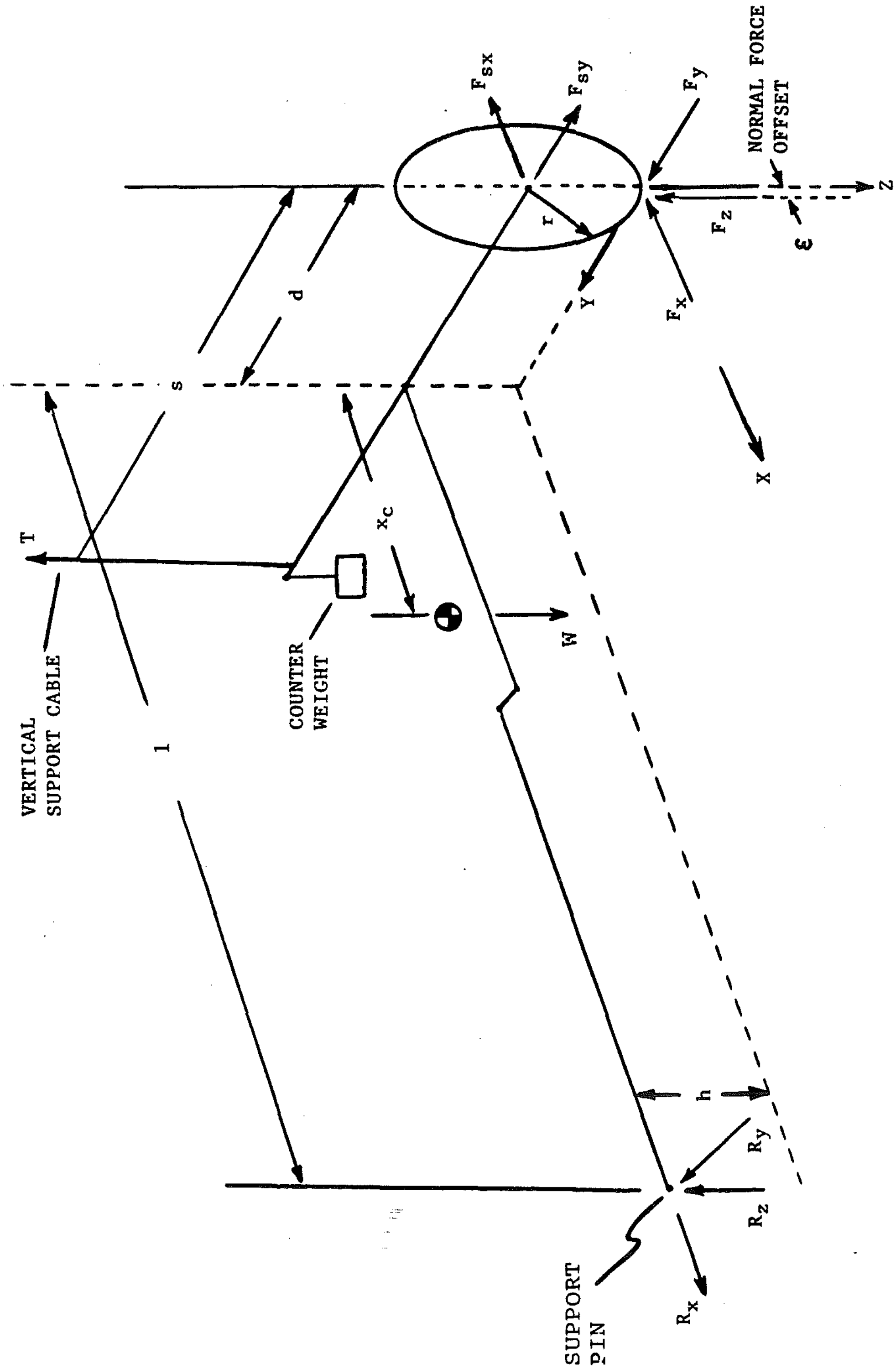

Figure A-1 Test Cart Forces and Geometry

R_z = reaction at pin in Z direction

T = tension in vertical support cable

F_x = longitudinal force on tire

F_y = lateral cornering force on tire

F_z = normal force on tire

F_{sx} = side force exerted in X direction by the load cell

F_{sy} = side force exerted in Y direction by the load cell

It is pointed out that the X-Y-Z axis system has its origin at the tire contact point. This axis system was described in detail in Chapter 2.

When using the test cart, the forward support pin is moved to various positions which correspond to fixed slip angles, α, for the tire. Thus, the first step in using the test cart is to determine the required positions of the forward pin. Note that using a pin to support the front of the test cart ensures that no moments are generated in addition to the reaction forces R_x, R_y, and R_z.

The method for determining the positions for the forward support pin is explained with the aid of Figure A-2. This Figure shows a top view of the test cart rotated through an exaggerated angle α. The test cart rotates about the point shown in Figure A-2 such that the connection point between the cart and the load cell remains fixed in space. This allows for successive measurements to be taken without moving the load cell. The load cell is configured to exert a side force F_s as shown. Although the side force has

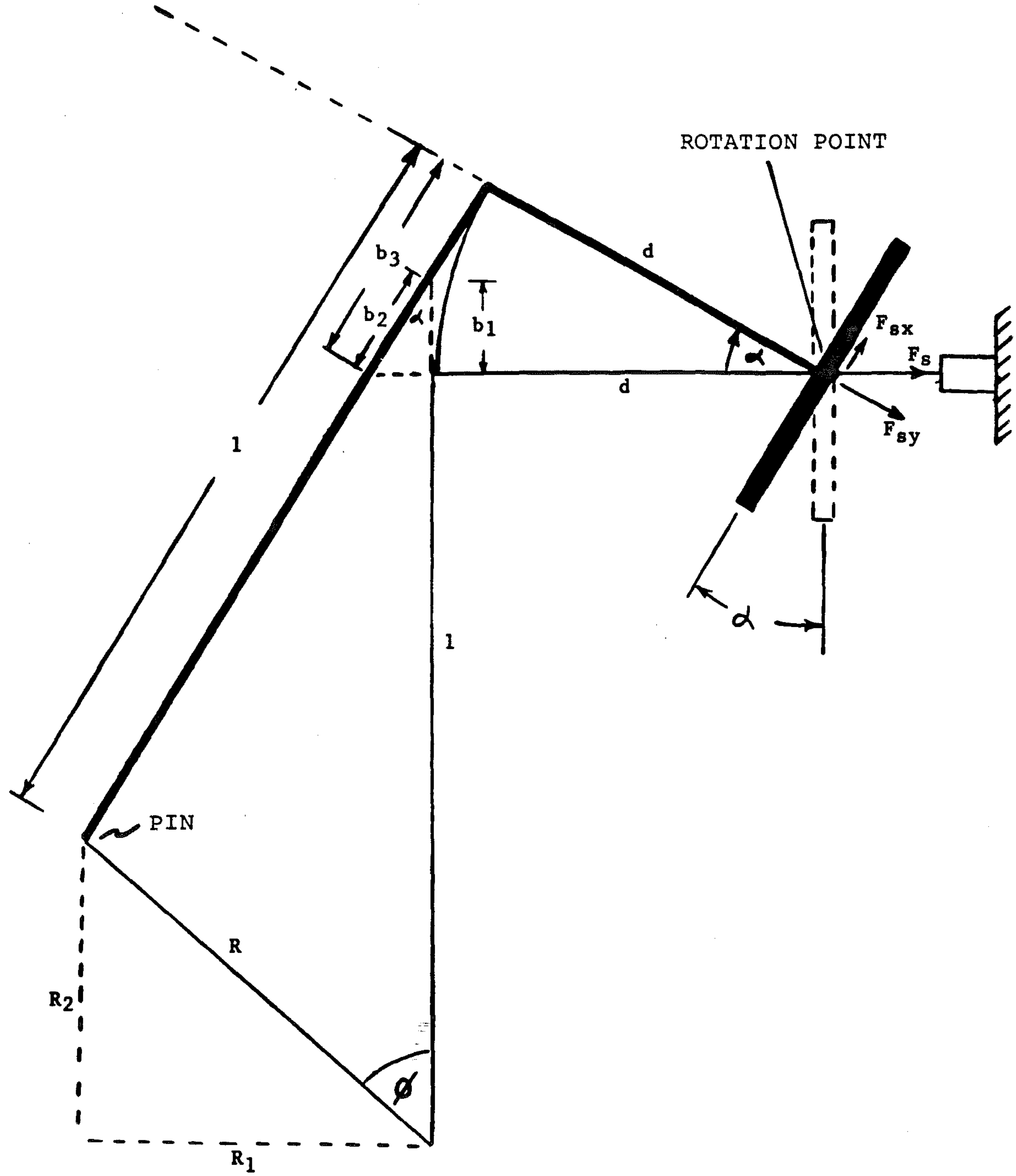

Figure A-2 Determining the Placement of The Test Cart Support Pin components along both the X and Y tire axes, the load cell experiences an axial force only.

In Figure A-2, the distances R, R_1, and R_2 are defined as follows:

R_1 = lateral distance pin is moved to create angle α

R_2 = longitudinal distance pin is moved to create angle α

R = total distance pin is moved

It is convenient to find distances R_1 and R_2 which correspond to integer slip angles. Because the length, l, is large compared to the width d, the distance R can be approximated as

$$R = l\alpha \tag{A-1}$$

However, for large slip angles, this approximation is not particularly good. The best method for setting up the test cart is to determine R_1 and R_2 by directly using the dimensions shown in Figure A-2.

The dimensions b_1, b_2, and b_3 shown in Figure A-2 are expressed in terms of the basic test cart dimensions as follows:

$$b_1 = \frac{d - d\cos(\alpha)}{\sin(\alpha)} \tag{A-2a}$$

$$b_2 = \frac{d - d\cos(\alpha)}{\sin(\alpha)\cos(\alpha)} \tag{A-2b}$$

$$b_3 = d\tan(\alpha) \tag{A-2c}$$

The distance R can then be found from the following equation:

$$R = a + b - 2ab\cos(\alpha) \qquad \text{(A-3)}$$

where the constants a and b are given by

$$a = 1 + b_1 \qquad \text{(A-4a)}$$

$$b = 1 - b_3 + b_2 \qquad \text{(A-4b)}$$

Finally, the required distances R_1 and R_2 are found to be

$$R_1 = R\sin(\emptyset) \qquad \text{(A-5a)}$$

$$R_2 = R\cos(\emptyset) \qquad \text{(A-5b)}$$

where the angle $\emptyset$ is given as

$$\emptyset = \sin{-1}\left(\frac{b}{R}\sin(\alpha)\right) \qquad \text{(A-6)}$$

Thus, given the test cart dimensions d and l the distances R_1 and R_2 can be found for any desired slip angle. Once R_1 and R_2 have been obtained, the proper locations for the support pin along the forward support bar (see Figure 3-1) can be measured.

Distances for R_1 and R_2 were determined for slip angles of 1 through 8 degrees. Holes were drilled along the support bar at the front of the treadmill to correspond to these distances. Thus the test cart could be easily adjusted simply by moving the pin to the appropriate hole.

With the treadmill belt moving, the test cart was rotated to a known slip angle α. The side force F_s necessary to hold the cart in the fixed position was measured. The load cell used for this testing had a range of 0 - 100 lbf. The components of the load cell side force F_{sx} and F_{sy} are given by:

$$F_{sx} = F_s \sin(\alpha) \tag{A-7a}$$

$$F_{sy} = F_s \cos(\alpha) \tag{A-7b}$$

The normal force F_z and the lateral cornering force F_y are found by using six statics equations for the test cart as it is shown in Figure A-1. These are given below.

$$F_x = R_x - F_x - F_{sx} = 0 \tag{A-8a}$$

$$F_y = R_y + F_y - F_{sy} = 0 \tag{A-8b}$$

$$F_z = -R_z + W - T - Fz = 0 \tag{A-8c}$$

$$M_x = R_y h - R_z d + Wd - Ts - F_{sy} r = 0 \tag{A-8d}$$

$$M_y = R_z l - R_x h - Wx_c + F_{sx} r + F_z \varepsilon = 0 \tag{A-8e}$$

$$M_z = R_y l - R_x h = 0 \tag{A-8f}$$

In order to solve these equations for the desired forces F_y and F_z, it is assumed that the rolling resistance force F_x depends only on the normal force F_z. Then F_x can be written in terms of F_z using the coefficient of rolling resistance f_r defined in Chapter 3 (see equation 3-2).

$$F_x = f_r F_z \tag{A-9}$$

Note that without equation (A-9), equations (A-8) have seven unknowns (F_x, F_y, F_z, R_x, R_y, R_z, and T) and hence cannot be solved. However, if equation (A-9) is assumed to be valid, the desired forces can be found using the following sequential solution:

$$F_z = \frac{W(1-x_c)(s-d) + F_{sy}(rl) + F_{sx}(rs-hs-rd)}{f_r(hs + rd - sr) + ls} \qquad \text{(A-10)}$$

$$F_x = f_r F_z \qquad \text{(A-11)}$$

$$R_x = f_r F_z + F_{sx} \qquad \text{(A-12)}$$

$$R_y = \frac{F_z f_r d + F_{sx} d}{l} \qquad \text{(A-13)}$$

$$F_y = F_{sy} - R_y \qquad \text{(A-14)}$$

$$R_z = \frac{R_x h + W x_c - F_{sx} r - F_z f_r r}{l} \qquad \text{(A-15)}$$

$$T = W - R_z - F_z \qquad \text{(A-16)}$$

These equations make it possible to determine all of the unknown forces given only F_s and f_r. It is emphasized that the equations must be solved in the order given. Only the equation for F_z is an explicit solution. Although it is possible to obtain explicit solutions for all of the forces, the expressions are cumbersome and there is no advantage to doing this.

For the purposes of examining wheelchair motion, only the forces F_x, F_y, and F_z are of interest. However, when the treadmill testing was done, all of the forces in equations (A-10) through (A-16) were calculated. This was done so that a calculated value for the tension in the support cable, T, could be found. This calculated value was compared to a measured value of T which was obtained using a spring scale linked to the vertical support cable. Note that it is not necessary to experimentally measure the tension in the support cable, but doing this provides one means of checking the consistency of results. For the treadmill results presented in this thesis, the difference between the value of T obtained from the spring scale and the value of T obtained from equation (A-16) was consistently less than 7%.

Note that equations (A-10) through (A-16) can be used even if the slip angle is zero. This is the method that was used for determining camber force. The left wheel of the test cart was cambered inward at the top (toward the center of the cart) and the side force F_s was measured. In this case, $F_{sx} = 0$ and $F_{sy} = F_s$. The lateral camber force was then determined using equations (A-10) through (A-16). Appendix B gives the treadmill results for the forces F_y and F_z as obtained for the seven tire types listed in Table 3-1.

Finally, it is noted that approximate solutions to equations (A-10) through (A-16) can be obtained by assuming that the rolling resistance force is negligible. In this case

$$F_x = F_{sx} = f_r = 0 \tag{A-17a}$$

and

$$F_y = F_{sy} = F_s \tag{A-17b}$$

This gives

$$F_z = \frac{W(1-x_c)(s-d) + F_{sy}rl}{ls} \tag{A-18}$$

If it is assumed that x_c is much smaller than the total length, l, (the c.g. is almost directly over the test cart axle) then equation (A-18) becomes:

$$F_z = \frac{F_{sy}r + W(s-d)}{s} \qquad \text{(A-19)}$$

The advantage to using these approximations is that the forces of interest, F_y and F_z, can be found directly from the load cell reading, F_s, using equations (A-17b) and (A-19). This simplifies the calculations somewhat. Also, note that assuming the approximations just given are valid, equation (A-19) indicates that if the test cart load, W, is constant, F_z is proportional to the lateral force F_y. These is the reason for the linear lines of constant test cart load shown if Figure 3-4a.

It was found that using the approximations just discussed, the calculated values of F_y and F_z changed by only a few percent. As expected, the largest error occurs for larger test cart loads. The F_y and F_z values presented in Appendix B were calculated using the full set of equations (A-10) through (A-16) without any approximations.

APPENDIX B

RESULTS OF TEST CART AND TREADMILL TIRE TESTING

This appendix gives the results of the treadmill testing that was done for each of the wheelchair tires listed in Table 3-1. Also given at the end of the appendix are the empirical coefficients which correspond to experimentally determined tire forces.

The results presented here represent the numerical values for lateral cornering force and camber force as found using the test cart and load cell. The method used to calculate the cornering force F_y from the measured side force F_s at the load cell was given in Appendix A.

Appendix B is divided into three parts. The first section gives cornering force results for each tire subjected to slip angles of 1 through 8 degrees. The second section gives camber force results for the five 24 inch tires subject to camber angles of 2, 5, and 8 degrees. Finally, the last section contains the empirical coefficients corresponding to the best fit curves as described in Chapter 4. The results given in this appendix are plotted in Figures 3-4a through 3-4g and in Figures 3-7a through 3-7e.

For clarity in reading the results tables, note that: W is total test cart weight, W(N) is test cart weight in Newtons, FZ is the calculated normal force on the tire, and FY is the calculated lateral cornering force on the tire.

TIRE : AIRLESS GREY (AG)
CONSTANT SLIP ANGLE = 1 DEG

		POUNDS FORCE		NEWTONS	
W	W(N)	FZ	FY	FZ	FY
82.	364.8	43.79	11.44	194.77	50.90
111.	493.8	58.70	13.75	261.09	61.14
140.	622.8	73.97	16.84	329.06	74.92
169.	751.7	88.32	17.95	392.89	79.83
198.	880.7	101.58	16.67	451.85	74.17
227.	1009.7	115.21	16.21	512.47	72.13

TIRE : AIRLESS GREY (AG)
CONSTANT SLIP ANGLE = 2 DEG

		POUNDS FORCE		NEWTONS	
W	W(N)	FZ	FY	FZ	FY
82.	364.8	47.82	20.15	212.71	89.62
111.	493.8	63.28	23.64	281.47	105.15
140.	622.8	78.73	27.12	350.22	120.65
169.	751.7	93.27	28.62	414.86	127.33
198.	880.7	107.63	29.74	478.77	132.30
227.	1009.7	121.45	29.68	540.22	132.04

TIRE : AIRLESS GREY (AG)
CONSTANT SLIP ANGLE = 3 DEG

		POUNDS FORCE		NEWTONS	
W	W(N)	FZ	FY	FZ	FY
82.	364.8	51.43	27.99	228.78	124.49
111.	493.8	67.62	33.05	300.77	147.02
140.	622.8	83.25	36.92	370.31	164.23
169.	751.7	97.59	38.02	434.11	169.11
198.	880.7	112.69	40.72	501.28	181.12
227.	1009.7	126.50	40.66	562.72	180.85

TIRE : AIRLESS GREY (AG)
CONSTANT SLIP ANGLE = 4 DEG

		POUNDS FORCE		NEWTONS	
W	W(N)	FZ	FY	FZ	FY
82.	364.8	54.63	34.96	243.01	155.51
111.	493.8	71.35	41.19	317.38	183.21
140.	622.8	86.97	45.04	386.86	200.35
169.	751.7	102.22	48.11	454.72	214.00
198.	880.7	116.58	49.22	518.60	218.93
227.	1009.7	130.76	49.95	581.66	222.17

TIRE : AIRLESS GREY (AG)
CONSTANT SLIP ANGLE = 5 DEG

		POUNDS FORCE		NEWTONS	
W	W(N)	FZ	FY	FZ	FY
82.	364.8	56.88	39.89	253.00	177.46
111.	493.8	73.76	46.49	328.09	206.78
140.	622.8	90.45	52.68	402.36	234.33
169.	751.7	105.88	56.13	470.98	249.66
198.	880.7	120.78	58.41	537.26	259.81
227.	1009.7	134.59	58.35	598.70	259.54

TIRE : AIRLESS GREY (AG)
CONSTANT SLIP ANGLE = 6 DEG

		POUNDS FORCE		NEWTONS	
W	W(N)	FZ	FY	FZ	FY
82.	364.8	58.55	43.60	260.42	193.92
111.	493.8	75.94	51.33	337.82	228.32
140.	622.8	92.98	58.27	413.60	259.20
169.	751.7	108.58	62.09	482.97	276.20
198.	880.7	123.83	65.14	550.82	289.77
227.	1009.7	137.64	65.08	612.26	289.49

TIRE : AIRLESS GREY (AG)
CONSTANT SLIP ANGLE = 7 DEG

		POUNDS FORCE		NEWTONS	
W	W(N)	FZ	FY	FZ	FY
82.	364.8	59.82	46.46	266.11	206.69
111.	493.8	77.55	54.93	344.98	244.36
140.	622.8	94.93	62.62	422.25	278.53
169.	751.7	110.86	67.19	493.15	298.89
198.	880.7	126.82	71.78	564.13	319.31
227.	1009.7	140.63	71.72	625.57	319.03

TIRE AIRLESS GREY (AG)
CONSTANT SLIP ANGLE = 8 DEG

		POUNDS FORCE		NEWTONS	
W	W(N)	FZ	FY	FZ	FY
82.	364.8	60.37	47.74	268.52	212.36
111.	493.8	79.13	58.48	351.98	260.13
140.	622.8	96.12	65.35	427.55	290.67
169.	751.7	112.57	71.06	500.75	316.07
198.	880.7	128.34	75.23	570.87	334.65
227.	1009.7	142.50	75.94	633.88	337.80

TIRE : EVEREST AND JENNINGS PNEUMATIC (EJP)
CONSTANT SLIP ANGLE = 1 DEG

		POUNDS FORCE		NEWTONS	
W	W(N)	FZ	FY	FZ	FY
82.	364.8	43.64	11.09	194.11	49.34
111.	493.8	58.60	13.46	260.67	59.89
140.	622.8	73.01	14.64	324.77	65.14
169.	751.7	87.23	15.43	388.04	68.63
198.	880.7	101.46	16.21	451.30	72.08
227.	1009.7	114.94	15.40	511.27	68.51

TIRE : EVEREST AND JENNINGS PNEUMATIC (EJP)
CONSTANT SLIP ANGLE = 2 DEG

		POUNDS FORCE		NEWTONS	
W	W(N)	FZ	FY	FZ	FY
82.	364.8	47.85	20.19	212.86	89.81
111.	493.8	63.55	24.14	282.67	107.39
140.	622.8	79.43	28.50	353.32	126.76
169.	751.7	93.47	28.88	415.75	128.47
198.	880.7	107.69	29.65	479.01	131.91
227.	1009.7	121.54	29.65	540.63	131.88

TIRE : EVEREST AND JENNINGS PNEUMATIC (EJP)
CONSTANT SLIP ANGLE = 3 DEG

		POUNDS FORCE		NEWTONS	
W	W(N)	FZ	FY	FZ	FY
82.	364.8	51.65	28.42	229.74	126.42
111.	493.8	67.70	33.15	301.13	147.44
140.	622.8	84.48	39.46	375.80	175.53
169.	751.7	99.44	41.82	442.31	186.03
198.	880.7	113.84	42.99	506.37	191.21
227.	1009.7	127.51	42.58	567.17	189.42

TIRE : EVEREST AND JENNINGS PNEUMATIC (EJP)
CONSTANT SLIP ANGLE = 4 DEG

		POUNDS FORCE		NEWTONS	
W	W(N)	FZ	FY	FZ	FY
82.	364.8	55.39	36.57	246.39	162.67
111.	493.8	72.88	44.43	324.20	197.62
140.	622.8	89.47	50.32	397.98	223.82
169.	751.7	104.41	52.67	464.45	234.27
198.	880.7	119.72	55.80	532.55	248.19
227.	1009.7	133.57	55.79	594.17	248.16

TIRE : EVEREST AND JENNINGS PNEUMATIC (EJP)
CONSTANT SLIP ANGLE = 5 DEG

		POUNDS FORCE		NEWTONS	
W	W(N)	FZ	FY	FZ	FY
82.	364.8	58.35	43.06	259.57	191.55
111.	493.8	76.73	52.84	341.29	235.05
140.	622.8	94.20	60.67	419.02	269.85
169.	751.7	108.95	62.61	484.65	278.50
198.	880.7	124.25	65.72	552.71	292.36
227.	1009.7	138.47	66.50	615.93	295.80

TIRE EVEREST AND JENNINGS PNEUMATIC (EJP)
CONSTANT SLIP ANGLE = 6 DEG

		POUNDS FORCE		NEWTONS	
W	W(N)	FZ	FY	FZ	FY
82.	364.8	60.01	46.74	266.94	207.93
111.	493.8	79.25	58.43	352.52	259.89
140.	622.8	96.70	66.21	430.13	294.51
169.	751.7	111.98	69.31	498.13	308.32
198.	880.7	127.63	73.19	567.74	325.57
227.	1009.7	141.84	73.96	630.95	329.00

TIRE : EVEREST AND JENNINGS PNEUMATIC (EJP)
CONSTANT SLIP ANGLE = 7 DEG

		POUNDS FORCE		NEWTONS	
W	W(N)	FZ	FY	FZ	FY
82.	364.8	61.46	49.98	273.37	222.34
111.	493.8	80.83	61.99	359.56	275.74
140.	622.8	99.32	72.06	441.81	320.53
169.	751.7	115.31	76.70	512.94	341.16
198.	880.7	130.24	79.00	579.32	351.42
227.	1009.7	145.16	81.32	645.69	361.73

TIRE : EVEREST AND JENNINGS PNEUMATIC (EJP)
CONSTANT SLIP ANGLE = 8 DEG

		POUNDS FORCE		NEWTONS	
W	W(N)	FZ	FY	FZ	FY
82.	364.8	62.52	52.40	278.08	233.07
111.	493.8	81.85	64.33	364.09	286.17
140.	622.8	100.84	75.50	448.54	335.84
169.	751.7	117.16	80.88	521.16	359.79
198.	880.7	131.01	80.86	582.78	359.69
227.	1009.7	147.34	86.25	655.41	383.67

TIRE : SILVER STAR PNEUMATIC 75PSI (SS)
CONSTANT SLIP ANGLE = 1 DEG

		POUNDS FORCE		NEWTONS	
W	W(N)	FZ	FY	FZ	FY
82.	364.8	42.71	9.10	189.98	40.46
111.	493.8	58.05	12.27	258.22	54.60
140.	622.8	72.10	12.67	320.71	56.35
169.	751.7	86.13	13.05	383.12	58.04
198.	880.7	100.55	14.24	447.27	63.34
227.	1009.7	114.21	13.82	508.03	61.48

TIRE : SILVER STAR PNEUMATIC 75PSI (SS)
CONSTANT SLIP ANGLE = 2 DEG

		POUNDS FORCE		NEWTONS	
W	W(N)	FZ	FY	FZ	FY
82.	364.8	47.11	18.60	209.58	82.74
111.	493.8	62.44	21.77	277.77	96.82
140.	622.8	76.86	22.95	341.89	102.09
169.	751.7	91.81	25.32	408.41	112.61
198.	880.7	106.41	26.90	473.36	119.65
227.	1009.7	120.63	27.68	536.58	123.11

TIRE : SILVER STAR PNEUMATIC 75PSI (SS)
CONSTANT SLIP ANGLE = 3 DEG

		POUNDS FORCE		NEWTONS	
W	W(N)	FZ	FY	FZ	FY
82.	364.8	50.91	26.84	226.47	119.37
111.	493.8	66.97	31.57	297.89	140.43
140.	622.8	82.30	34.73	366.07	154.48
169.	751.7	96.88	36.29	430.93	161.43
198.	880.7	110.92	36.68	493.41	163.16
227.	1009.7	125.32	37.85	557.44	168.36

TIRE : SILVER STAR PNEUMATIC 75PSI (SS)
CONSTANT SLIP ANGLE = 4 DEG

		POUNDS FORCE		NEWTONS	
W	W(N)	FZ	FY	FZ	FY
82.	364.8	53.75	33.02	239.09	146.89
111.	493.8	70.52	39.31	313.68	174.86
140.	622.8	86.57	44.03	385.06	195.85
169.	751.7	100.96	45.19	449.09	201.02
198.	880.7	115.00	45.58	511.56	202.73
227.	1009.7	129.94	47.92	578.01	213.17

TIRE : SILVER STAR PNEUMATIC 75PSI (SS)
CONSTANT SLIP ANGLE = 5 DEG

		POUNDS FORCE		NEWTONS	
W	W(N)	FZ	FY	FZ	FY
82.	364.8	55.64	37.18	247.49	165.38
111.	493.8	73.11	45.00	325.21	200.19
140.	622.8	89.69	50.88	398.94	226.31
169.	751.7	105.16	54.38	467.78	241.91
198.	880.7	118.84	53.98	528.64	240.13
227.	1009.7	133.77	56.32	595.05	250.52

TIRE : SILVER STAR PNEUMATIC 75PSI (SS)
CONSTANT SLIP ANGLE = 6 DEG

		POUNDS FORCE		NEWTONS	
W	W(N)	FZ	FY	FZ	FY
82.	364.8	56.77	39.72	252.55	176.69
111.	493.8	74.40	47.90	330.95	213.05
140.	622.8	92.04	56.08	409.39	249.45
169.	751.7	108.04	60.74	480.58	270.18
198.	880.7	122.62	62.29	545.44	277.08
227.	1009.7	137.54	64.61	611.81	287.41

TIRE : SILVER STAR PNEUMATIC 75PSI (SS)
CONSTANT SLIP ANGLE = 7 DEG

		POUNDS FORCE		NEWTONS	
W	W(N)	FZ	FY	FZ	FY
82.	364.8	57.35	41.06	255.12	182.63
111.	493.8	76.20	51.90	338.95	230.88
140.	622.8	94.16	60.82	418.85	270.53
169.	751.7	110.68	66.62	492.34	296.33
198.	880.7	125.62	68.93	558.77	306.64
227.	1009.7	140.17	70.47	623.52	313.46

TIRE : SILVER STAR PNEUMATIC 75PSI (SS)
CONSTANT SLIP ANGLE = 8 DEG

		POUNDS FORCE		NEWTONS	
W	W(N)	FZ	FY	FZ	FY
82.	364.8	57.74	41.98	256.82	186.73
111.	493.8	76.72	53.15	341.27	236.41
140.	622.8	95.36	63.55	424.18	282.70
169.	751.7	112.57	70.86	500.73	315.21
198.	880.7	127.49	73.17	567.11	325.46
227.	1009.7	143.46	77.78	638.14	345.97

TIRE INVACARE MAG-SPIDER WEB (IM)
CONSTANT SLIP ANGLE = 1 DEG

		POUNDS FORCE		NEWTONS	
W	W(N)	FZ	FY	FZ	FY
82.	364.8	42.70	9.09	189.95	40.42
111.	493.8	56.91	9.84	253.14	43.78
140.	622.8	70.93	10.21	315.53	45.40
169.	751.7	84.76	10.16	377.03	45.19
198.	880.7	98.40	9.71	437.72	43.19
227.	1009.7	112.21	9.64	499.12	42.86

TIRE : INVACARE MAG-SPIDER WEB (IM)
CONSTANT SLIP ANGLE = 2 DEG

		POUNDS FORCE		NEWTONS	
W	W(N)	FZ	FY	FZ	FY
82.	364.8	45.63	15.41	202.97	68.55
111.	493.8	60.39	17.36	268.62	77.22
140.	622.8	75.15	19.31	334.29	85.90
169.	751.7	89.35	20.06	397.43	89.23
198.	880.7	103.73	21.20	461.42	94.31
227.	1009.7	117.90	21.93	524.46	97.53

TIRE : INVACARE MAG-SPIDER WEB (IM)
CONSTANT SLIP ANGLE = 3 DEG

		POUNDS FORCE		NEWTONS	
W	W(N)	FZ	FY	FZ	FY
82.	364.8	48.71	22.08	216.65	98.21
111.	493.8	63.82	24.81	283.90	110.36
140.	622.8	78.77	27.15	350.37	120.77
169.	751.7	93.69	29.48	416.77	131.13
198.	880.7	108.44	31.41	482.37	139.71
227.	1009.7	122.98	32.92	547.04	146.45

TIRE : INVACARE MAG-SPIDER WEB (IM)
CONSTANT SLIP ANGLE = 4 DEG

		POUNDS FORCE		NEWTONS	
W	W(N)	FZ	FY	FZ	FY
82.	364.8	50.83	26.71	226.09	118.81
111.	493.8	66.48	30.61	295.74	136.16
140.	622.8	81.78	33.73	363.79	150.03
169.	751.7	96.70	36.05	430.16	160.35
198.	880.7	111.63	38.36	496.55	170.65
227.	1009.7	126.89	41.45	564.45	184.37

TIRE : INVACARE MAG-SPIDER WEB (IM)
CONSTANT SLIP ANGLE = 5 DEG

		POUNDS FORCE		NEWTONS	
W	W(N)	FZ	FY	FZ	FY
82.	364.8	52.37	30.11	232.97	133.94
111.	493.8	68.02	33.99	302.56	151.22
140.	622.8	83.85	38.27	372.99	170.25
169.	751.7	99.67	42.54	443.35	189.25
198.	880.7	114.77	45.24	510.51	201.24
227.	1009.7	130.38	49.10	579.98	218.40

TIRE : INVACARE MAG-SPIDER WEB (IM)
CONSTANT SLIP ANGLE = 6 DEG

		POUNDS FORCE		NEWTONS	
W	W(N)	FZ	FY	FZ	FY
82.	364.8	52.99	31.52	235.73	140.20
111.	493.8	69.35	36.94	308.46	164.33
140.	622.8	85.16	41.20	378.83	183.27
169.	751.7	101.15	45.84	449.93	203.91
198.	880.7	116.78	49.69	519.45	221.05

TIRE : INVACARE MAG-SPIDER WEB (IM)
CONSTANT SLIP ANGLE = 7 DEG

		POUNDS FORCE		NEWTONS	
W	W(N)	FZ	FY	FZ	FY
82.	364.8	53.24	32.12	236.83	142.89
111.	493.8	70.11	38.68	311.87	172.07
140.	622.8	86.45	44.08	384.55	196.09
169.	751.7	102.60	49.08	456.37	218.34
198.	880.7	118.75	54.08	528.22	240.57
227.	1009.7	134.16	57.51	596.78	255.82

TIRE : INVACARE MAG-SPIDER WEB (IM)
CONSTANT SLIP ANGLE = 8 DEG

		POUNDS FORCE		NEWTONS	
W	W(N)	FZ	FY	FZ	FY
82.	364.8	53.13	31.94	236.32	142.07
111.	493.8	70.15	38.85	312.04	172.80
140.	622.8	86.47	44.21	384.63	196.67
169.	751.7	102.95	49.96	457.95	222.23
198.	880.7	119.62	56.09	532.08	249.48
227.	1009.7	135.19	59.88	601.37	266.36

TIRE : EVEREST AND JENNINGS AIRLESS (EJA)
CONSTANT SLIP ANGLE = 1 DEG

		POUNDS FORCE		NEWTONS	
W	W(N)	FZ	FY	FZ	FY
82.	364.8	41.39	6.27	184.09	27.89
111.	493.8	56.51	9.01	251.38	40.10
140.	622.8	70.90	10.17	315.40	45.23
169.	751.7	84.92	10.52	377.74	46.81
198.	880.7	98.93	10.86	440.06	48.32
227.	1009.7	113.10	11.58	503.09	51.53

TIRE : EVEREST AND JENNINGS AIRLESS (EJA)
CONSTANT SLIP ANGLE = 2 DEG

		POUNDS FORCE		NEWTONS	
W	W(N)	FZ	FY	FZ	FY
82.	364.8	44.51	13.01	197.98	57.85
111.	493.8	60.37	17.33	268.52	77.09
140.	622.8	75.86	20.87	337.45	92.81
169.	751.7	90.06	21.62	400.60	96.15
198.	880.7	104.07	21.96	462.92	97.67
227.	1009.7	118.05	22.28	525.13	99.09

TIRE : EVEREST AND JENNINGS AIRLESS (EJA)
CONSTANT SLIP ANGLE = 3 DEG

		POUNDS FORCE		NEWTONS	
W	W(N)	FZ	FY	FZ	FY
82.	364.8	45.75	15.72	203.53	69.94
111.	493.8	63.99	25.18	284.63	112.00
140.	622.8	80.02	29.89	355.96	132.94
169.	751.7	94.59	31.43	420.74	139.79
198.	880.7	109.33	33.35	486.32	148.35
227.	1009.7	123.68	34.46	550.15	153.30

TIRE : EVEREST AND JENNINGS AIRLESS (EJA)
CONSTANT SLIP ANGLE = 4 DEG

		POUNDS FORCE		NEWTONS	
W	W(N)	FZ	FY	FZ	FY
82.	364.8	46.98	18.41	209.00	81.90
111.	493.8	66.65	30.98	296.46	137.81
140.	622.8	83.03	36.46	369.35	162.16
169.	751.7	98.50	39.96	438.16	177.75
198.	880.7	113.61	42.66	505.34	189.78
227.	1009.7	127.95	43.77	569.17	194.71

TIRE : EVEREST AND JENNINGS AIRLESS (EJA)
CONSTANT SLIP ANGLE = 5 DEG

		POUNDS FORCE		NEWTONS	
W	W(N)	FZ	FY	FZ	FY
82.	364.8	48.92	22.64	217.60	100.71
111.	493.8	68.36	34.76	304.08	154.60
140.	622.8	85.27	41.38	379.32	184.08
169.	751.7	101.64	46.83	452.11	208.32
198.	880.7	116.91	49.92	520.06	222.03
227.	1009.7	131.44	51.41	584.67	228.69

TIRE : EVEREST AND JENNINGS AIRLESS (EJA)
CONSTANT SLIP ANGLE = 6 DEG

		POUNDS FORCE		NEWTONS	
W	W(N)	FZ	FY	FZ	FY
82.	364.8	51.36	27.99	228.47	124.50
111.	493.8	70.05	38.48	311.58	171.18
140.	622.8	87.12	45.47	387.51	202.24
169.	751.7	103.82	51.67	461.82	229.83
198.	880.7	119.09	54.74	529.73	243.47
227.	1009.7	134.15	57.40	596.72	255.31

TIRE : EVEREST AND JENNINGS AIRLESS (EJA)
CONSTANT SLIP ANGLE = 7 DEG

		POUNDS FORCE		NEWTONS	
W	W(N)	FZ	FY	FZ	FY
82.	364.8	53.41	32.50	237.57	144.55
111.	493.8	71.34	41.38	317.34	184.06
140.	622.8	88.57	48.71	393.96	216.68
169.	751.7	105.07	54.49	467.39	242.39
198.	880.7	120.51	57.93	536.04	257.69
227.	1009.7	135.74	60.97	603.78	271.19

TIRE : EVEREST AND JENNINGS AIRLESS (EJA)
CONSTANT SLIP ANGLE = 8 DEG

		POUNDS FORCE		NEWTONS	
W	W(N)	FZ	FY	FZ	FY
82.	364.8	54.00	33.85	240.20	150.59
111.	493.8	71.90	42.68	319.83	189.87
140.	622.8	89.10	49.97	396.34	222.30
169.	751.7	105.41	55.34	468.88	246.14
198.	880.7	121.18	59.53	539.05	264.79
227.	1009.7	135.87	61.39	604.38	273.06

TIRE : ESSEM RUBBER CASTER (ER)
CONSTANT SLIP ANGLE = 1 DEG

		POUNDS FORCE		NEWTONS	
W	W(N)	FZ	FY	FZ	FY
73.	324.7	40.79	5.84	181.46	25.98
102.	453.7	55.95	6.00	248.86	26.67
131.	582.7	71.11	6.15	316.32	27.36
160.	711.7	86.04	5.89	382.71	26.20
189.	840.7	101.15	6.01	449.94	26.75
218.	969.7	116.10	5.76	516.43	25.60

TIRE : ESSEM RUBBER CASTER (ER)
CONSTANT SLIP ANGLE = 2 DEG

		POUNDS FORCE		NEWTONS	
W	W(N)	FZ	FY	FZ	FY
73.	324.7	43.66	11.31	194.19	50.32
102.	453.7	58.81	11.47	261.59	51.02
131.	582.7	73.76	11.22	328.09	49.89
160.	711.7	89.11	11.77	396.39	52.36
189.	840.7	104.01	11.49	462.67	51.09
218.	969.7	119.28	11.84	530.57	52.66

TIRE : ESSEM RUBBER CASTER (ER)
CONSTANT SLIP ANGLE = 3 DEG

		POUNDS FORCE		NEWTONS	
W	W(N)	FZ	FY	FZ	FY
73.	324.7	46.48	16.74	206.77	74.46
102.	453.7	61.85	17.30	275.11	76.96
131.	582.7	76.80	17.05	341.62	75.85
160.	711.7	91.72	16.79	408.00	74.68
189.	840.7	106.52	16.30	473.82	72.52
218.	969.7	122.21	17.46	543.61	77.68

TIRE : ESSEM RUBBER CASTER (ER)
CONSTANT SLIP ANGLE = 4 DEG

		POUNDS FORCE		NEWTONS	
W	W(N)	FZ	FY	FZ	FY
73.	324.7	48.96	21.51	217.78	95.69
102.	453.7	64.84	23.08	288.44	102.65
131.	582.7	79.69	22.63	354.49	100.65
160.	711.7	94.62	22.36	420.87	99.48
189.	840.7	109.41	21.88	486.69	97.32
218.	969.7	124.68	22.23	554.58	98.87

TIRE : ESSEM RUBBER CASTER (ER)
CONSTANT SLIP ANGLE = 5 DEG

		POUNDS FORCE		NEWTONS	
W	W(N)	FZ	FY	FZ	FY
73.	324.7	51.61	26.63	229.55	118.47
102.	453.7	67.80	28.79	301.58	128.07
131.	582.7	82.75	28.54	368.10	126.97
160.	711.7	97.68	28.28	434.49	125.81
189.	840.7	112.05	27.00	498.44	120.08
218.	969.7	127.94	28.55	569.13	126.99

TIRE : ESSEM RUBBER CASTER (ER)
CONSTANT SLIP ANGLE = 6 DEG

		POUNDS FORCE		NEWTONS	
W	W(N)	FZ	FY	FZ	FY
73.	324.7	53.90	31.09	239.75	138.31
102.	453.7	70.08	33.24	311.75	147.87
131.	582.7	85.45	33.79	380.11	150.32
160.	711.7	100.07	32.94	445.13	146.51
189.	840.7	114.66	32.05	510.01	142.58
218.	969.7	130.13	32.80	578.83	145.90

TIRE : ESSEM RUBBER CASTER (ER)
CONSTANT SLIP ANGLE = 7 DEG

		POUNDS FORCE		NEWTONS	
W	W(N)	FZ	FY	FZ	FY
73.	324.7	56.46	36.09	251.15	160.55
102.	453.7	72.33	37.63	321.74	167.41
131.	582.7	87.90	38.58	391.01	171.61
160.	711.7	102.62	37.92	456.49	168.70
189.	840.7	117.01	36.65	520.47	163.01
218.	969.7	132.89	38.18	591.10	169.85

TIRE : ESSEM RUBBER CASTER (ER)
CONSTANT SLIP ANGLE = 8 DEG

		POUNDS FORCE		NEWTONS	
W	W(N)	FZ	FY	FZ	FY
73.	324.7	58.47	40.03	260.07	178.08
102.	453.7	74.74	42.36	332.44	188.42
131.	582.7	89.90	42.51	399.88	189.08
160.	711.7	104.31	41.26	464.00	183.55
189.	840.7	118.90	40.39	528.91	179.65
218.	969.7	134.78	41.92	599.52	186.45

TIRE : POLYURETHANE CASTER (PU)
CONSTANT SLIP ANGLE = 1 DEG

		POUNDS FORCE		NEWTONS	
W	W(N)	FZ	FY	FZ	FY
73.	324.7	40.70	5.64	181.03	25.10
102.	453.7	55.76	5.61	248.02	24.94
131.	582.7	70.94	5.78	315.56	25.71
160.	711.7	86.10	5.94	383.00	26.44
189.	840.7	101.26	6.10	450.42	27.14
218.	969.7	116.20	5.84	516.88	25.97

TIRE : POLYURETHANE CASTER (PU)
CONSTANT SLIP ANGLE = 2 DEG

		POUNDS FORCE		NEWTONS	
W	W(N)	FZ	FY	FZ	FY
73.	324.7	42.92	9.90	190.93	44.04
102.	453.7	58.09	10.07	258.39	44.78
131.	582.7	73.59	10.85	327.35	48.25
160.	711.7	88.65	10.81	394.31	48.07
189.	840.7	103.05	9.54	458.40	42.42
218.	969.7	118.31	9.89	526.29	43.98

TIRE : POLYURETHANE CASTER (PU)
CONSTANT SLIP ANGLE = 3 DEG

		POUNDS FORCE		NEWTONS	
W	W(N)	FZ	FY	FZ	FY
73.	324.7	44.80	13.51	199.28	60.09
102.	453.7	60.82	15.30	270.52	68.05
131.	582.7	75.57	14.65	336.16	65.18
160.	711.7	90.73	14.82	403.59	65.90
189.	840.7	105.57	14.36	469.60	63.90
218.	969.7	120.40	13.90	535.57	61.82

TIRE : POLYURETHANE CASTER (PU)
CONSTANT SLIP ANGLE = 4 DEG

		POUNDS FORCE		NEWTONS	
W	W(N)	FZ	FY	FZ	FY
73.	324.7	47.07	17.89	209.39	79.56
102.	453.7	62.66	18.86	278.73	83.90
131.	582.7	78.37	20.04	348.59	89.13
160.	711.7	92.89	18.99	413.21	84.46
189.	840.7	107.21	17.53	476.88	77.97
218.	969.7	122.25	17.47	543.80	77.70

TIRE : POLYURETHANE CASTER (PU)
CONSTANT SLIP ANGLE = 5 DEG

		POUNDS FORCE		NEWTONS	
W	W(N)	FZ	FY	FZ	FY
73.	324.7	48.37	20.41	215.17	90.80
102.	453.7	64.69	22.79	287.75	101.37
131.	582.7	80.29	23.76	357.14	105.69
160.	711.7	95.24	23.52	423.64	104.62
189.	840.7	109.24	21.46	485.92	95.47
218.	969.7	123.86	20.60	550.98	91.62

TIRE : POLYURETHANE CASTER (PU)
CONSTANT SLIP ANGLE = 6 DEG

		POUNDS FORCE		NEWTONS	
W	W(N)	FZ	FY	FZ	FY
73.	324.7	49.75	23.11	221.31	102.79
102.	453.7	66.48	26.27	295.71	116.86
131.	582.7	81.76	26.63	363.68	118.48
160.	711.7	97.23	27.40	432.50	121.87
189.	840.7	111.24	25.35	494.81	112.75
218.	969.7	125.35	23.49	557.58	104.50

TIRE : POLYURETHANE CASTER (PU)
CONSTANT SLIP ANGLE = 7 DEG

		POUNDS FORCE		NEWTONS	
W	W(N)	FZ	FY	FZ	FY
73.	324.7	51.94	27.36	231.02	121.69
102.	453.7	68.34	29.91	303.98	133.03
131.	582.7	83.93	30.86	373.32	137.29
160.	711.7	98.36	29.63	437.54	131.81
189.	840.7	113.20	29.18	503.55	129.82
218.	969.7	127.22	27.14	565.89	120.72

TIRE : POLYURETHANE CASTER (PU)
CONSTANT SLIP ANGLE = 8 DEG

		POUNDS FORCE		NEWTONS	
W	W(N)	FZ	FY	FZ	FY
73.	324.7	53.46	30.36	237.81	135.04
102.	453.7	69.85	32.89	310.73	146.32
131.	582.7	85.54	34.04	380.51	151.44
160.	711.7	100.09	33.02	445.20	146.87
189.	840.7	114.11	31.00	507.59	137.87
218.	969.7	129.36	31.33	575.42	139.36

TIRE : AG
CONSTANT CAMBER ANGLE = 2 DEG

		POUNDS FORCE		NEWTONS	
W	W(N)	FZ	FY	FZ	FY
82.	364.8	39.67	2.59	176.47	11.52
111.	493.8	53.87	3.37	239.65	15.01
140.	622.8	67.85	3.67	301.82	16.33
169.	751.7	81.72	3.74	363.50	16.62
198.	880.7	95.77	4.18	426.03	18.61
227.	1009.7	109.46	3.84	486.89	17.10

TIRE : AG
CONSTANT CAMBER ANGLE = 5 DEG

		POUNDS FORCE		NEWTONS	
W	W(N)	FZ	FY	FZ	FY
82.	364.8	41.02	5.47	182.45	24.35
111.	493.8	55.56	6.98	247.12	31.05
140.	622.8	69.91	8.08	310.97	35.95
169.	751.7	83.89	8.39	373.14	37.31
198.	880.7	97.89	8.71	435.42	38.76
227.	1009.7	111.51	8.25	496.04	36.72

TIRE : AG
CONSTANT CAMBER ANGLE = 8 DEG

		POUNDS FORCE		NEWTONS	
W	W(N)	FZ	FY	FZ	FY
82.	364.8	41.69	6.92	185.44	30.76
111.	493.8	56.30	8.58	250.45	38.18
140.	622.8	70.47	9.28	313.46	41.30
169.	751.7	84.73	10.19	376.88	45.34
198.	880.7	99.01	11.12	440.41	49.46
227.	1009.7	112.63	10.66	501.02	47.42

TIRE : EJP
CONSTANT CAMBER ANGLE = 2 DEG

		POUNDS FORCE		NEWTONS	
W	W(N)	FZ	FY	FZ	FY
82.	364.8	40.12	3.52	178.47	15.67
111.	493.8	54.34	4.30	241.73	19.14
140.	622.8	68.38	4.69	304.19	20.85
169.	751.7	82.27	4.76	365.97	21.16
198.	880.7	96.22	4.93	428.00	21.95
227.	1009.7	110.31	5.45	490.70	24.24

TIRE : EJP
CONSTANT CAMBER ANGLE = 5 DEG

		POUNDS FORCE		NEWTONS	
W	W(N)	FZ	FY	FZ	FY
82.	364.8	41.69	6.89	185.44	30.63
111.	493.8	55.95	7.75	248.87	34.46
140.	622.8	71.00	10.29	315.81	45.78
169.	751.7	84.66	9.88	376.59	43.95
198.	880.7	98.89	10.66	439.87	47.41
227.	1009.7	113.30	11.85	503.98	52.73

TIRE : EJP
CONSTANT CAMBER ANGLE = 8 DEG

		POUNDS FORCE		NEWTONS	
W	W(N)	FZ	FY	FZ	FY
82.	364.8	42.73	9.13	190.09	40.61
111.	493.8	56.96	9.91	253.35	44.08
140.	622.8	71.74	11.89	319.13	52.90
169.	751.7	86.15	13.08	383.23	58.19
198.	880.7	100.19	13.46	445.68	59.87
227.	1009.7	114.34	14.09	508.63	62.70

TIRE : SS
CONSTANT CAMBER ANGLE = 2 DEG

		POUNDS FORCE		NEWTONS	
W	W(N)	FZ	FY	FZ	FY
82.	364.8	39.90	3.04	177.47	13.54
111.	493.8	54.05	3.67	240.43	16.33
140.	622.8	68.03	3.91	302.60	17.38
169.	751.7	81.91	3.97	364.37	17.67
198.	880.7	95.86	4.16	426.42	18.49
227.	1009.7	128.60	44.68	572.03	198.74

TIRE : SS
CONSTANT CAMBER ANGLE = 5 DEG

		POUNDS FORCE		NEWTONS	
W	W(N)	FZ	FY	FZ	FY
82.	364.8	41.43	6.33	184.28	28.14
111.	493.8	55.82	7.47	248.31	33.25
140.	622.8	70.08	8.31	311.72	36.97
169.	751.7	84.11	8.69	374.16	38.68
198.	880.7	97.97	8.68	435.80	38.61
227.	1009.7	112.18	9.46	499.02	42.07

TIRE : SS
CONSTANT CAMBER ANGLE = 8 DEG

		POUNDS FORCE		NEWTONS	
W	W(N)	FZ	FY	FZ	FY
82.	364.8	41.71	6.93	185.52	30.81
111.	493.8	56.59	9.12	251.71	40.55
140.	622.8	71.38	11.11	317.53	49.43
169.	751.7	85.53	11.74	380.46	52.21
198.	880.7	99.72	12.44	443.59	55.34
227.	1009.7	113.86	13.06	506.48	58.09

TIRE : IM
CONSTANT CAMBER ANGLE = 2 DEG

		POUNDS FORCE		NEWTONS	
W	W(N)	FZ	FY	FZ	FY
82.	364.8	39.22	1.59	174.44	7.07
111.	493.8	53.24	1.95	236.81	8.67
140.	622.8	67.11	1.99	298.54	8.86
169.	751.7	81.05	2.19	360.54	9.73
198.	880.7	94.85	2.05	421.89	9.14
227.	1009.7	108.73	2.15	483.65	9.56

TIRE : IM
CONSTANT CAMBER ANGLE = 5 DEG

		POUNDS FORCE		NEWTONS	
W	W(N)	FZ	FY	FZ	FY
82.	364.8	40.00	3.27	177.93	14.55
111.	493.8	53.98	3.55	240.13	15.80
140.	622.8	68.05	3.99	302.69	17.77
169.	751.7	82.06	4.35	365.02	19.35
198.	880.7	96.04	4.62	427.21	20.54
227.	1009.7	110.04	4.95	489.46	22.03

TIRE : IM
CONSTANT CAMBER ANGLE = 8 DEG

		POUNDS FORCE		NEWTONS	
W	W(N)	FZ	FY	FZ	FY
82.	364.8	40.08	3.43	178.26	15.27
111.	493.8	54.69	5.07	243.29	22.56
140.	622.8	68.64	5.28	305.34	23.47
169.	751.7	82.55	5.39	367.18	23.98
198.	880.7	96.60	5.82	429.70	25.88
227.	1009.7	110.67	6.31	492.29	28.09

TIRE : EJA
CONSTANT CAMBER ANGLE = 2 DEG

		POUNDS FORCE		NEWTONS	
W	W(N)	FZ	FY	FZ	FY
82.	364.8	39.20	1.57	174.37	6.97
111.	493.8	53.27	2.04	236.95	9.06
140.	622.8	67.27	2.35	299.24	10.47
169.	751.7	81.21	2.55	361.25	11.34
198.	880.7	95.00	2.41	422.58	10.72
227.	1009.7	108.83	2.40	484.10	10.68

TIRE : EJA
CONSTANT CAMBER ANGLE = 5 DEG

		POUNDS FORCE		NEWTONS	
W	W(N)	FZ	FY	FZ	FY
82.	364.8	39.82	2.89	177.11	12.85
111.	493.8	54.37	4.40	241.85	19.57
140.	622.8	68.39	4.76	304.22	21.16
169.	751.7	82.46	5.23	366.81	23.28
198.	880.7	96.61	5.86	429.72	26.05
227.	1009.7	110.62	6.25	492.07	27.79

TIRE : EJA
CONSTANT CAMBER ANGLE = 8 DEG

		POUNDS FORCE		NEWTONS	
W	W(N)	FZ	FY	FZ	FY
82.	364.8	40.28	3.89	179.18	17.30
111.	493.8	54.89	5.52	244.18	24.56
140.	622.8	69.01	6.08	306.96	27.04
169.	751.7	83.83	8.16	372.87	36.28
198.	880.7	97.37	7.50	433.13	33.35
227.	1009.7	111.26	7.61	494.89	33.85

EMPIRICAL TIRE COEFFICIENTS

THE FOLLOWING COEFFICIENTS CAN BE USED TO EMPIRICALLY PREDICT CORNERING FORCE AND ROLLING RESISTANCE FORCE AS DESCRIBED IN CHAPTER 4. THE COEFFICIENTS ARE BASED ON THE BEST FITTING THIRD ORDER POLYNOMIAL WHICH FITS THE TIRE FORCE RESULTS WHICH WERE OBTAINED USING THE TEST CART AND TREADMILL. THE TREADMILL RESULTS CORRESPONDING TO THESE COEFFICIENTS ARE GIVEN IN TABULAR FORM AT THE BEGINNING OF THIS APPENDIX AND IN GRAPHICAL FORM IN CHAPTERS 2 AND 3 OF THE THESIS TEXT.

THE COEFFICIENTS WERE COMPUTED USING THE PROGRAM PWRSTAR WHICH USES A LEAST SQUARES TECHNIQUE. [4.4] THE BEST FIT IN A LEAST SQUARES SENSE RESULTS IN A THIRD ORDER POLYNOMIAL HAVING FOUR TERMS. FOR PROGRAMMING PURPOSES THE ZEROTH ORDER TERM WAS DISCARDED IN ORDER TO ENSURE THAT ALL OF THE PREDICTED FORCES ARE ZERO WHEN THE NORMAL FORCE F_z IS ZERO. IN EVERY CASE THE ZEROTH ORDER TERMS ARE SMALL, BUT FOR COMPLETENESS THEY ARE ALSO LISTED HERE. ALSO LISTED IS THE CORRELATION COEFFICIENT (R) OF THE BEST FIT POLYNOMIAL. R VALUES CLOSE TO 1 CORRESPOND TO BETTER POLYNOMIAL FITS (NOT TO MORE ACCURATE RESULTS).

THE COEFFICIENTS ARE USED TO COMPUTE TIRE FORCES AS DESCRIBED IN CHAPTER 4. (EQUATION 4-1).

$$F = (a \times F_z) + (b \times F_z \times F_z) + (c \times F_z \times F_z \times F_z) + d$$

WHERE F_z IS THE NORMAL FORCE ON THE TIRE (IN NEWTONS), d IS THE ZEROTH ORDER COEFFICIENT WHICH HAS BEEN DISCARDED, AND F CAN BE EITHER THE CORNERING FORCE F_y OR THE ROLLING RESISTANCE FORCE F_x DEPENDING ON WHICH SET OF COEFFICIENTS ARE BEING USED. FOR COMPUTIN CORNERING FORCE EACH TIRE WHICH WAS TESTED HAS 8 SET OF COEFFICIENTS a, b, AND c, CORRESPONDING TO THE EIGHT SLIP ANGLES WHICH WERE TESTED USING THE TREADMILL AND TEST CART. THUS THE CORNERING FORCE COEFFICIENTS ARE GOOD FOR INTEGER SLIP ANGLES IN THE RANGE ZERO TO 8 DEGREES. VALUES OF CORNERING FORCE FOR NON-INTEGER SLIP ANGLES MUST BE INTERPOLATED. THE UPPER LIMIT ON Fz IS 500N. THE COEFFICIENTS ARE LISTED BY TIRE (SEE TABLE 3-1).

Tire	a	b	c	d	R
ROLLING RESISTANCE COEFFICIENTS					
EJA	1.95068E-2	-2.65456E-5	5.38569E-8	-6.23000E-3	.999
IM	1.20231E-2	-3.62874E-6	2.47265E-8	4.82082E-3	.999
EJP	1.48242E-2	-2.77966E-5	2.70203E-8	8.49772E-3	.997
SS	1.81750E-2	-5.30452E-5	6.26485E-8	6.77434E-3	.999
AG	-1.22211E-3	1.42569E-4	-1.70013E-7	-8.50931E-3	.999
ER	9.19876E-3	3.21731E-5	-1.54890E-8	1.51131E-2	.999
CORNERING FORCE COEFFICIENTS					
EJA					
ALPHA = 1	1.98189E-1	-1.73690E-4	-3.90765E-8	-2.42543E-1	.996
2	3.17287E-1	2.37231E-5	-5.19682E-7	-2.16646E-1	.998
3	3.07205E-1	5.56659E-4	-1.11809E-6	-6.19382E-1	.997
4	2.93374E-1	9.48220E-4	-1.52567E-6	-6.72709E-1	.998
5	3.65706E-1	8.27195E-4	-1.34621E-6	-3.78725E-1	.999
6	5.31375E-1	2.66275E-4	-7.41407E-7	-1.71293E-1	.999
7	6.75259E-1	-2.13245E-4	-2.69438E-7	-3.42661E-2	.999
8	6.96379E-1	-2.23784E-4	-2.97540E-7	3.52819E-2	.999

Tire	a	b	c	d	R
IM					
ALPHA = 1	3.58427E-1	-9.11580E-4	7.31398E-7	9.00047E-3	.999
2	5.09691E-1	-1.01940E-3	7.68241E-7	4.51666E-2	.999
3	6.80230E-1	-1.29672E-3	9.95998E-7	1.35024E-1	.999
4	8.10033E-1	-1.53026E-3	1.19312E-6	-2.64639E-3	.999
5	8.32849E-1	-1.39033E-3	1.04160E-6	1.45601E-1	.999
6	8.40706E-1	-1.27670E-3	9.12153E-7	9.47246E-2	.999
7	7.88546E-1	-9.29083E-4	5.50323E-7	9.95372E-2	.999
8	7.74272E-1	-8.86877E-4	5.64815E-7	1.46869E-1	.999
EJP					
ALPHA = 1	3.35695E-1	-4.40024E-4	9.33529E-8	3.56009E-2	.999
2	5.30394E-1	-4.86746E-4	-8.41244E-8	-7.55427E-1	.999
3	6.31923E-1	-3.16612E-4	-3.67544E-7	1.27679E-1	.999
4	8.25503E-1	-6.47171E-4	-6.40109E-8	-3.18040E-2	.999
5	8.99986E-1	-5.39797E-4	-2.33609E-7	-1.46733E-1	.999
6	9.29075E-1	-4.47427E-4	-3.16601E-7	-1.56425E-1	.999
7	9.19489E-1	-2.36651E-4	-5.02252E-7	-1.33110E-1	.999
8	9.84140E-1	-4.15714E-4	-3.08961E-7	-2.50519E-1	.999
SS					
ALPHA = 1	3.00952E-1	-4.38212E-4	1.68247E-7	-1.31133E-1	.996
2	5.84062E-1	-1.08108E-3	7.88194E-7	9.51884E-2	.999
3	7.61038E-1	-1.14356E-3	5.69103E-7	-9.66171E-2	.999
4	8.81072E-1	-1.20144E-3	5.34230E-7	-2.37569E-1	.999
5	8.54826E-1	-7.28898E-4	-1.11906E-8	-1.59808E-1	.999
6	8.22513E-1	-4.40673E-4	-2.27546E-7	-9.67396E-3	.999
7	7.53144E-1	3.15524E-5	-6.98151E-7	-2.64325E-2	.999
8	7.77852E-1	-7.30789E-5	-4.72285E-7	-9.23439E-2	.999
AG					
ALPHA = 1	2.68912E-1	6.28921E-5	-6.18542E-7	-8.62854E-3	.997
2	5.42135E-1	-6.12264E-4	1.14320E-7	5.50084E-2	.999
3	7.51468E-1	-1.00052E-3	4.23781E-7	-5.51555E-4	.999
4	8.78984E-1	-1.07359E-3	3.75928E-7	-2.62351E-3	.999
5	8.86993E-1	-7.67556E-4	2.04054E-8	1.17411E-1	.999
6	9.22619E-1	-6.89697E-4	-6.90660E-8	1.09482E-1	.999
7	9.46552E-1	-6.50317E-4	-6.81895E-8	1.61335E-1	.999
8	9.52619E-1	-5.63006E-4	-1.52079E-7	4.47684E-2	.999
ER					
ALPHA = 1	2.43038E-1	-6.86099E-4	6.05735E-7	9.13370E-2	.998
2	4.59856E-1	-1.31249E-3	1.19560E-6	1.78319E-1	.997
3	6.90894E-1	-1.97964E-3	1.78667E-6	3.01852E-2	.999
4	8.18698E-1	-2.11332E-3	1.72893E-6	-1.57005E-3	.999
5	9.82602E-1	-2.45591E-3	1.96530E-6	-1.23941E-1	.999
6	1.07234E-0	-2.50068E-3	1.86841E-6	-7.90585E-2	.999
7	1.21599E-0	-2.83152E-3	2.12777E-6	-4.35083E-2	.999
8	1.34947E-0	-3.14277E-3	2.34825E-6	-1.21222E-1	.999

Tire	a	b	c	d	R
PU					
ALPHA = 1	2.23684E-1	-6.15377E-4	5.44997E-7	1.67082E-1	.995
2	3.86729E-1	-1.00143E-3	8.04368E-7	4.74344E-2	.996
3	5.23715E-1	-1.30470E-3	1.01454E-6	-2.04435E-3	.999
4	6.58717E-1	-1.57865E-3	1.15352E-6	-4.26528E-2	.999
5	6.764413E-1	-1.33156E-3	7.30949E-7	-6.44.83E-2	.999
6	7.11494E-1	-1.23550E-3	5.29445E-7	2.51131E-2	.999
7	8.796300E-1	-1.77214E-3	1.05365E-6	1.01676E-2	.999
8	1.008872E-0	-2.18213E-3	1.46919E-6	1.46919E-6	.999

APPENDIX C

```
**********************************************************************
*                                                                    *
*                         PROGRAM WCHAIR                             *
*                                                                    *
*                 A PROGRAM WHICH CAN BE USED TO                     *
*          SIMULATE THE MOTION OF FREE ROLLING WHEELCHAIRS           *
*                                                                    *
*                               BY                                   *
*                                                                    *
*                       TIMOTHY J. COLLINS                           *
*             GRADUATE STUDENT : MECHANICAL ENGINEERING              *
*                     UNIVERSITY OF VIRGINIA                         *
*                     VERSION 1  MAY, 1987                           *
*                                                                    *
*              SUPPORTED BY THE UNIVERSITY OF VIRGINIA               *
*               CENTER FOR REHABILITATION ENGINEERING                *
*                   NIHR GRANT NO. G00-83-00072                      *
*                                                                    *
**********************************************************************

**********************************************************************
*                                                                    *
* I. PROGRAM DESCRIPTION                                             *
*                                                                    *
*        THIS  PROGRAM  IS  USED TO SIMULATE THE  MOTION  OF  A      *
*    FREELY  ROLLING WHEELCHAIR.   THE PROGRAM IS INTENDED AS  A     *
*    TOOL  TO INVESTIGATE THOSE FACTORS THAT ARE RELATED TO  THE     *
*    DIRECTIONAL STABILITY OF REAR CASTER WHEELCHAIRS.  HOWEVER,     *
*    THE PROGRAM IS COMPLETELY GENERAL AND CAN BE APPLIED TO ANY     *
*    WHEELCHAIR, PROVIDED THE PROPER INPUTS ARE GIVEN.               *
*        GIVEN  A  SET  OF  INITIAL  CONDITIONS,   THE  PROGRAM      *
*    CALCULATES  A WHEELCHAIR'S TRAJECTORY AND VELOCITY  OVER  A     *
*    USER   SPECIFIED  INTERVAL  OF  TIME.    SEVERAL  DIFFERENT     *
*    VARIABLES  MAY BE SPECIFIED INTERACTIVELY BEFORE EACH  TEST     *
*    CASE.   THE DEFAULT VALUES FOR ALL PHYSICAL VARIABLES (SUCH     *
*    AS  WHEELCHAIR MASS) ARE TAKEN AS THOSE  MEASURED  DIRECTLY     *
*    FROM  AN EVEREST AND JENNINGS "PREMIER" MANUAL REAR  CASTER     *
*    WHEELCHAIR.                                                     *
*        THIS PROGRAM DESCRIPTION ASSUMES SOME FAMILIARITY WITH      *
*    THE MASTER'S THESIS TEXT "AN ANALYSIS OF PARAMETERS RELATED     *
*    TO  THE DIRECTIONAL STABILITY OF REAR CASTER  WHEELCHAIRS".     *
*    (T. COLLINS , AUGUST 1987)                                      *
*        NOTE   THAT   BECAUSE  THE  PROGRAM  WAS  WRITTEN   TO      *
*    INVESTIGATE  THE BEHAVIOR OF REAR CASTER  WHEELCHAIRS,  THE     *
*    TERMINOLOGY  WHICH  IS USED REFERS TO SUCH  A  CHAIR.   FOR     *
*    EXAMPLE,  THE TERMS FRONT,  REAR,  RIGHT, AND LEFT REFER TO     *
*    POSITIONS WITH RESPECT TO A REAR CASTER WHEELCHAIR.             *
**********************************************************************
```

```
*************************************************************************
*                                                                       *
* II. PROGRAM LIMITATIONS                                               *
*                                                                       *
*          THE  WHEELCHAIR  MOTION  IS CONSIDERED TO  BE  PLANER.       *
*      PITCH AND ROLL EFFECTS ARE NEGLECTED,  EXCEPT THAT A QUASI-      *
*      STATIC  METHOD  OF  APPROXIMATING  LATERAL  LOAD   TRANSFER      *
*      IS INCORPORATED.                                                 *
*          THE  PROGRAM  AUTOMATICALLY CHECKS THE SLIP ANGLES  AT       *
*      EACH  TIRE AND THE TOTAL NORMAL LOAD CARRIED BY EACH  TIRE.      *
*      IF  EITHER OF THESE EXCEEDS THE LIMITS OF THE  EXPERIMENTAL      *
*      DATA  USED  TO  SUPPORT THE  PROGRAM,  ERROR  MESSAGES  ARE      *
*      ISSUED.   THE  PROGRAM IS CURRENTLY SET SUCH THAT  10  SUCH      *
*      WARNING MESSAGES CAUSES EXECUTION TO TERMINATE.   LIMITS ON      *
*      SLIP  ANGLE ARE 8 DEGREES AND ON NORMAL LOAD ARE 450 N  PER      *
*      TIRE.                                                            *
*                                                                       *
*      SOME CAUSES FOR PROGRAM TERMINATION ARE:                         *
*                                                                       *
*      (1)  NATURAL  TERMINATION  WHEN A  REAR  CASTER  WHEELCHAIR      *
*           BECOMES UNSTABLE.                                           *
*      (2)  SPECIFICATION  OF A LARGE INITIAL  LATERAL  VELOCITY.       *
*           THIS  MAY  RESULT  IN INITIAL SLIP  ANGLES  WHICH  ARE      *
*           GREATER  THAN  8  DEGREES OR  IN  AN  INITIAL  LATERAL      *
*           LOAD TRANSFER WHICH IS TOO GREAT, RESULTING IN  NORMAL      *
*           FORCES GREATER THAN 450N.                                   *
*                                                                       *
*          IF  LARGE  FORCES OR ACCELERATIONS  ARE  PRESENT,  THE       *
*      PROGRAM MAY HAVE TROUBLE TRACKING THE MOTION AND CONVERGING      *
*      TO  A DEFINITE SOLUTION.   THIS IS TYPIFIED BY VALUES WHICH      *
*      OSCILLATE  ABOUT  SOME  VALUE  RATHER  THAN  INCREASING  OR      *
*      DECREASING UNIFORMLY.   THIS IS ESPECIALLY A PROBLEM IF TOO      *
*      LARGE A TIME STEP IS CHOSEN.                                     *
*                                                                       *
*************************************************************************
*                                                                       *
*III. EXECUTION TIME                                                    *
*                                                                       *
*         ALTHOUGH   THE  TIME  STEP  FOR  SUCCESSIVE  ITERATIONS       *
*      WITHIN THE PROGRAM CAN BE SPECIFIED,  IT IS FOUND THAT .001      *
*      SEC  IS  THE  LARGEST  VALUE THAT  LEADS  TO  A  CONVERGING      *
*      SOLUTION.  RUNNING  THE PROGRAM ON A CDC  CYBER  865,  THIS      *
*      RESULTS  IN  A REAL TIME EXECUTION OF ABOUT 15  SECONDS  IN      *
*      ORDER TO SIMULATE 5 SECONDS OF WHEELCHAIR MOTION.  HOWEVER,      *
*      THE  SAME RUN TAKES APPROXIMATELY 15 MINUTES USING AN  AT&T      *
*      PERSONAL COMPUTER.   BECAUSE THE SOLUTION PROCEDURE ASSUMES      *
*      CONSTANT ACCELERATION OVER EACH TIME STEP,  IT IS ESSENTIAL      *
*      THAT  A SMALL ENOUGH STEP BE CHOSEN.  FURTHERMORE,  IF LESS      *
*      THAN  12  DIGITS ARE CARRIED  FOR  NUMERICAL  CALCULATIONS,      *
*      ROUND OFF ERROR MAY BECOME A SERIOUS PROBLEM.                    *
*************************************************************************
```

```
*************************************************************************
*                                                                       *
* IV. UNITS                                                             *
*                                                                       *
*    ANY  CONSISTENT  SET OF UNITS CAN  BE  USED.   ALL  DEFAULT        *
*    VALUES ARE GIVEN IN THE MKS SYSTEM.   IF IT IS NECESSARY TO        *
*    RUN  MANY  TRIALS  USING A DIFFERENT  SYSTEM,  THE  DEFAULT        *
*    VALUES CAN BE EASILY CHANGED BY ALTERING THE DATA  SUPPLIED        *
*    IN THE BLOCK DATA ROUTINE.                                         *
*                                                                       *
*************************************************************************

*************************************************************************
*                                                                       *
*  V. DESCRIPTION OF PROGRAM COMPONENTS                                 *
*                                                                       *
*************************************************************************
*                                                                       *
* (1) NAMED COMMON BLOCKS AND VARIABLES HELD                            *
*                                                                       *
*      DIMEN  - GEOMETRIC DIMENSIONS OF WHEELCHAIR                      *
*      MASSPR - MASS AND INERTIA PROPERTIES                             *
*      LATFOR - LATERAL TIRE FORCES                                     *
*      LONFOR - LONGITUDINAL TIRE FORCES                                *
*      NORFOR - NORMAL TIRE FORCES                                      *
*      C1VAR  - KINEMATIC VARIABLES AND TOTAL EXTERNAL                  *
*               FORCE ACTING IN THE C1 DIRECTION (PARALLEL)             *
*               TO THE "FORWARD DIRECTION" OF THE WHEELCHAIR            *
*      C2VAR  - KINEMATIC VARIABLES AND TOTAL EXTERNAL.                 *
*               FORCE ACTING IN THE C2 DIRECTION.                       *
*      CASANG - KINEMATIC VARIABLES FOR THE CASTER WHEELS.              *
*      GLOBAL - KINEMATIC  VARIABLES IN THE FIXED INERTIAL              *
*               REFERENCE FRAME. NOTE, THE C1-C2 REFERENCE.             *
*               FRAME IS FIXED IN THE MOVING WHEELCHAIR.                *
*      SLIPAN - SLIP ANGLES ASSOCIATED WITH EACH WHEEL.                 *
*      PTVEL  - VELOCITIES OF THE POINTS WHERE EACH TIRE.               *
*               IS ASSUMED TO TOUCH THE GROUND.                         *
*      CDAMP  - FRICTIONAL DAMPING MOMENTS AT CASTER PINS.              *
*      CAMTOE - TOE AND CAMBER ANGLES FOR MAIN WHEELS.                  *
*      TIRES  - ARRAYS WHICH HOLD THE EMPIRICAL CONSTANTS               *
*               USED TO COMPUTE TIRE FORCES.                            *
*      YCOEFF - CORNERING FORCE EMPIRICAL CONSTANTS FOR                 *
*               FIVE DIFFERENT TIRE TYPES.  ONE TYPE IS                 *
*               SELECTED PER RUN.                                       *
*      XCOEFF - LONGITUDINAL (ROLLING RESISTANCE) EMPIRICAL             *
*               CONSTANTS FOR FIVE TIRE TYPES.                          *
*      FORMOD - COEFFICIENTS USED TO MODIFY THE MAGNITUDE               *
*               OF TIRE FORCES.  USED TO MODIFY YCOEFF OR               *
*               XCOEFF SO AS TO MODEL HYPOTHETICAL TIRES.               *
*      TIME   - TIME AND PRINTER CONTROL CONSTANTS.                     *
*                                                                       *
*************************************************************************
```

```
**************************************************************************
*                                                                        *
* (2) SPECIFIABLE VARIABLE DESCRIPTIONS                                  *
*     NOTE: VALUES IN PARENTHESIS ARE DEFAULT VALUES                     *
*                                                                        *
*     DIMENSIONS                                                         *
*                                                                        *
*        D1 - CG TO LEFT WHEEL LATERAL DISTANCE        (.265 METERS)     *
*        D2 - CG TO RIGHT WHEEL LATERAL DISTANCE       (.265 METERS)     *
*        S1 - CG TO FRONT AXLE FORWARD DISTANCE        (.345 METERS)     *
*        S2 - CG TO CASTER PINS BACKWARD DISTANCE      (.175 METERS)     *
*        L1 - CASTER PIN TO CASTER CG DISTANCE         (.058 METERS)     *
*        L  - CASTER PIN TO CASTER CONTACT POINT       (.080 METERS)     *
*        T1 - CG TO LEFT CASTER PIN LATERAL DISTANCE   (.240 METERS)     *
*        T2 - CG TO RIGHT CASTER PIN LATERAL DISTANCE  (.240 METERS)     *
*        H  - HEIGHT OF CG ABOVE GROUND                (.610 METERS)     *
*                                                                        *
*     MASS PROPERTIES                                                    *
*                                                                        *
*        IZ - TOTAL MOMENT OF INERTIA ABOUT Z AXIS     (5.6 KG-M-M)      *
*       IZP - MOMENT OF INERTIA OF CASTER ABOUT PIN    (.02 KG-M-M)      *
*         M - TOTAL MASS                               (95 KG)           *
*        MC - CASTER ASSEMBLY MASS                     (1.2 KG)          *
*                                                                        *
*     FORCE / FORCE RELATED VARIABLES                                    *
*                                                                        *
*     FCIMP - LATERAL INITIAL IMPULSE AT CG            (0  N-METER)      *
*     FTIMP - LATERAL INITIAL IMPULSE AT MAIN TIRES    (0 N-METER)       *
*     DUIMP - DURATION FOR FCIMP OR FTIMP              (0 SECONDS)       *
*     ROLLK - ROLL COEFFICIENT                         (1.0)             *
*     MAF   - FRICTION MOMENT AT LEFT CASTER           (.1 N-METER)      *
*     MBF   - FRICTION MOMENT AT RIGHT CASTER          (.1 N-METER)      *
*     CAMCOF- CAMBER COEFFICIENT                       (0)               *
*     CAMANG- CAMBER ANGLE                             (0 DEGREES)       *
*     TOEANG- TOE ANGLE                                (0 DEGREES)       *
*     TXMOD - MODIFYING FACTOR FOR TIRE X FORCES       (0)               *
*     TYMOD - MODIFYING FACTOR FOR TIRE Y FORCES       (1)               *
*     CXMOD - MODIFYING FACTOR FOR CASTER X FORCES     (0)               *
*     CYMOD - MODIFYING FACTOR FOR CASTER Y FORCES     (1)               *
*  TIRY(3,8)- EMPIRICAL LATERAL OR CORNERING FORCE                       *
*             COEFFICIENTS FOR SLIP ANGLES 0 - 8                         *
*             DEGREES.  TIRY VALUES ARE SELECTED                         *
*             BY SELECTING ONE OF FIVE TIRE TYPES                        *
*             WHICH WERE TESTED EXPERIMENTALLY.                          *
*   TIRX(3) - EMPIRICAL LONGITUDINAL FORCE                               *
*             COEFFICIENTS, ALSO SELECTED BY                             *
*             CHOOSING ONE OF FIVE TIRE TYPES.                           *
*                                                                        *
*     KINEMATIC VARIABLES                                                *
*                                                                        *
*        UD - INITIAL FORWARD VELOCITY  (UD ="UDOT")   (.75 METER/S)     *
*        VD - INITIAL LATERAL VELOCITY                 (0.0 METER/S)     *
*         E - INITIAL ANGLE OF LEFT CASTER (ETA)       (0 DEGREES)       *
*         B - INITIAL ANGLE OF RIGHT CASTER (BETA)     (0 DEGREES)       *
```

```
*    TIME AND PRINTER CONTROL CONSTANTS                                    *
*                                                                          *
*   TTOTAL - MAXIMUM TOTAL TIME FOR MOTION SIMULATION (10 SEC)             *
*    TSTEP - TIME STEP FOR EACH PROGRAM ITERATION       (.001 SEC)         *
*     PINT - TIME INTERVAL BETWEEN VARIABLE PRINTOUTS (.20 SEC)            *
*   PRCTRL - 1.0 = PRINT KEY VARIABLES ONLY            (1.0)               *
*            ANY OTHER NUMBER = PRINT ALL VARIABLES                        *
*                                                                          *
****************************************************************************
*                                                                          *
* (3) NON-SPECIFIABLE VARIABLES                                            *
*                                                                          *
*     FAY,FBY,FDY,FEY - LATERAL FORCES ON TIRES                            *
*     FAX,FBX,FDX,FEX - LONGITUDINAL FORCES ON TIRES                       *
*     U,UDD - LOCAL DISPLACEMENT,ACCELERATION IN C1 DIRECTION              *
*             (UDD = "U DOUBLE DOT")                                       *
*     V,VDD - LOCAL DISPLACEMENT, ACCELERATION IN C2 DIRECTION             *
*     FC1,FC2 - TOTAL FORCE IN C1 AND C2 DIRECTIONS                        *
*     ED,EDD,BD,BDD - VELOCITIES AND ACCELERATIONS OF CASTERS              *
*                     IN THEIR LOCAL REFERENCE FRAMES                      *
*     X,XD,XDD - GLOBAL KINEMATIC VARIABLES IN FIXED X DIRECTION           *
*     Y,YD,YDD - GLOBAL KINEMATIC VARIABLES IN FIXED Y DIRECTION           *
*     THE,THED,THEDD - ROTATIONAL KINEMATIC VARIABLES                      *
*     KE - TOTAL KINETIC ENERGY OF SYSTEM                                  *
*     SLIPA,SLIPB,SLIPD,SLIPE - SLIP ANGLE FOR EACH TIRE                   *
*     VAX,VBX,VDX,VDX - VELOCITIES OF TIRE CONTACT POINTS IN               *
*                       THE TIRE'S LOCAL X DIRECTION                       *
*     VAY,VBY,VDY,VEY - VELOCITIES OF TIRE CONTACT POINTS IN               *
*                       THE TIRES'S LOCAL Y DIRECTION                      *
*     T - CURRENT TIME, USED BY MAIN DO LOOP                               *
*                                                                          *
****************************************************************************
*                                                                          *
* (4) EMPIRICAL COEFFICIENT ARRAYS                                         *
*                                                                          *
*         THE ARRAYS EJAY(3,8),  IMY(3,8),  EJPY(3,8),  SSY(3,8)           *
*     AND  AGY(3,8) CONTAIN EMPIRICAL LATERAL FORCE  COEFFICIENTS          *
*     FOR  FIVE DIFFERENT TIRE TYPES.  ONE OF THE FIVE ARRAYS  IS          *
*     SELECTED AND ASSIGNED TO THE ARRAY TIRY(3,8).   THESE COEF-          *
*     FICIENTS  APPROXIMATE  THE  LATERAL FORCE ON A  TIRE  USING          *
*     THIRD  ORDER POLYNOMIALS WITH NORMAL FORCE AS THE  INDEPEN-          *
*     DENT VARIABLE.   THE 8 ARRAY COLUMNS CORRESPOND TO  COEFFI-          *
*     CIENTS  FOR  8  DIFFERENT INTEGER SLIP  ANGLES.   FOR  NON-          *
*     INTEGER  SLIP ANGLES,  THE PROGRAM USES THE NEAREST  HIGHER          *
*     AND LOWER INTEGER SLIP ANGLE,  ALONG WITH A LINEAR INTERPO-          *
*     LATION TO OBTAIN THE LATERAL FORCE.                                  *
*        THE ARRAYS EJAX(3), IMX(3), EJPX(3), SSX(3), AND AGX(3)           *
*     HOLD  SIMILAR COEFFICIENTS USED TO  CALCULATE  LONGITUDINAL          *
*     FORCE  DEPENDING UPON WHICH TIRE IS SELECTED.   ONLY  THREE          *
*     COEFFICIENTS  ARE REQUIRED FOR EACH TIRE BECAUSE LONGITUDI-          *
*     NAL FORCE IS ASSUMED INDEPENDENT OF SLIP ANGLE AND HENCE IS          *
*     DETERMINED ONLY BY THE VALUE OF THE NORMAL FORCE.                    *
*        EMPIRICAL  COEFFICIENTS  FOR A TYPICAL  SET  OF  CASTER           *
*     WHEELS  ARE  STORED  IN THE ARRAY  CASY(3,8)  AND  CASX(3).          *
```

```
*     ALTHOUGH  INDIVIDUAL CASTER TYPES CANNOT BE SELECTED,  DIF-         *
*     FERENT  CASTERS  CAN BE SIMULATED BY  SPECIFYING  DIFFERENT         *
*     VALUES FOR CXMOD AND CYMOD.                                         *
*                                                                         *
***************************************************************************
*                                                                         *
* (4) OUTPUT FILES                                                        *
*                                                                         *
*     TAPE6 - KEY VARIABLE LISTING (ALWAYS PRINTED), AND A LIST-          *
*             ING OF ALL INITIAL SPECIFIABLE VARIABLE VALUES              *
*     TAPE7,TAPE8,TAPE9,TAPE10 - PRINTED IF PRCTRL DOES NOT EQUAL 1.0     *
*     TAPE 11 - PRINTED ONLY IF WARNING MESSAGES ARE GIVEN                *
*                                                                         *
*     CONTENTS                                                            *
*       TAPE6 : X,Y,THE,THED,THEDD,UD,VD,KE                               *
*       TAPE7 : SLIPA,SLIPB,SLIPD,SLIPE,VAX,VAY,VBX,VBY,                  *
*               VDX,VDY,VEX,VEY                                           *
*       TAPE8 : FAX,FBX,FDX,FEX,FC1,FAY,FBY,FDY,FEY,FC2,                  *
*               FAZ,FBZ,FDZ,FEZ                                           *
*       TAPE9 : U,UD,UDD,V,VD,VDD,E,ED,EDD,B,BD,BDD                       *
*       TAPE10: X,XD,XDD,Y,YD,YDD,THE,THED,THEDD,KE                       *
*       TAPE11: T(=CURRENT TIME), SLIPA,SLIPB,SLIPD,SLIPE                 *
*               AND/OR FAZ,FBZ,FDZ,FEZ                                    *
*                                                                         *
***************************************************************************
*                                                                         *
* (5) OTHER VARIABLES                                                     *
*                                                                         *
*          ALL  OTHER VARIABLES ARE USED ONLY LOCALLY BY  INDIVI-         *
*     DUAL  SUBROUTINES.   THESE  ARE DESCRIBED BY USING  COMMENT         *
*     LINES WHEN NECESSARY.   NOTE THAT AUXILLARY VARIABLES WHICH         *
*     HAVE  NO  PARTICLAR  MEANING BUT  ARE  USED  FOR  TEMPORARY         *
*     STORAGE ALWAYS BEGIN WITH THE LETTER Z.  (E.G. Z1,Z1,Z3,...)        *
*                                                                         *
***************************************************************************
```

```
************************************************************************
**                 BEGIN EXECUTION OF MAIN PROGRAM                    **
************************************************************************

      PROGRAM WCHAIR(INPUT,OUTPUT,TAPE6,TAPE7,TAPE8,TAPE9,TAPE10,TAPE11)
      COMMON /TIME/   TTOTAL,TSTEP,PINT,PRCTRL
      INTEGER COUNT,PRFLAG

C+++++++++++++++++++++++++++++++++++++++++
C SPECIFY VARIABLES, SET FLAG FOR PRINTING
C AND PLACE HEADINGS IN OUTPUT FILES
C+++++++++++++++++++++++++++++++++++++++++
      CALL SETUP
      PRFLAG = PINT/TSTEP
      COUNT = PRFLAG
      CALL HEADRS(PRCTRL)
C+++++++++++++++++++++++++++++++++++++++++
C BEGIN PRIMARY PROGRAM LOOP
C+++++++++++++++++++++++++++++++++++++++++
      DO 99  T = 0,TTOTAL+TSTEP,TSTEP
         CALL SLIP
         CALL STATICS(T)
         IF ((COUNT.EQ.PRFLAG).AND.(PRCTRL.EQ.1.0)) THEN
            CALL PRKEY(T)
            COUNT = 0
         ELSE IF (COUNT.EQ.PRFLAG) THEN
            CALL PRCUR(T)
            COUNT = 0
         END IF
         CALL MECHAN(T)
         CALL DYNAM(T)
         CALL UPDATE
         COUNT = COUNT + 1
99    CONTINUE
      END



************************************************************************
* SUBROUTINE SETUP ALLOWS THE USER TO INTERACTIVELY SPECIFY THE INITIAL *
* CONDITIONS FOR EACH RUN OF THE PROGRAM.  THIS INCLUDES ALTERATION OF  *
* SPECIFIABLE VARIABLES AS PREVIOUSLY LISTED, AS WELL AS THE SELECTION  *
* OF A SPECIFIC TIRE TYPE. (SEE THESIS TEXT)                            *
************************************************************************

      SUBROUTINE SETUP
      COMMON /DIMEN/  D1,D2,S1,S2,L1,L,T1,T2,H
      COMMON /MASSPR/ IZ,IZP,M,MC,GR
      COMMON /LATFOR/ FAY,FBY,FDY,FEY,FTIMP,FCIMP,DUIMP
      COMMON /NORFOR/ FAZ,FBZ,FDZ,FEZ,ROLLK
      COMMON /C1VAR/  U,UD,UDD,FC1
      COMMON /C2VAR/  V,VD,VDD,FC2
      COMMON /CASANG/ E,ED,EDD,B,BD,BDD
      COMMON /GLOBAL/ X,XD,XDD,Y,YD,YDD,THE,THED,THEDD,KE
```

```
      COMMON /CDAMP/  MAF,MBF
      COMMON /CAMTOE/ CAMANG,CAMCOF,TOEANG
      COMMON /TIRES/  TIRY(3,8),TIRX(3),CASY(3,8),CASX(3)
      COMMON /YCOEFF/ EJAY(3,8),IMY(3,8),EJPY(3,8),SSY(3,8),AGY(3,8)
      COMMON /XCOEFF/ EJAX(3),IMX(3),EJPX(3),SSX(3),AGX(3)
      COMMON /FORMOD/ TXMOD,TYMOD,CXMOD,CYMOD
      COMMON /TIME/   TTOTAL,TSTEP,PINT,PRCTRL
      REAL    L1,L,IZ,IZP,MAF,MBF,M,MC,KE,IMX,IMY
      INTEGER CHOICE,TIRSEL
      CHARACTER TIRTYP*5
C+++++++++++++++++++++++++++++++++++++++
C PRINT CURRENT VALUES TO SCREEN
C+++++++++++++++++++++++++++++++++++++++
10    PRINT*,'CURRENT VALUES FOR SPECIFIABLE VARIABLES ARE:'
      WRITE(*,1000) 'D1=',D1,'M=',M,'FTIMP=',FTIMP,'D2=',D2,
     *              'MC=',MC,'FCIMP=',FCIMP,'S1=',S1,'IZ=' ,
     *               IZ,'DUIMP=',DUIMP,'S2=',S2,'IZP=',IZP ,
     *              'TXMOD=',TXMOD,'L1=',L1,'UD=',UD,'TYMOD=',
     *               TYMOD,'L=',L,'VD=',VD,'CXMOD=',CXMOD,
     *              'T1=',T1,'E=',E,'CYMOD=',CYMOD,'T2=',T2,
     *              'B=',B,'CAMCOF=',CAMCOF,'H=',H,'MAF=',MAF,
     *              'CAMANG=',CAMANG,'ROLLK=',ROLLK,'MBF=',MBF,
     *              'TOEANG=',TOEANG,'TTOTAL=',TTOTAL,'TSTEP=',
     *               TSTEP,'PINT=',PINT,'PRCTRL=',PRCTRL
1000  FORMAT (/,10(2(A12,F7.3),A14,F7.3,/),/,3(A10,F8.5),A11,F3.1,/)
C+++++++++++++++++++++++++++++++++++++++
C SELECT VARIABLES TO SPECIFY
C+++++++++++++++++++++++++++++++++++++++
      PRINT*, 'WHICH OF THE FOLLOWING ARE TO BE SPECIFIED?'
      PRINT*
      PRINT*,  ' 1    GEOMETRIC VARIABLES'
      PRINT*,  ' 2    DAMPING MOMENTS AT CASTER PINS'
      PRINT*,  ' 3    TIME AND PRINTER CONTROL CONSTANTS'
      PRINT*,  ' 4    LOCAL VELOCITIES (UD AND VD)'
      PRINT*,  ' 5    LOCAL CASTER ANGLES (E AND B)'
      PRINT*,  ' 6    INITIAL LATERAL IMPULSE FORCES'
      PRINT*,  ' 7    MASS AND INERTIA VALUES'
      PRINT*,  ' 8    ROLL STIFFNESS RATIO (ROLLK)'
      PRINT*,  ' 9    CAMBER ANGLE FOR MAIN WHEELS'
      PRINT*,  '10    TOE ANGLE FOR MAIN WHEELS'
      PRINT*,  '11    TIRE FORCE MODIFYING COEFFICIENTS'
      PRINT*,  '12    QUIT : CONTINUE WITH PROGRAM'
      PRINT*
      READ*, CHOICE
      IF ((CHOICE.LT.1) .OR. (CHOICE.GT.12)) THEN
         PRINT*,'CHOICE OUT OF RANGE, SELECT 1 THROUGH 12'
         GO TO 10
      END IF
C+++++++++++++++++++++++++++++++++++++++
C READ INPUT FOR CHOSEN VARIABLES, RETURN
C TO MAKE ANOTHER SELECTION
C+++++++++++++++++++++++++++++++++++++++
      GO TO (15,20,25,30,35,40,45,50,55,60,65,70),CHOICE
15    PRINT*,'GIVE D1,D2,S1,S2,L1,L,T1,T2,H'
```

```
      READ*,  D1,D2,S1,S2,L1,L,T1,T2,H
      GO TO 10
20    PRINT*,'GIVE MAF AND MBF'
      READ*,  MAF,MBF
      GO TO 10
25    PRINT*,'GIVE TTOTAL, TSTEP, PINT, AND PRCTRL'
      READ*,  TTOTAL,TSTEP,PINT,PRCTRL
      GO TO 10
30    PRINT*,'GIVE UD AND VD'
      READ*,  UD,VD
      GO TO 10
35    PRINT*,'GIVE E AND B  (IN DEGREES)'
      READ*,  E,B
      GO TO 10
40    PRINT*,'GIVE FTIMP,FCIMP, AND DUIMP'
      READ*,  FTIMP,FCIMP,DUIMP
      GO TO 10
45    PRINT*,'GIVE M,MC,IZ,IZP'
      READ*,  M,MC,IZ,IZP
      GO TO 10
50    PRINT*,'GIVE ROLLK'
      READ*, ROLLK
      GO TO 10
55    PRINT*,'GIVE CAMBER ANGLE (IN DEGREES) AND CAMBER COEFFICIENT'
      PRINT*,'GIVE ONLY WHOLE NUMBER CAMBER ANGLES (1,2,3,...)'
      READ*, CAMANG,CAMCOF
      GO TO 10
60    PRINT*,'GIVE TOEANG  (IN DEGREES)'
      READ*,TOEANG
      GO TO 10
65    PRINT*, 'GIVE TXMOD,TYMOD,CXMOD,CYMOD'
      READ*, TXMOD,TYMOD,CXMOD,CYMOD
      GO TO 10
70    CONTINUE
      PRINT*
C+++++++++++++++++++++++++++++++++++++++
C SELECT ONE OF FIVE MAIN WHEEL TYPES
C+++++++++++++++++++++++++++++++++++++++
      PRINT*, 'SELECT ONE OF THE FOLLOWING TIRE TYPES'
      PRINT*
      PRINT*, ' 1   EJA (EVEREST AND JENNINGS AIRLESS)'
      PRINT*, ' 2   IM  (INVACARE MAG-SPIDER WEB)'
      PRINT*, ' 3   EJP (EVEREST AND JENNINGS PNEUMATIC)'
      PRINT*, ' 4   SS  (SILVER STAR PNEUMATIC)'
      PRINT*, ' 5   AG  (AIRLESS GREY RUBBER)'
      READ*,TIRSEL
C+++++++++++++++++++++++++++++++++++++++
C ASSIGN EMPIRICAL COEFFICIENTS TO BE
C USED BY THE MAIN PROGRAM TO THE ARRAYS
C TIRY AND TIRX.  USE PERMANTLY STORED
C ARRAY VALUES FOR THE TIRE SELECTED
C+++++++++++++++++++++++++++++++++++++++
      IF (TIRSEL.EQ.1) THEN
        DO 80  I = 1,3
```

```
                DO 75  J = 1,8
                TIRY(I,J) = EJAY(I,J)
      75        CONTINUE
              TIRX(I) = EJAX(I)
      80      CONTINUE
              TIRTYP = 'EJA'
            ELSE IF (TIRSEL.EQ.2) THEN
              DO 90  I = 1,3
                DO 85  J = 1,8
                TIRY(I,J) = IMY(I,J)
      85        CONTINUE
              TIRX(I) = IMX(I)
      90      CONTINUE
              TIRTYP = 'IM'
            ELSE IF (TIRSEL.EQ.3) THEN
              DO 100  I = 1,3
                DO 95  J = 1,8
                TIRY(I,J) = EJPY(I,J)
      95        CONTINUE
              TIRX(I) = EJPX(I)
      100     CONTINUE
              TIRTYP = 'EJP'
            ELSE IF (TIRSEL.EQ.4) THEN
              DO 110  I = 1,3
                DO 105 J = 1,8
                TIRY(I,J) = SSY(I,J)
      105       CONTINUE
              TIRX(I) = SSX(I)
      110     CONTINUE
              TIRTYP = 'SS'
            ELSE IF (TIRSEL.EQ.5) THEN
              DO 120 I = 1,3
                DO 115 J = 1,8
                TIRY(I,J) = AGY(I,J)
      115       CONTINUE
              TIRX(I) = AGX(I)
      120     CONTINUE
              TIRTYP = 'AG'
            ELSE
              PRINT*,'TIRE CHOICE NOT IN RANGE 1 - 5'
              GO TO 65
            END IF
      C+++++++++++++++++++++++++++++++++++++++++
      C WRITE FINAL SELECTIONS TO TAPE6
      C+++++++++++++++++++++++++++++++++++++++++
            WRITE(6,1500) TIRTYP
      1500  FORMAT(/,'TIRE SELECTED = ',A10,/)
            WRITE(6,1000) 'D1=',D1,'M=',M,'FTIMP=',FTIMP,'D2=',D2,
           *              'MC=',MC,'FCIMP=',FCIMP,'S1=',S1,'IZ=' ,
           *               IZ,'DUIMP=',DUIMP,'S2=',S2,'IZP=',IZP ,
           *              'TXMOD=',TXMOD,'L1=',L1,'UD=',UD,'TYMOD=',
           *               TYMOD,'L=',L,'VD=',VD,'CXMOD=',CXMOD,
           *              'T1=',T1,'E=',E,'CYMOD=',CYMOD,'T2=',T2,
           *              'B=',B,'CAMCOF=',CAMCOF,'H=',H,'MAF=',MAF,
```

```
     *                'CAMANG=',CAMANG,'ROLLK=',ROLLK,'MBF=',MBF,
     *                'TOEANG=',TOEANG,'TTOTAL=',TTOTAL,'TSTEP=',
     *                 TSTEP,'PINT=',PINT

C+++++++++++++++++++++++++++++++++++++++
C CONVERT ANGLES TO RADIANS, INITIALIZE
C KE, XD, YD TO MACH SPECIFIED CONDITIONS
C+++++++++++++++++++++++++++++++++++++++
      E = E * 0.0174532
      B = B * 0.0174532
      TOEANG = TOEANG * 0.0174532
      KE = 0.5*M*(UD*UD + VD*VD)
      XD = UD
      YD = VD
      RETURN
      END



**************************************************************************
* SUBROUTINE SLIP CALCULATES THE CURRENT SLIP ANGLE AT EACH OF THE FOUR  *
* WHEELCHAIR TIRES.                                                      *
**************************************************************************

      SUBROUTINE SLIP
      COMMON /DIMEN/  D1,D2,S1,S2,L1,L,T1,T2,H
      COMMON /C1VAR/  U,UD,UDD,FC1
      COMMON /C2VAR/  V,VD,VDD,FC2
      COMMON /CASANG/ E,ED,EDD,B,BD,BDD
      COMMON /GLOBAL/ X,XD,XDD,Y,YD,YDD,THE,THED,THEDD,KE
      COMMON /SLIPAN/ SLIPA,SLIPB,SLIPD,SLIPE
      COMMON /CAMTOE/ CAMANG,CAMCOF,TOEANG
      COMMON /PTVEL/  VAX,VAY,VBX,VBY,VDX,VDY,VEX,VEY
      REAL   L1,L
      COSE = COS(E)
      SINE = SIN(E)
      COSB = COS(B)
      SINB = SIN(B)
C+++++++++++++++++++++++++++++++++++++++
C CALCULATE VELOCITY OF EACH TIRE CONTACT
C POINT (IN TIRE FIXED REFERENCE FRAME)
C+++++++++++++++++++++++++++++++++++++++
      VAX = (UD+(THED*T1))*COSE + (VD-(THED*S2))*SINE
      VAY = (VD-(THED*S2))*COSE - (UD+(THED*T1))*SINE - ED*L
      VBX = (UD-(THED*T2))*COSB + (VD-(THED*S2))*SINB
      VBY = (VD-(THED*S2))*COSB - (UD-(THED*T2))*SINB - BD*L
      VDX = UD + THED*D1
      VDY = VD + THED*S1
      VEX = UD - THED*D2
      VEY = VD + THED*S1
C+++++++++++++++++++++++++++++++++++++++
C CORRECT FOR PRESENCE OF TOE ANGLE
C+++++++++++++++++++++++++++++++++++++++
      IF (TOEANG.NE.0.) THEN
```

```
            Z1 =  VEX*COS(TOEANG) + VEY*SIN(TOEANG)
            Z2 = -VEX*SIN(TOEANG) + VEY*COS(TOEANG)
            Z3 =  VDX*COS(TOEANG) - VDY*SIN(TOEANG)
            Z4 =  VDX*SIN(TOEANG) + VDY*COS(TOEANG)
            VEX = Z1
            VEY = Z2
            VDX = Z3
            VDY = Z4
         END IF
C+++++++++++++++++++++++++++++++++++++++
C CALCULATE SLIP ANGLES
C+++++++++++++++++++++++++++++++++++++++
      SLIPA = ATAN (ABS(VAY/VAX)) * 57.295779
      SLIPB = ATAN (ABS(VBY/VBX)) * 57.295779
      SLIPD = ATAN (ABS(VDY/VDX)) * 57.295779
      SLIPE = ATAN (ABS(VEY/VEX)) * 57.295779
      RETURN
      END



***********************************************************************
* SUBROUTINE STATICS CALCULATES THE CURRENT NORMAL FORCE ACTING ON EACH  *
* WHEELCHAIR TIRE.  THIS IS DONE USING THE CURRENT VALUES FOR THE ROAD   *
* FORCES (FAX,FBX,FDX,FEX,FAY,FBY,FDY,FEY) ON EACH TIRE.  A QUASI-STATIC *
* METHOD IS USED WHICH ASSUMES THAT THE WHEELCHAIR DOES NOT ROLL.        *
***********************************************************************

      SUBROUTINE STATICS(T)
      COMMON /DIMEN/  D1,D2,S1,S2,L1,L,T1,T2,H
      COMMON /MASSPR/ IZ,IZP,M,MC,GR
      COMMON /NORFOR/ FAZ,FBZ,FDZ,FEZ,ROLLK
      COMMON /C1VAR/  U,UD,UDD,FC1
      COMMON /C2VAR/  V,VD,VDD,FC2
      COMMON /CASANG/ E,ED,EDD,B,BD,BDD
      REAL   L1,L,IZ,IZP,M,MC
      SAVE NWARN1
      DATA NWARN1 /0/
C+++++++++++++++++++++++++++++++++++++++
C CALCULATE LATERAL AND LONGITUDINAL
C DISTANCE OF EACH TIRE CONTACT POINT
C FROM THE WHEELCHAIR CENTER OF GRAVITY
C+++++++++++++++++++++++++++++++++++++++
      AX = L * COS(E) + S2
      AY = L * SIN(E) + T1
      BX = L * COS(B) + S2
      BY =-L * SIN(B) + T2
      Z1 = 1.0/(ROLLK + 1.0)
      Z2 = 1.0 - Z1
C+++++++++++++++++++++++++++++++++++++++
C SEQUENTIALLY SOLVE STATIC EQUATIONS
C TO DETERMINE NORMAL FORCES
C+++++++++++++++++++++++++++++++++++++++
      TERM1 = FC2*H*Z1*(S1+AX) - FC1*H*AY - M*GR*S1*AY
```

```
      TERM2 = S1*(AY+BY) + AY*BX + AX*BY
      TERM3 = FC2*H*(Z2*S1/D1 - Z1*AX/AY) + FC1*H
      FBZ = -TERM1/TERM2
      FEZ = (FBZ*(BX + AX*BY/AY) - TERM3)/(S1*(1.0 + D2/D1))
      FDZ = FEZ*D2/D1 + FC2*H*Z2/D1
      FAZ = FBZ*BY/AY + FC2*H*Z1/AY
C+++++++++++++++++++++++++++++++++++++
C CHECK TO ENSURE THAT NORMAL FORCES ARE
C WITHIN THE ALLOWED RANGE, IF NOT PRINT
C WARNING TO SCREEN AND CURRENT VALUES
C+++++++++++++++++++++++++++++++++++++
      IF (MAX(FAZ,FBZ,FDZ,FEZ).GT.450) THEN
         PRINT*,'**** WARNING!!  SEE TAPE 11  ****'
         PRINT*,'**** NORMAL FORCE > 450 N    ****'
         WRITE(11,2000) 'T = ',T,'FAZ = ',FAZ,'FBZ = ',FBZ,'FDZ = ',
     *                    FDZ,'FEZ = ',FEZ
2000     FORMAT(A4,F8.6,4(A9,F7.2))
C+++++++++++++++++++++++++++++++++++++
C KEEP TRACK OF WARNINGS ISSUED, IF
C NUMBER OF WARNINGS EXCEEDS 10, STOP
C+++++++++++++++++++++++++++++++++++++
         NWARN1 = NWARN1 + 1
         IF (NWARN1.GT.10) STOP 'TEST CASE TERMINATED'
      END IF
      RETURN
      END



*********************************************************************
* SUBROUTINE MECHAN USES THE SLIP ANGLES CALCULATED BY SLIP AND THE   *
* FORCES CALCULATED BY STATICS TO DETERMINE THE CURRENT LONGITUDINAL  *
* AND LATERAL ROAD FORCE ACTING ON EACH WHEELCHAIR TIRE.  THIS IS DONE *
* USING EXPERIMENTALLY DETERMINED EMPIRICAL CONSTANTS.  NOTE THAT THE  *
* DIRECTION OF EACH TIRE FORCE ALWAYS OPPOSES THE THE CORRESPONDING   *
* VELOCITY COMPONENT FOR A GIVEN TIRE. IF A TIRE HAS A LATERAL VELOCITY *
* DIRECTED ALONG ITS POSITIVE LOCAL X AXIS, THE LATERAL FORCE WILL BE  *
* DIRECTED ALONG THE NEGATIVE LOCAL X AXIS.                           *
*********************************************************************

      SUBROUTINE MECHAN(T)
      COMMON /LATFOR/ FAY,FBY,FDY,FEY,FTIMP,FCIMP,DUIMP
      COMMON /LONFOR/ FAX,FBX,FDX,FEX
      COMMON /NORFOR/ FAZ,FBZ,FDZ,FEZ,ROLLK
      COMMON /SLIPAN/ SLIPA,SLIPB,SLIPD,SLIPE
      COMMON /PTVEL/  VAX,VAY,VBX,VBY,VDX,VDY,VEX,VEY
      COMMON /CAMTOE/ CAMANG,CAMCOF,TOEANG
      COMMON /TIRES/  TIRY(3,8),TIRX(3),CASY(3,8),CASX(3)
      COMMON /FORMOD/ TXMOD,TYMOD,CXMOD,CYMOD
      SAVE NWARN2
      DATA NWARN2 /0/
```

```
C++++++++++++++++++++++++++++++++++++++
C CHECK TO ENSURE THAT ALL SLIP ANGLES
C ARE LESS THAN 8 DEGREES. (E.G. THAT NO
C SLIPPING HAS BEGUN)  IF NOT, PRINT
C WARNING AND CURRENT VALUES
C++++++++++++++++++++++++++++++++++++++
      IF (MAX(SLIPA,SLIPB,SLIPD,SLIPE).GT.8.) THEN
         PRINT*,'**** WARNING!!  SEE TAPE 11  ****'
         PRINT*,'**** SLIP ANGLE ) 8 DEGREES  ****'
         WRITE(11,2500) 'T = ',T,'SLIPA = ',SLIPA,'SLIPB = ',SLIPB,
     *                 'SLIPD = ',SLIPD,'SLIPE = ',SLIPE
2500     FORMAT(A4,F8.6,4(A9,F7.3))
         NWARN2 = NWARN2 + 1
         IF (NWARN2.GT.10) STOP 'TEST CASE TERMINATED'
      END IF
C++++++++++++++++++++++++++++++++++++++
C CALCULATE LATERAL FORCE ON LEFT CASTER
C++++++++++++++++++++++++++++++++++++++
      I = INT(SLIPA)
      J = I + 1
      Z1 = POLYFT(CASY,I,FAZ)
      Z2 = POLYFT(CASY,J,FAZ)
      FAY = SIGN((SLIPA - I)*(Z2-Z1) + Z1 , -VAY) * CYMOD
C++++++++++++++++++++++++++++++++++++++
C CALCULATE LATERAL FORCE ON RIGHT CASTER
C++++++++++++++++++++++++++++++++++++++
      I = INT(SLIPB)
      J = I + 1
      Z1 = POLYFT(CASY,I,FBZ)
      Z2 = POLYFT(CASY,J,FBZ)
      FBY = SIGN((SLIPB - I)*(Z2-Z1) + Z1 , -VBY) * CYMOD
C++++++++++++++++++++++++++++++++++++++
C CALCULATE LATERAL FORCES ON MAIN WHEELS
C++++++++++++++++++++++++++++++++++++++
      IF((FTIMP.NE.0.).AND.(T.LE.DUIMP)) THEN
         FDY = FTIMP
         FEY = FTIMP
      ELSE
         I = INT(SLIPD)
         J = I + 1
         Z1 = POLYFT(TIRY,I,FDZ)
         Z2 = POLYFT(TIRY,J,FDZ)
         FDY = SIGN((SLIPD - I)*(Z2-Z1) + Z1 , -VDY) * TYMOD
         I = INT(SLIPE)
         J = I + 1
         Z1 = POLYFT(TIRY,I,FEZ)
         Z2 = POLYFT(TIRY,J,FEZ)
         FEY = SIGN((SLIPE - I)*(Z2-Z1) + Z1 , -VEY) * TYMOD
      END IF
C++++++++++++++++++++++++++++++++++++++
C CALCULATE LONGITUDINAL FORCES
C++++++++++++++++++++++++++++++++++++++
      FAX = SIGN(CASX(1)*FAZ+CASX(2)*FAZ**2+CASX(3)*FAZ**3,-VAX)*CXMOD
      FBX = SIGN(CASX(1)*FBZ+CASX(2)*FBZ**2+CASX(3)*FBZ**3,-VBX)*CXMOD
```

```
      FDX = SIGN(TIRX(1)*FDZ+TIRX(2)*FDZ**2+TIRX(3)*FDZ**3,-VDX)*TXMOD
      FEX = SIGN(TIRX(1)*FEZ+TIRX(2)*FEZ**2+TIRX(3)*FEZ**3,-VEX)*TXMOD
C++++++++++++++++++++++++++++++++++++++++
C CORRECT FOR PRESENCE OF TOE OR CAMBER
C++++++++++++++++++++++++++++++++++++++++
      IF(CAMANG.NE.0.) THEN
         I = INT(CAMANG)
         FDY = FDY + CAMCOF*POLYFT(TIRY,I,FDZ)
         FEY = FEY - CAMCOF*POLYFT(TIRY,I,FEZ)
      END IF
      IF(TOEANG.NE.0.) THEN
         Z1 = FEX*COS(TOEANG) - FEY*SIN(TOEANG)
         Z2 = FEX*SIN(TOEANG) + FEY*COS(TOEANG)
         Z3 = FDX*COS(TOEANG) + FDY*SIN(TOEANG)
         Z4 =-FDX*SIN(TOEANG) + FDY*COS(TOEANG)
         FEX = Z1
         FEY = Z2
         FDX = Z3
         FDY = Z4
      END IF
      END

C++++++++++++++++++++++++++++++++++++++++++
C FUNCTION POLYFIT USES THE LATERAL FORCE
C COEFFICIENTS TO COMPUTE THE LATERAL FORCE
C ON A TIRE GIVEN THE NORMAL FORCE AND AN
C INTEGER VALUE SLIP ANGLE.
C++++++++++++++++++++++++++++++++++++++++++

      FUNCTION POLYFT(A,K,FZ)
      DIMENSION A(3,8)
      IF (K.GT.8) THEN
         K = 8
      END IF
      IF (K.EQ.0) THEN
         POLYFT = 0.0
      ELSE
         POLYFT = A(1,K)*FZ + A(2,K)*FZ**2 + A(3,K)*FZ**3
      END IF
      RETURN
      END



************************************************************************
* SUBROUTINE DYNAM CALCULATES THE CURRENT ACCELERATION OF THE          *
* WHEELCHAIR CENTER OF MASS AND OF THE INDIVIDUAL CASTER WHEELS.       *
************************************************************************

      SUBROUTINE DYNAM(T)
      COMMON /DIMEN/  D1,D2,S1,S2,L1,L,T1,T2,H
      COMMON /MASSPR/ IZ,IZP,M,MC,GR
      COMMON /LATFOR/ FAY,FBY,FDY,FEY,FTIMP,FCIMP,DUIMP
      COMMON /LONFOR/ FAX,FBX,FDX,FEX
```

```
      COMMON /C1VAR/  U,UD,UDD,FC1
      COMMON /C2VAR/  V,VD,VDD,FC2
      COMMON /CASANG/ E,ED,EDD,B,BD,BDD
      COMMON /GLOBAL/ X,XD,XDD,Y,YD,YDD,THE,THED,THEDD,KE
      COMMON /CDAMP/  MAF,MBF
      REAL   L1,L,IZ,IZP,MAF,MBF,M,MC
C++++++++++++++++++++++++++++++++++++++
C COMPUTE SEVERAL CONSTANTS WHICH MUST BE
C USED FOR ALL ACCELERATION CALCULATIONS
C++++++++++++++++++++++++++++++++++++++
      COSE = COS(E)
      SINE = SIN(E)
      COSB = COS(B)
      SINB = SIN(B)
      SDIF = SIN(E-B)
      CDIF = COS(E-B)
      Z1 = T1*COSE - S2*SINE
      Z2 = T1*SINE + S2*COSE
      Z3 = T2*COSB + S2*SINB
      Z4 = T2*SINB - S2*COSB
      Z5 = L1*MC/M/IZP
      Z6 = M/L1/MC
      Z7 = 1.0 -L*M/MC/L1
      Z8 = FDY + FEY
      Z9 = FDX + FEX
      Z10 = M*THEDD
      Z11 = M*THED*THED
C++++++++++++++++++++++++++++++++++++++
C CHOOSE FRICTION AT CASTERS TO OPPOSE
C CASTER MOTION.  IF CASTERS ARE NOT
C ROTATING SET FRICTION DAMPING TO ZERO.
C++++++++++++++++++++++++++++++++++++++
      IF (ED.NE.0.) THEN
          Z12 = SIGN(MAF,-ED)
        ELSE
          Z12 = 0.0
      END IF
      IF (BD.NE.0.) THEN
          Z13 = SIGN(MBF,-BD)
        ELSE
          Z13 = 0.0
      END IF
C++++++++++++++++++++++++++++++++++++++
C CALCULATE NET FORCE ON CENTER OF MASS
C IN C1 AND C2 DIRECTIONS USING CURRENT
C TIRE FORCE VALUES.
C++++++++++++++++++++++++++++++++++++++
      FC1 = FDX + FEX + FAX*COSE - FAY*SINE + FBX*COSB - FBY*SINB
      IF((FCIMP.NE.0.).AND.(T.LE.DUIMP)) THEN
         FC2 = FDY + FEY + FAX*SINE + FAY*COSE + FBX*SINB + FBY*COSB
     *         + FCIMP
      ELSE
         FC2 = FDY + FEY + FAX*SINE + FAY*COSE + FBX*SINB + FBY*COSB
      END IF
```

```
C+++++++++++++++++++++++++++++++++++++++
C COMPUTE DESIRED ACCELERATIONS
C+++++++++++++++++++++++++++++++++++++++
      UDD = FC1/M + THED*VD
      VDD = FC2/M - THED*UD
      THEDD = ( FDX*D1 - FEX*D2 + Z8*S1 + FAX*Z1 -
     *          FAY*(Z2+L) - FBX*Z3 + FBY*(Z4-L) ) / IZ
      BDD   = ( Z13*Z6 + FBY*Z7 + FAX*SDIF + FAY*CDIF +
     *          Z8*COSB - Z9*SINB + Z10*Z4 - Z11*Z3 ) * Z5
      EDD   = ( Z12*Z6 + FAY*Z7 - FBX*SDIF + FBY*CDIF +
     *          Z8*COSE - Z9*SINE - Z10*Z2 + Z11*Z1 ) * Z5
      RETURN
      END



************************************************************************
* SUBROUTINE UPDATE USES THE ACCELERATIONS COMPUTED IN SUBROUTINE DYNAM *
* TO UPDATE THE CURRENT VALUES FOR POSITION AND VELOCITY.  THE ACCELERA- *
* TIONS FOUND FROM DYNAM ARE ASSUMED CONSTANT OVER A SINGLE TIME STEP.  *
* UPDATE ALSO TRANSFORMS THE CURRENT VALUES OF LOCAL DISPLACEMENT,      *
* VELOCITY, AND ACCELERATION TO THE FIXED INERTIAL FRAME (E.G. TO THE   *
* GLOBAL X,Y FRAME)                                                     *
************************************************************************

      SUBROUTINE UPDATE
      COMMON /MASSPR/ IZ,IZP,M,MC,GR
      COMMON /C1VAR/  U,UD,UDD,FC1
      COMMON /C2VAR/  V,VD,VDD,FC2
      COMMON /CASANG/ E,ED,EDD,B,BD,BDD
      COMMON /GLOBAL/ X,XD,XDD,Y,YD,YDD,THE,THED,THEDD,KE
      COMMON /TIME/   TTOTAL,TSTEP,PINT,PRCTRL
      REAL IZ,IZP,M,MC,KE
C+++++++++++++++++++++++++++++++++++++++
C CALCULATE LOCAL DISPLACEMENT, VELOCITY
C AND ACCELERATION IN C1 AND C2 DIRECTIONS
C+++++++++++++++++++++++++++++++++++++++
      U = 0.0
      V = 0.0
      CALL ITRATE(U,UD,UDD,TSTEP)
      CALL ITRATE(V,VD,VDD,TSTEP)
C+++++++++++++++++++++++++++++++++++++++
C TRANSFORM TO GLOBAL REFERENCE FRAME,
C X,Y ARE WITH RESPECT TO A FIXED ORIGIN
C AND DO NOT MOVE OR ROTATE WITH THE
C WHEELCHAIR
C+++++++++++++++++++++++++++++++++++++++
      COST = COS(THE)
      SINT = SIN(THE)
      X = X + (U*COST - V*SINT)
      Y = Y + (U*SINT + V*COST)
      XD = UD*COST - VD*SINT
      YD = UD*SINT + VD*COST
      XDD = UDD*COST - VDD*SINT
```

```
      YDD = UDD*SINT + VDD*COST
C++++++++++++++++++++++++++++++++++++++
C UPDATE ANGULAR DISPLACEMENTS, VELOCITIES
C AND ACCELERATIONS.
C++++++++++++++++++++++++++++++++++++++
      CALL ITRATE(B,BD,BDD,TSTEP)
      CALL ITRATE(E,ED,EDD,TSTEP)
      CALL ITRATE(THE,THED,THEDD,TSTEP)
C++++++++++++++++++++++++++++++++++++++
C UPDATE VALUE OF TOTAL KINETIC ENERGY
C++++++++++++++++++++++++++++++++++++++
      KE = 0.5*(M*(UD*UD + VD*VD) + IZ*THED*THED)
      RETURN
      END



***********************************************************************
* SUBROUTINE ITRATE USES CLASSICAL FORMULAS FOR MOTION WITH CONSTANT    *
* ACCELERATION TO COMPUTE DISPLACEMENT AND VELOCITY CHANGES FOR A SINGLE *
* TIME STEP.  ITRATE IS CALLED BY SUBROUTINE DYNAM.                     *
***********************************************************************

      SUBROUTINE ITRATE(DISP,VEL,ACCEL,TSTEP)
      DISP = DISP + VEL*TSTEP + 0.5*ACCEL*TSTEP*TSTEP
      VEL = VEL + ACCEL*TSTEP
      RETURN
      END



***********************************************************************
* SUBROUTINE HEADRS PRINTS HEADINGS AT THE TOP OF EACH OUTPUT FILE TO BE *
* PRINTED.  THE NUMBER OF OUTPUT FILES DEPENDS UPON THE SPECIFIED VALUE  *
* OF PRCTRL.                                                            *
***********************************************************************

      SUBROUTINE HEADRS(PRCTRL)
      WRITE  (6,3000)
      IF (PRCTRL.NE.1.) THEN
         WRITE  (7,3500)
         WRITE  (8,4000)
         WRITE  (9,4500)
         WRITE  (10,5000)
      END IF
3000  FORMAT (3X,'T',11X,'X',8X,'Y',7X,'THE',5X,'THED',4X,'THEDD',
     *        7X,'UD',7X,'VD',7X,/)
3500  FORMAT (3X,'T',6X,'SLIPA',6X,'SLIPB',6X,'SLIPD',6X,'SLIPE',
     *        7X,'VAX',8X,'VAY',8X,'VBX',8X,'VBY',8X,'VDX',8X,'VDY',
     *        8X,'VEX',8X,'VEY',/)
4000  FORMAT (2X,'T',8X,'FAX',4X,'FBX',4X,'FDX',4X,'FEX',4X,'FC1',
     *        8X,'FAY',8X,'FBY',8X,'FDY',8X,'FEY',5X,'FC2',5X,'FAZ',
     *        5X,'FBZ',5X,'FDZ',5X,'FEZ',/)
4500  FORMAT (3X,'T',9X,'U',9X,'UD',8X,'UDD',9X,'V',9X,'VD',9X,'VDD',
```

```
     *         9X,'E',9X,'ED',9X,'EDD',9X,'B',9X,'BD',9X,'BDD',/)
5000  FORMAT (3X,'T',10X,'X',11X,'XD',11X,'XDD',11X,'Y',12X,'YD',
     *         10X,'YDD',10X,'THE',9X,'THED',9X,'THEDD',7X,'KE',/)
      RETURN
      END



*******************************************************************
* SUBROUTINE PRCUR PRINTS THE CURRENT VALUES OF SEVERAL VARIABLES TO THE *
* OUTPUT FILES.  IF PRCTRL = 1.0 ENTRY BEGINS AT THE ENTRY STATEMENT     *
* "PREKEY" AND ONLY KEY VARIABLES ARE PRINTED.  FOR ANY OTHER VALUE OF   *
* PRCTRL, ALL VARIABLES ARE PRINTED.  PRCUR IS CALLED FROM THE MAIN      *
* PROGRAM AT TIMES CORRESPONDING TO THE SPECIFIED VALUE OF PINT.         *
*******************************************************************

      SUBROUTINE PRCUR(T)
      COMMON /LATFOR/ FAY,FBY,FDY,FEY,FTIMP,FCIMP,DUIMP
      COMMON /LONFOR/ FAX,FBX,FDX,FEX
      COMMON /NORFOR/ FAZ,FBZ,FDZ,FEZ,ROLLK
      COMMON /C1VAR/  U,UD,UDD,FC1
      COMMON /C2VAR/  V,VD,VDD,FC2
      COMMON /CASANG/ E,ED,EDD,B,BD,BDD
      COMMON /GLOBAL/ X,XD,XDD,Y,YD,YDD,THE,THED,THEDD,KE
      COMMON /SLIPAN/ SLIPA,SLIPB,SLIPD,SLIPE
      COMMON /PTVEL/  VAX,VAY,VBX,VBY,VDX,VDY,VEX,VEY
      COMMON /CDAMP/  MAF,MBF
      REAL    KE
      WRITE  (7,5500) T,SLIPA,SLIPB,SLIPD,SLIPE,VAX,VAY,
     *                VBX,VBY,VDX,VDY,VEX,VEY
      WRITE  (8,6000) T,FAX,FBX,FDX,FEX,FC1,FAY,FBY,FDY,
     *                FEY,FC2,FAZ,FBZ,FDZ,FEZ
      WRITE  (9,5500) T,U,UD,UDD,V,VD,VDD,E,ED,EDD,B,BD,BDD
      WRITE  (10,6500) T,X,XD,XDD,Y,YD,YDD,THE,THED,THEDD,KE
      ENTRY PRKEY(T)
      WRITE  (6,7000) T,X,Y,THE,THED,THEDD,UD,VD
5500  FORMAT (F5.2,12E11.3)
6000  FORMAT (F5.2,2X,5F7.1,4E11.3,5F8.1)
6500  FORMAT (F5.2,1X,9E13.4,F7.2)
7000  FORMAT (F5.2,3X,7F9.4)
      END



*******************************************************************
* BLOCK DATA INITIALIZES ALL SPECIFIABLE AND NON-SPECIFIABLE VARIABLES.  *
* IF IT IS DESIRABLE TO CHANGE SEVERAL INITIAL CONDITIONS FOR MANY DIFF- *
* ERENT TEST CASES, THIS CAN BE DONE BY MODIFYING BLOCK DATA RATHER THAN *
* BY SPECIFYING EACH CHANGE INTERACTIVELY FOR EACH TEST CASE.            *
*******************************************************************

      BLOCK DATA
      COMMON /DIMEN/  D1,D2,S1,S2,L1,L,T1,T2,H
      COMMON /MASSPR/ IZ,IZP,M,MC,GR
```

```
      COMMON /LATFOR/ FAY,FBY,FDY,FEY,FTIMP,FCIMP,DUIMP
      COMMON /LONFOR/ FAX,FBX,FDX,FEX
      COMMON /NORFOR/ FAZ,FBZ,FDZ,FEZ,ROLLK
      COMMON /C1VAR/  U,UD,UDD,FC1
      COMMON /C2VAR/  V,VD,VDD,FC2
      COMMON /CASANG/ E,ED,EDD,B,BD,BDD
      COMMON /GLOBAL/ X,XD,XDD,Y,YD,YDD,THE,THED,THEDD,KE
      COMMON /SLIPAN/ SLIPA,SLIPB,SLIPD,SLIPE
      COMMON /PTVEL/  VAX,VAY,VBX,VBY,VDX,VDY,VEX,VEY
      COMMON /CDAMP/  MAF,MBF
      COMMON /CAMTOE/ CAMANG,CAMCOF,TOEANG
      COMMON /TIRES/  TIRY(3,8),TIRX(3),CASY(3,8),CASX(3)
      COMMON /YCOEFF/ EJAY(3,8),IMY(3,8),EJPY(3,8),SSY(3,8),AGY(3,8)
      COMMON /XCOEFF/ EJAX(3),IMX(3),EJPX(3),SSX(3),AGX(3)
      COMMON /FORMOD/ TXMOD,TYMOD,CXMOD,CYMOD
      COMMON /TIME/   TTOTAL,TSTEP,PINT,PRCTRL
      REAL   L1,L,IZ,IZP,MAF,MBF,M,MC,KE,IMY,IMX
      DATA   D1,D2,S1,S2 /.265,.265,.345,.175/
      DATA   L1,L,T1,T2,H /.058,.08,.24,.24,.61/
      DATA   IZ,IZP,M,MC,GR /5.6,.02,95.,1.2,9.81/
      DATA   FCIMP,DUIMP,FTIMP,FAX,FBX,FDX,FEX /40.,.10,5*0./
      DATA   FAY,FBY,FDY,FEY,FAZ,FBZ,FDZ,FEZ,ROLLK /8*0.,1./
      DATA   TXMOD,TYMOD,CXMOD,CYMOD /0.,1.,0.,1./
      DATA   U,UD,UDD,FC1,V,VD,VDD,FC2,E,ED,EDD,B,BD,BDD /0.,.75,12*0./
      DATA   X,XD,XDD,Y,YD,YDD,THE,THED,THEDD,KE /10*0./
      DATA   SLIPA,SLIPB,SLIPD,SLIPE /4*0./
      DATA   VAX,VAY,VBX,VBY,VDX,VDY,VEX,VEY /8*0./
      DATA   MAF,MBF,CAMANG,CAMCOF,TOEANG /.1,.1,0.,0.,0./
      DATA   TTOTAL,TSTEP,PINT,PRCTRL /10.,.001,.20,1./
      DATA EJAX  / 1.95068E-2,-2.65456E-5, 5.38569E-8 /
      DATA IMX   / 1.20231E-2,-3.62874E-6, 2.47265E-8 /
      DATA EJPX  / 1.48242E-2,-2.77966E-5, 2.70203E-8 /
      DATA SSX   / 1.81750E-2,-5.30452E-5, 6.26485E-8 /
      DATA AGX   / 1.22211E-3, 1.42569E-4,-1.70013E-7 /
      DATA CASX  / 9.19876E-3, 3.21731E-5,-1.54898E-8 /
      DATA EJAY  / 1.98189E-1,-1.73690E-4,-3.90765E-8,
     *             3.17207E-1, 2.37231E-5,-5.19682E-7,
     *             3.07205E-1, 5.56659E-4,-1.11809E-6,
     *             2.93374E-1, 9.48220E-4,-1.52567E-6,
     *             3.65706E-1, 8.27195E-4,-1.34621E-6,
     *             5.31375E-1, 2.66275E-4,-7.41407E-7,
     *             6.75259E-1,-2.13245E-4,-2.69438E-7,
     *             6.96379E-1,-2.23784E-4,-2.97540E-7 /
      DATA IMY   / 3.58427E-1,-9.11580E-4, 7.31398E-7,
     *             5.09691E-1,-1.01940E-3, 7.68241E-7,
     *             6.80230E-1,-1.29672E-3, 9.95998E-7,
     *             8.10033E-1,-1.53026E-3, 1.19312E-6,
     *             8.32849E-1,-1.39033E-3, 1.04160E-6,
     *             8.40706E-1,-1.27670E-3, 9.12153E-7,
     *             7.88546E-1,-9.29083E-4, 5.50323E-7,
     *             7.74272E-1,-8.86877E-4, 5.64815E-7 /
      DATA EJPY  / 3.35695E-1,-4.40024E-4, 9.33529E-8,
     *             5.30394E-1,-4.86746E-4,-8.41244E-8,
     *             6.31923E-1,-3.16612E-4,-3.67544E-7,
```

```
     *             8.25503E-1,-6.47171E-4,-6.40109E-8,
     *             8.99986E-1,-5.39797E-4,-2.33609E-7,
     *             9.29075E-1,-4.47427E-4,-3.16601E-7,
     *             9.19489E-1,-2.36651E-4,-5.02252E-7,
     *             9.84140E-1,-4.15714E-4,-3.08961E-7 /
      DATA SSY   / 3.00952E-1,-4.38212E-4, 1.68247E-7,
     *             5.84062E-1,-1.08108E-3, 7.88194E-7,
     *             7.61038E-1,-1.14356E-3, 5.69103E-7,
     *             8.81072E-1,-1.20144E-3, 5.34230E-7,
     *             8.54826E-1,-7.28898E-4,-1.11986E-8,
     *             8.22513E-1,-4.40673E-4,-2.27546E-7,
     *             7.53144E-1, 3.15524E-5,-6.98151E-7,
     *             7.77852E-1,-7.30789E-5,-4.72285E-7 /
      DATA AGY   / 2.68912E-1, 6.28921E-5,-6.18542E-7,
     *             5.42135E-1,-6.12264E-4, 1.14320E-7,
     *             7.51468E-1,-1.00052E-3, 4.23781E-7,
     *             8.78984E-1,-1.07359E-3, 3.75928E-7,
     *             8.86993E-1,-7.67556E-4, 2.04054E-8,
     *             9.22619E-1,-6.89697E-4,-6.90660E-8,
     *             9.46552E-1,-6.50317E-4,-6.81895E-8,
     *             9.52619E-1,-5.63006E-4,-1.52079E-7 /
      DATA CASY  / 2.43038E-1,-6.86099E-4, 6.05735E-7,
     *             4.59856E-1,-1.31249E-3, 1.19560E-6,
     *             6.90894E-1,-1.97964E-3, 1.78667E-6,
     *             8.18698E-1,-2.11332E-3, 1.72893E-6,
     *             9.82602E-1,-2.45591E-3, 1.96530E-6,
     *             1.07234E-0,-2.50068E-3, 1.86841E-6,
     *             1.21599E-0,-2.83152E-3, 2.12777E-6,
     *             1.34947E-0,-3.14277E-3, 2.34825E-6 /
      END
```

APPENDIX D

ESTIMATION OF DEFAULT PARAMETERS

The default parameters used by program WCHAIR were given in Table 8-1. Most of the default values were either measured directly or were assigned a known typical value. For example, the width dimensions d_1 or d_2 (see Figure 6-1) could be directly measured from the Everest and Jennings rear caster wheelchair. The assumed total mass of 95 kg corresponds to a user with mass 75kg and a wheelchair with mass 20kg. These are known to be reasonable values. Of course, all of the parameters will vary for different wheelchairs and different users. It is desirable to choose default parameters which are representative of a typical wheelchair/user combination.

Of the parameters given in Table 8-1, three were slightly more difficult to estimate than the others. These were the center of gravity position, the moment of inertia values, and the frictional moments at the caster pins. This appendix is intended to briefly outline the methods that were used to obtain reasonable values for each of these quantities.

CENTER OF GRAVITY POSITION

As mentioned previously, it was not possible to obtain the Everest and Jennings rear caster wheelchair for an extended period of testing. For this reason, the longitudinal position and vertical height of the center of gravity were estimated using data collected by E.V. Mochel. [D.1] Mochel determined the position of the center of gravity for a 75kg ISO (International Organization for Standardization) test dummy seated in an Invacare Rolls 500 STS wheelchair. This is a manual front caster wheelchair. The center of gravity was found to be a distance of 13.5cm from the rear axle of the front caster wheelchair at a height of 61cm. Note that the default mass used by program WCHAIR assumes a user of mass 75 kg. This value was chosen to correspond to the ISO dummy used by Mochel. Later in this appendix, moment of inertia values for the ISO dummy will be discussed.

The rear axle on the front caster wheelchair used by Mochel corresponds approximately to the back of the seat. Because the Invacare wheelchair and the rear caster Everest and Jennings wheelchair have nearly the same mass, it is reasonable to expect that the center of gravity position for the Everest and Jennings chair will also be about 13.5cm from the seat back (again assuming a 75kg test dummy). Adding to this value a distance of 4cm from the back of the seat to the caster pins means that the distance (s_2) from the caster pins to the center of gravity is approximately 17.5 cm (see Figure 9-1).

The seat height for both the Everest and Jennings rear caster wheelchair and the Invacare front caster wheelchair used by Mochel was measured to be 48 cm (19 in). Since both wheelchairs have nearly the same mass, the center of gravity heights should be approximately equal. Thus, the height of

61 cm found by mochel was used as the value for h.

It is emphasized that the default values are only reasonable estimates. The effect of varying the center of gravity position was discussed in Chapters 8 and 9.

MOMENT OF INERTIA VALUES

The moment of inertia of the 75 kg ISO test dummy was determined to be 3.1 kg-m^2 by T.M. Duffey. [D.2] This value corresponds to a vertical axis passing through the dummy's center of gravity. The ISO dummy was designed to have mass properties similar to those found for a typical wheelchair user.

The mass moment of inertia of a typical manual wheelchair was experimentally determined by using a torsional pendulum. The pendulum consisted of a slender steel rod welded between two small metal plates as shown in Figure D-1. The upper plate was clamped to a rigid frame so that the pendulum would hang freely. A wheelchair was suspended at the lower plate by passing a flat steel bar under the seat frame and then clamping that bar to the lower plate using two C-clamps. The wheelchair was clamped such that the lower plate was located at the wheelchair center of mass.

The suspended wheelchair was then carefully rotated through a small angle theta and released. By measuring the period of the resulting oscillations, it was possible to determine the moment of inertia, I.

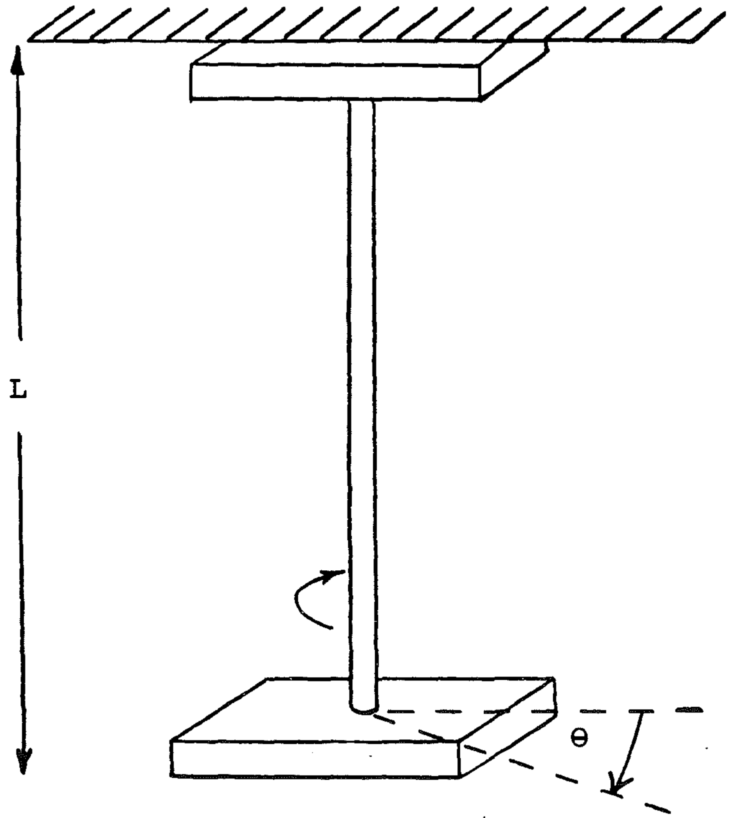

Figure D-1 Torsional Pendulum for Determining Moments of Inertia

The relationship between the period of oscillation, T, the wheelchair moment of inertia, I, and the material properties of the steel rod is given by

$$T = 2\pi\sqrt{\frac{I}{K_t}} \tag{D-1}$$

where K_t is the torsional rigidity of the rod. K_t can be found by suspending a mass with a known moment of inertia such as a solid cylinder from the pendulum and observing its period of oscillation. Once K_t is determined, I values can be found for a wheelchair or any other mass that can easily be mounted at its center of gravity to the lower pendulum plate.

The torsional pendulum used for this research consisted of a 1/8 (.32 cm) inch diameter steel rod of length 33 1/2 inches (85.1 cm). A 50 lbf (222 N) solid cylinder was used to calibrate the pendulum. The value of K_t for this rod was found to be 0.66 (ft-lbf)/rad. The value for I for an Invacare Rolls IV manual front caster wheelchair was found to be 2.3 kg-m^2.

Because the center of mass of the wheelchair and the seated dummy do not coincide, the total moment of inertia is not simply the sum of the value found by Duffey for the ISO dummy and value obtained from the torsional pendulum for the wheelchair. Instead a small correction is required. This is done by determining the position of the dummy center of mass, the wheelchair center of mass, and the combined center of mass. With these positions known, the parallel axis theorem for moments of inertia is used to compute the total moment of inertia. When this was done, the resulting total moment of inertia, I_z was found to be 5.6 kg-m^2 as given in Table 8-1. This is 0.2 kg-m^2 higher than would have been obtained by simply adding the two values already given for the dummy only and the chair only (3.1 kg-m^2 + 2.3 kg-m^2)

FRICTIONAL MOMENTS AT CASTER PINS

Because the friction at the caster pins is extremely small, it is difficult to measure directly. An approximate value was obtained by lifting the wheelchair off the ground so that the two casters were free to pivot. A spring scale was hooked to one of the casters at a known distance from the caster pin. By measuring the distance to the caster pin and the force required to slowly turn the caster, the frictional moment was found to be approximately 0.10 N-m.